



THE UNIVERSITY OF QUEENSLAND
AUSTRALIA

**siRNA screening of the kinome identified Aurora A kinase
as a therapeutic target gene in cervical cancer**

Fawzi Faisal A. Bokhari, M.Sc.

A thesis submitted for the degree of Doctor of Philosophy at

The University of Queensland in 2014

The University of Queensland Diamantina Institute

Abstract

HPV oncogenes disable a number of tumour suppressor pathways, including p53 and Rb, contributing to the transformed phenotype. Loss of these critical host cell functions may also provide an opportunity to selectively target the destruction of HPV-transformed cells. We have performed an siRNA screen using the kinome (779 genes) library to identify genes that when depleted are synthetically lethal with HPV transformation. The primary and validation screens have confirmed Aurora A kinase (AURKA) as a potential synthetic lethal target selective for HPV transformed cells. AURKA has been further investigated using the selective small molecule inhibitor MLN8237. We found that MLN8237 was significantly more potent towards the HPV transformed cells. The effect was not a consequence of targeting mitosis as two other mitotic inhibitors, PLK1 inhibitor (BI2536) and taxol, demonstrated no selectivity. Analysis of the nuclear structure and DNA content showed that Aurora A inhibition promoted a high level of polyploidy in non-HPV treated cells whilst this same degree of polyploidy was associated with apoptosis in the HPV-transformed cell lines. Whereas Bcl-2 over expression in HeLa cells had no effect on sensitivity to MLN8237, Mcl-1 overexpressing HeLa cells were less sensitive to the MLN8237 in comparison to the parental cell line, which may suggest the involvement of Noxa or Puma pro-apoptotic proteins in the induction of the apoptosis in the HPV-transformed cells. The transfection of the non-HPV C33A cervical cancer and SCC25 squamous cell carcinoma cell lines with the HPV16 oncogenic E7 increased sensitivity to MLN8237 between 3 >10 fold suggesting that the sensitivity to MLN8237-dependent killing was a direct consequence of HPV E7 expression. Xenograft experiments with cervical cancer cell lines in immunodeficient mice showed MLN8237 inhibited growth of HPV and non-HPV xenografts during treatment with 30mg/kg MLN8237 once a day for 10 consecutive days. However, outgrowth of tumour was noticed from the second day post-treatment in the non-HPV tumour group whereas the HPV-induced tumour group did not show cancer recurrence for 50 days post-treatment. These findings suggest that MLN8237 represent a promising novel therapeutic targeted agent against HPV-transformed cervical cancer.

Declaration by author

This thesis is composed of my original work, and contains no material previously published or written by another person except where due reference has been made in the text. I have clearly stated the contribution by others to jointly-authored works that I have included in my thesis.

I have clearly stated the contribution of others to my thesis as a whole, including statistical assistance, survey design, data analysis, significant technical procedures, professional editorial advice, and any other original research work used or reported in my thesis. The content of my thesis is the result of work I have carried out since the commencement of my research higher degree candidature and does not include a substantial part of work that has been submitted to qualify for the award of any other degree or diploma in any university or other tertiary institution. I have clearly stated which parts of my thesis, if any, have been submitted to qualify for another award.

I acknowledge that an electronic copy of my thesis must be lodged with the University Library and, subject to the General Award Rules of The University of Queensland, immediately made available for research and study in accordance with the *Copyright Act 1968*.

I acknowledge that copyright of all material contained in my thesis resides with the copyright holder(s) of that material. Where appropriate I have obtained copyright permission from the copyright holder to reproduce material in this thesis.

Publications during candidature

Blake, S.J., **Bokhari, FB.**, McMillan, N.A. (2012). RNA interference for viral infections. *Curr Drug Targets*, Oct; 13(11):1411-20

Publications included in this thesis

No publications included.

Contributions by others to the thesis

Technical assistance from Mr Max Ranall (ARVEC Unit UQDI) for the design and optimisation of the kinome screen.

Statement of parts of the thesis submitted to qualify for the award of another degree

None.

Acknowledgements

“In the name of Allah, the most gracious, the most merciful”

Thank you Allah for helping me to finish this PhD thesis.

I would like to start the first acknowledgment in this section with the person who pushed me to go throughout all the postgraduate studies Masters and PhD. The person whom I will never forget and I wish he is now with me sharing with me these moments. But many times what we wish never comes to reality. To the person that I have lost in the mid of my PhD, to his soul; to my Father: I have made it to the end of the journey Dad. I hope this thesis will make your soul as happy as you would have been with me today. I owe you a lot and thank you is not even enough to what you have done for me; and all words will not be adequate to describe my feelings. I love you Dad.

This PhD work would have not been done without the financial support I have received from the generous government of the Kingdom of Saudi Arabia and the support I had from the funding of Associate Professor Brian Gabrielli at the UQDI and Professor Nigel McMillan at Griffith University. Thank you all for your great support.

Honestly I do not know how to thank my great supervisors, both Associate Professor Brian Gabrielli and Professor Nigel McMillan. I owe you a huge thank you for all what you have done with me. I HAVE LEARNT SO MUCH FROM YOU BOTH. Thank you for your usual support, understandings, guiding me throughout my PhD, and providing me with opportunities to learn and develop my skills to become a scientist. Your doors have been always open for guidance, discussions, ideas, and questions. Thank you so much.

Special thanks also go to my previous associate supervisor Professor Tom Gonda who guided me throughout the beginning of this project. Your feedback and guidance have been always appreciated.

To all the Gabrielli lab members, you have been great friends and colleagues to be with. I would like to specifically thank Dr Loredana Spoerri for her helps in reviewing my Materials and Methods

Chapter of this thesis and for her continuous advices. Also, I will never forget to say thank you McMillan lab members past and present, I have enjoyed being with you all.

Any work in this life has ups and downs and moments where you need special squad to make you feel you are still alive. To my amazing friends in Australia and in Saudi Arabia who helped me overcome all the hectic moments I have been through during this project (YES! Those Thursday nights at the La Dolce Vita Café having coffee, helped me so much).

Last, but of course not least, this section is devoted to those who really being part of my life. Firstly, to my Mother, any word in this life will not be enough to convey my feelings towards you. Thank you for being with me all the time, for the support you gave me, for the advices that always put me on top of this life, thank you for everything you have given me. Without you, not only my PhD but also my whole life will be tasteless. I love you Mom. Secondly, my wife Nahla, the person who left everything behind to join me in this journey; thank you for all the cares you gave me, helps and encouragements. I would thank Allah everyday throughout my life for giving me such a great person like you. I owe you so much Nahla and, of course, I love you. To my brothers and sisters, Bassem, Ashwaq, AbdulRahman, and Ghazal. You are the great companion gifts from Allah to me in this life. Your support and helps were key players in finishing this work; thank you so much, I love you all. To my sons, who are my real eyes in this life, Faisal and AbdulRahman. All the pain, stress, and challenges resolve when I see your great smiles and hug you. You have been always and will remain the bright side of my life.

Keywords

siRNA, AURKA, AURKB, Haspin, GSG2, cervical cancer, HPV, synthetic lethality.

Australian and New Zealand Standard Research Classifications (ANZSRC)

ANZSRC code: 111207, Molecular Targets, 50%

ANZSRC code: 111201, Cancer Cell Biology, 30%

ANZSRC code: 111203, Cancer Genetics, 20%

Fields of Research (FoR) Classification

FoR code: 0604, Genetics 50%

FoR code: 0601, Biochemistry and Cell Biology, 25%

FoR code: 1112, Oncology and Carcinogenesis, 25%

Table of Contents

Abstract.....	ii
Acknowledgements.....	vi
List of Tables	xiv
List of Figures.....	xv
List of Abbreviations	xvii
1 Literature Review	1
1.1 Human papillomavirus (HPV)	1
1.1.1 The structure of HPV	2
1.1.2 Viral proteins	4
1.1.2.1 The HPV E6 oncogene	4
1.1.2.2 HPV E7 oncogene	5
1.1.3 HPV life cycle.....	6
1.1.3.1 Infection and uncoating	6
1.1.3.2 Genome maintenance and proliferative phase.....	7
1.1.3.3 Genome amplification	8
1.1.3.4 Packaging of viral genome and virus release	9
1.2 Cell Cycle	9
1.2.1 G ₁	10
1.2.2 DNA synthesis (S-phase).....	11
1.2.3 G ₂	12
1.2.4 Mitosis (M)	13
1.2.5 SAC/p53 cross-talking	15
1.3 The molecular basis of cancer.....	15
1.3.1 Sustaining proliferative signalling	15
1.3.2 Evasion growth suppressors.....	17
1.3.3 Resisting cell death	19
1.3.4 Enabling replicative immortality	20

1.3.5	Inducing angiogenesis.....	21
1.3.6	Activating invasion and metastasis.....	23
1.4	Programmed cell death (apoptosis).....	24
1.4.1	Anoikis signaling	26
1.5	Cervical cancer	27
1.5.1	Risk factors	27
1.5.2	Signs and symptoms	28
1.5.3	Types of cervical neoplasia.....	28
1.5.4	Diagnosis of cervical neoplasia	28
1.5.5	Management of cervical neoplasia.....	29
1.5.6	Vaccination	30
1.6	Ribonucleic acid interference (RNAi)	32
1.6.1	Use of siRNA in cancer therapies.....	33
1.6.2	Efforts to knockdown E6 and E7 HPV oncogenes using siRNA	34
1.7	Synthetic lethality screening.....	35
1.8	Hypothesis	38
1.9	Aims.....	38
1.10	Significance.....	39
2	Materials and methods	40
2.1	Materials	40
2.1.1	Western blotting solutions	40
2.1.2	Tissue culturing solutions and reagents	40
2.1.3	Inhibitors	41
2.1.4	Antibodies	41
2.1.5	siRNA high-throughput synthetic lethal screen reagents/consumables.....	42
2.2	Methods	42
2.2.1	Cell culture.....	42
2.2.1.1	Cell propagation and subculturing.....	43
2.2.1.2	Long-term storage of cells.....	43
2.2.2	Optimization of siRNA screening conditions	43

2.2.2.1	Cell seeding density.....	43
2.2.2.2	Optimizing transfection reagents and concentration.....	44
2.2.3	siRNA primary screening.....	45
2.2.4	siRNA validation screening.....	45
2.2.5	Resazurin cell viability assay.....	45
2.2.6	Adenylate kinase cytotoxicity assay.....	46
2.2.7	Nucleotide incorporation assay (5-ethynyl-2'-deoxyuridine or EdU Assay).....	46
2.2.8	Quantitative cell imaging.....	47
2.2.9	Flow cytometry.....	47
2.2.10	Time-lapse microscopy.....	47
2.2.11	Immunoblotting.....	48
2.2.12	Cell doubling-time.....	48
2.2.13	Xenograft mice models.....	49
2.2.14	Screening Statistical Methods.....	49
2.2.15	Immunofluorescence staining.....	50
3	siRNA screening of the kinome identified potential therapeutic target genes in cervical cancer.....	52
3.1	Introduction.....	52
3.2	Results.....	53
3.2.1	Screening Optimization.....	53
3.2.2	Primary Screening.....	58
3.2.2.1	Cell Viability.....	58
3.2.2.2	Cytotoxicity.....	61
3.2.2.3	Cell Number.....	63
3.2.2.4	Hit Selection.....	67
3.2.3	siRNA Secondary Screening.....	68
3.2.3.1	Cell Viability.....	68
3.2.3.2	Cytotoxicity.....	69
3.2.3.3	Cell Numbers.....	71
3.2.3.4	Final hit selection.....	72

3.2.4	Confirming AURKA and AURKB knockdown by the ON-TARGETplus SMARTpool siRNA	74
3.3	Discussion	74
4	Aurora B small molecule inhibitor, ZM447439, is not selective for HPV-transformed cell lines.....	80
4.1	Introduction.....	80
4.2	Results.....	81
4.2.1	Inhibiting AURKA, AURKB, and Haspin is specific to HPV-induced cell lines	81
4.2.2	Aurora B small-molecule inhibitor (ZM 447439) selectivity	85
4.2.3	Suppression of Aurora B activity by ZM 447439 induces accumulation of 4N and >4N DNA contents	87
4.3	Discussion	90
5	Aurora A small molecule inhibitor, MLN8237, is selective for HPV-transformed cervical cancer cells	94
5.1	Introduction.....	94
5.2	Results.....	95
5.2.1	MLN8237 showed selectivity for HPV-transformed cervical cancer cell lines	95
5.2.2	Non-HPV squamous cell carcinoma (SCC) showed resistance to MLN8237	97
5.2.3	Treatment with MLN8237 induced apoptosis and polyploidy in cervical cancer cell lines	98
5.2.4	MLN8237 induced polyploidy of all tested cell lines tested using immunofluorescence staining.....	101
5.2.5	Time-lapse microscopy showed longer mitotic delay in HPV-transformed cell lines	104
5.2.6	Sensitivity to MLN8237 is a direct consequence of expression of HPV E7	108
5.2.7	Over-expression of Mcl-1 reduced sensitivity to MLN8237	109
5.2.8	Assessing the mechanism of MLN8237-induced apoptosis in HPV and non-HPV cervical cancer cell lines.....	110
5.2.9	MLN8237 inhibits tumour growth in mouse xenograft model.....	112

5.3 Discussion.....	114
6 General discussion, conclusion, and future directions.....	120
6.1 General Discussion	120
6.2 Conclusions and future directions.....	124
Bibliography	127
Appendix 1 Customized high-content imaging protocols for the tested cell lines.....	174
Appendix 2 Example of how cell seeding density was determined.....	177
Appendix 3 Example of other transfection reagents and concentrations.....	178
Appendix 4 siRNA primary screen candidates detail.....	180
Appendix 5 Relative AURKA and AURKB protein levels	186
Appendix 6 Dose-response for cervical cancer HPV and non-HPV cell lines treated with MLN8237.....	188
Appendix 7 Dose-response for cervical cancer squamous cell carcinoma (SCC) cell lines treated with MLN8237.....	190
Appendix 8 Dose-response for C33A and SCC-25 HPV16E7-transfected cell lines treated with MLN8237.....	192

List of Tables

Table 1.1.	Main functions of proteins expressed by the high-risk human papillomaviruses	4
Table 2.1.	Commonly used Western blotting solutions	40
Table 2.2.	Commonly used tissue culturing solutions and reagents	40
Table 2.3.	Inhibitors used throughout the project	41
Table 2.4.	Commonly used antibodies and their corresponding species and dilutions.....	41
Table 2.5.	Reagents and consumables used in the screening processes.....	42
Table 3.1.	List of all cell lines and their corresponding seeding densities used throughout the primary and secondary siRNA screens	54
Table 3.2.	Selected hits for the validation screen.....	67

List of Figures

Figure 1.1. Evolutionary associations between different human papillomaviruses subtypes.	2
Figure 1.2. Illustration of the HPV genome.	3
Figure 1.3. Cell cycle phases. Illustration of the Cyclins and cyclin-dependent kinaes associated with the cell cycle phases. Modified from (Niehrs and Acebron, 2012).....	11
Figure 1.4. Mitotic stages and principles of SAC.	14
Figure 1.5. Biological hallmarks of cancer.	16
Figure 1.6. Apoptosis mechanism regulated by the Bcl-2 family.	26
Figure 1.7. Pap smear specimen collection.	30
Figure 1.8. SiRNA pathway mechanism: where the dicer produces ds-siRNA from ds-RNA and the RISC upload it for target-specific mRNA degradation with the help of Ago2. From Rutz and Scheffold (Rutz and Scheffold, 2004).	34
Figure 1.9. Illustration of synthetic lethality concept.	38
Figure 2.1. Example of how the Z-score was calculated in the siRNA screening stages of this project.	50
Figure 3.1. Summary of cell metabolic activity measured in HaCaT, CaSki and C33A cell lines using DharmaFECT 3 at 0.05% lipid concentration.	55
Figure 3.2. Summary of adenylate kinase activity measured in HaCaT, CaSki, and C33A cell lines using DharmaFECT 3 at a 0.05% lipid concentration.	56
Figure 3.3. Summary of HaCaT, CaSki, and C33A cell line cell count measurements using DharmaFECT 3 at 0.05% lipid concentration.	57
Figure 3.4. Cell viability of the primary screening of the human kinome library.	60
Figure 3.5. Adenylate kinase activity of the primary screening of the human kinome library.	62
Figure 3.6. Cell numbers of the primary screening of the human kinome library.	64
Figure 3.7. S-phase% determination of the primary screening of the human kinome library.	66

Figure 3.8. Validated target hits using Dharmacon ON-TARGETplus SMARTpool siRNA based on the viability assay.	69
Figure 3.9. Validated target hits based on adenylate kinase activity.	70
Figure 3.10. siRNA-validated target hits based on cell count.	71
Figure 3.11. Summary of selected target hits based on three cell biological assays	73
Figure 3.12. AURKA and AURKB ON-TARGETplus SMARTpool siRNA successfully decreased protein level	74
Figure 4.1. PLK1 small molecule inhibitor (BI-2536) and paclitaxel did not show selectivity towards either HPV or non-HPV cervical cancer cell lines.	84
Figure 4.2. Aurora B small-molecule inhibitor ZM 447439 showed no selectivity towards HPV-transformed cervical cancer cells.	87
Figure 4.3. ZM447439 induced aneuploidy and high apoptotic profiles on time-dependent manner in all tested cell lines regardless of their HPV-transformation status.	90
Figure 5.1. C33A non-HPV cervical cancer cell lines showed least sensitivity to MLN8237.	96
Figure 5.2. The non-HPV squamous cell carcinoma cell lines are less sensitive to MLN8237.	97
Figure 5.3. MLN8237 induced high apoptotic profile in HPV-transformed cervical cancer cell lines A)	100
Figure 5.4. MLN8237 disrupt normal mitosis.	103
Figure 5.5. Time-lapse microscopy confirms high mitotic delay of HPV-transformed cells treated with MLN8237 followed by second mitosis and subsequent apoptosis.	108
Figure 5.6. Transfection of non-HPV cell lines with HPV16 E7 increased sensitivity to MLN8237.	108
Figure 5.7. Mcl-1 over expression reduced the sensitivity to MLN8237.	110
Figure 5.8. Analysis of cell lysate from cervical cancer HPV and non-HPV cell lines.	111
Figure 5.9. MLN8237 arrest tumour growth in vivo in a mouse xenograft model.	113

List of Abbreviations

DNA	Deoxyribonucleic acid
dsDNA	Double-stranded deoxyribonucleic acid
HPV	Human papillomavirus
bp	Base pair
LCR	Long control region
E1	Early oncogene 1
E2	Early oncogene 2
E3	Early oncogene 3
E4	Early oncogene 4
E5	Early oncogene 5
E6	Early oncogene 6
E7	Early oncogene 7
L1	Late protein 1
L2	Late protein 2
ORF	Open reading frame
mRNA	Messenger RNA
RNA	Ribonucleic acid
p53	Protein 53
MDM2	Mediator of DNA damage 2
E6AP	Early oncogene 6 associated protein
CBP	CREB-binding protein
Bax	Bcl2-associated X protein
TNFR1	Tumour necrosis factor receptor 1
pRb	Retinoblastoma protein
CDK4	Cyclin dependent kinase 4
CDK2	Cyclin dependent kinase 2
G1	Gap/Growth 1
G2	Gap/Growth 2
S-phase	Synthesis phase
E2F1	E2F transcription factor 1
p21	Protein 21
p27	Protein 27
M	Mitosis
CDKI	Cyclin dependent kinase inhibitor
CDK	Cyclin dependent kinase
JNK	c-Jun N-terminal kinase
MAPK	Mitogen-activated protein kinase
ERK	Extracellular signal regulated protein kinase
NF- κ B	Nuclear factor kappa B
TNF	Tumour necrosis factor

Caspase	Cysteine-aspartic proteases
Bcl-2	B-cell CLL/lymphoma 2
BH	Bcl-2 homology
BH1	Bcl-2 homology 1
BH2	Bcl-2 homology 2
BH3	Bcl-2 homology 3
BH4	Bcl-2 homology 4
Bcl-xl	Bcl2-like 1
Bcl-w	Bcl2-like 2
Mcl-1	Myeloid cell leukemia sequence 1
Bim	Bcl2-like 11
Bid	BH3 interacting domain death agonist
Bad	Bcl2-associated agonist of cell death
Bik	Bcl2-interacting killer
Puma	Bcl2 binding component 3
Noxa/PMAIP1	Phorbol-12-myristate-13-acetate-induced protein 1
Bmf	Bcl2 modifying factor
Hrk	Harakiri, Bcl2 interacting protein
Bak	Bcl2-antagonist/killer 1
p600	Protein 600
SCC	Squamous cell carcinoma
CIN	Cervical intraepithelial neoplasia
FIGO	International Federation of Gynaecology and Obstetrics
SCI	Cervical squamocolumnar
Pap test	Papanicolaou test
ACOG	American College of Obstetrician and Gynaecologist
ACS	American cancer society
RNAi	Ribonucleic acid interference
siRNA	Small interfering ribonucleic acid
shRNA	Short-hairpin ribonucleic acid
dsRNA	double-stranded ribonucleic acid
ssRNA	Single-stranded ribonucleic acid
STAT3	Signal transducer and activator of transcription 3
VEGF	Vascular endothelial growth factor A
MMP2	Matrix metalloproteinase 2
qPCR	Quantitative polymerase chain reaction
HFDM	Hydration-of-freeze-dried-matrix
KRAS	Kirsten rat sarcoma viral oncogene homolog
TBK1	Tank-binding kinase 1
CHK1	Checkpoint kinase 1
PBS	Phosphate-buffered saline
TBS	Tris-buffered saline

DMEM	Dulbecco's modified eagle medium
gH2AX	H2A histone family, member X
α -Tubulin	Alpha tubulin
ATCC	American Type Culture Collection
EDTA	Ethylenediaminetetraacetic Acid
mL	Milliliter
mM	Millimolar
μ M	Micromolar
nM	Nanomolar
pM	Picomolar
V/V	Volume per volume
W/V	Weight per volume
h	Hours
min	Minutes
PLK1	Polo-like kinase 1
siNT	Non-targeting siRNA
EdU	5-ethynyl-2'-deoxyuridine
μ M	Microgram
PMSF	Phenylmethylsulfony fluoride
SDS-PAGE	SDS-polyacrylamide gel electrophoresis
SD	Standard deviation
Wee1	wee-like protein kinase 1
COPB2	coatamer protein complex subunit beta 2
GSG2	Germ cell associated 2
PRKCN/PRKD3	Protein kinase D3
PIK3CA	Phosphatidylinositol-4,5-bisphosphate 3-kinase, catalytic subunit alpha
KSR2	Kinase suppressor of ras 2
AURKA	Aurora kinase A
AURKB	Aurora kinase B
AURKC	Aurora kinase C
CDC2L2	Cell division cycle 2-like protein kinase 2
CDC2L1	Cell division cycle 2-like protein kinase 1
ERN1	Endoplasmic reticulum to nucleus signalling 1
HRI	Heme regulated initiation factor 2 alpha kinase
STK39	Serine threonine kinase 39
CDKN1C	Cyclin-dependent kinase inhibitor 1C
TLK1	Tousled-like kinase 1
CHUK	Conserved helix-loop-helix ubiquitous kinase
MAPK12	Mitogen-activated protein kinase 12
CALM3	Calmodulin 3
CDKL1	Cyclin-dependent kinase-like 1

ANGPT4	Angiopoietin 4
CDC2/POLD1	Polymerase (DNA directed), delta 1, catalytic subunit
STK22C	Testis-specific serine kinase 3
DCK	Deoxycytidine kinase
RSP6KA3	Ribosomal protein S6 kinase
PIK3R3	Phosphoinositide-3-kinase regulatory subunit (gamma)
MYLK2	Myosin light chain kinase 2
hH3Thr3	Phosphorylates histone H3 at threonine 3
CPC	Chromosomal passenger complex
INCENP	Inner centromeric protein
MAD2	MAD2 mitotic arrest deficient-like 1
BubR1	BUB1 mitotic checkpoint serine/threonine kinase B
MLN8237	Aurora A kinase specific small molecule inhibitor
ZM447439	Aurora B kinase small molecule inhibitor

1 Literature Review

1.1 Human papillomavirus (HPV)

Papillomaviruses comprise several groups of viruses, which have been detected in different mammalian species. Due to the medical significance of human papillomaviruses (HPVs), intensive investigations have been conducted on them, and, as a result, more than 100 different types have been identified (Bernard, 2005). HPVs are a group of icosahedral capsids containing 72 capsomers with double-stranded (ds) DNA genome of about 8,000 base pairs (bp) (Nyitray et al., 2010). Based on their DNA sequence homology, HPVs can be divided into five subgroups, namely alpha, beta, gamma, mu, and nu, each of which is involved in different life cycle progression and disease association (Figure 1.1) (Bernard et al., 2010, Ekstrom et al., 2011).

Based on the phylogenetic tree which was generated from the detected alpha-HPVs, three subtypes of alpha-HPVs were identified (de Villiers et al., 2004a, Schiffman et al., 2005). Firstly, the low-risk 1 group mainly includes HPVs which cause benign genital warts and oral lesions (Schiffman et al., 2005). Second, low-risk 2 HPVs are responsible for benign vaginal cells (Narechania et al., 2005). Finally, high-risk alpha-HPV, may result in cervical neoplasia and cancer (Castle et al., 2007).

The second-largest HPV group is beta-HPV. This may pose problems for immunocompromised individuals or people with inherited defects (Ramos et al., 2002). In addition, it is thought that beta-HPV may be involved in the development non-melanoma skin cancer in the general population (Harwood et al., 2004).

Like beta-HPVs, the majority of gamma-HPVs may only cause asymptomatic infections in immunodeficient individuals; these can be detected by skin swabs or mucosal rinses (Bottalico et al., 2011, Gottschling et al., 2009). The remaining mu and nu-HPVs have only three human members which have been identified, all of which result in cutaneous papillomas (de Villiers et al., 2004b).

1.1.1 The structure of HPV

All papillomaviruses share a similar genomic structure and a non-enveloped icosahedral capsid. The viral particles comprise a circular dsDNA molecule of 8,000 bp bound to cellular histone and encompassed in a capsid which has 72 pentameric capsomers. The HPV genome is divided into three main regions, as follows: the non-coding long control region (LCR) with an average of 1,000 bp; the protein-coding early region of approximately 4,000 bp; protein-coding late region of about 3,000 bp. There are six different early proteins which are encoded by the viral genome (E1–E7) and two late proteins (L1 and L2) (Figure 1.2).

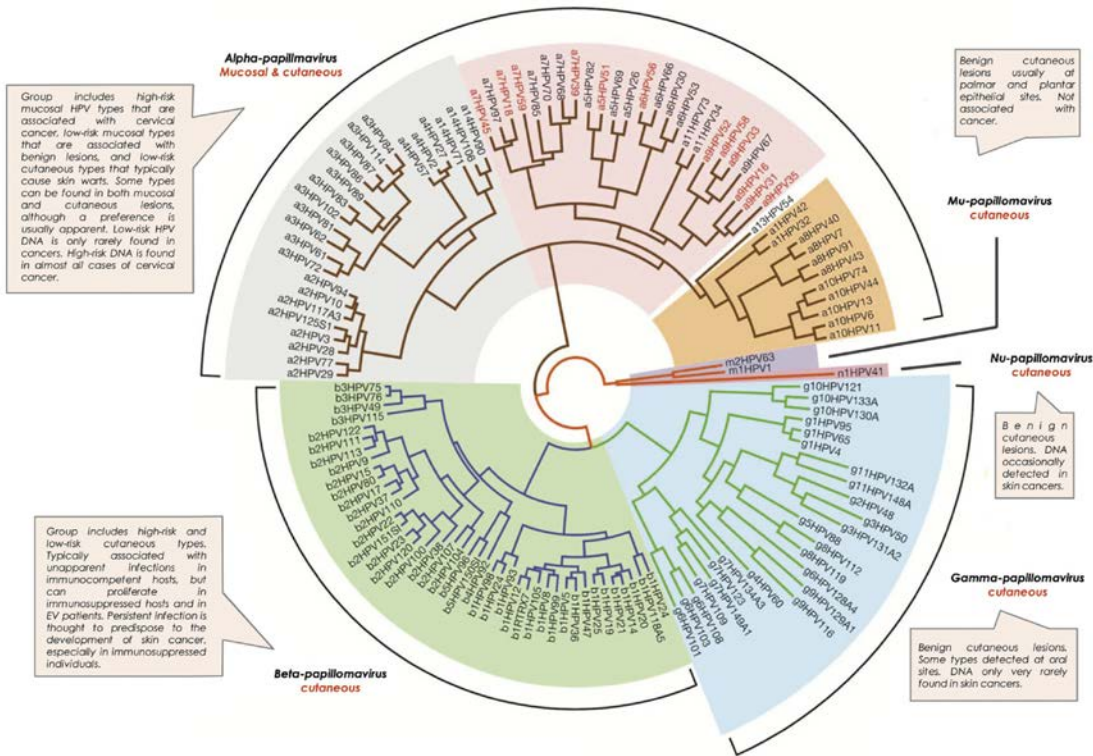


Figure 1.1. Evolutionary associations between different HPV subtypes. From (Doorbar et al., 2012).

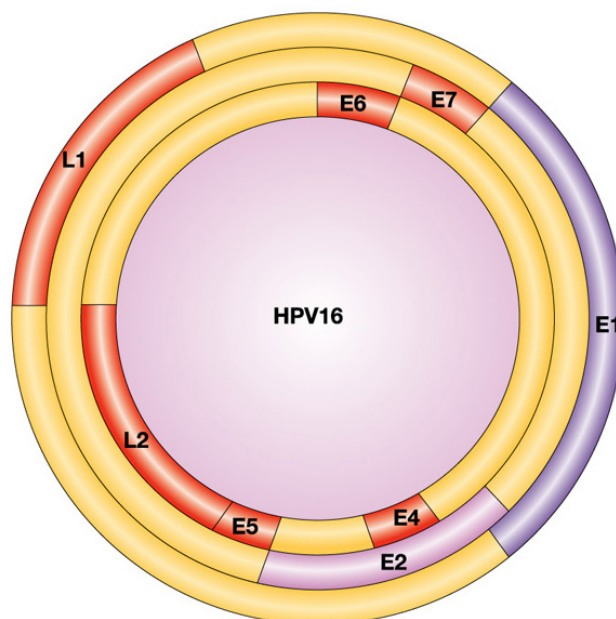


Figure 1.2. Illustration of the HPV genome. The three circles show the possible open reading frames (ORFs) where the sense strand can be translated. From (Frazer, 2004).

The LCR (also known as the upper regulatory region) regulates the DNA replication via the p97 core promoter by controlling the transcription of the ORFs (Apt et al., 1996). The LCR is also thought to have the highest degree of variation in the viral genome, as well as *cis* components which are responsible for replication and transcription of the papillomavirus DNA. The second region responsible for DNA replication and oncogenic transformation is early proteins region (McLaughlin-Drubin et al., 2008, McLaughlin-Drubin and Munger, 2009). Of interest, E6 and E7 are key players in this region, and are particularly essential for the cellular neoplastic transformation process. The latter oncogenic early proteins appear to interfere with essential normal cellular tumour suppressor proteins, where E6 binds and degrades protein 53 (p53) whilst E7 antagonises the function of the retinoblastoma protein (pRb) (Brooks et al., 2002, Gao et al., 2002, Shin et al., 2010). The third region of the HPV genomic structure is the late region, which has two late proteins, namely L1 and L2. L1 is the major element of the icosahedral capsid whereas the L2 protein binds with the papillomavirus DNA and package it into the viral capsid (Chen et al., 2000, Holmgren et al., 2005).

1.1.2 Viral proteins

As indicated above, HPV is composed of an 8 kb genome which has eight major proteins, six located in the ‘early’ region and two in the ‘late’ region. Each of these proteins has distinctive features and plays a role or a set of roles during the viral life cycle. Table 1.1 demonstrates the main function of each viral protein, whilst sections 1.1.2.1 and 1.1.2.2 focus on E6 and E7, as they play vital roles in the transformation status and maintaining tumourigenicity during malignancy.

Table 1.1. Main functions of proteins expressed by the high-risk HPVs

Protein	Role in the virus lifecycle
L1	Major capsid protein which assembles in capsomers and capsids. Also, encodes neutralising epitope.
L2	Minor capsid protein. Expedites virion assembly and interacts with cell receptors.
E1	Essential for viral DNA replication (ATP-dependent DNA helicase).
E2	Plays a vital role in viral replication and segregation. Binds the viral transcriptional promoter as a dimer. Orchestrates cellular gene expression and encapsidation.
E4	Virion assembly and release. Has the ability to induce cell cycle arrest (G ₂ arrest) and remodels the cyokeratin network.
E5	Plays a major role in cell proliferation and differentiation.
E6	Prevents apoptosis and differentiation. Also induces DNA synthesis.
E7	Stimulates cell proliferation and it controls the cell cycle.

1.1.2.1 The HPV E6 oncogene

The HPV E6 oncoprotein is about 160 amino acids in size, and has the ability to induce and maintain cellular transformation, albeit inefficiently. To date, it is known that the main target of the E6 oncoprotein is p53, also known as the guardian of the genome (Bai et al., 2006). The high-risk HPV E6 oncoprotein binds to p53 and causes its proteasomal degradation with the help of the 26S proteasome. Although the level of p53 is very low in normal cells, the deregulated overexpression of E7 causes this p53 level to increase due to the suppression of the mediator of DNA damage 2 (MDM2) – mediated proteasomal degradation of p53 in normal cells (Ainsworth et al., 2008, Eichten et al., 2002). The process of p53 degradation occurs through a trimeric complex which includes E6, E6-associated protein (E6AP), and p53. E6AP is an E3 ubiquitin ligase which ubiquitinates p53 and targets it for degradation by proteasome (Zanier et al., 2005). HPV E6 also

has the ability to downregulate p53 activity through CREB-binding protein (CBP) and p300. The role of the E6AP in the degradation of p53 is essential; however, it has been reported that degradation of p53 could be achieved without the presence of E6AP (Massimi et al., 2008).

High-risk HPV E6 oncoprotein also plays a vital role in preventing apoptosis via a p53-independent mechanism that entails the suppression of the *Bax* gene and the inhibition of Bax protein, a pro-apoptotic protein required for apoptosis, in human keratinocytes (Liu et al., 2008). The high-risk HPV E6 oncoprotein can also hinder apoptosis by binding to the tumour necrosis factor receptor 1 (TNFR1) and prevent its apoptotic signaling (Filippova et al., 2002).

Unlike the high-risk HPV E6 oncoprotein, the low-risk HPV E6 oncoprotein does not bind E6AP to form a trimeric complex (E6/E6AP/p53). It has the ability to bind to the p53 but with a minimal effect (Massimi et al., 2008, Zanier et al., 2005). The binding of the low-risk HPV E6 oncoprotein to the p53 does not degrade p53 due to the very low affinity of the binding process. However, the accumulation of p53 after the DNA damage in cells expressing low-risk HPV E6 oncoprotein causes the cells to be arrested in the G₁ phase of the cell cycle (Pietsch and Murphy, 2008).

While high-risk HPV E6 targets p53 and inhibit its normal function, HPV E6 has also been found to bind to other cellular target proteins. It has been reported that high-risk HPV E6 targets and degrades E6 targeted protein 1. This protein has homology with GTPase-activating proteins, and this suggests that HPV E6 might modulate G protein signalling (Gao et al., 1999). In addition, in 2007, Jeong and colleagues reported that HPV E6 binds to the cystic fibrosis transmembrane receptor-associated ligand and hinders its normal function in a PDZ domain-dependent manner (Jeong et al., 2007).

1.1.2.2 HPV E7 oncogene

The HPV E7 oncoprotein is approximately 100 amino acids in size. This oncoprotein is known to bind to the pRb and inhibit its binding to the E2F transcription factor (Barrow-Laing et al., 2010, Zhang et al., 2006). (Barrow-Laing et al., Zhang et al., 2006). Normally, pRb protein is phosphorylated by two major complexes, namely cyclin D1/cyclin-dependent kinase 4 (CDK4) and cyclin E/CDK2; this process causes pRb to dissociate from E2F, allowing E2F-dependent

transcription and normal S-phase progression. HPV E7 binds to the hypophosphorylated pRb and hinders its interaction with the E2F. As a result, cells overexpressing the HPV E7 oncogene will lose checkpoint control at the G₁/S transition, and subsequently undergo uncontrolled cellular proliferation (Dyson, 1998, Zhang et al., 2010). It has been also reported that E7 causes degradation of pRb through the ubiquitin-proteasome-mediated pathway (Liu et al., 2006). The binding of E7 to pRb occurs via the LXCXE motif present in the E7 protein (Bischof et al., 2005).

Although pRb is the preferred target of HPV E7, studies have shown that other cellular target proteins may interact with HPV E7. HPV E7 binds to the histone deacetylase through Mi2, which results in E2F-dependent transcription and subsequent cell proliferation (Longworth and Laimins, 2004). In addition, HPV E7 has shown to bind to CDK2/cyclin A and cyclin E and stimulates these kinases to phosphorylate pRb and promote transcription of S-phase genes. Reports have revealed the binding of HPV E7 to CDK inhibitors p27 and p21 (Shin et al., 2009, Zehbe et al., 1999). This binding removes the checkpoint control at G₁/S in the cell cycle promoting unregulated cell cycle progression.

1.1.3 HPV life cycle

Dissimilar types of life cycle organization are evident in different HPV groups. Moreover, most of the work on HPV has focused on high-risk HPVs. Still, based on these many different studies and analyses, a general lifecycle pattern has been worked out: the characterised lifecycles forms can be modified and then applied to other HPV groups.

1.1.3.1 *Infection and uncoating*

HPV infections act in a similar way to many other microorganism infections where infectious particles require access to the human cells. In HPV, access to the basal layer is required and in some HPV types break in the stratified epithelium may be essential (Burd, 2003, Flores et al., 1999). Different reports have demonstrated that viral DNA from beta-HPV can be amplified by polymerase chain reaction (PCR) from plucked hair follicles (Boxman et al., 2001, Wolf et al., 2004, Pfister, 2003).

Because of the high association between high-risk HPV and cervical cancer, the growth of cervical lesion can be expedited via infection of columnar cells (Burd, 2003). The nature of the cell surface receptor which is initially required to facilitate viral infection is not clear, although several studies have suggested the involvement of heparin sulphate (Giroglou et al., 2001, Richards et al., 2013). Upon viral entry, the uncoating occurs via the interruption of the intracapsomeric disulphide bond; subsequently, the virions migrate to the nucleus where they inaugurate their genomes as multi-copy extrachromosomal plasmids sustained at about 20-100 viral copies per infected basal cells (Doorbar et al., 2012, Stubenrauch and Laimins, 1999).

1.1.3.2 *Genome maintenance and proliferative phase*

Once virions migrate to the nucleus, E1 and E2 proteins are expressed to maintain the HPV DNA as an episome and to enable precise genomic segregation throughout the cell division process (Wilson et al., 2002, You et al., 2004). E2 has been found to regulate transcription and to be able to recruit viral E1 helicase to the viral origin of replication (Kim and Lambert, 2002, Blakaj et al., 2009). Viral helicase is different from cellular helicase, and, therefore, they are disconnected during genome maintenance and amplification. Additionally, E2 plays a role in genome partitioning through basal cell division (McPhillips et al., 2006, Jang et al., 2009). However, during cell division, other E-binding-proteins are thought to be essential in the joining of viral episomes to the cellular chromatin (McPhillips et al., 2006, McBride et al., 2006, Dao et al., 2006).

The role of E6 and E7 is still unclear in the infected basal cells, particularly when it comes to infections associated with the low-risk HPVs, which do not result in neoplasia (Doorbar et al., 2012). The E6 and E7 viral protein roles have been intensively investigated intensively due to their involvement in driving cell proliferation in the basal and parabasal cell layers. E7 is known to be associated with pRb, a negative regulator of the cell cycle (Bischof et al., 2005, Huh et al., 2005, Shaikh et al., 2012). In normal cells, pRb associates with E2F and prevents S-phase entry. The association of E7 with pRb supersedes E2F and results in the expression of proteins required for DNA replication. During natural infection, the ability of E7 to initiate S-phase progression is limited to cells with low levels of p21/p27, or to those expressing a high level of E7 protein (Noya et al., 2001). In addition, viral E6 protein mediates p53 degradation, which consequently prevents

apoptosis in response to unscheduled S-phase entry initiated by E7 (Yugawa and Kiyono, 2009, Delury et al., 2013). It also has been reported that E6 is able to associate with other pro-apoptotic proteins such as Bax and Bak (Thomas and Banks, 1999, Saha et al., 2012). Targeting different therefore, E6 is considered a predisposing factor in initiating HPV-related cancers though an accumulating likelihood that errors in host DNA to go unchecked.

It has been also reported that E6 viral protein is capable of stimulating cell proliferation independently of E7 through its C-terminal PDZ-ligand domain (Pim et al., 2012). In addition to the roles of E6 and E7, other viral proteins, namely E1, E2, E4 and E5 are expressed before the genome amplification to confirming maintenance of the viral episome at a low copy number (Middleton et al., 2003).

1.1.3.3 *Genome amplification*

Where the viral genome is replicated and basal cells are divided, one of the daughter cells migrates from the basal layer to enter the differentiation programme and further proceeds further towards maturation of the epithelium. The expression of viral proteins E6 and E7 in the upper epithelial layers facilitates the re-entry into S-phase, and hence, the copy number of the viral genome increases. The amplification of the viral genome is thought to occur at a transcriptional level, where the late promoter located within the E7 ORF is upregulated (Bodily and Laimins, 2011, Bedell et al., 1991). This upregulation is believed to occur due to the increase levels of E1 and E2. In addition, E4 and E5 contribute to the viral genome amplification. E5 stabilises epidermal growth factor receptor (EGFR) and enhances EGF signalling and mitogen-activated protein kinase (MAPK) activity (Genther et al., 2003, Pim et al., 1992). Moreover, independently of EGFR, it modulates extracellular signal-regulated protein kinase (ERK) 1 and 2 in addition to p38 (Crusius et al., 2000).

The MAPKs ERK 1 and 2 are essential modulators of nuclear E1 (Yu et al., 2007). This indirect correlation between E5 and E1 increases the accumulation of E1 in the nucleus and consequently, enhances viral DNA replication through the induction of DNA damage response (Moody et al., 2007). E4 is a viral protein that accumulates in cells which support virus synthesis; as a result, it is believed that E4 is primarily involved in virus release or transmission (McIntosh et al., 2008, Wang

et al., 2004a). However, it is also thought that E4 may contribute indirectly to viral genome amplification (Wilson et al., 2005, Wang et al., 2009a).

1.1.3.4 Packaging of viral genome and virus release

The final stage of the HPV life cycle involves the expression of L1 and L2, which will facilitate genome packaging. The expression of these two viral proteins switches the message production from E1^{E4}, E5 to E1^{E4}, L1 to allow genome packaging (Johansson et al., 2012, Milligan et al., 2007). It has also been also thought that E4 contributes to the release of the virions and viral infectivity in the upper epithelial layers (Wang et al., 2004a, McIntosh et al., 2008). The contribution of E4 is thought to occur via the disruption of keratin structure, thereby compromising the common association of the cornified envelope.

1.2 Cell Cycle

The cell cycle usually refers to the growth and division of cells, which consists of two essential phases. The first is the interphase, which is also subdivided into the G₁ phase (growth phase), S phase (DNA replication), and G₂ phase (preparation of the cell to enter mitosis and divide) (Ford and Pardee, 1999, Williams and Stoeber, 2012) (Figure 1.3). The second phase is mitosis (M phase), where cell divides; this may also be subdivided into the prophase, prometaphase, metaphase, anaphase, telophase, and cytokinesis. In the cell cycle, G₀ forms the resting state, where the cell is reversibly withdrawn from the cell cycle as a result of high cell density or mitogen deprivation (Williams and Stoeber, 2012).

Progression throughout the cell cycle is controlled by the CDK and cyclins (Malumbres and Barbacid, 2006). Cyclins D-CDK4, D-CDK6 and E-CDK2 control the advancement of the G₁ phase whereas cyclins A-CDK2 and B-CDK1 control the progression of the S and G₂ phases, respectively (Nigg, 2001, Planas-Silva and Weinberg, 1997, De Boer et al., 2008). Furthermore, cyclin B-CDK1 is responsible for the progression through the mitotic phase. As cells progress from one phase to another, they pass through cell-cycle checkpoints to ensure the correct order of events (Hartwell and Weinert, 1989). If aberrant or incomplete has been found, these checkpoints then transmit signs to

effectors, such as CDK inhibitors (CKIs), which are able to induce cell-cycle arrest until the problem is solved (Musacchio and Salmon, 2007). Disruption of these orchestrated cell-cycle events underlies the uncontrolled cell proliferation, which is a major hallmark of the malignant phenotype (Beamish et al., 2004, Gabrielli et al., 1999). Thus, it can be noted that tight regulation of the cell-cycle events is required to ensure the fidelity of cell division.

1.2.1 G₁

Upon the completion of cytokinesis the cell enters the first stage of the cell cycle, which is referred to as Gap 1 (G₁). At this stage the cell needs to accumulate the energy sources and materials required to move through various cell cycle stages. Most cells spend the majority of their time during the cell cycle at this stage with a few exceptions. As mentioned above, cell cycle events are orchestrated by numbers of CDKs. In G₁, the most important target of the CDKs is the pRb (Kato et al., 1993). The cyclin-CDK-complex, most notably cyclin D-CDK, phosphorylates pRb on different residues. For instance, the cyclin E-CDK2 complex, for example, phosphorylates E2F-5 (Arroyo and Raychaudhuri, 1992). This notably occurs only in the late G₁ phase. Phosphorylation of pRb allows the release of pRb from the E2F transcription factor and consequently, allows cells to move through the next stage of cell cycle, namely S-phase, by recruiting p300/CBP co-activators. Other important agents in the G₁ phase are the CDK inhibitors (CKIs). The CKI family negative regulators in G₁ include at least three proteins, specifically p21^{Cip1}, p27^{Kip1}, and p57^{Kip2} (Nakayama and Nakayama, 1998, Sherr and Roberts, 1999). It has been reported that p27^{Kip1} is degraded in the late G₁ and plays a crucial role in controlling cell growth at the transition from G₁ to S-phase (Nakayama et al., 2001).

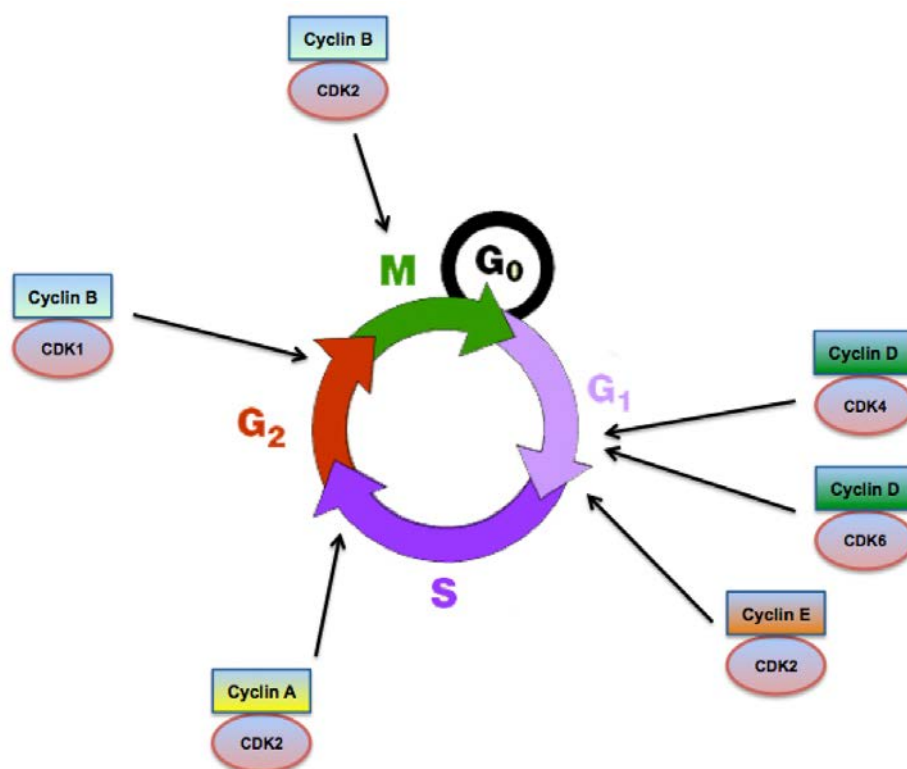


Figure 1.3. Cell cycle phases. Illustration of the cyclins and CDKs associated with the cell cycle phases. Modified from (Niehrs and Acebron, 2012).

1.2.2 DNA synthesis (S-phase)

DNA replication is performed and arranged by group of enzymes and proteins which associate with each other to perfectly duplicate the genetic information of the cell. Decades ago, fluorescence microscopy with bromodeoxyuridine (BrdU) was used to determine how the DNA synthesis commences. It was found that newly synthesised DNA is confined to what are known as ‘replication foci’ or ‘replication site’ (O’Keefe et al., 1992). Co-localizations of several replication factors at these sites show that they assemble at these locations (Hozak et al., 1993). Given the length of the genome and the bidirectional replication fork, it was noted that early S-phase requires about 5 to 6 replicons (Jackson and Pombo, 1998, Ma et al., 1998). In addition, active replication forks for each factory should range from approximately few units in early S-phase to thousands in late S-phase. Early in the 21st century, it was found that the large replication factors that had been identified at late S-phase do not originate from small factors; instead, they are assembled *de novo*

during S-phase (Leonhardt et al., 2000). When chromatin becomes ready for replication (also known as the licensed state), initiator proteins prepare for the formation of the pre-replicative complexes (pre-RCs) on the replication origins (Prasanth et al., 2004). These initiators include the origin recognition complex (ORC), Cdc6/18, Cdt1, and the mini-chromosome maintenance (MCM) proteins (Nishitani and Lygerou, 2004, Nishitani et al., 2001). Activation of licensed origins basically depends on CDK and Dbf4-dependent kinase (DDK) (Shimada and Komatsu, 2009, Devault et al., 2008). Cdk2-cyclin E has been found to play an essential role in initiating DNA replication. Activation by protein kinases is thought to result in modifications to the pre-RCs, which subsequently results in the association of Cdc45 to the MCM complex (Walter and Newport, 2000, Zou and Stillman, 2000). As a result, the replication origins become unwind, and replicating proteins such as RPA, polymerase α and polymerase ϵ are assembled at the initiation site. Once the replication of origins is activated, the MCM and Cdc45 move along with the other replication enzymes enlisted at the replication forks to successfully complete DNA replication (Pacek and Walter, 2004, Wong et al., 2011).

1.2.3 G₂

This stage of the cell cycle commences upon the completion of the DNA synthesis phase. It is relatively a short cell cycle phase compared to G₁ in most cell types, where cells undergo a DNA fidelity check for major errors and accumulate energy and materials required for cell division in mitosis. The progression from G₂ to M is Cdk1 in the complex, and dependent on Cyclin B1 dependent (Gavet and Pines, 2010, Porter and Donoghue, 2003), but the time timing of this complex activation depends on Cyclin A/Cdk2 (De Boer et al., 2008). The Cyclin B1 level increases during G₂, which subsequently gives the chance for Cdk1-Cyclin B1 complex the chance to accumulate. The formed complex is kept inactive by the phosphorylation of Cdk1 T14 and Y15 by Wee and Myt kinases (Mueller et al., 1995, Parker and Piwnica-Worms, 1992, Borgne and Meijer, 1996). The Cyclin B1-Cdk1 complex is then activated by Cdc25 phosphatases, which dephosphorylate Cdk1 sequentially at T14 and then Y15. Active Cyclin B1-Cdk1 has been identified in centrosomes shortly before they travel away from one another towards the end of G₂ (Jackman et al., 2003). Phosphorylation of the Cyclin B1-Cdk1 complex occurs at the cytoplasmic retention sequence on Cyclin B1, which results in nuclear translocation of the complex (Hagting et

al., 1999, Li et al., 1997a). Indeed, this relocalisation of the Cyclin B1-Cdk1 complex improves chromosome condensation and nuclear envelope breakdown.

1.2.4 Mitosis (M)

In this phase of the cell cycle, sister chromatids are segregated and the cell is divided to produce new daughter cells, each of which inherits a complete copy of the genome of its mother (Figure 1.4). Establishment of the mitotic phase is dependent on Cyclin B/Cdk, which is also known as M-phase promoting factor (MPF) (Nigg, 2001). Several mitotic events are orchestrated by extensive phosphorylation operated by CycB-Cdk1 or some other kinases (Dephoure et al., 2008, Hegemann et al., 2011). In mitosis, Cyclin B/Cdk1 maintains itself by a phosphorylation feedback loop where CycB-Cdk1 phosphorylates and activates Cdc25c (CycB-Cdk1 activator), while it phosphorylates and inactivates Wee1 (CycB-Cdk1 inactivator) (Novak and Tyson, 1993). Indeed, the activity of CycB-Cdk1 and other mitotic kinases is essential for a functional spindle assembly checkpoint (SAC). A SAC acts as a safeguard mechanism which delays cyclin degradation and transition to anaphase until spindle assembly is achieved. This is primarily accomplished by limiting the ubiquitin ligase anaphase promoting complex/cyclosome (APC/C) along with APC/C^{Cdc20} (Chen et al., 2008, Musacchio and Salmon, 2007). Unattached kinetochore triggers SAC effector proteins such as Mad2 and BubR1, which bind Cdc20 in a mitotic checkpoint complex (MCC), and subsequently, restrict APC/C activity (Musacchio and Salmon, 2007, Tipton et al., 2011).

The idea that Mad2 is an APC/C inhibitor has been confirmed by the ability of Mad2 to inhibit APC/C^{Cdc20} (Li et al., 1997b, Fang et al., 1998). In addition, it has been demonstrated that MCC encompasses Mad2, BubR1, Bub3, and Cdc20 (Sudakin et al., 2001). Although the C-Mad2-Cdc20 complex may be enough to warn the cell of unattached kinetochores, it has been demonstrated that this alone may not be sufficient to block the anaphase transition. This observation was confirmed, as BubR1/Mad3 is depleted with unattached kinetochore and formation of C-Mad2-Cdc20; yet SAC function is abolished (Hardwick et al., 2000, Nilsson et al., 2008).

Hence, BubR1/Mad3 functions downstream of C-Mad2-Cdc20 to block the anaphase onset of anaphase. Although SAC activation and delayed transition to anaphase have been thought to be a

consequence of unattached kinetochore, some findings suggest that SAC signalling networks can function independently of the kinetochore (Meraldi et al., 2004, Malureanu et al., 2009). For example, BubR1 was observed to bind to Bub3 throughout the cell cycle. Nevertheless, it was found that Bub3 is not essential for BubR1 to bind to the C-Mad2-Cdc20 complex. In fact, it is not required, nor does it enhance the capability of BubR1 and Mad2 to restrain APC/C^{Cdc20} *in vitro* (Tang et al., 2001, Fang, 2002, Lara-Gonzalez et al., 2011).

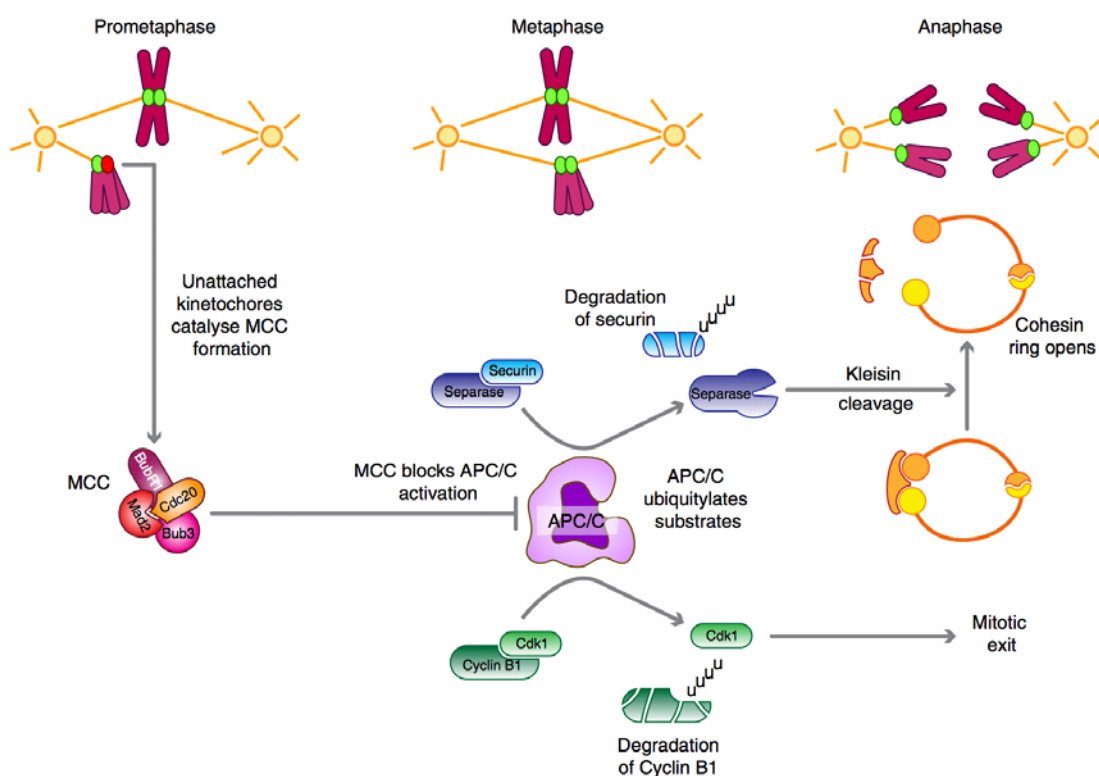


Figure 1.4. Mitotic stages and principles of SAC. During prometaphase, the mitotic checkpoint complex (MCC) is formed as a result of unattached kinetochore. The MCC consists of BubR1, Bub3, Mad2, and Cdc20; consequently, it inhibits APC/C activity. After the correction of all kinetochores attachment and chromosome alignment in metaphase, the MCC formation terminates, which gives the authority to Cdc20 to activate APC/C. This leads to the ubiquitylation and degradation of securin and Cyclin B1. Degradation of the securin releases separase, which allows the cleavage of the Scc1 kleisin subunit of the cohesion ring structure. This cleavage opens the ring, which in turn allows the sister chromatids to move apart during anaphase. Meanwhile, Cyclin B1 is degraded and, subsequently, Cdk1 is inactivated, allowing mitotic exit. From Lara-Gonzalez (Lara-Gonzalez et al., 2012).

1.2.5 SAC/p53 cross-talking

Treating normal cells with spindle-damaging agents such as nocodazole or taxol results in transient pre-anaphase arrest as a result of SAC activation. This arrest is then followed by aberrant mitotic exit without sister chromatid segregation and unsuccessful cytokinesis, a process known as mitotic slippage (Elhajouji et al., 1998). However, due to the post-mitotic G₁ checkpoint, the resulting tetraploid cells will be arrested in G₁; they will not further proceed to S phase, and as a result, polyploidisation will be prevented (Meek, 2000, Margolis et al., 2003). Like other cells, cells lacking p53, p21, or pRb arrest in mitosis as other cells but they do not arrest in G₁. Instead, they proceed to S phase, which results in endoreduplicated DNA despite the intact SAC (Marxer et al., 2013, Di Leonardo et al., 1997, Khan and Wahl, 1998). These observations confirmed that p53/pRb is required for G₁ postmitotic arrest. Hence, activation of p53 prevents cells from involvement in polyploidisation. It has been demonstrated that HeLa cells overexpressing dominant negative mutant Bub1 or HCT116 cells with a reduced level of Mad2 exit mitosis and endoreduplicate even though HCT116 cells have intact p53 (Michel et al., 2001, Taylor and McKeon, 1997).

1.3 The molecular basis of cancer

As described in many studies over the past decades, cancer disturbs the normal biological cellular activities, such as differentiation, growth, apoptosis and tissue integrity. Several genomic alterations of the genome underlie the development and formation of cancer. Hanahan and Weinberg (2011) described six biological capabilities which are acquired in the course of tumourigenesis and associated differentiation of a normal cell to a cancerous cell (Figure 1.5) (Hanahan and Weinberg, 2011).

1.3.1 Sustaining proliferative signalling

It is obvious that cancerous cells need to maintain chronic proliferative characteristics. In normal cellular activity, balanced growth-promoting signals are maintain throughout cell division to ensure cell homeostasis. As cancer cells become more independent, this phenomenon is totally disrupted by enabling signal cascades typically with the involvement of receptor tyrosine kinases (RTKs).

RTKs initiate signals from intracellular and extracellular as transmit points for signalling pathways within the cell. Many tyrosine kinases are found mutated or overexpressed at elevated levels in human cancers (Blume-Jensen and Hunter, 2001, Levitzki and Gazit, 1995). For example, epidermal growth factor receptor 3 (EGFR3) lacks amino acid 6-273 and increases RTK basal activity, which results in cell proliferation in glioblastoma, ovarian cancer, and non-small cell lung carcinoma (Nishikawa et al., 1994). In addition, somatic mutations in the EGFR 2 and 3 have been linked with bladder neoplastic disorder and cervical cancer. That is, somatic mutations may activate downstream pathways. In melanoma, it is becoming clear that reactivation of signalling downstream to RAF in the MAPK pathway is a pivotal mechanism of resistance to BRAF inhibition of melanoma therapeutics (Flaherty, 2010, Flaherty et al., 2010).

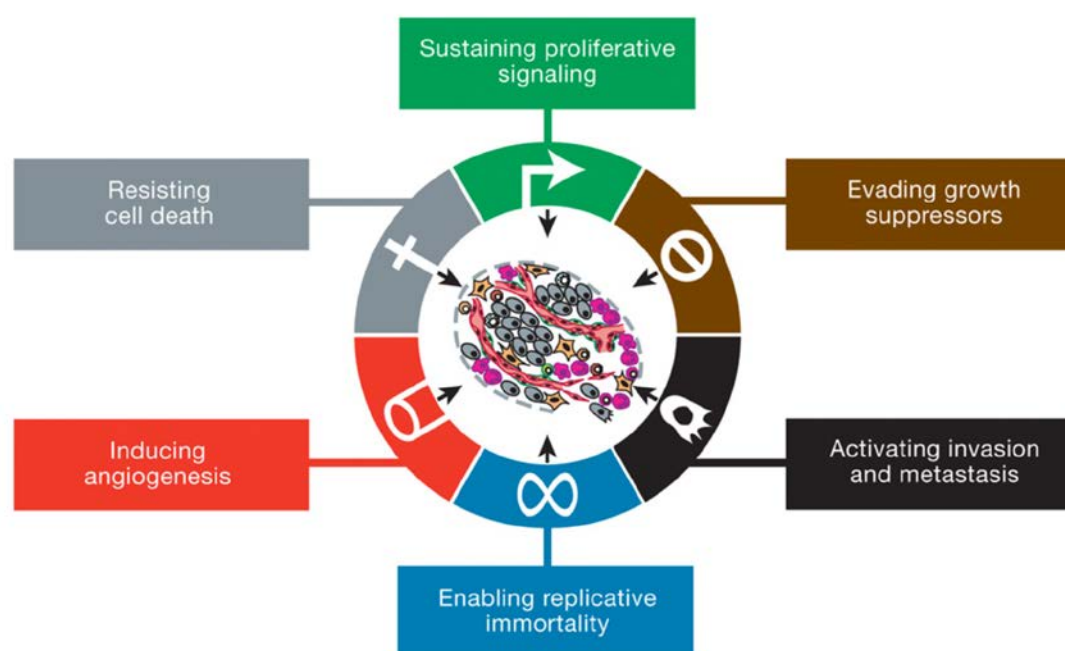


Figure 1.5. Biological hallmarks of cancer. Illustration of the six biological hallmarks acquired during cancer development. From Hanahan and Weinberg (Hanahan and Weinberg, 2011).

Another method of sustaining proliferative signalling of the cancerous cells is through the disruption of negative feedback loop, which enhances the proliferative signalling. For example, activation of PI3K/Akt/mTOR signalling by mutation or activation of the upstream signalling

pathway has been observed in many cancer types (Vivanco and Sawyers, 2002, Bjornsti and Houghton, 2004). This cascade is normally orchestrated by upstream RTKs, particularly insulin and insulin-like growth factor I (IGF-I) receptors (IGF-IRs) (Oldham and Hafen, 2003). In cancer cells, constitutive activation of the mTOR/Akt pathway will result in the induction of upstream feedback inhibition through IGF-I/insulin receptors. This feedback inhibition may have biological implications (Weinstein, 2002, Mills et al., 2001). First, it may cause hypersensitivity to mTOR inhibitors and inhibition of other elements of the activated pathway. Second, mTOR inhibition may result in feedback inhibition release, which perhaps activates IGF-I signalling and, as a result, decreases the anti-tumour effect of mTOR inhibitors. The interruption of these negative feedback loops has been noticed in many cancer types.

Another feature of some cancerous cells is the ability to bypass the senescence state. Some cells, such as human diploid fibroblasts, can undergo 60-80 doubling populations before they produce a senescence phenotype; at this point, they stop dividing but remain metabolically active and are able to survive for years (Dimri et al., 1995). This cell cycle arrest state occurs due to the activation of p53 and pRb (Artandi and DePinho, 2000, Hara et al., 1991). Therefore, alterations to these pathways by, for example, the expression of tumour viruses, for example, will result in bypassing the senescence state, giving the cells mastery over their own proliferative state.

1.3.2 Evasion growth suppressors

Loss or inactivation of tumour suppressor genes is a major advantage which cancerous cells use to over control the cellular proliferation machinery. Of these suppressor genes, pRb has been identified to be lost or inactivated in >70% of cancer types (Sherr, 2000, Nevins, 2001, Bartek et al., 1997). In the past few decades, efforts have been made throughout the last decades to understand how pRb can actually suppress tumour activity. In late 1980s, it was found that pRb activity is sequestered by viral oncoproteins such as SV40 large T antigen, adenovirus E1A, and HPV-E7 (Whyte et al., 1988, Munger et al., 1989, Dyson et al., 1990). Indeed, this observation revealed how viral oncoproteins initiate tumour formation. As a consequence of these findings, more efforts have been made to understand what other implications and involvements result from abrogating the pRb function. It is now obvious that many critical partners of the pRb are engaged in transcriptional

control (Cobrinik, 2005, Morris and Dyson, 2001). Abrogation of pRb suggests several mechanistic issues in human cancers. Firstly, high expression of CDK4 or Cyclin D by amplification or mutation has been observed to occur in several cancer types and; as a result, augments pRb phosphorylation. In addition, p16^{ink4a} as a CKI can be lost/mutated (Sherr, 2000, Morris and Dyson, 2001, Heilmann and Dyson, 2012). This increases the activity of CDK4 and Cyclin D, which results in pRb phosphorylation. Furthermore, the association of pRb with E2F abolishes its ability to modulate gene transcription (e.g. cervical carcinoma) (Salcedo et al., 2002, Guo et al., 2011). An additional facet is the mutation of the Rb locus itself, which causes unchecked E2F activity (Cobrinik, 2005, Wang et al., 1994). Taken together, these findings represent a model for explaining pRb actions in the cell cycle and defining the effect of pRb loss in cancers.

The transforming growth factor- β (TGF- β) signalling pathway is another instrumental tumour suppressor cascade which inhibits proliferation and induces apoptosis in different cell types (Mishra et al., 2005). The TGF- β achieves tumour suppression in several ways. For example, it inhibits cell proliferation by the induction of CKI p21^{Cip1} and p15^{Ink4b}, and thus halts cell proliferation (Gomis et al., 2006, Pardali et al., 2000, Seoane et al., 2004). In addition, *in vitro* investigation has shown that TGF- β increases the expression of death-associated protein kinase (DAPK) in hepatoma cell lines (Jang et al., 2002). This increasing level of expression triggers apoptosis.

Tumours are able to escape the TGF- β tumour suppressive mechanism in different ways. For example, in gliomas, p15^{Ink4b} is deleted and, as a result, prevent TGF- β -mediated induction of this gene in those neoplastic diseases is prevented (Jen et al., 1994). Moreover, overexpression of a proliferative driver like c-Myc or an oncogene like Cyclin D1 diminishes the effect of TGF- β on CKI or the expression of Ras signalling which inhibits Samds (Massague, 2008). As illustrated above, it is obvious that the evasion of tumour suppressor genes/pathways is a main criterion for a cancer cell to proliferate beyond the expected cellular lifespan.

1.3.3 Resisting cell death

Cells have a programmed cell death called apoptosis (see section 1.5). Briefly, the apoptotic mechanism is facilitated by upstream regulators and downstream effectors. These respond to stimuli, causing cells to undergo apoptosis as a result of cellular problems (e.g. DNA damage). Cancer cells, in contrast, have different characteristics where they resist or escape apoptosis to survive for a longer time. One of their resistance strategies involves the loss of a common tumour suppressor gene called TP53 (Muller and Vousden, 2014). TP53 is considered the most commonly mutated gene in neoplasia. Another approach that can be taken by tumour cells is by increasing the expression of anti-apoptotic proteins such as Bcl-2 or Bcl-x_l or decreasing the expression of the pro-apoptotic proteins like Bax, Bim or Puma (Lomonosova and Chinnadurai, 2008).

Tumour cells try to use different approaches to sustain their proliferative state. For example, they use an autophagic programme to resist cell death (Mathew and White, 2011). In autophagy, cells breakdown cellular organelles like ribosomes and mitochondria (Levine and Kroemer, 2008, Mizushima, 2007). As a result of this mechanism, catabolites will be recycled and used as a source of energy metabolism. The autophagic programme involves a key step where intracellular vesicles called autophagosomes envelop the intracellular organelles. This biological cascade helps the cell to generate low-molecular-weight metabolites which in turn provide the cell with sufficient nutrition in stressful conditions like cancer. Upon treating cancer patients with radiation or chemotherapy, it was observed that four forms of autophagy were demonstrated, namely cytoprotective, cytostatic, cytotoxic, and nonprotective autophagy (Gewirtz, 2014). It is difficult to predict which type will be induced by a particular therapy. Nevertheless, the way in which autophagic programme maintains the survival of the cell has been demonstrated in many human cancer cells, confirming that autophagy mediates tumour cell survival.

Forms of cellular death vary based on what signals cells may receive. Necrosis is another form of cellular death which has different properties from those of apoptosis (Proskuryakov and Gabai, 2010). Necrotic cells become enlarged and bloated, and then explode, releasing all of the intracellular contents to the surrounding environments (Galluzzi and Kroemer, 2008, Grivennikov et al., 2010). Because of this, necrotic cells are capable of recruiting inflammatory cells from the immune system to clean up the necrotic debris via their housekeeping function. However, calling

immune-inflammatory cells may not always be beneficial, such as in the case human cancers. These cells are can increase cancer cell proliferation and invasiveness under neoplastic conditions (Waters et al., 2013). Furthermore, because necrotic cells release their contents to the surrounding environment, some of the contents (e.g. interleukin [IL1]-1-alpha) can in fact cause neighbouring cells to proliferate, thereby sustaining cancer cell division.

1.3.4 Enabling replicative immortality

A remarkable feature which most cancer cells exhibit as opposed to normal cells is their ability to divide indefinitely, a feature that is called immortalisation (Hayflick, 2000). The expected lifespan and cell cycle rates limit cell division in normal cells. This trait is primarily controlled by two main mechanisms which cease proliferation, namely senescence and cell crisis (Campisi and d'Adda di Fagagna, 2007, Greenberg, 2005). In cell culture, when cells divide, they reach a point where they die or senesce. If these cells escape this process and continue dividing, they will reach a crisis state, where most of the population dies. However, some cells emerge again in the proliferation state and start dividing for a longer time, exhibiting the feature of immortalisation, which is basically a characteristic that most cell lines possess in virtue.

It is widely considered that telomere maintenance by telomerase contributes to the development of the immortalisation (Yang et al., 1999, Bodnar et al., 1998, Morales et al., 1999). Telomeres are repetitive DNA sequences at the end of the chromosome protected by a protein called shelterin, which prevents a DNA damage response (DDR) from arising (Martinez and Blasco, 2010). The enzyme telomerase has been shown to collaborate with oncogenes to help transforming primary human cells into cancerous cells (Hahn et al., 1999a). Accordingly, telomerase activation is in fact contributes to the transformation to malignancy. This finding has been further confirmed in that telomerase is inhibited via telomere shortening where cell death is observed (Hahn et al., 1999b, Zhang et al., 1999). Short telomeres and activation of DDR may be evident in cancer. Indeed, increased numbers of short telomeres correlate stringly with higher genomic instability (Blasco et al., 1997, Hemann et al., 2001).

Although telomerase activation is widely accepted to be a hallmark of cancer, however, it may not contribute to the initiation of cancer (Hackett and Greider, 2002). There are several mechanisms through which telomerase can be activated. Of these, Myc and Wnt as they act as transcriptional regulators of telomerase (Wu et al., 1999, Greider, 2012). Additional mechanisms may involve alternative splicing or epigenetic modifications (Kyo and Inoue, 2002). Furthermore, it has been reported that mutations which increase the transcriptional activity of the telomerase reverse transcriptase (TERT) promoter form binding motifs for E-twenty-six (ETS) transcription factors was described in melanoma (Huang et al., 2013). These observations suggest an abandonment of the role of telomerase. On the other hand, this could also be problematic, because lack of telomerase may result in higher chromosomal instability, which in fact make a solid base for cancer initiation (Feldser and Greider, 2007). Clearly, overviewing these findings demonstrate how telomerase deficiency may contribute to cancer development through chromosomal instability whilst telomerase activation may be needed for maintain tumour growth and further tumour progression (Ding et al., 2012).

1.3.5 Inducing angiogenesis

Angiogenesis is a normal mechanism in adult tissue which is transiently switched on. In contrast, tumour angiogenesis is different, as the cancer establishes neovascularisation to respond to nutrient and oxygen demands and to remove metabolic waste and carbon dioxide (Brown et al., 1999, Bergers and Benjamin, 2003). Without these pivotal energy resources, tumour vascularisation increases by up to 1-2mm.

Angiogenesis is affected by different factors which induce or restrict it. Of these, vascular endothelial growth factor (VEGF) is a key player in inducing angiogenesis via its direct effect on endothelial cells (Pepper et al., 1992). This observation has been confirmed through *in vitro* experiments, where VEGF was found to induce a capillary-like tubule structure via microvascular endothelial cells grown on collagen gel. Using murine embryos, it was demonstrated that the deletion of a single VEGF allele during embryonic vasculogenesis resulted in abnormal blood vessels growth and was ultimately fatal (Carmeliet et al., 1996). Tumours were quiescent between proliferation and apoptosis, and were then converted to the angiogenic phenotype, a conversion

process known as the ‘angiogenic switch’ (Bergers and Benjamin, 2003). VEGF acts as a mediator for tumour growth to establish new blood vessels from neighbouring capillaries to fuel-up energy resources. As the tumour growth progresses, the mass becomes hypoxic as a result of the distance from the supporting capillaries. Indeed, this observation has been confirmed in glioblastoma, as VEGF messenger RNA (mRNA) was expressed at higher levels in the hypoxic area of the tumour (Shweiki et al., 1992).

Activation of oncogenes such HER2, Kras, Hras, and Bcl-2 has been linked to increasing VEGF expression (Rak et al., 2000). In head and neck cancer, a high expression of VEGF was correlated with the expression of HER2 and EGFR (P et al., 2002). In addition to the aforementioned functions of VEGF, it has central role in protecting the neovasculature of the tumour by inducing the antiapoptotic Bcl-2 and survivin (Harmey and Bouchier-Hayes, 2002, Tran et al., 1999). Moreover, due to its effect on the secretion and activation of enzymes engaged in the degradation of the extracellular matrix, VEGF has the ability to establish further blood vessels (Unemori et al., 1992). All these findings illustrate the importance of VEGF in angiogenesis and its role VEGF in supporting cancer further cancer growth.

There is accumulating evidence that bone marrow-derived cells (BMDCs) contribute to tumour angiogenesis and growth (Jain and Duda, 2003, Wu et al., 2007). Neutrophils (Nozawa et al., 2006), macrophages (Ribatti et al., 2007) and monocytes (Conejo-Garcia et al., 2005), have been found to contribute to the growth of new blood vessels, and as a result, facilitate tumour growth and expansion (Bertolini et al., 2006, Kerbel, 2008). Kaplan and colleagues reported that the hemopoietic progenitor cells, VEGF receptor (VEGFR) 1+ cells, which are haematopoietic progenitor cells, could actually contribute to the spread of metastases (Kaplan et al., 2005). In fact, these cells reach the metastatic site before cancerous cells, where they form a pre-metastatic gathering spot for BMDCs.

VEGFR1+ has been found to modify the microenvironment at the metastatic site, preparing it for the tumour cells by upregulating several cytokines and integrins. Moreover, Gao *et al.* (2008) demonstrated that endothelial progenitor cells (EPCs) actually contribute to the angiogenesis in the

micro-metastatic phase and angiogenesis may then accelerate and move towards the possibly lethal macro-static stage (Gao et al., 2008). This observation was further confirmed when short-hairpin RNA (shRNA) against *Id1* blocked the EPCs' function, and subsequently, inhibited angiogenesis in the micro-metastatic state. BMDCs represent a growing area of interest in cancer biology, and extensive efforts are being made to understand how they contribute to cancer growth.

1.3.6 Activating invasion and metastasis

Although tumour metastasis is primary the cause of cancer-related death in 90% of advanced (metastasized) cancer cases, the process through which invasion and metastasis occur is not totally understood (Mehlen and Puisieux, 2006). There are several types of cancer metastasis is common (e.g. melanoma) (Bhatia et al., 2009) whilst in others, it is very rare (e.g. basaloid squamous carcinoma) (Boyd et al., 2011). Moreover, how the size of the tumour may contributes to tumour invasion and metastasis is still unclear (Mehlen and Puisieux, 2006). Reports have indicated that small tumours form micro-metastases. Cells from micro-metastases can remain viable in the body for years where they can proliferate again after doses of chemotherapy and radiotherapy. In mouse models, it was observed that up to 1×10^6 cells leave the primary mouse tumour and engage in the metastatic cascade (Weinberg, 2006).

About 90% of all human cancers originate from epithelial tissues, and are therefore considered carcinomas. An epithelium is considered a line of defence against exogenous toxins and infectious agents. Epithelial cells are characterised by their close anchorage in the tissue, which prevent motility. Adhesion between cell to cell from a similar type of cells is controlled by calcium transmembrane protein such as cadherins (Christofori, 2003). Abrogation of normal cadherin functions, E-cadherin in particular, has been observed in invasive cancer cells (Herzig et al., 2007). E-cadherin has been linked to adopt mesenchymal phenotype in epithelia, a transition process known as epithelial mesenchymal transition (EMT) (Voulgari and Pintzas, 2009). In addition, B-catenin is another important player which supports the EMT (Gordon and Nusse, 2006). This occurs because a large amount of B-catenin is associated with E-cadherin and they become free once E-cadherin is down-regulated. Thus, they can be found free in the cytosol and might move to the nucleus. At the nuclear level, B-catenin binds to Tcf/LEF, where it promotes EMT.

As indicated above, EMT is crucial for the invasiveness of cancer. Twist an EMT transcription-inducing factor has known functions which are implicated in cell motility throughout early embryogenesis (Yang et al., 2004, Yang et al., 2006). In vertebrates, Twist is mainly expressed in the neural crest (Soo et al., 2002). The metastatic behaviour and invasiveness of 4T1 mammary carcinoma cells were observed to be decreased when Twist is suppressed (Yang et al., 2004). Furthermore, it was demonstrated that a major reason beyond this finding was Twist induced downregulation of E-cadherin. Another remarkable function of Twist is the ability to hinder Myc-induced apoptosis. In addition, high Twist expression has been found in melanoma and neuroblastoma (Yang et al., 2006). Unsurprisingly, both melanoma and neuroblastoma cells originate from the neural crest, where Twist is active.

Different transcription factors affect the EMT, including cytokines and stromal cells. Moreover, cells of the innate system are also pivotal in the context of metastasis (Qian and Pollard, 2010). Macrophages, for example, produce TNF-alpha in large amounts, and have been observed to generate EGF in case of breast cancer. Colony stimulating factor-1 (CSF-1) is able to enlist tumour-associated macrophages (TAMs) when expressed by cancer cells, which results in the production of EGF (Wyckoff et al., 2004). Therefore, these cells reciprocally activate one another. Activation of the EGF-signalling pathway results in the release of CSF-1, which stimulates motility and metastasis. Research on breast cancer models has indicated that the absence of CSF-1 and thus TAMs, does not actually halt the proliferation of primary tumours (Lin et al., 2001). Instead, lack of CSF-1 and TAMs prevent metastasis. Research efforts are still required to elucidate the molecular mechanism by which invasion and metastasis occur as well as what factors influence them, and how they could be suppressed. As indicated above, more cancer-related deaths occur due to metastasis than a result of the primary tumours.

1.4 Programmed cell death (apoptosis)

Apoptosis is a crucial process which can be triggered by different cellular autonomous and non-autonomous mechanisms, and its evasion may lead to carcinogenesis, tumour progression, or resistance to treatment (Fulda, 2010, Lowe et al., 2004). Apoptosis is characterised by classical

biological and morphological features such as cellular contraction, DNA fragmentation and membrane blebbing (Hengartner, 2000). The underlying mechanisms triggering apoptosis are not entirely understood. However, damage to the DNA or some other essential key regulators is usually considered a key initial event followed by different cell stress responses (Rich et al., 2000). Several stress-inducible players are engaged in transmitting apoptotic signals, including c-Jun N-terminal kinase (JNK), MAPK, ERK or nuclear factor kappa B (NF- κ B) (Davis, 2000, Karin et al., 2002). Furthermore, there are two types of signalling pathways which initiate apoptosis, namely intrinsic and extrinsic pathways (Ashkenazi, 2002, Green and Kroemer, 2004).

In the extrinsic pathway, the cellular death receptors are members of the TNFR gene superfamily, which encompasses more than 20 proteins with wide range of biological roles (Walczak and Krammer, 2000). Members of this family share a cysteine-rich extracellular domain of 80 amino acids called the ‘death domain’, which plays a pivotal role in transmitting death signals from the extracellular surface to the intracellular pathways (Elmore, 2007). On the other hand, the intrinsic pathway involves a mitochondrial pathway, primarily through activation of cysteine-aspartic proteases (caspases), which are key apoptotic proteins (Green and Kroemer, 2004). The regulatory mechanisms of these mitochondrial events arise through the Bcl-2 family of proteins (Elmore, 2007). Once the external mitochondrial membrane is disrupted, different proteins are commonly found within the inner and outer mitochondrial membranes, including cytochrome *c*, Smac/DIABLO, Omi/HtrA2, AIF and endonuclease G (Saelens et al., 2004). The Bcl-2 family functions to control mitochondrial permeability via pro-apoptotic or anti-apoptotic genes; members of this family have conserved regions termed Bcl-2 homology (BH) domains. The anti-apoptotic genes hold up to four similar regions of sequence homology (BH1 – BH4) including Bcl-2, Bcl-xl, Bcl-w, Mcl-1 and A1 (van Delft and Huang, 2006). In contrast, pro-apoptotic genes are divided into two groups based on their distinct functions and features. The BH3-only protein includes Bim, Puma, Bid, Bad, Bik, Noxa, Bmf, and Hrk whilst Bax and Bak contain different BH domains (BH1, 2, and 3) (Figure 1.6).

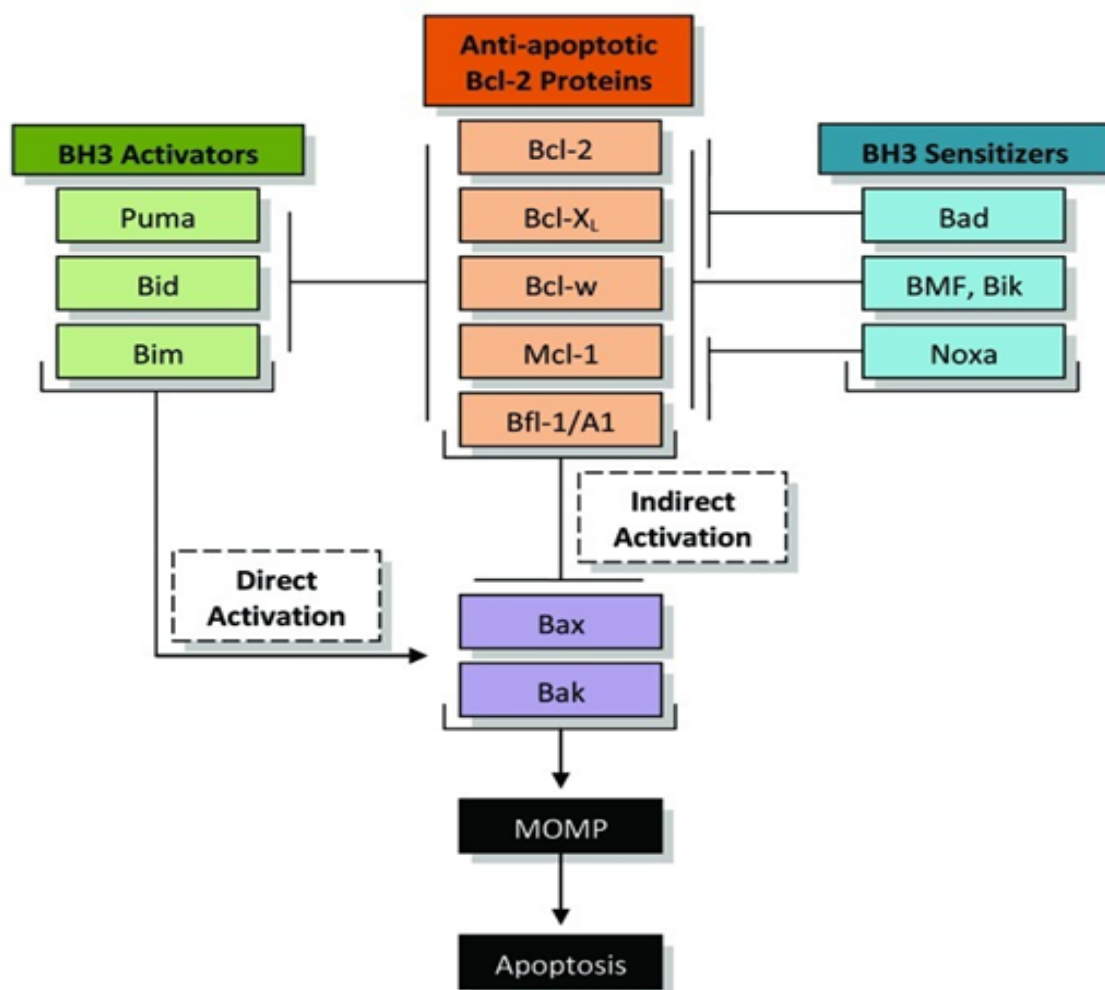


Figure 1.6. Apoptosis mechanism regulated by the Bcl-2 family. The anti-apoptotic proteins inhibit Bax and Bak activity. Upregulation of the BH3-only protein interrupts this association and results in the release of Bax and Bak. This causes the mitochondrial outer membrane permeabilisation (MOMP) to release cytochrome *c* and subsequent induction of apoptosis. The anti-apoptotic proteins also inhibit Puma, Bid, and Bim. The BH-3 sensitisers can interrupt this interaction, which allow the release of Bax and Bakt thereby inducing apoptosis. From Liu and Wang (Liu and Wang, 2012).

1.4.1 Anoikis signaling

Anoikis is a form of apoptosis which is activated when normal cells try to divide in the absence of a matrix and can be induced either by intrinsic or extrinsic pathways (Guadamillas et al., 2011). Failure to enter the anoikis pathway is a feature of cellular transformation. A key requirement for the HPV lifecycle is that cells continue to synthesise DNA and cell divide (McLaughlin-Drubin and

Munger, 2009). Therefore, avoiding anoikis might be an essential strategy in HPV replication. A major protein was found to be implicated in this mechanism is p600 (DeMasi et al., 2005, Huh et al., 2005). HPV E7 binding can deplete p600; consequently, it inhibits anoikis and block detached cells from undergoing apoptosis. This process will contribute positively to viral transformation.

1.5 Cervical cancer

Cervical cancer is considered one of the most common neoplastic disorders that affecting females. Worldwide, approximately 470,000 new cases are encountered annually, with about 80% of these cases reported from developing countries (Monteiro et al., 2006, Pettersson et al., 2010). Most cervical cancer cases belong to one of two histological lineages, based on whether they emerge in the squamous or glandular cervical epithelium. About 80% of the cases are squamous cell carcinomas (SCCs) whereas the remaining 20% are glandular malignancies (adenocarcinomas) (Badaracco et al., 2010, Duenas-Gonzalez et al., 2010, Monteiro et al., 2006, Pettersson et al., 2010). HPV remains the main cause of cervical cancer accounting for about 99.7% of cases; most of these case are caused by the high-risk HPV types 16 and 18 (Beaudenon and Huibregtse, 2008).

1.5.1 Risk factors

There are several risk factors which contribute to an increased risk of cervical cancer along with the HPV infection. These risk factors may include the following:

- Multiple sexual partners (Monteiro et al., 2006);
- Smoking (Ann L. Coker, 2008, Shehnaz K. Hussain, 2009);
- Parity (Misra et al., 2009);
- Sexually transmitted infections (Monteiro et al., 2006);
- Diet (Garcia-Closas et al., 2005, Shannon et al., 2002, Tomita et al., 2010); and
- Oral contraceptive (Laura G Currin, 2009).

1.5.2 Signs and symptoms

Cervical neoplasia is commonly asymptomatic in the early stage of cancer (Matsumoto et al., 2010, Kai et al., 2009). However, the most common clinical presentation would be abnormal vaginal bleeding, postcoital bleeding and intermenstrual or postmenopausal bleeding. If the bleeding is heavy, anaemia can be found in the lab report. Offensive vaginal discharge may also be observed. Throughout the progress of the disease a lower back pain might be experienced (Bullard Dunn, 2010). Moreover, if the cancer has reached the bladder, haematuria might be found (Spahn et al., 2005). Similarly, if the disease has spread into the rectum it can lead to rectal bleeding and tenesmus (Chan et al., 2009).

1.5.3 Types of cervical neoplasia

There are three common subtypes of cervical neoplasia, namely SCC, pre-invasive SCC and microinvasive SCC. The SCCs are the most common. About 60% of low-grade cervical intraepithelial neoplasia (CIN) cases regress, and the risk of developing invasive carcinoma from low-grade CIN is approximately 1% (Mitchell et al., 1994). Moreover, about one-third of CIN III cases will progress and develop into cervical cancer in 10-20 years if the disease is not treated. Similarly, an average of one-third of CIN I cases will regress depending on the age, immunity and smoking habits of the patient, as well as the causative HPV types (Kietpeerakool and Srisomboon, 2009, Mitchell et al., 1994). Microinvasive squamous carcinoma describes the progress of the cancer past the basement membrane of the epithelium and invasion into the tissue beyond. Once this invasion is detectable microscopically in the cervical stroma, it is called superficial or microinvasive (Goncalves et al., 2009). Furthermore, this invasion stage presents the first stage in the International Federation of Gynaecology and Obstetrics (FIGO) staging system for cervical cancer (Pecorelli et al., 2009, Pecorelli and Odicino, 2003).

1.5.4 Diagnosis of cervical neoplasia

The most common routine diagnostic method for cervical carcinomas is the Pap smear test, collected from the cervical transformation zone located between the original cervical squamocolumnar, SCI, and the new SCI, followed by colposcopic examination (Figure 1.7) (Glick et al., 2012, Insinga et al., 2004). The Pap smear is a screening test used to determine preinvasive lesions for early treatment. The procedure involves scraping cells from the squamocolumnar

junction of the cervical tissue. There is a strong correlation between the initiation of the Pap smear screening programme and a reduction in the cervical cancer mortality rate (De Vincenzo et al., 2009, Sait, 2011). Moreover, lack or provision of this type of screening programme is still a major issue in the developing countries that makes cervical neoplasia has a high incidence in these countries.

Both the American College of Obstetricians and Gynaecologists (ACOG) and the American Cancer Society (ACS) have suggested that the screening should be performed every two to three years if negative results have been returned for three consecutive Pap smear tests (Sawaya et al., 2001, Sawaya et al., 2003). In addition to the Pap smear test, colposcopy is another diagnostic tool which is used usually for two purposes - determining the best site for biopsy and ruling out any invasive diseases (Chase et al., 2009).

1.5.5 Management of cervical neoplasia

The management of cervical cancer is stage driven. In early stages of cervical malignancy surgical procedures can be performed with a survival rate of 85% up to 5 years (Rojas-Espallat and Rose, 2005). In contrast, patients with advanced cervical neoplastic disorders may require multiple therapeutic approaches for good survival rates to be obtained. There are several surgical procedures which can be used to treat cervical cancer based on the stage and progress of the disease. These may include basic surgical approaches such as ablation, destruction or excisional methods, or advanced surgical methods such as radical hysterectomy (Allam et al., 2005, Nam et al., 2002, Penna et al., 2005).

Advanced cases of cervical cancer often require a combination of different therapeutic approaches such as radiation therapy and chemotherapy after the surgical procedure (Lyng et al., 2000, Strauss et al., 2008). However, there are some factors that negatively affect the use of these therapeutic approaches. In radiation therapy, for example, hypoxia and rapid tumour growth are challenging obstacles when it comes to achieving a satisfactory rate of successful treatment. Furthermore, the use of chemotherapy as a treatment for patients with recurrent or metastatic cancer is merely palliative (Benedet et al., 2003, Robati et al., 2008). At present, the most common chemotherapeutic agent that is used to treat cervical cancer is cisplatin (Kaern et al., 1996). The response rate with

cisplatin is about 20 to 30%, with an overall survival time of 7 months. A better survival rate has been observed when cisplatin is combined with topotecan (camptothecin derivative), with an overall survival rate for the patient group of about 15.4 months (Monk et al., 2005). As described above, cervical cancer has a poor prognosis at later stages of the disease, and the current treatment options have limitations. Therefore, the use of genetic approaches may help in developing better treatment options, particularly in term of selective type of treatments with fewer side effects.

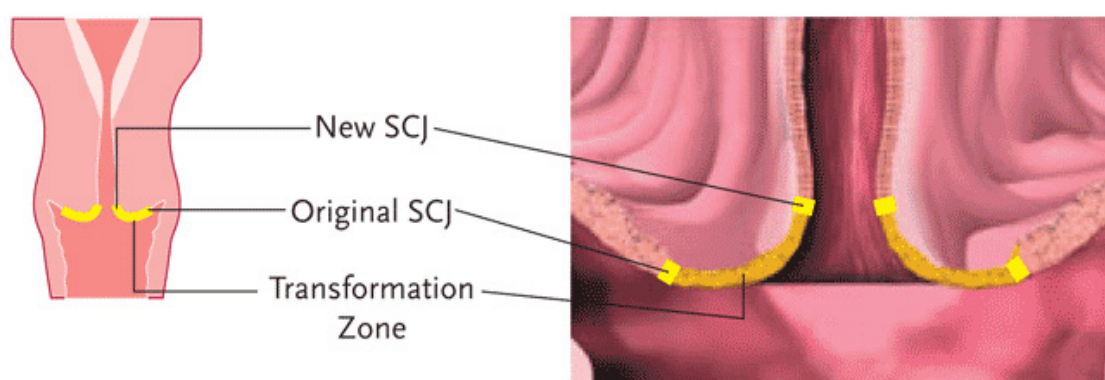


Figure 1.7. Pap smear specimen collection. The specimen is collected from the transformation zone located between the original cervical squamocolumnar junction and the new formed one. From Merck & Co. (Co., 2008).

1.5.6 Vaccination

As indicated above, the primary cause of cervical neoplasia is HPV. High-risk HPV types 16, 18 and 45 cause approximately 75% of cervical carcinomas whilst the other 25% are associated with high-risk HPV types 31, 33, 35, 39, 51, 52, 56, 58, 59, 66 and 68 (Smith et al., 2007, Capri et al., 2011, Giuliano et al., 2008). Cervical cancer can be avoided using two preventive measures, as follows: (i) regular Pap test screenings and (ii) by vaccination against HPVs. There are currently two vaccines available, namely Gardasil (by Merck, Sharpe & Dohme) and Cervarix (by GlaxoSmithKline) (Draper et al., 2013, Wang and Roden, 2013). Both vaccines encompass virus-like particles (VLPs) of the recombinant L1 capsid protein; Gardasil protects against HPV 6, 11, 16 and 18, while Cervarix antagonises HPV 16 and 18. Gardasil also contains aluminium hydroxyphosphate sulphate whilst Cervarix includes aluminium hydroxide with monophosphoryl lipid A (ASO4) (Schwarz et al., 2010, Haupt and Sings, 2011).

The composition of both vaccines is believed to result in 60-100 times the antibody titres of those produced by natural infection. The vaccine is given intramuscularly into the deltoid muscle at different time points. Cervarix is administered at 0, 1 and 6 months, whereas Gardasil is given at 0, 2 and 6 months. The age at which the vaccines can be given has been standardised at 9 years old upwards in the UK and Europe, whereas in the US the vaccine cannot be given to females older than 26 years old. The Gardasil vaccine has also been approved for boys (15 to 26 years old) in Europe and the US.

Whilst it has been reported that the Cervarix vaccine can produce a high antibody titre up to 9.5 years post vaccination (Petaja et al., 2011, Romanowski et al., 2009, Naud et al., Sep. 17-22-2011), it has been found that Gardasil can produce similar antibody trend but for shorter period (up to 5 years) post vaccination (Haupt and Sings, 2011, Petaja et al., 2011). The latter provided a high efficacy of 96% in preventing persistent infection with HPV 6, 11, 16 and 18 in addition to a similar efficacy reported in preventing genital warts formation (Garland et al., 2007, Bonati and Garattini, 2009). Gardasil has also been found to exhibit 100% protection efficacy against vulvar and vaginal neoplasia. Furthermore, Gardasil has been found to be effective in HPVs which are not included within the vaccine but have closer genetic types, such as HPV 45 (60% efficacy), 31 and 52 (32-36 efficacy) (La Torre et al., 2007). The highest antibody titres in both vaccines were found in the age group of 10 to 14 years in females injected with the vaccine (Schwarz et al., 2012). In the case of Cervarix, vaccine efficacy for cervical intra-epithelial neoplasia II (CIN II) was 98.1% for HPV types 16 and 18 combined (Paavonen et al., 2009).

As first generation vaccines, both Cervarix and Gardasil have demonstrated promising results. However, the need for developing better second-generation vaccines is pivotal. To date, the second-generation vaccine is still under clinical trial and has tremendous advantages over the previous generation. The newly developed vaccine is a nonavalent (9-valent) vaccine which antagonises the previous four HPV genotypes (6, 11, 16 and 18) in addition to five new genotypes (31, 33, 45, 52 and 58). It is believed to decrease the risk of cervical cancer by an additional 15-30%. As indicated above, the data on the vaccine provide a good starting point for preventing cervical cancer. However, it will be a long time before total protection can be seen. Therefore, the need to develop

therapy for cervical carcinomas is paramount, particularly when it comes to covering those who may become infected with other HPVs not included in the vaccine, and subsequently, acquire cervical cancer, or women not been immunised and have already developed this neoplastic disease.

1.6 Ribonucleic acid interference (RNAi)

The discovery of RNAi, a highly selective and specific natural process which knocks down the expression of targeted genes, presents a potentially valuable tool for personalised cancer therapy (Singh et al., 2011, Wang et al., 2011b). Target-specific RNAi has the potential to knock down abnormal, overexpressed molecular targets which are required for the survival of patients' tumours. Like any other new therapeutic agents, there are several problems involved in using RNAi agents, and these need to be addressed in order to transfer RNAi technology from the laboratory to the bedside. These issues may include comparison between different RNAi agents (such as siRNA and shRNA), possible off-target effects and effective delivery (Tanaka et al., 2010, Sioud, 2010). Although the primary use of siRNA and shRNA is to deplete target genes, they have distinct features and delivery modes and should be used based on the goal of the project. For example, shRNA is delivered to the nucleus via retroviral (Araki and Konieczny, 2012), adenoviral (El-Armouche et al., 2007), and more recently lentiviral viral vectors (Hung et al., 2010). It has a long lifespan that may span years; therefore, it is highly favourable for chronic diseases.

On the other hand, siRNA which will be used in this project, has a short lifespan, usually degrading within 72-96 hours. They are short double-stranded nucleotides usually 21 – 27 bp in length with a two nucleotide 3' overhang (Figure 1.8) (Singh et al., 2011, Wang et al., 2011b, He et al., 2009). These are produced from longer dsRNA via the cellular endoRNase Dicer III (Doi et al., 2003). The guide or the antisense strand binds to a large protein complex called the RNA induced silencing complex (RISC), which will then target and cleave the mRNA. The argonaute 2 protein is the major component of RISC, as it is responsible for mRNA degradation, as well as formation of the single-stranded RNA (ssRNA).

Given their precise and effective RNAi triggering activity, there are many studies that support the use of siRNA as a potential biodrug (Izquierdo, 2005, Ozpolat et al., 2014). SiRNA that it interferes with translation and not DNA transcription; therefore, it has no effect on the chromosomal DNA.

This advantage significantly reduces concerns about possible gene alterations which might result from DNA-based therapies.

1.6.1 Use of siRNA in cancer therapies

The use of siRNA as a therapeutic agent has paved the way in developing treatments for diseases such as cancer. SiRNA is of inherently effective because it uses the endogenous RNAi pathway, resulting in precise targeting of disease-associated genes, and is appropriate for any gene with a complementary sequence (Leung and Whittaker, 2005). Because cancer is basically a genetic disease, many crucial genes associated with different cancer types have been discovered, their mutations have been determined and the pathways through which they act have been characterised. Despite this knowledge, we have not been able to develop many truly effective cancer-specific therapies. This is where siRNAs come in. In fact, a number of siRNA-focused-libraries have been designed and are commercially available to target sets of genes with common features. These include the kinome library, which target kinases, or larger libraries such as for the whole genome (Adhim et al., 2013, Dutta et al., 2010).

Efforts have also been made to design specific siRNA to target dominant oncogenes, or viral oncogenes involved in carcinogenesis. For example, siRNA has been used *in vitro* and *in vivo* using a pancreatic carcinoma model (Huang et al., 2011). The design of specific RNAi was able to knockdown STAT-3, and consequently, inhibit the expression of VEGF and matrix metalloproteinase (MMP)-2 resulting in tumour inhibition. SiRNA was also evaluated in prostate cancer metastasised to bone and local lymph nodes (Minakuchi et al., 2004). SiRNA was formulated with atelocollagen to target EZH2 or p110-alpha in a xenograft model which was also injected with reporter luciferase and monitored using bioluminescence imaging. Injection of siRNA was performed intravenously and 28 days post-treatment in a study on; here, the treated group showed no increase in luminescence, whereas the control group demonstrated significant metastasis to the thorax, jaws and legs (Minakuchi et al., 2004). Although siRNA-mediated gene silencing for cancer therapies has been investigated in cell culture systems and mouse models and have shown promising results, such therapies have not yet been extended to clinical use (Gavrilov and Saltzman, 2012, Wang et al., 2009b). The main challenge which remains is the optimisation of delivery.

Developing an optimum delivery system should minimise the off-target effect and nonspecific immune response that is caused by the administration of the siRNAs.

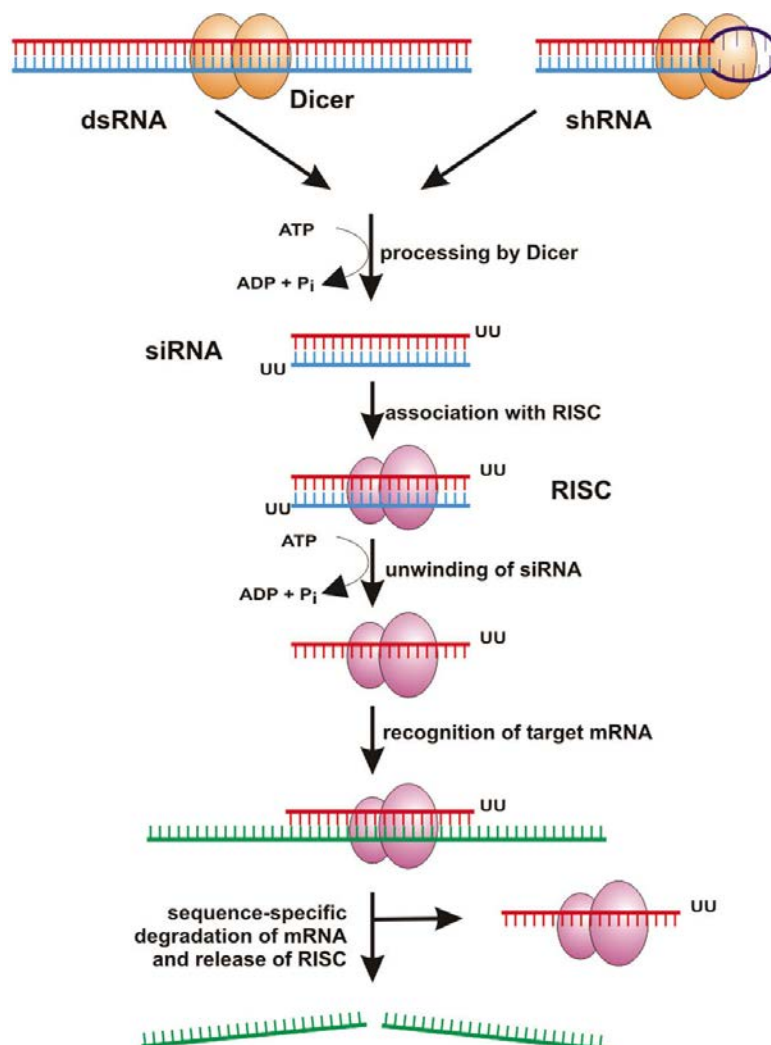


Figure 1.8. The siRNA pathway mechanism. The dicer produces ds-siRNA from dsRNA and the RISC upload it for target-specific mRNA degradation with the help of Ago2. From Rutz and Scheffold (Rutz and Scheffold, 2004).

1.6.2 Efforts to knockdown E6 and E7 HPV oncogenes using siRNA

There are several studies that have focused on depleting the oncogenic activity of E6 and E7 to restore functional pRb and p53, respectively. Wu and colleagues described novel findings using specific siRNAs to target E6 and E7 of HPV *in vitro* and *in vivo* (Wu et al., 2011b). The study illustrated the use of hydration-of-freeze-dried-matrix (HFDM) to formulate stable and efficient siRNA delivery to silence E6 and E7. The *in vitro* data revealed significant knockdown of both

oncogenes; this was confirmed by low mRNA using quantitative PCR (qPCR). Additionally, TC-1 tumour cells were inoculated into mice and formulated E6/E7 siRNA was administered on days 1, 4 and 7 after cell inoculation. SiRNA-treated mice had significantly prolonged survival, with a median of 31 days, in comparison to the control group, at 21 days. Putral *et. al.* also investigated the use of siRNA targeting E6 to target both E6 and E7 simultaneously (Putral *et al.*, 2005). The depletion of these phenomenal HPV oncogenes resulted in remarkable reduction in cellular viability and induction of the senescence phenotype. Furthermore, the effect of silencing E6 and E7 by these siRNAs enhanced the chemotherapeutic effect of cisplatin, a chemotherapeutic which is used for advanced cervical cancer treatment, in HeLa cells.

In another report, Jonson and colleagues, they have investigated the role of siRNAs to silence E6 and E7 oncogenes in cervical cancer (Jonson *et al.*, 2008). They designed specific siRNAs targeting E6/E7 to restore normal p53 and pRb functions. SiRNAs were directly injected into the tumour site every three days for 35 days, along with non-targeting control siRNA or saline. The therapeutic siRNA targeting E6/E7 significantly inhibited the tumour growth in the mouse model of cervical cancer. The aforementioned studies described the use of siRNA as a powerful tool to silence the E6/E7 oncogenes and provide evidence of their treatment capabilities.

1.7 Synthetic lethality screening

Our understanding of some of the molecular mechanisms of cancer progression has paved the way for researchers to provide better treatment options. As discussed above, the major problem in almost all cancer patients, particularly those with advanced metastases, remains the relative lack of available treatment options and the fact that the success rate of these options is often very low. Therefore, alternatives need to be developed. The siRNA synthetic lethality screening concept has been used as a tool to discover novel target genes, which can be then exploited to develop targeted anti-cancer agents. Knocking down oncogenes will result in shrinking of the tumour, and eventually provide a successful cure for cancer patients. This concept has been proven experimentally in HPV (Jonson *et al.*, 2008). In addition, incorporation of viral oncogenes such as HPV E6 and E7 will make use of other normal genes, which are non-oncogenic by themselves, but the survival of the HPV E6 and E7-expressing cells will depends on these genes. Hence, the knockdown of these genes

will be lethal for the cells expressing HPV E6 and E7. These genes, which are essential for the survival of HPV E6 and E7-expressing cells are known to be lethal genes (Scholl et al., 2009a).

Two genes are called synthetically lethal if gene abrogation of either alone is not lethal, but abrogation of both leads to death or significant decrease in an organism's fitness (Nijman and Friend, 2013, Nijman, 2011). Synthetic lethal interactions may occur through different means; for instance, multiple-partial defects may present together in a single linear pathway, or defects in parallel pathways may lead to the synthesis of a common gene product (Canaani, 2009). A third model of synthetic lethality can constitute independent parallel survival pathways, each serving as a salvage pathway in the absence of the other (Figure 1.9). The underlying principle of synthetic lethality provides novel insights into selective anticancer design by utilising the presence of synthetic lethal partners of mutant/defective, cancer-related genes. Accordingly, given a mutated gene in a cancer cell, a knockdown using siRNA to silence the activity of one of its synthetic lethal partners would cause a lethal condition in cancer cells (Brough et al., 2011). Meanwhile, little or only minor damage in healthy cells would be expected, consistent with the synthetic lethality of the genes, and thus constituting a selective anti-cancer therapy.

There are many examples of a synthetic lethality approach being used successfully to identify novel target genes (Luo et al., 2009, Tarailo et al., 2007, Ashworth, 2008). For example, Barbie and colleagues sought to identify synthetic lethal genes that associate with KRAS-driven cancers using high-throughput siRNA screens (Barbie et al., 2009). They found about 45 genes from the first initial screen targeting different kinases. Upon validating these 45 genes, they found that the non-canonical I κ B *TBK1* was selectively required in cells that contain mutant KRAS. In these cells, TBK1 activates the NF- κ B anti-apoptotic signalling pathway, which involve c-Rel and Bcl-xl that are important for survival. Their observations highlighted the synthetic lethality interactions between KRAS and TBK1, and revealed that the TBK1 and NF- κ B signalling pathway are essential in KRAS mutant tumours. These results suggest that the TBK1 gene can be a potential therapeutic target.

In another study, a synthetic lethality RNAi screen was performed to target 1,011 human genes, including kinases and phosphatases, to identify synthetic lethal interactions in cancer cells harbouring mutant KRAS (Scholl et al., 2009b). The researchers found that the cells are dependent

on mutant KRAS exhibit sensitivity to the suppression of the serine/threonine kinase *STK33* irrespective of tissue origin, whereas *STK33* is not required by KRAS-independent cells. They also reported that *STK33* promotes cancer cell viability by regulating the suppression of mitochondrial apoptosis mediated through selective S6K1-induced inactivation of the agonist BAD selectively in mutant KRAS-dependent cells. Thus, *STK33* was identified as a potential target for the treatment of mutant KRAS-driven cancers (Scholl et al., 2009b).

Synthetic lethality screens have also been used to identify genes which affect drug sensitivity. In 2009, Azorsa and colleagues performed a high-throughput RNAi screens targeting 572 known kinases to identify genes which would sensitise pancreatic cancer cells to gemcitabine when silenced (Azorsa et al., 2009). Initially, they found several kinases which when lost potentiated the growth-inhibitory effects of gemcitabine in pancreatic cancer cells. However, upon validating these targets, the checkpoint kinase 1 (CHK1) was shown to exhibit the greatest potentiation among other genes. The researchers examined the dose response of gemcitabine treatment in the presence of CHK1 siRNA, and found a three to ten-fold decrease in EC_{50} for CHK1 siRNA-treated cells versus control siRNA-treated cells. Their observations positively contributed to the use of synthetic lethality screens using RNAi to identify sensitising targets to chemotherapeutic agents. Taken together, these studies demonstrate the potential of RNAi screens when it comes to discovering functional dependencies created by oncogenic mutations. Such dependencies may enable therapeutic intervention in cancers involving genetic alterations which cannot be corrected through drug therapy; this is the basis of this thesis.

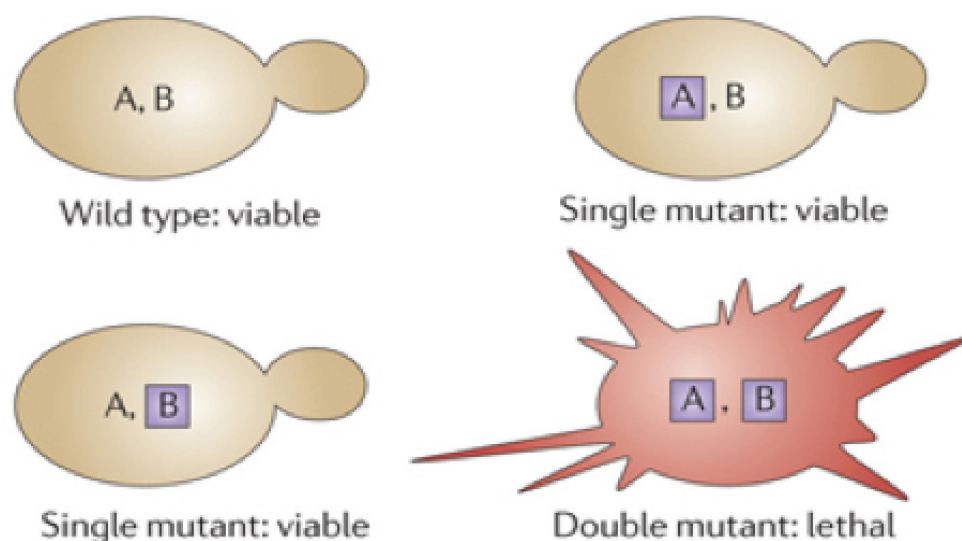


Figure 1.9. Illustration of the synthetic lethality concept. If either gene is mutated the cell remains viable but simultaneous mutation of both genes results in cell death. From Chan and Giaccia (Chan and Giaccia, 2011).

1.8 Hypothesis

Cervical cancer, when driven by the expression of the HPV E6 and E7 oncogenes, may become dependent on expression of other cellular genes for full transformation. These genes form a part of a network required for survival of cervical cancer cells. The loss of these secondary genes in cervical cancer cells will result in their death while normal (or non-HPV) cells are not affected.

1.9 Aims

To identify genes that when silenced are only lethal with the HPV-transformed cervical cancer cells but not with the non-HPV cervical cancer cells. To achieve this general aim, several objectives need to be completed including:

- Establishing a high-throughput siRNA screening protocols that are applicable to be used in the primary and secondary siRNA screens;
- Performing an siRNA high-throughput screen using the kinome library that consists of 779 gene to identify novel target genes in cervical cancer;
- Confirming these target hits using different form of siRNA to eliminate any off-target effects that was found through the primary screen;

- Investigate the most enriched hit(s).
- Demonstrate the ability to inhibit these hits *in vitro* and *in vivo* to show cervical cancer treatment potentials.

1.10 Significance

Like many other cancers, cervical cancer has poor prognosis in advanced stages where patients' survival rate is significantly low (7 – 15.4 months). The side effects and the dramatic limitations of the current therapeutic agents have led to the notion of developing targeted therapy for cervical neoplasia pursuing better treatment options. Synthetic lethal siRNA screens provide a powerful tool that is able to identify novel target genes in different cancer models. In this project, the finding of synthetic lethal genes that when depleted become only lethal to the HPV E6/E7 expressing cells will be a novel finding and may provide potential for cervical cancer treatment. Additionally, there are many small molecule inhibitors that have been developed for different kinases within the kinome library. Some of these small molecule inhibitors have been approved for clinical trials. The identification of a target with a clinically proven small molecule inhibitor would provide a chance to translate the findings of this project to the clinical settings in a relatively short timeframe.

2 Materials and methods

2.1 Materials

2.1.1 Western blotting solutions

Table 2.1. Commonly used Western blotting solutions

Solution	Composition
PBS (pH 7.4)	137mM NaCl, 2.7mM KCl, 4.3mMNa ₂ HPO ₄ , 1.47mMKH ₂ PO ₄
TBS (pH 7.4)	50mM Tris, 150mM NaCl
Running Buffer	25mM Tris, 192mM glycine, 0.1% SDS
Transfer Buffer	25mM Tris, 192mM Glycine, 0.1% SDS, 20% methanol
Stripping Buffer	100mM β-mercaptoethanol, 2% SDS, 62.5mM Tris (pH6.7)
Sample Buffer (5X)	62.5mM Tris, 30% glycerol, 2% SDS, 0.04% bromophenol blue, 1% β-mercaptoethanol
Ponceau Stain	1% Ponceau Stain, 1% glacial acetic acid
Blocking solution	5% skim powder milk in 1x PBS containing 0.05% Tween 20 (PBST) or TBS containing 0.1% Tween 20 (TBST)

2.1.2 Tissue culturing solutions and reagents

Table 2.2. Commonly used tissue culturing solutions and reagents

Solution/Reagent	Composition/Supplier
10X PBS	NaCl 80g, KCl ₂ g, Na ₂ H PO ₄ 14.4g, KH ₂ PO ₄ 2.4g per 2 L (used as 1x PBS)
Trypsin/Versene/PBS	0.025% Trypsin, 1% Versene, 1x PBS
DMEM	Gibco Invitrogen
DMEM/F12	Gibco Invitrogen
L-Glutamine	Invitrogen
Sodium Pyruvate	Invitrogen

2.1.3 Inhibitors

Table 2.3. Inhibitors used throughout the project

Inhibitor (Supplier)	Target
MLN8237 (Millennium)	Aurora A (30 μ M – 30 nM)
ZM447439 (Enzo Life Sciences)	Aurora B (30 μ M – 30 nM)
BI-2536 (Selleckchem)	Polo-like kinase 1 (100 nM – 100 pM)
Paclitaxel (Sigma)	Microtubule depolymerisation (30 nM –30 pM)
Etoposide (Sigma)	Topoisomerase II poison, arrests cells at G2 phase (50 μ M – 50 nM)

2.1.4 Antibodies

Table 2.4. Commonly used antibodies and their corresponding species and dilutions

Antibody (Supplier)	Species	Dilution
BIM (Cell Signalling, Cat # 2819)	Mouse	1:500
Mcl-1 (Cell Signalling, Cat # 4752)	Rabbit	1:500
Bcl-2 (Cell Signalling, Cat # 2876)	Rabbit	1:500
PARP (Cell Signalling, Cat # 9542)	Rabbit	1:1000
Bcl-xl (Cell Signalling, Cat # 2762)	Rabbit	1:500
p53 (Cell Signalling, Cat # 9282)	Rabbit	1:1000
BAD (Cell Signalling, Cat # 9292)	Rabbit	1:500
Aurora A (BD Biosciences, Cat # 610939)	Mouse	1:500
Aurora B (BD Biosciences, Cat # 611082)	Mouse	1:250
Noxa (Abcam, Cat # ab13654)	Mouse	1:250
α -Tubulin (Sigma-Aldrich, Cat # T9026)	Mouse	WB 1:5000, IF 1:500
γ H2AX (Cell Signalling, Cat # 2577)	Rabbit	IF 1:500
Anti-Mouse Alex Fluor 488 conjugate (Invitrogen, Cat # A-11001)	Goat	IF 1:250
Anti-Mouse Alex Fluor 488 conjugate (Invitrogen, Cat # A-21235)	Goat	IF 1:250

2.1.5 siRNA high-throughput synthetic lethal screen reagents/consumables

Table 2.5. Reagents and consumables used in the screening processes

Reagent/Consumables (Supplier)	Application
siGENOME (SMARTpools of 4 siRNA duplexes) (Dharmacon) Cat # G-003505-E2-05	Kinome screening library
siGENOME Non-Targeting siRNA #3 (Dharmacon) Cat # D-001210-03-50	Negative control siRNA used in the primary screen
ON-TARGETplus Non-Targeting individual siRNA (Dharmacon): #1, Cat # D-001810-01-50 #2, Cat # D-001810-02-50 #3, Cat # D-001810-03-50 #4, Cat # D-001810-01-50	Negative control siRNA used in the validation screen
ON-TARGETplus Non-Targeting Pool siRNA (Dharmacon) Cat # D-001810-10-50	Negative control siRNA used in the validation screen
ToxiLight bioassay kit (Adenylate kinase assay) (Lonza, Cat # LT07-217)	Cytotoxicity assay
Lipofectamin 2000 Transfection Reagent (Invitrogen, Cat # 11668019)	Transfection reagent
DharmaFECT 1 (Thermo Scientific, Cat # T-2001-03)	Transfection reagent
DharmaFECT 2 (Thermo Scientific, Cat # T-2002-03)	Transfection reagent
DharmaFECT 3 (Thermo Scientific, Cat # T-2003-03)	Transfection reagent
DharmaFECT 4 (Thermo Scientific, Cat # T-2004-03)	Transfection reagent
5x siRNA buffer (Thermo Scientific, Cat # B-002000-UB-100)	Resuspension buffer
384-well black clear flat bottom plates (Corning, Cat # 3712)	Cell culturing plates
384-well white walled plates (Corning, Cat # 35761)	Luminescence assays
Clear 96-well V-bottom plates (Corning, Cat # 3894)	Transfection master mix reservoir
Nucleotide incorporation assay (EdU)	16mM CuSO ₄ , 275mM Ascorbic Acid, 22µM Cy5 Azide, and 1M Tris HCl (pH 8.5)

2.2 Methods

2.2.1 Cell culture

All cervical cancer cell lines were originally obtained from the American Type Culture Collection (ATCC) except for the C33A-HPV16-E7. Cervical cancer cell lines (HeLa, CaSki, ME-180, SiHa, C33A, HT3, and C33A-HPV16-E7) were maintained in complete Dulbecco's Modified Eagle Medium (DMEM) (GIBCO, Invitrogen, Mulgrave, Victoria, Australia) supplemented with 10% serum supreme (Biowhittaker, Lonza, Mt Waverley, Victoria, Australia), 1mM sodium pyruvate

(GIBCO) and 2mM L-glutamine (GIBCO) at 37°C and 5% CO₂. Squamous cell carcinoma cell lines were kindly given by Associate Professor Nicholas Saunders (The University of Queensland Diamantina Institute, Brisbane, Australia) and were cultured in DMEM/F12 (1:1) (GIBCO) containing 10% serum supreme (Lonza) at 37°C and 5% CO₂.

2.2.1.1 Cell propagation and subculturing

Cells in T-75 tissue culture flasks were washed with 5mL 1x PBS and then 1mL 0.25% trypsin-EDTA was added to the flask and incubated at 37°C and 5% CO₂ for 3-5 minutes for subsequent cell detachment from the flask. Trypsin was then inactivated by 5mL of complete DMEM culture medium. Cells are usually split using 1mL cell suspension and 9mL complete medium (1 in 10).

2.2.1.2 Long-term storage of cells

Cells were first detached from the tissue culture flasks by washing the cells with 5mL 1x PBS and then trypsinize the cells with 1mL of 0.25% trypsin-EDTA. Trypsin was then inactivated by 5mL of complete DMEM culture medium using normal trypsinization procedures within the previous materials and methods section. Cells are then transferred to 10mL tubes and centrifuged at 400x g for 5 minutes. Cell pellet was gently resuspended with the cell-freezing solution (10% DMSO and 90% complete DMEM culture medium) and then each mL was transferred into freezing cryovials (Greiner Bio-one, USA). Cryovials are kept in the cell-freezing container at -80°C overnight before transferring into the liquid nitrogen tank.

2.2.2 Optimization of siRNA screening conditions

2.2.2.1 Cell seeding density

All cell lines tested underwent this stage for optimizing proper seeding density in 384-well plates. Cells were seeded at maximum seeding density (approximately 3,000 cells/well) then a dilution series was performed. Cells were then incubated at 37°C and 5% CO₂ for 72 h prior to harvesting. Cells were subject to EdU labelling as described in section 2.2.7 of this chapter. A comparison between S-phase% generated by the EdU labelling and cell number was then performed. Cell density was considered optimum at the highest point where DNA replication occurred (Appendix 2).

2.2.2.2 Optimizing transfection reagents and concentration

Transfection was optimized for all tested cell lines throughout the primary and secondary siRNA screening processes using four DharmaFECT transfection reagents, DharmaFECT 1 – 4, (Thermo Scientific) in addition to Lipofectamine 2000 (Invitrogen) with four different lipid concentrations (0.2%, 0.1%, 0.05%, and 0.025%) to ensure the highest possible transfection efficiency in all tested cell lines. At this experiment, siRNA against the Polo-like kinase 1 (PLK1) and non-sense scrambled siRNA were used as positive and negative controls, respectively. The following protocol was optimized to facilitate one 384-well plate. Therefore, if more plates to be incorporated, calculations should be performed.

2.2.2.2.1 Lipid preparation

In a 96-well plate, 30 μ L of Opti-MEM only was dispensed in all wells of rows B to D. Following, 300 μ L of Opti-MEM only was dispensed into six 1.5mL microfuge tubes to enable lipid/ Opti-MEM mix. In these six tubes, 7.5 μ L from each lipid (DharmaFECT 1 to 4 and Lipofectmaine 2000, in addition to a no lipid tube) was transferred and mixed with the Opti-Mem and left at room temperature for at least 5 min. A 60 μ L of the lipid/Opti-MEM mix was transferred to each well of row A of the plate. A 30 μ L from row A was then transferred down for dilution series (30 μ L from row A to B, B to C, and C to D). Excess was left in row D of the plates.

2.2.2.2.2 siRNA preparation

PLK1 and non-targeting siRNAs were diluted from the stock [1 μ M] to 412nM in Opti-MEM as a working concentration. Also, 1x siRNA buffer/ Opti-MEM (4:6) was prepared for mock transfection. In a new 96-well plate, 20 μ L of the PLK1 siRNA was dispensed into the wells of columns 2-6 of rows A-D of the plate. Also, 20 μ L of the non-targeting scrambled siRNA was dispensed into the wells in columns 8-12 of rows A-D of the plate. The same volume was transferred into wells of columns 1 and 7 for mock transfection.

2.2.2.2.3 siRNA/lipid preparation

In a new 384-well plate, 6 μ L from the lipid/ Opti-MEM mix was mixed with 7 μ L from the siRNA/ Opti-MEM mix using the liquid handling robotic platform SciClone ALH3000 (Caliper Life

Sciences). The plate was then left for 20-30 min at room temperature for siRNA/lipid complexes to equilibrate.

2.2.2.2.4 *Reverse transfection*

In the siRNA/lipid 384-well plate, 25 μ l of the cell suspension with appropriate seeding density was dispensed using the WellMate bulk dispenser (Thermo Fisher Scientific) into each well containing the siRNA/lipid complexes making final lipid concentrations of 0.2%, 0.1%, 0.05%, and 0.025%; and siRNA final concentration as 50nM. Plate was then incubated at 37°C and 5% CO₂ for 72 h prior to harvesting with the assays described in sections 2.2.5, 2.2.6, 2.2.7, and 2.2.8 of this chapter.

2.2.3 siRNA primary screening

The same procedures that were mentioned in sections 2.2.2.2.1 through 2.2.2.2.4 were followed. However, because only a single transfection reagent, DharmaFECT 3, was used at this stage in addition to one lipid concentration, 0.05%; thus, all volumes were adapted based on these two conditions. The Dharmacon Human siGENOME® SMARTpool® siRNA Library for Protein Kinases (targeting 779 genes) was stored at a concentration of 1 μ M. This library has 4 siRNA duplexes targeting the same gene in different sites of the mRNA. The library was used at 50nM final concentration in 384-well plates at a final volume of 38 μ l that includes 13 μ l of siRNA/lipid mix as described in sections 2.2.2.2.1 through 2.2.2.2.4. The Polo-like kinase 1 (PLK1) and scrambled non-targeting siRNA were included as positive and negative controls, respectively. All cells were incubated at 37°C with 5% CO₂ for 72 hours prior to harvesting with the assays described in sections 2.2.5, 2.2.6, 2.2.7, and 2.2.8 of this chapter.

2.2.4 siRNA validation screening

Dharmacon ON-TARGETplus SMARTpool siRNAs were used for the validation screen. The library was resuspended in 1x siRNA buffer to 1 μ M stock concentration and was used at a final concentration of 40nM.

2.2.5 Resazurin cell viability assay

Resazurin (or Alamar Blue) is a dye based on a mitochondrial respiration measurement assay. Briefly, resazurin itself has a weak fluorescence signalling until it is reduced to a pink colour,

resorufin, by viable cells. All resazurin experiments were performed on Corning 384-well black clear flat bottom plates. Cells were seeded and then incubated overnight at 37°C with 5% CO₂. Upon incubation, siRNA (as explained in the transfection sections) or the small molecules were introduced and incubated in the same incubation condition for 72 h. Following, resazurin dye was introduced at a final concentration of 44 µM made in complete DMEM culture medium then incubated at 37°C with 5% CO₂ for 75-90 minutes. All plates were subject to fluorescence signal detection with an excitation of 554nm and an emission of 590nm using FLUOstar microplate reader (BMG LabTech). Cells' viability was normalised to media only control.

2.2.6 Adenylate kinase cytotoxicity assay

Cytotoxicity was determined using Toxilight bioassay kit (Lonza) according to the manufacturer protocol. The kit quantitatively measures the luminescence signal of adenylate kinase that is released from damaged cells to the surrounding media. The reaction engages the addition of ADP as a substrate for adenylate kinase. In the presence of adenylate kinase, the ADP is converted into ATP for assay bioluminescence. This method exploits an enzyme luciferase that catalyses the formation of light from ATP and luciferin., The procedures involved recovering 8µl of cell media after 72 h siRNA transfection from the transfection plates and transferred it into 384-well Corning white plates. Following, 8µL of the adenylate kinase reagent was added and incubated for 20 min at room temperature in the dark. The luminescence signal was then detected using the FLUOstar microplate reader (BMG LabTech) where the gain was adjusted on 4059 with single lens emission filter, 1 multichromatics, and double orbital shaking with 4mm at 150rpm.

2.2.7 Nucleotide incorporation assay (5-ethynyl-2'-deoxyuridine or EdU Assay)

Following 72 h siRNA transfection and the recovery of 8µL for the adenylate assay, and the addition of resazurin dye mixed with the EdU that give final concentrations of 44nM and 10nM in the 384-well plates, respectively; plates were washed with 1x PBS. Cells were then fixed with 3.7% (v/v) formaldehyde in 1x PBS, washed with 1x PBS, permeabilized with 0.5% (v/v) Triton X-100, washed with 1x PBS, and then blocked with 3% (w/v) BSA in PBS with 0.1% (v/v) Tween-20 (PBST-BSA). Plates were then washed with 1x PBS before the click reaction took place. Click reaction had four main components: CuSO₄ 16mM, Cy5 azide 22µM, 400mM TRIS HCl pH 8.5, and freshly made ascorbate acid 275mM. Tris HCl and ascorbate solutions were in bulk reservoir

whereas CuSO₄ and the Cy5 azide were dispensed into clear 96-well V-bottom plates. The 96-well V-bottom plate of Cy5 was also used as mixing stations for all components before they are introduced into the 384-well plates. Following preparation, all reagents were then mixed with samples at final concentration of 100mM Tris HCl pH 8.5, 4mM CuSO₄, 2μM Cy5 Azide, and 50mM sodium ascorbate. Reaction was left at room temperature for 15-20 minutes in a dark place. Following the click reaction, plates were washed with 1x PBS and samples were stained with 400nM 4',6-diamidino-2-phenylindole (DAPI) in 3% BSA for one hour at room temperature and EdU-labelled DNA percentage was generated using the Cellomics ArrayScan VTI analyser (Thermo Fischer Scientific).

2.2.8 Quantitative cell imaging

The original processed plates that were used to generate the EdU-labelled DNA percentage were at the same time used to generate cell numbers throughout the primary and secondary screens using the Cellomics ArrayScan VTI automated inverted epifluorescent microscope (Thermo Fisher Scientific). Image acquisition and analysis were performed using the manufacturer provided software, Cellomics ArrayScan VTI Compartmental Analysis V.3.0. A detailed imaging protocol can be seen at Appendix 1.

2.2.9 Flow cytometry

All tested cells were exposed to final concentrations of 5μM Aurora A kinase small molecule inhibitor MLN8237 (Millennium Inc.), 5μM ZM447439 (Enzo Life Science), or DMSO (vehicle) for 24, 48, or 72 hours. Cell were permeabilized by incubation with 70% ethanol at -20°C and resuspended in 50 μg/mL propidium iodide and 20 units/mL RNase-A (Roche Diagnostics). DNA content was measured by flow cytometry using BDFACS-Canto II (BD Biosciences, San Jose, CA) and data analysed with FlowJo software (FlowJo Co.).

2.2.10 Time-lapse microscopy

Cells were seeded at 2.5×10^5 in 6-well tissue culture plate and incubated at 37°C with 5% CO₂ until they reached at least 50% confluency. All cells were then either treated with a final concentration of 5μM MLN8237 or equal volume of DMSO (vehicle). After treatment a time-lapse microscopy experiment was performed using a Zeiss Axiovert 200M Cell Observe microscope equipped with an

incubation chamber at 37°C and 5% CO₂. Images were captured at 20 minutes intervals using Zeiss AxioCam. Images were analysed using ImageJ V1.46r (National Institutes of Health, USA) with a minimum of 150 cells per condition per cell line analysed. Time of cellular mitotic entry, an event characterised by a bright cell wall and round-up-like morphology of the cell with intact membrane, was tracked by the previously mentioned mitosis characteristics. Cellular exit from mitosis was observed and assessed for successful cellular division, failure of cytokinesis, or cell death.

2.2.11 Immunoblotting

Cells were seeded at 7.5×10^5 in 10 cm dishes and treated either with DMSO only (vehicle) or a final concentration of 5 μ M MLN8237 and incubated at 37°C with 5% CO₂ for 24, 48, and 72 hours. Cells were harvested and collected at each time-point and pellets were stored at -80°C until processing. Total cell pellets were lysed in NETN lysing buffer with 1 mM phenylmethylsulfonyl fluoride (PMSF), Protease inhibitor cocktail (5 μ g.mL aprotinin, pepstatin A, and leupeptin mix; Sigma Aldrich), 0.1% SDS, 100 mM NaCl, , 0.3 mM Na₃VO₄, 10 mM NaF, and 25 mM B-glycerophosphate. The Bio-Rad Protein Assay solution was added to the lysis supernatant for equalisation, and; a standard curve was generated using bovine serum albumin (BSA). Equalised protein concentration lysates were boiled for 5 minutes with 20% sample buffer before samples were resolved using SDS-PAGE gel electrophoresis with 10%, 12.5%, or 15% SDS-polyacrylamide gels. Transfer to either Hybond-C Extra nitrocellulose or polyvinylidene difluoride (PVDF) membranes was achieved by using a Trans-Blot semi-dry transfer cell apparatus (Bio-Rad). The protein of interest was detected after adding the suitable primary antibody, which was incubated overnight at 4°C followed by the appropriate horseradish peroxidase conjugated secondary antibodies for 1 hour at room temperature. Protein band visualization was performed using Western Lightening Plus ECL chemiluminescent reagents (Perkin Elmer) with the ChemiDoc gel system and software (Vilber Lourmat).

2.2.12 Cell doubling-time

Cells were seeded in at 3.5×10^5 10cm dishes and incubated for 48, 96 and 120 hours at 37°C with 5% CO₂. Cells were trypsinized, collected, and counted in each time-point. Cell doubling time was obtained using an online cell doubling time calculator (Roth V. 2006 <http://www.doubling-time.com/compute.php>).

2.2.13 Xenograft mice models

Nude-strain immunodeficient mice 6-weeks old females were purchased from UQBR. All animal studies were conducted based on the approved University of Queensland Animal Ethics number UQDI/427/12/CCQ. The 36 mice had been assigned into three groups: (i) CaSki; (ii) HeLa, and; (iii) C33A. For each group of 12 mice, 6 mice were used for the treatment with MLN8237 and 6 for the vehicle control only. One million of cells from each cell type (CaSki, HeLa, and C33A) inoculated subcutaneously in the right flank. When tumour size reached approximately 20-25mm³, which was measured using manual caliper, 100µL oral treatment of 30 mg/kg of the MLN8237 Aurora A small molecule inhibitor by Millennium was administered daily for 10 consecutive days. Mice were then followed up daily by scoring any tumour regrowth or until culled.

2.2.14 Screening Statistical Methods

Different approaches of statistics can be used in high-throughput siRNA screenings. In the present thesis, a Z-score was used for data interpretation (Birmingham et al., 2009). The Z-score is the distance from the mean based on standard deviation. Z-score is usually used to normalize data in siRNA screens where it counts the total population, which will provide strength of a single sample in the total data context. This assumes that variations in screenings are between plates not within the plate. All data from the primary and secondary screens were collected and initially analysed in Microsoft Excel 2008 (v. 12.2.9). The screening was performed in triplicates in both the primary and secondary stages. That is, the standard deviation was calculated for each sample followed by the Z-score for data normalization. The Z-score for each replicate was calculated separately and then a mean Z-score of three replicates was calculated for final interpretation. The Z-score was calculated based on the formula:

$$Z = \frac{X - \mu}{SD}$$

where X is the raw value, μ is the population mean, and SD is the standard deviation of the population. Figure 2.1 shows an example of how the Z score was calculated.

2.2.15 Immunofluorescence staining

Cells were cultured on 10cm plates containing poly-L-lysine coated glass coverslips in the absence (DMSO only) or presence of 5 μ M MLN8237 for 24, and 48 h. Coverslips were recovered and fixed with -20°C absolute methanol and stored at -20°C until processing. Coverslips were washed with 1x PBS and rehydrated in blocking buffer (3% BSA and 0.1% powder skim milk) for 1 hour at room temperature. Cells were then incubated with the primary antibodies diluted in the blocking buffer for 24 hours at 4°C . Coverslips were washed six times with 1x PBS and cells were then incubated with corresponding secondary fluorescence antibodies and DAPI DNA stain for 30 minutes at room temperature in a dark atmosphere. Upon incubation, all coverslips were washed six times with 1x PBS and air-dried before they were mounted on glass slides using prolong gold (Invitrogen).

WellID	Gene Name	replicate 1	replicate 2	replicate 3	Z-Score 1	Z-Score 2	Z-Score 3	Mean Z-Score
1A01	AVPR1B	21.3502399	19.3729373	19.9127454	-0.3520197	-0.8347087	-0.8480059	-0.678244765
1A02	CDKN3	24.567474	25.1853516	27.9087075	0.49514295	0.75981807	1.4931151	0.916025372
1A03	AVPR1A	25.7633106	25.9705489	25.1544354	0.81003083	0.97522221	0.68669754	0.823983529
1A04	CDKN2D	29.2922882	28.5616203	32.0240623	1.7392818	1.68603405	2.69804117	2.041119007
1A05	AURKC	27.2727273	24.4515539	25.9409969	1.20749068	0.55851445	0.91699325	0.894332794
1A06	CDKN2C	21.4903357	21.6257007	23.4538535	-0.3151296	-0.2167054	0.18878774	-0.114349088
1A07	AURKB	19.4673123	18.3021451	17.3505275	-0.8478325	-1.1284605	-1.5981922	-1.191495072
1A08	CDKN2B	26.0635281	26.2099125	26.1570618	0.88908415	1.04088714	0.98025443	0.970075238
1A09	ATR	22.6247987	22.5036532	21.8058808	-0.0164027	0.02414443	-0.2937187	-0.095325647
1A10	CDKN1C	28.3767535	26.3506448	32.6395459	1.49820306	1.0794944	2.87824733	1.818648263
1A11	ATM	20.5951679	23.1733333	22.7186053	-0.5508454	0.20785861	-0.026484	-0.123156932
1A12	CDKN1B	25.8064516	24.475	26.8807051	0.82139073	0.56494644	1.19212842	0.859488528
1A13	ASP	19.6680498	22.6298797	19.5844791	-0.7949743	0.05877229	-0.9441183	-0.560106752
1A14	CDKN1A	21.7088056	22.6309379	22.4653538	-0.2576021	0.05906259	-0.100633	-0.099724182

WellID	Gene Name	replicate 1	replicate 2	replicate 3	Z-Score 1	Z-Score 2	Z-Score 3	Mean Z-Score
1A01	AVPR1B	21.3502399	19.3729373	19.9127454	-0.3520197	-0.8347087	-0.8480059	-0.678244765
1A02	CDKN3	24.567474	25.1853516	27.9087075	0.49514295	0.75981807	1.4931151	0.916025372
1A03	AVPR1A	25.7633106	25.9705489	25.1544354	0.81003083	0.97522221	0.68669754	0.823983529
1A04	CDKN2D	29.2922882	28.5616203	32.0240623	1.7392818	1.68603405	2.69804117	2.041119007
1A05	AURKC	27.2727273	24.4515539	25.9409969	1.20749068	0.55851445	0.91699325	0.894332794
1A06	CDKN2C	21.4903357	21.6257007	23.4538535	-0.3151296	-0.2167054	0.18878774	-0.114349088
1A07	AURKB	19.4673123	18.3021451	17.3505275	-0.8478325	-1.1284605	-1.5981922	-1.191495072
1A08	CDKN2B	26.0635281	26.2099125	26.1570618	0.88908415	1.04088714	0.98025443	0.970075238
1A09	ATR	22.6247987	22.5036532	21.8058808	-0.0164027	0.02414443	-0.2937187	-0.095325647
1A10	CDKN1C	28.3767535	26.3506448	32.6395459	1.49820306	1.0794944	2.87824733	1.818648263
1A11	ATM	20.5951679	23.1733333	22.7186053	-0.5508454	0.20785861	-0.026484	-0.123156932
1A12	CDKN1B	25.8064516	24.475	26.8807051	0.82139073	0.56494644	1.19212842	0.859488528
1A13	ASP	19.6680498	22.6298797	19.5844791	-0.7949743	0.05877229	-0.9441183	-0.560106752
1A14	CDKN1A	21.7088056	22.6309379	22.4653538	-0.2576021	0.05906259	-0.100633	-0.099724182

Figure 2.1. Example of how the Z-score was calculated in the siRNA screening stages of this project. The above diagram illustrates an example of how the Z score was calculated from the raw data. Yellow colour

indicates raw data of a single sample (well); Green colour shows the whole population from where the standard deviation and the mean of the total population were calculated; Orange colour indicates the calculated Z score for one replicate; and Blue colour shows the mean Z score from all three replicates, which in fact was used for data interpretation.

3 siRNA screening of the kinome identified potential therapeutic target genes in cervical cancer

3.1 Introduction

Although many anticancer agents have been developed over the past decades, the mission to achieve a selective anticancer agents has not been accomplished yet (Brzezniak et al., 2013, Takahashi et al., 2012, Verstovsek, 2013, Zeng et al., 2008). The unspecific targeting that occurs using current anticancer agents has led to the notion of trying to develop better treatment options. To achieve this ultimate goal, different techniques have demonstrated the ability to identify novel target genes that when depleted affect only cancer cells but not normal cells (Kollareddy et al., 2012). In genetics, synthetic lethality is defined as a combination of mutations in two or more genes leading to cellular death (Dai et al., 2013, Dong et al., 2010, Porcelli et al., 2012). The concept of synthetic lethality screening via RNAi became a method of choice for many researchers for the purpose of identifying novel target genes that are selective for cancer cells. I utilized this concept in the present project to identify novel target genes in cervical cancer.

A strong relationship between high-risk human papillomavirus (HPV) and genital cancers has been well-established over the past decades (Peralta-Zaragoza et al., 2012). Cervical cancer is the second-leading cause of cancer-related death among women worldwide. Approximately 470,000 cases are diagnosed annually, and the mortality rate is about 280,000. The most common high-risk HPV types involved in this neoplastic disorder are HPV types 16 and 18. Upon the integration of the viral DNA with the host DNA, several genetic interactions occur. E6 and E7 primarily disrupt p53 and the retinoblastoma protein (pRb), respectively. This oncogenic interaction results in interrupted cell cycles, independent cellular growth, immune response escape, and the accumulation of further mutations, all contributing to cancer formation (Wang et al., 2013, Sima et al., 2008, Gu et al., 2011). In the present study, I used a cervical cancer model to apply the concept of a synthetic lethality screen using small interfering RNA (siRNA) to identify novel target genes that, when silenced, kill E6/E7-expressing cells but not normal or non-HPV cells.

Developing robust, high-throughput screens requires optimal conditions to ensure maximum transfection efficiency with the lowest possible cytotoxicity (Nebane et al., 2013, Henderson and Azorsa, 2013, Kahle et al., 2010). Key considerations during optimization are: cell seeding density,

lipid type and concentration, siRNA concentration, cell line selection, the selection of positive and negative siRNA controls, and developing proper cell-biological assays to monitor the screens. In this project, the Dharmacon Human siGENOME® SMARTpool® siRNA Libraries for Protein Kinases (targeting 779 genes of the kinome library) was selected for the primary screen. The library consists of a pool of four siRNAs targeting each gene at different sites. Combinations of three cell lines were chosen for the optimization and the primary screen, including CaSki (cervical cancer HPV16 cell line), C33A (cervical cancer non-HPV cell line), and HaCaT (non-cervical cancer, non-HPV, spontaneously immortalized keratinocyte cell line). This combination allows for confidence in comparing cervical cancer HPV-transformed cell lines against cervical cancer non-HPV cell line. The availability of the HaCaT cell line added an extra value for results validity as it demonstrates the closest available cell culture system to normal keratinocyte. Additionally, another two HPV-transformed cell lines were added to the validation screen, HeLa (cervical cancer HPV18) and SiHa (cervical cancer HPV16). At the validation screening stage, a different form of siRNA from Dharmacon was used that called ON-TARGETplus SMARTpool siRNA. The latter has a 2'-O-methyl chemical modification. The sense strand is modified to preclude uptake by the RNA-induced silencing complex and favours only antisense loading. The 2'-O-methyl modified siRNA has a better silencing capability and low off-target activity (Jackson et al., 2006).

This chapter illustrates the importance of performing optimization experiments prior to any large-scale siRNA screening. It also demonstrates the novel candidates of the primary screen, which were participating in the killing of the HPV-transformed cells but not others. The chapter also shows the findings of the validation screening, which was carried out to validate the target hits that were found in the primary screen. The validated target genes were then taken for further validation experiments throughout this project.

3.2 Results

3.2.1 Screening Optimization

As indicated in the introduction, three cell lines—HaCaT, CaSki, and C33A—were selected for the optimization processes and the primary screening. This combination of HPV and non-HPV cell lines gives the potential to compare the findings of the loss-of-function siRNA screen.

Firstly, cells were seeded in maximum cell numbers in 384-well plates, and a dilution series was performed to obtain a proper seeding density, with approximately 85% confluency, in 72 h. The optimum seeding density for each cell line was selected based on the highest number of cells in S-phase as determined by the EdU (5-ethynyl-2'-deoxyuridine) assay, which is incorporated during DNA synthesis in a quick-click chemistry reaction (Appendix 2). Table 3.1 lists the required seeding density for each cell line used throughout the primary and the secondary screens.

Table 3.1. List of all cell lines and their corresponding seeding densities used throughout the primary and secondary siRNA screens

Cell line	Seeding density (cells/well in a 384-well plate format)	Doubling time \pm SD
CaSki	2100	28 \pm 1.8
HaCaT	550	20 \pm 6.1
C33A	2600	26.1 \pm 1.6
HeLa	500	21 \pm 1.7
SiHa	1000	22 \pm 0.24

Next, five different transfection reagents (DharmaFECT 1–4 and Lipofectamine 2000) were examined with four different lipid concentrations (0.2%, 0.1%, 0.05%, and 0.025%) to obtain the maximum possible transfection efficiency with minimal cytotoxicity. In this experiment, positive and negative control siRNAs were included for transfection efficiency measurements, including polo-like kinase 1 (PLK1), a serine/threonine kinase and a key mitotic regulator that induces apoptosis and inhibits cell growth in the majority of cancer cells upon depletion. Also, a non-targeting siRNA was included as a negative control. Four cell-based biological assays were used for results interpretation, including cell metabolic activity, cytotoxicity, S-phase %, and cell number as outlined below.

Lipids and siRNAs were mixed and dispensed into 384-well plates, and cells were seeded for reverse transfection. All cells were transfected with a final concentration of 50nM PLK1 of either or non-targeting siRNA. Cells were then incubated at 37°C for 72 h prior to harvesting. Cell metabolic activity was evaluated by adding resazurin dye at a concentration of 44 μ M. Resazurin is a weak dye that reduces to a highly fluorescent pink, resorufin, as a result of irreversible chemical reduction based on mitochondrial respiration (Gonzalez and Tarloff, 2001, O'Brien et al., 2000). Regardless of the cell line, high lipid concentrations—0.2% and 0.1%—showed cytotoxicity, whereas

transfection efficiency was lost at the 0.025% concentration (Appendix 3). Among all lipid concentrations and transfection agents, DharmaFECT 3 transfection agent showed a strong reduction in cell viability that was observed at a 0.05% lipid concentration in cells transfected with PLK1 siRNA when compared to the non-targeting siRNA transfected cell lines (Figure 3.1).

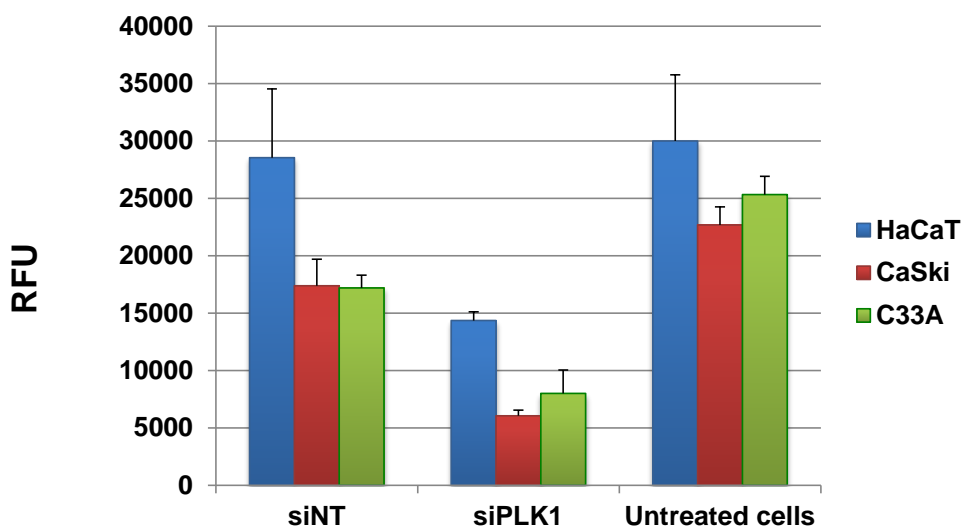


Figure 3.1. Summary of cell metabolic activity measured in HaCaT, CaSki and C33A cell lines using DharmaFECT 3 at 0.05% lipid concentration. Cells were seeded and reverse transfected with 50nM siRNA against PLK1, and non-targeting siRNA was included as a negative control. At 72 h transfection, cells were labelled with 44 μ M resazurin dye. Cells were incubated for 75 min at 37°C. Cell metabolic activity was then measured fluorimetrically by the FLUOStar plate reader. Each point is the mean and standard error mean (SEM) of quadruplicate determinations. The knockdown of the PLK1 by the siRNA resulted in remarkable reduction of the cell viability in all the three cell lines compared to the control siRNA. The non-targeting siRNA also showed reduction in the metabolic activity of the tested cell lines suggesting a level of toxicity compared to the untreated cells.

In addition, cytotoxicity was measured using a commercially available adenylate kinase kit, which was used according to the manufacturer's protocol (ToxiLight[®] Non-destructive Cytotoxicity BioAssay Kit, Lonza, Australia). From the primary 384-well plate, 8 μ L were recovered to another plate for the cytotoxicity assay. An adenylate kinase substrate was added to the cells and incubated for 20 min at room temperature. The luminescence signals of the adenylate kinase activity were then measured using the FLUOStar plate reader. The results of the DharmaFECT 3 testing at a 0.05% lipid concentration showed high adenylate kinase activity level indicated by the luminescence signals only in C33A cells when PLK1 was depleted (Figure 3.2). Although both

CaSki and HaCaT cell lines showed remarkable increase in the adenylate kinase activity level, cells transfected with siNT control showed elevated luminescence signals that may suggest strong cytotoxicity. This cytotoxicity might be confirmed when cells transfected with siNT are compared with the untreated cells, as they both show relatively similar luminescence activity. This cytotoxicity resulted in a marginal significant difference between cells transfected with siPLK1 and those transfected with siNT ($P = 0.1$). Other lipid concentration and transfection reagent data are shown in Appendix 3.

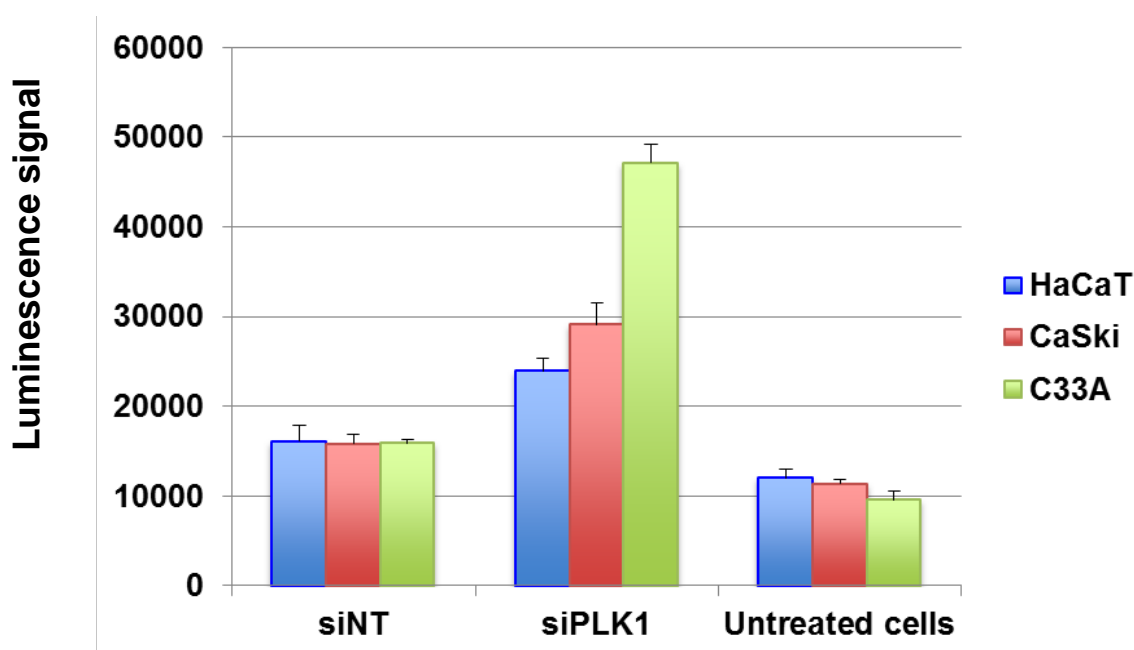


Figure 3.2. Summary of adenylate kinase activity measured in HaCaT, CaSki, and C33A cell lines using DharmaFECT 3 at a 0.05% lipid concentration. Cells were seeded and reverse transfected with 50nM siRNA against PLK1, and non-targeting scrambled siRNA was included as a negative control. At 72 h transfection, 8 μ L of the media were recovered for the cytotoxicity assay using a commercially available kit. An equal volume of the adenylate kinase substrate was added to the cells, plates were incubated for 20 min, and the luminescence signals were then measured by the FLUOStar plate reader. Each point is the mean and standard error mean (SEM) of quadruplicate determinations. The luminescence signals showed high activity of adenylate kinase when PLK1 was depleted in CaSki and C33A cells. This trend was less in HaCaT compared to the siNT control. The siNT also showed marginally high adenylate kinase activity considering the PLK1 and untreated data. Significant difference was calculated using One-Way ANOVA test by Prism V6.0.

To count cell number, cells in primary plates were fixed and stained with 400nM DAPI in 3% BSA and then subjected to cell number assessment using the Cellomics analyser. The knockdown of PLK1 using DharmaFECT 3 at 0.05% in all cell lines resulted in at least six to eight-fold reduction in cell numbers (Figure 3.3).

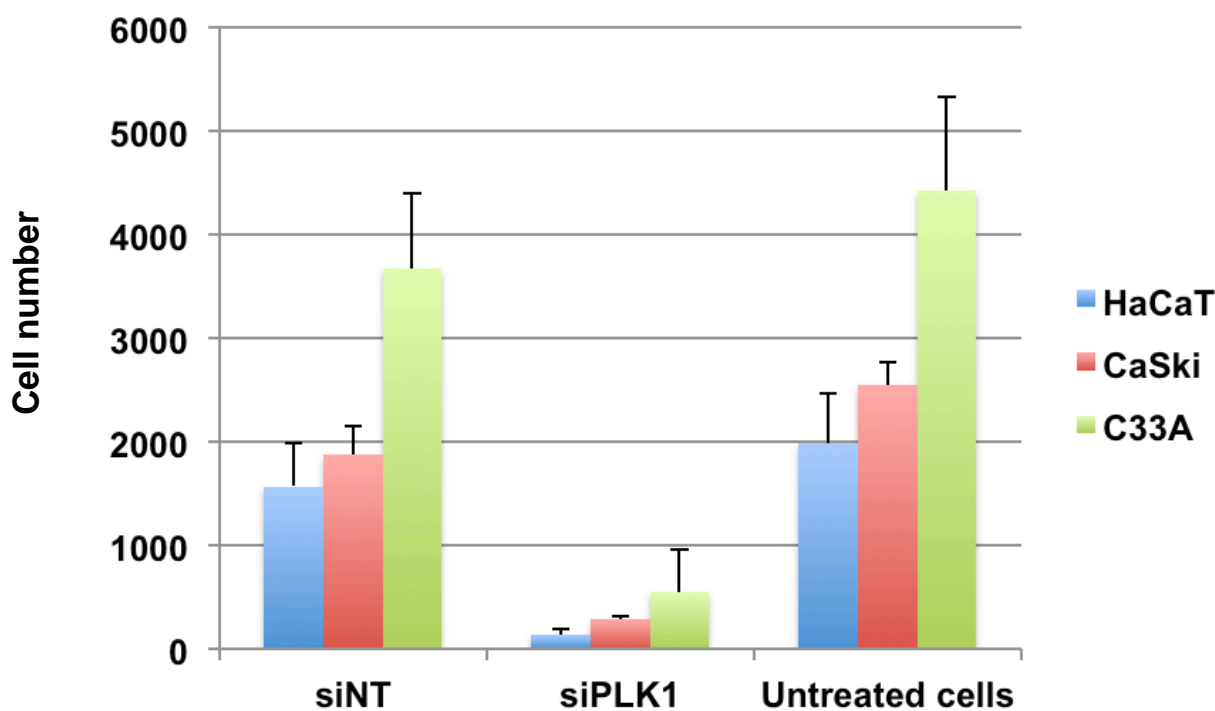


Figure 3.3. Summary of HaCaT, CaSki, and C33A cell line cell count measurements using DharmaFECT 3 at 0.05% lipid concentration. Cells were seeded and reverse transfected with 50nM siRNA against PLK1, and non-targeting scrambled siRNA was included as a negative control. At 72 h, cells were fixed and stained with 400nM DAPI stain in 3% BSA. Cells were counted using the Cellomics analyser. Each point is the mean and standard error mean (SEM) of quadruplicate determinations. The knockdown of the PLK1 by siRNA demonstrated obvious reduction in all cell lines. This was confirmed by the siNT control and the untreated cells. *P* value was calculated, ($p = 0.03$), using a two-tailed paired t test by Prism V6.0.

It was noted that the depletion of PLK1 left all cell lines with more metabolically active cells (Figure 3.1) compared to cell numbers (Figure 3.3). In this project, the metabolic activity assay is performed at first instant and then these plates underwent various washing stages before the Cellmoics ArrayScan VTI generates cell numbers. This may suggests technical variability due to washing steps, which may resulted in more cells to detach from the plates. Overall, DharmaFECT 3 at a 0.05% lipid concentration demonstrated the maximum possible transfection efficiency when

compared with the other lipid reagents (Appendix 3 shows examples of other transfection reagents and lipid concentrations data using different biological assays). This observation was determined via cell viability, cytotoxicity, and cell number assays. Optimizing conditions, such as seeding density, lipid type and concentration, and validating biological assays, are essential factors for successful high-throughput screens. This part of the project was essential to establishing a robust screening platform before the primary and secondary screens could take place.

3.2.2 Primary Screening

The main aim of this project was to identify target genes that, when silenced, kill only E6/E7-expressing cells but have no (or minor) effect on non-HPV/normal cells. These targets might be potential therapeutic targets for cervical cancer. A high-throughput siRNA screen was carried out using a combination of an HPV-transformed cervical cancer cell line (CaSki) and a non-HPV cervical cancer cell line (C33A), in addition to a non-HPV, non-cervical cancer cell line (HaCaT). The screening was performed in the Arrayed RetroViral Expression Cloning (ARVEC) Facility at the University of Queensland Diamantina Institute using Dharmacon Human siGENOME® SMARTpool® siRNA Libraries for Protein Kinases (targeting 779 genes of the kinome library). Transfection complexes were prepared and dispensed into 384-well plates. Cells were then added for reverse transfection. All plates were incubated at 37°C for 72 h prior to harvesting. The kinome library was screened at a final concentration of 50nM; the screening was performed in triplicate.

3.2.2.1 Cell Viability

To assess cell viability, resazurin dye was added to cells at a final concentration of 44µM and plates were incubated for 75 min at 37°C. Fluorescence signals were determined using a FLUOStar plate reader. The Z-score of each cell line was calculated and then all genes were sorted according to the minimum CaSki viability Z-value, as shown in (Figure 3.4A). Because I was interested in genes that only affect the viability of the HPV-transformed cell line, CaSki. Thus, gene is considered a potential target if the CaSki Z-score was -2 or lower and the C33A/HaCaT Z-score is -0.5 or higher. Firstly, the results revealed that PLK1, wee-like protein kinase 1 (WEE1), and coatomer protein complex subunit beta 2 (COPB2) were on the top of the gene list that affects the viability of all cell types, although there were differential responses among cell lines (Figure 3.4B). Unsurprisingly, PLK1 and WEE1 kinases play critical roles in cell cycles, and their depletion induces G₂/M arrest

(de Oliveira et al., 2012, Magnussen et al., 2012). There was only four genes came under the category of affecting CaSki by -2 (or less) Z-score with -0.5 (or higher) on C33A and HaCaT viability—GSG2 (Haspin), PRKCN, PIK3CA, and KSR2. Of these genes, the germ cell associated 2 (GSG2/Haspin) has been newly reported to be a crucial regulator of in cell cycle (Higgins, 2010). In addition, Aurora A kinase (AURKA) depletion caused a strong reduction in the viability of CaSki and HaCaT with Z-scores being -2.9 and -2.5 , respectively. Surprisingly, the C33A metabolic activity was not affected by the knockdown of AURKA where Z-score of the viability level remained as high as 1.5 . The results also revealed another group of genes that affect HaCaT and C33A viability but had a lesser effect on CaSki cells. Within this group, the depletion of the cell division cycle 2-like protein kinase 2 (CDC2L2) affected HaCaT and C33A viability, and resulted in lower Z-scores, 0.1 and 0.06 , respectively; when compared with the CaSki Z-score of 0.4 . On the other hand, the depletion of the same family member, CDC2L1, resulted in a Z-score of 0.05 and 0.08 in HaCaT and CaSki cells, respectively. The aforementioned gene had a very low impact on C33A viability by showing a Z-score of 1.2 .

With all the data taken together and based on the selection criteria, this cell-based assay has revealed that the depletion of GSG2 (Haspin), PRKCN, and PIK3CA caused a serious effect on CaSki viability (Z-score ≤ -2), but the effect was less on HaCaT or C33A viability (Z-score > -0.5). Another important finding using this assay was the effect of AURKA depletion on CaSki and HaCaT metabolic activity compared to C33A. The latter is a classic example of a potential target gene that when silenced affect only HPV-transformed but not non-HPV cervical cancer cells. However, HaCaT was added as a negative control but, unfortunately, the depletion of AURKA in HaCaT demonstrated low metabolic activity as seen in CaSki. CaSki is an HPV-transformed cervical cancer cells, whereas C33A is non-HPV cervical cancer cell line. HaCaT is a spontaneous immortalized keratinocytes that is non-HPV..

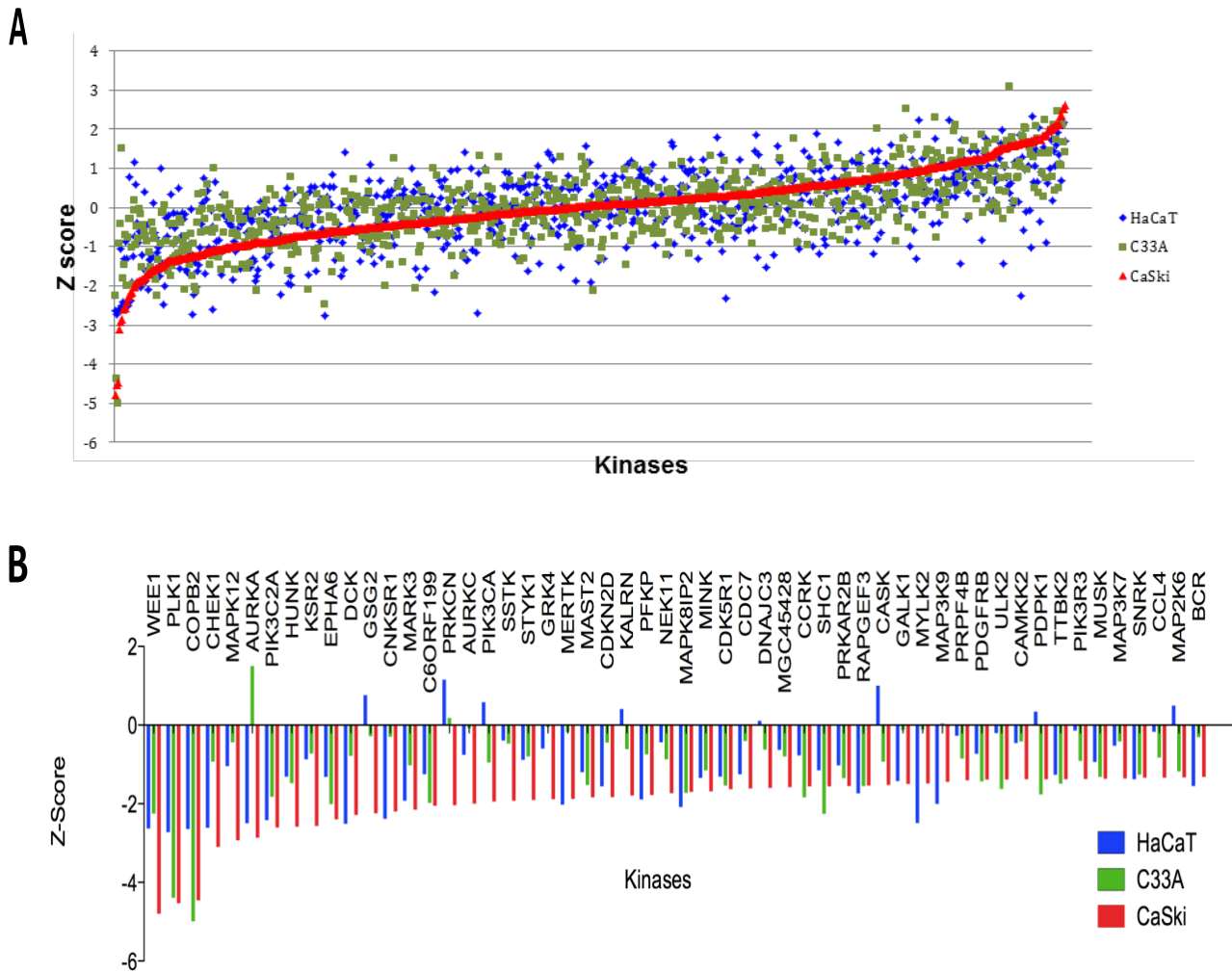


Figure 3.4. Cell viability of the primary screening of the human kinome library. **A** The Dharmacon Human siGENOME® SMARTpool® siRNA Library for Protein Kinases (targeting 779 genes) was screened at a final concentration of 50nM. A pool of four siRNAs targeted each gene. Transfection complexes were prepared and dispensed into 384-well plates for reverse transfection. After 72 h, resazurin dye was added into each well at a 44µM final concentration, and plates were incubated for 75 min at 37°C before being read by the FLOUStar plate reader for fluorescence detection. Each data point represents a mean Z-score of three replicates. **B** Zoom-in image of figure 3.4A to show the top 55 hits based on the cell viability assay sorted based on minimal CaSki Z-scores.

3.2.2.2 Cytotoxicity

Another cell-based assay that can help in finding target genes is the cytotoxicity assay. This assay is based on the leakage of the cytoplasmic adenylate kinase enzyme into the surrounding media once the cell membrane is disrupted. After 72 h post-transfection, 8 μ L of the media from each well of the primary plates was recovered to another 384-well plate for this purpose. The adenylate kinase substrate was then added to each well, and plates were incubated for 20 min at room temperature before the luminescence signals were detected using the FLUOStar plate reader.

The Z-score was calculated for each cell line, and genes were sorted according to the highest CaSki Z-score, as shown in (Figure 3.5A). The Z-scores that were set for selecting potential genes that affect CaSki cell integrity based on adenylate kinase activity were >1 Z-score for CaSki with <0.5 Z-score for C33A. The screening results demonstrated that the depletion of Aurora kinases A, B, and C affected CaSki cell integrity, causing high adenylate kinase activity in the cell media (Figure 3.5B). However, this strong effect was not seen in C33A. Furthermore, two other target genes, endoplasmic reticulum to nucleus signalling 1 (ERN1; also called ERI1) and heme regulated initiation factor 2 alpha kinase (HRI; also known as EIF2AK1), had the same effect as the Aurora kinases. The knockdown of these two kinases was highly cytotoxic to CaSki, with a lesser effect on C33A. On the other hand, the results revealed that STK39, CDKN1C, TLK1, CHUK, WEE1, and COPB2 had high luminescence signals on both cervical cancer cell lines, suggesting that the depletion of these genes was vital in CaSki and C33A cells. Although the HaCaT cell line was not included in this assay, the data revealed that the Aurora kinases are important when compared with the cell viability assay.

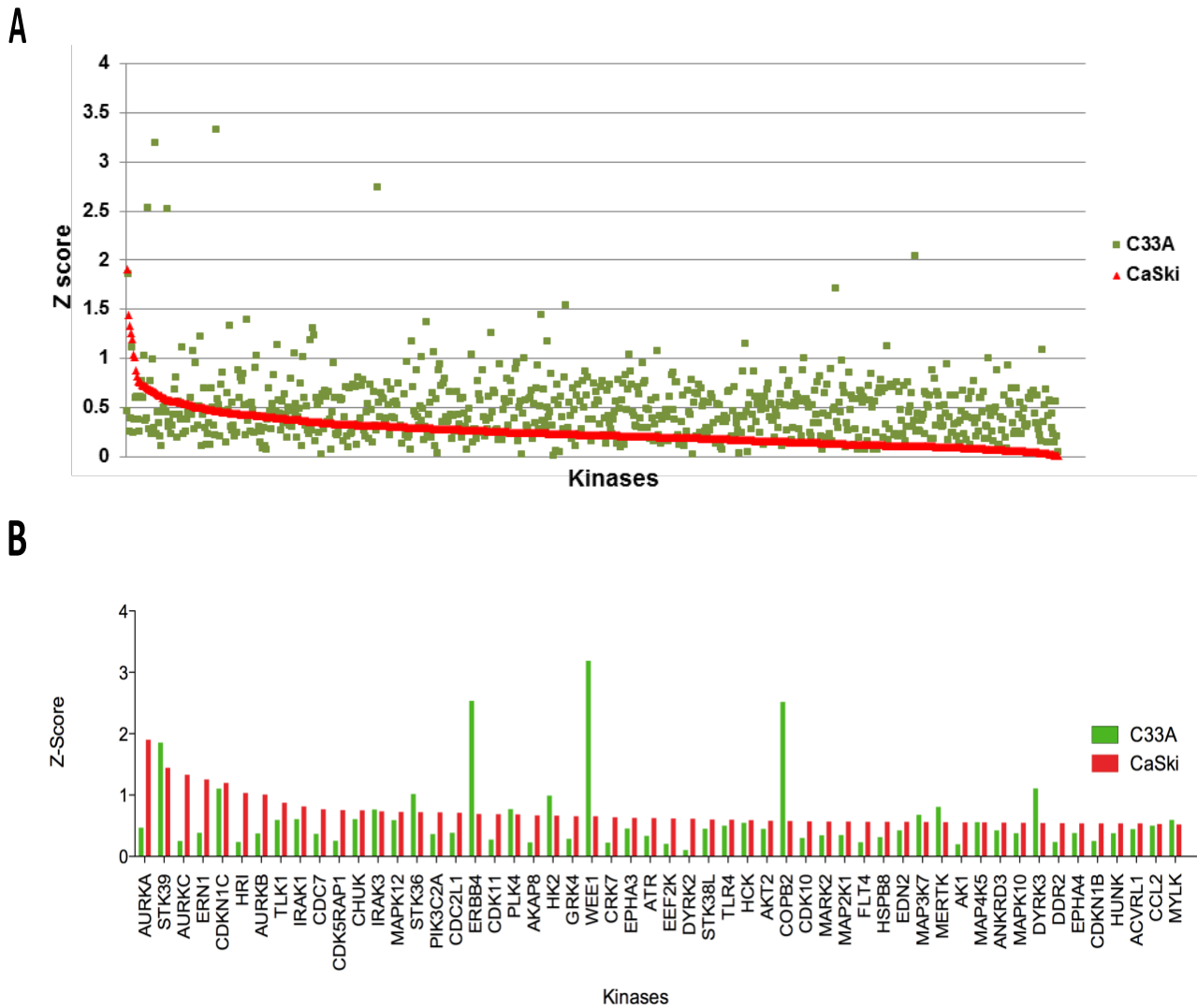


Figure 3.5. Adenylate kinase activity of the primary screening of the human kinome library. **A** The adenylate kinase substrate was added into each well and plates were incubated for 20 min at room temperature. Plates were then read by the FLUOStart plate reader for luminescence signal detection. Each data point represents a mean Z-score of three replicates. **B** Zoom-in image of figure 3.5A to show the top 55 hits based on cytotoxicity, sorted based on maximum CaSki Z-values.

3.2.2.3 Cell Number

Cell numbers for all cell lines were generated using the ArrayScan VTI analyser (Cellomics). All genes were sorted according to the minimum Z-score of CaSki that represents the lowest cell number of CaSki cells, as shown in (Figure 3.6A). The selection criteria for potential target genes were similar to the cell viability were CaSki Z-scores -2 (or less) with C33A/HaCaT Z-score of -0.5 (or higher). Unsurprisingly, the results demonstrated that PLK1 and WEE1 are at the top of the hits list, affecting all three cell lines and showing results consistent with the cell viability results (Figure 3.6B). Furthermore, the depletion of the Aurora A kinase caused a remarkable reduction in CaSki cell counts in comparison to C33A and HaCaT. Interestingly, the knockdown of GSG2 (Haspin) revealed an interesting result, as it resulted in the severe reduction of the CaSki cell count, whereas HaCaT and C33A were far less affected. Only two other genes came under the selection criteria; these include MAPK12 and PRKCN. Although this project focuses on the identification of genes that, when silenced, affect only HPV-transformed cells, the results revealed that the depletion of Aurora B kinases resulted in a similar reduction pattern for both cervical cancer cell lines, CaSki and C33A, but not for HaCaT. The latter finding may add a new area of interest in terms of finding genes that affect cervical cancer cells regardless of their HPV dependency.

The target genes that were found using the cell count measurement show high consistency when compared with the cell viability and cytotoxicity biological assays. Both WEE1 and PLK1 affected all cell lines, whereas GSG2 and Aurora A kinases showed a better outcome in affecting the HPV-transformed cell line, CaSki, with less effect on C33A and HaCaT.

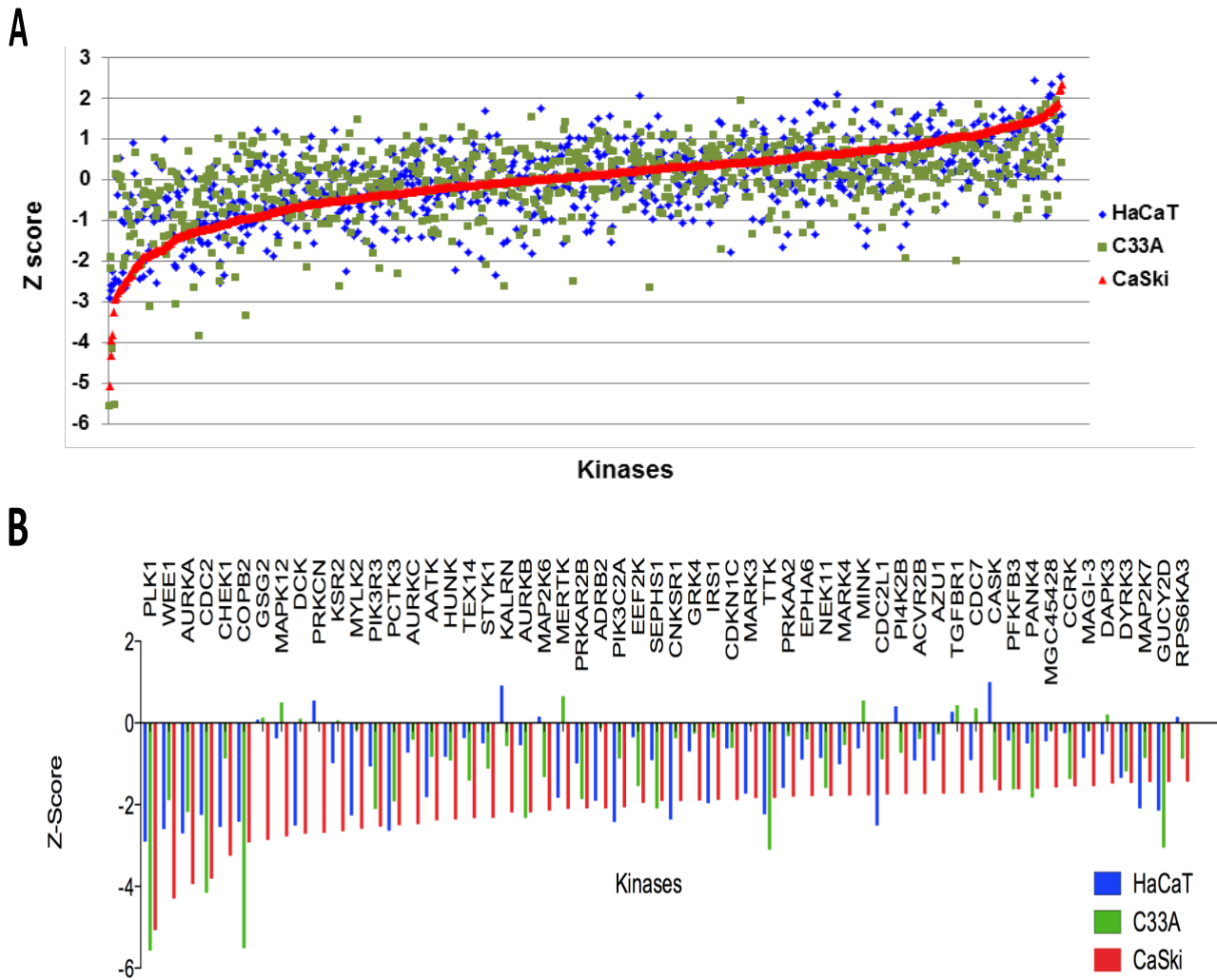


Figure 3.6. Cell numbers of the primary screening of the human kinome library. A Cells were fixed and stained with 400nM DAPI stain in 3% BSA and a cell count was performed by the ArrayScan VTI analyser (Cellomics). Each data point represents a mean Z-score of three replicates. **B** Zoom-in image of figure 3.6A to show the top 55 hits based on cell number, sorted based on the minimal CaSki Z-score.

3.2.2.3.1 *S-Phase Determination*

To determine the S-phase% of DNA replication, cells were labelled with 10 μ M EdU for 90 min before harvesting. In the present experiment, all genes were listed according to the minimum DNA replication of CaSki cells, represented by the minimum Z-score. The selection criteria used for potential target genes were similar to the previous criteria used in cell viability and cell number (Figure 3.7A). The results revealed that the knockdown of CDC2 caused all cell lines to have minimum DNA replication (Figure 3.7B). This finding was consistent with the cell number data, where the knockdown of the CDC2 gene was found to affect the cell numbers of all cell lines, regardless of their HPV dependency (Figure 3.7B). Additionally, based on the selection criteria of CaSki Z-score -2 (or less) whilst C33A/HaCaT should have -0.5 (or higher) Z-score, the data revealed that the depletion of CALM3 and CDKL1 were the top hits affecting CaSki DNA replication, with a lesser effect on HaCaT and C33A replication. Furthermore, some genes affect only cervical cancer cells' DNA replication, with minimal effect on the HaCaT cells, such as ANGPT4. However, sorting the genes based on the minimum DNA replication of CaSki cells did not show any overlapping genes, apart from the CDC2, with the previous assays. This is because cells were sorted based on blocking CaSki cells from entering S-phase regardless of what the other two cell lines show.

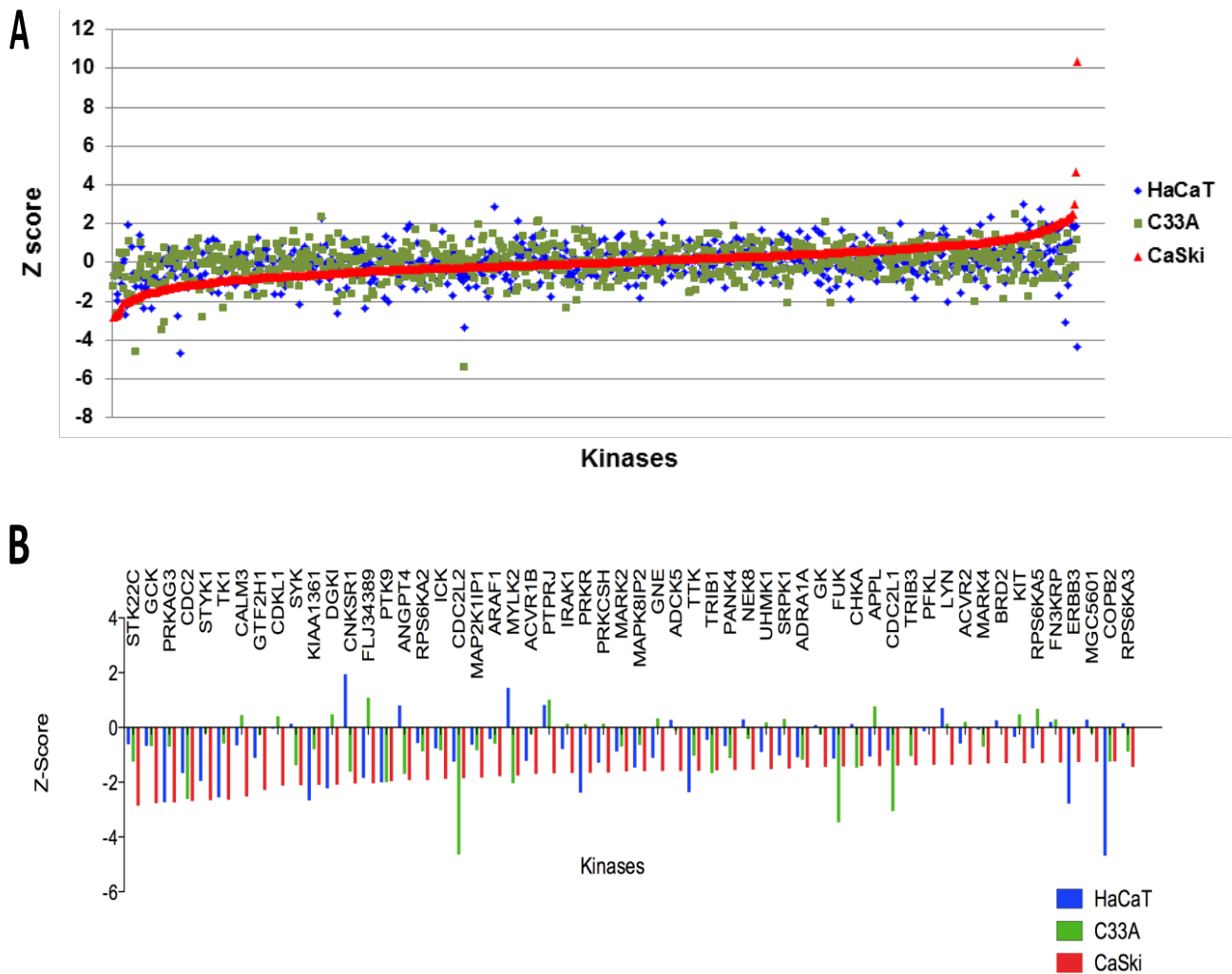


Figure 3.7. S-phase% determination of the primary screening of the human kinome library. A All cells were labelled with 10 μ M EdU. Cells were then subjected to click-reaction conditions and stained with 400nM DAPI in 3% BSA. Positive nuclei were detected using the ArrayScan VTI analyser (Cellomics). Each data point represents a mean Z-score of three replicates. **B** Zoom-in image of figure 3.7A to show the top 55 hits based on S-phase determination, sorted based on the minimal CaSki Z-score.

3.2.2.4 Hit Selection

Each biological assay that was used throughout the screening process has a main aim of use. For example, cells that die within the first 24 h because of a depletion of a particular gene may reflect a low bioluminescence signal of the adenylate kinase activity by 72 h as the signals weaken. Therefore, an additional parameter such as cell viability and/or cell number may be used to help interpret the results. Also, some cells might be metabolically active, viable, but their DNA stops replicating because of the silencing of a gene that affect DNA replication. Thus, the use of multi-biological parameters helps interpreting the results and, consequently, helps in selecting the best target genes. According to the cell biological assays that were conducted to monitor this screening, genes were divided into several categories, including genes that affect CaSki only (cervical cancer HPV-transformed cells), genes that affect cervical cancer cells only (CaSki and C33A cells), and genes that affect all cells (HaCaT, CaSki, and C33A). Because this project was designed to focus on the killing of HPV-transformed cells, the selection of hits was based on targets that, when depleted, caused major reduction in the cell viability and cell numbers of CaSki, but not for HaCaT or C33A. Both cytotoxicity and nucleotide incorporation assays were used as additional measures for more confidence in the selected hits. Based on these criteria, only 54 genes were selected for the validation screen later in this project (Table 3.2). Details of each candidate can be seen in Appendix 4.

Table 3.2. Selected hits for the validation screen

AURKB	MAPK12	RAGE	CKS1B	SSTK
AURKA	PKIA	FLJ10074	RSPH10B	IRAK3
PIK3R3	PIK3CA	CSNK1D	DCK	EGFR
DUSP10	TGFBR1	HUNK	NEK8	DGKE
BCL2	PRPSAP2	MAP3K2	MAP3K7	SYK
MARK3	PTPRJ	BMPR2	MAPK10	MINK
GSG2	MYLK2	PRKCN	GRK4	MAP2K6
CNKSRI	TEX14	MERTK	RPS6KA3	CASK
STK16	NEK7	STK22C	ACVRL1	CAMK1D
PRKAR2B	MAGI-3	PDIK1L	KSR2	AURKC
EPHA2	ADRB2	DAPK1	ANGPT4	-----

3.2.3 siRNA Secondary Screening

To validate genuine kinases and exclude any targets that were implicated by off-target siRNA effects, a secondary siRNA screening was performed using a new set of siRNA, the ON-TARGETplus SMARTpool siRNA (Dharmacon). This is a pool of four siRNAs per gene and differs from the previous Dharmacon Human siGENOME® SMARTpool® siRNA library, which was used in the primary screen, as it has been chemically modified by adding a 2'-O-methyl group to the sense strand. Also, the pool of four siRNA used at the primary screen were targeting different seeding regions than the regions that are targeted using the ON-TARGETplus SMARTpool siRNA. The main reason beyond using these ON-TARGETplus SMARTpool siRNA primarily was to reduce off-target effects. The library was screened at a final concentration of 40nM.

At this time, more cell lines were incorporated into the validation screen to increase confidence in the selected target genes and reduce cell line bias. The two cervical cancer HPV-transformed cell lines, HeLa (HPV18) and SiHa (HPV16), were added to the previous cell lines panel. As before, each cell line underwent optimization experiments, including seeding density, optimal transfection reagent and lipid concentration experiments were carried out for the newly incorporated cell lines. The same cell-based biological assays were used for the 54 targets throughout the validation screen.

The same statistical method was used to standardize the results through the Z-score (Chapter 2, 2.2.14 Screening Statistical Methods). In addition, the main hit validation criterion was based on *targets that repeated the same patterns/effects seen in the primary screen*. In other words, if the gene showed the same pattern that was noticed in the primary screen, it was considered a validated gene.

3.2.3.1 Cell Viability

To assess cell viability, cells were subject to the resazurin assay. The Z-scores were calculated and all genes were ranked based on the minimal viability of the CaSki HPV16-transformed cell line. Based on the selection criterion, only seven of 54 target hits demonstrated the same patterns noticed in the primary screen (Figure 3.8). Of these, the depletion of the testis-specific serine kinase 3 TSSK3 (STK22C) had a lethal effect on all cervical cancer cell lines but not on HaCaT. Surprisingly, the knockdown of GSG2 (Haspin) showed a strong reduction in the viability of HeLa

HPV-transformed cell line (Z-score -2.6). The impact of depleting Haspin did not demonstrate the same effect on the other HPV-transformed cell lines, CaSki and SiHa. The depletion of Haspin, however, had only a minor effect on C33A and HaCaT. Because the main aim of this project was to find novel target genes that, when silenced, kill only E6/E7-expressing cells but not others; the only target that met this criterion partially was Haspin. Additionally, it is highly essential to select final target genes based on all the biological assays used throughout the screening process rather on a single parameter.

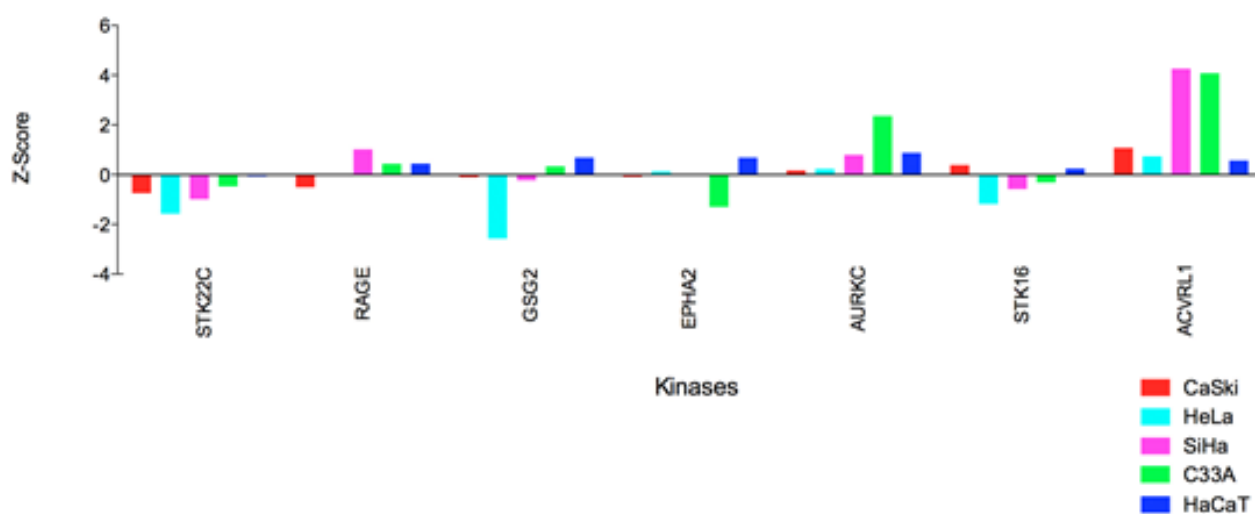


Figure 3.8. Validated target hits using Dharmacon ON-TARGETplus SMARTpool siRNA based on the viability assay. All cells were reverse transfected with the chemically modified siRNA at a final concentration of 40nM. The resazurin dye was added into each well of the 384-well plates at 44uM for fluorescence detection. All genes were sorted based on the lowest Z-score value of the HPV-transformed cell line, CaSki (HPV16). Out of the 54 genes tested, these hits repeated the effect that was seen in the primary screen. Each data point represents a mean Z-score of three replicates.

3.2.3.2 Cytotoxicity

According to the selection criterion of the validated targets, of the 54 screened genes, only 18 kinases repeated the same pattern that was noticed throughout the primary siRNA screen (Figure 3.9). Among all the validated genes, the depletion of both Aurora kinases A and B demonstrated a high level of adenylate kinase activity on the CaSki cells when compared with the other HPV-transformed cell lines. Although HaCaT is not an HPV-positive cell line, it showed higher luminescence signals than the other non-HPV cell line, C33A, and the HPV-transformed cell line,

SiHa. Notably, the knockdown of GSG2 (Haspin) and the deoxycytidine kinase (DCK) were found to affect the cell integrity of CaSki and HeLa, leading to high level of adenylate kinase leakage. This effect was less in SiHa, C33A, and HaCaT. Another interesting target that demonstrated high cytotoxicity to HPV-transformed cell lines but not the others was serine/threonine kinase 16 (STK16). The knockdown of STK16 showed relatively higher luminescence signals in CaSki, HeLa, and SiHa when compared with C33A and HaCaT. Furthermore, mitogen-activated protein kinase 12 (MAPK12) and the ribosomal protein S6 kinase (RSP6KA3) showed high adenylate kinase activity on the cervical cancer, HPV-transformed cell lines and HaCaT, but not on the other cervical cancer, non-HPV cell line, C33A. Although the cytotoxicity assay revealed interesting targets that are worth further investigation, target selection based on different biological parameters was necessary to ensure consistency and the main focus of the project remains on those targets that, when depleted, affect the cell integrity of HPV-positive cell lines but not others, such as AURKB, AURKA, GSG2, DCK, and STK16.

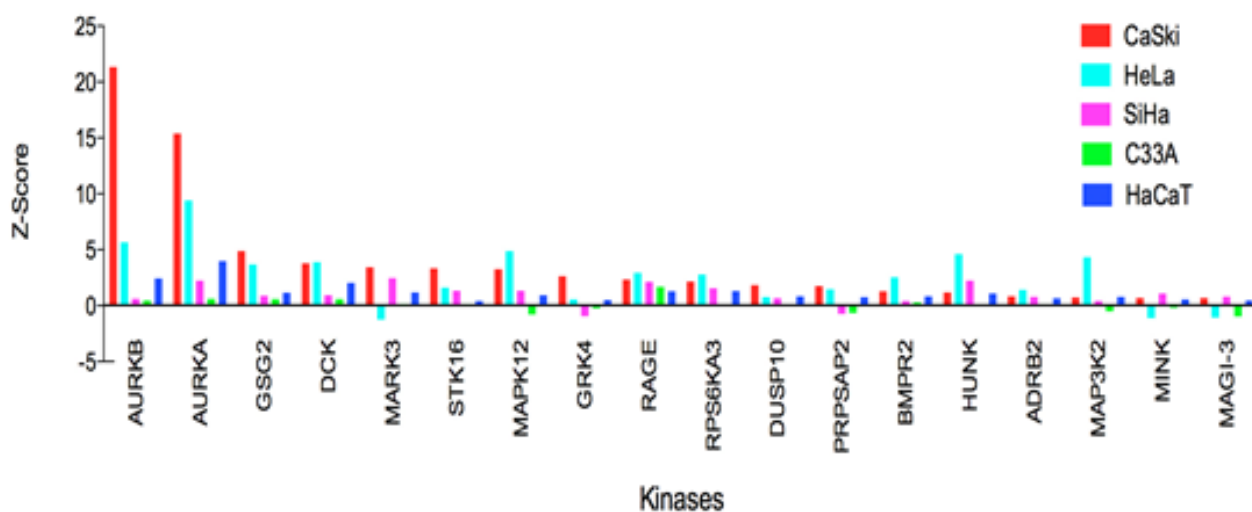


Figure 3.9. Validated target hits based on adenylate kinase activity. Cells were reverse transfected with a pool of four ON-TARGETplus SMARTpool siRNAs at a final concentration of 40nM. Upon transfection, the adenylate kinase substrate was added into each well and luminescence signals were detected. The represented 18 candidate genes were sorted based on the highest Z-score value of the CaSki (HPV16) cell line. Each data point represents a mean Z-score of three replicates.

3.2.3.3 Cell Numbers

Cell numbers can reflect the viable cells within the plates. Of the 54 genes, only 14 genes repeated the patterns that were noticed during the primary screen. Upon calculating the Z-score, all genes were ranked based on the lowest CaSki Z-score, which reflects the lowest cell number counted in the wells (Figure 3.10). Aurora B kinase (AURKB) was on the top of the candidate hits. The depletion of the latter had a severe impact on the viability of all cervical cancer cell lines, regardless of their HPV background. However, this effect was not seen in HaCaT, non-HPV, and non-cervical cancer cell lines. Furthermore, the silencing of the Aurora A kinase (AURKA) also demonstrated remarkable reduction in cell numbers in both CaSki and HeLa, Z-scores of -9.3 and -7.2, respectively. This effect was not seen in SiHa (Z-score -0.2). Both non-HPV cell lines had higher Z-values compared to SiHa but far less compared to CaSki and HeLa HPV-transformed cell lines. Moreover, the depletion of the phosphoinositide-3-kinase regulatory subunit (gamma) (PIK3R3) and myosin light chain kinase 2 (MYLK2) showed low cell numbers in all HPV-transformed cell lines but not in C33A and HaCaT. In addition, both GSG2 (Haspin) and STK16 had a similar effect on CaSki and HeLa, demonstrating low Z-scores when compared to other cell lines. The data obtained from the cell count are relatively consistent with the cytotoxicity results, suggesting confidence in the validated target hits. Aurora kinases A and B, together with GSG2, STK16, and PIK3R3, are promising validated candidate genes based on the cell number data.

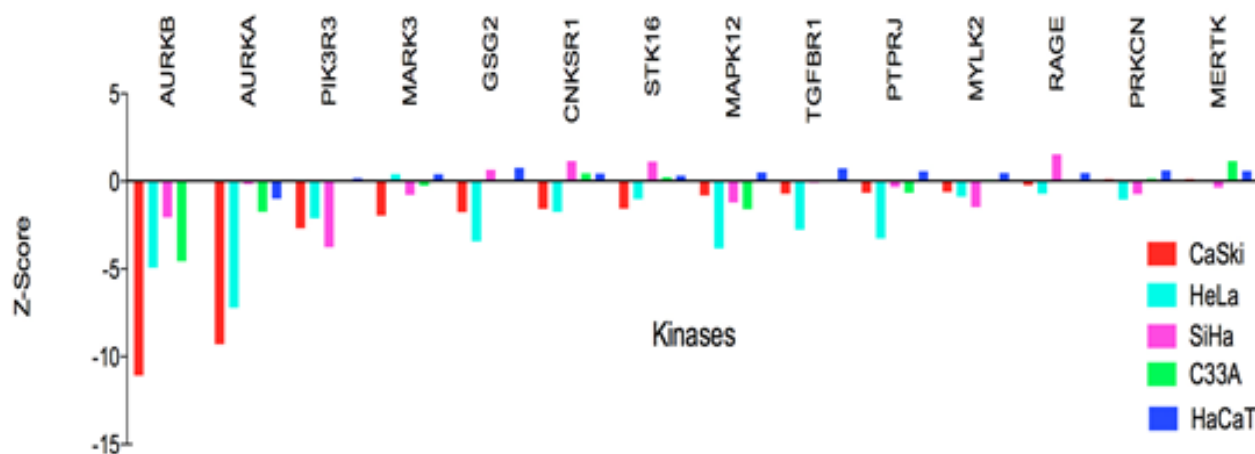


Figure 3.10. siRNA-validated target hits based on cell count. Following siRNA transfection, cells were fixed and stained with 400nM DAPI in 3% BSA and counted using the ArrayScan VTI analyser (Cellomics). Z-

scores were calculated and genes ranked based on the lowest Z-values of the CaSki cells. Each data point represents a mean Z-score of three replicates.

3.2.3.4 *Final hit selection*

The main aim of this project was to find novel target genes that when depleted become only lethal to cervical cancer HPV-transformed cells but not others. Furthermore, to ensure results consistency and to increase confidence in selecting real target hits, four different assays were used based on two different forms of pool siRNAs (siGENOME SMARTpool and the ON-TARGETplus SMARTpool siRNA), although the EdU assay used during the secondary siRNA screen did not show targets with similar patterns to those selected from the primary siRNA screening; this is primarily because of the purpose of the present work sought to look for genes that when deplete affect cell viability (cell killing) rather than DNA. To exclude off-target effects and to validate hits, a secondary screen was conducted and more HPV-transformed cell lines were incorporated, HeLa and SiHa. Based on the criterion of genes when silenced affect only HPV-transformed cells with minor effect on non-HPV cells, only 6 genes were validated to have this effect. These genes are AURKB, AURKA, GSG2, STK16, CNKSR1, and PIK3R3. Figure 3.11 summarizes the effect of these genes on a panel of cervical cancer HPV-transformed and non-HPV cell lines as well as HaCaT cell line.

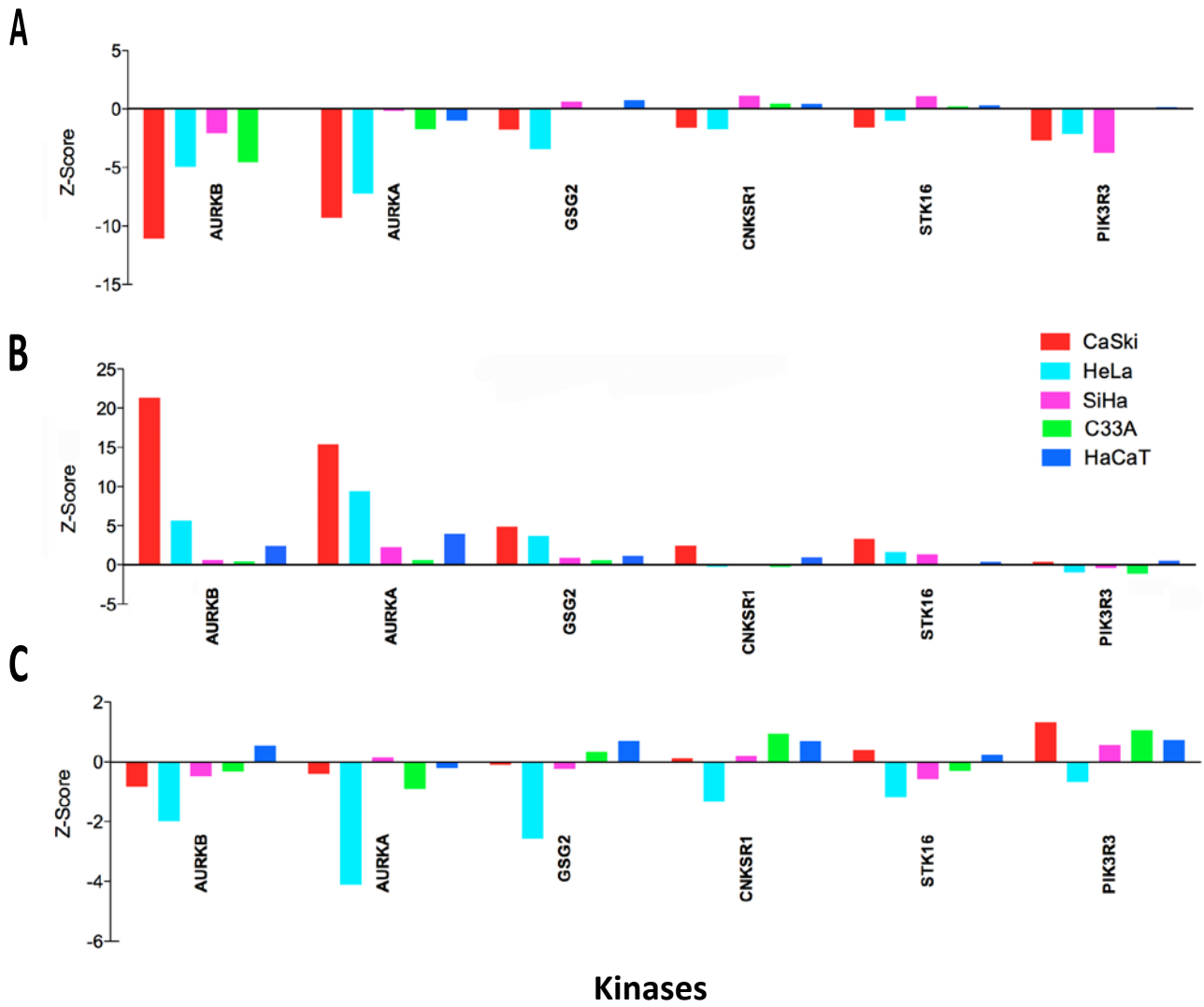


Figure 3.11. Summary of selected target hits based on three cell biological assays : including A cell number; B cytotoxicity; and C cell viability.

3.2.4 Confirming AURKA and AURKB knockdown by the ON-TARGETplus SMARTpool siRNA

Both AURKA and AURKB are mitotic regulators that showed interesting selectivity to the majority of the HPV-transformed cervical cancer cell lines and both targets have commercially available small molecule inhibitors. Therefore, the ON-TARGETplus SMARTpool siRNA against AURKA and AURKB were used to confirm the knockdown by Western blotting. Both siRNA were used at a final concentration of 20nM. The data demonstrates that the silencing of AURKA and AURKB by the ON-TARGETplus SMARTpool siRNA was able to reduce the protein levels when compared to the non-targeting siRNA in all the tested cell lines (Figure 3.12 – densitometry data are shown in Appendix 5). These data also support the previously shown data of AURKA and AURKB using different biological assays throughout the primary and the secondary screens, as these targets are real target hits.

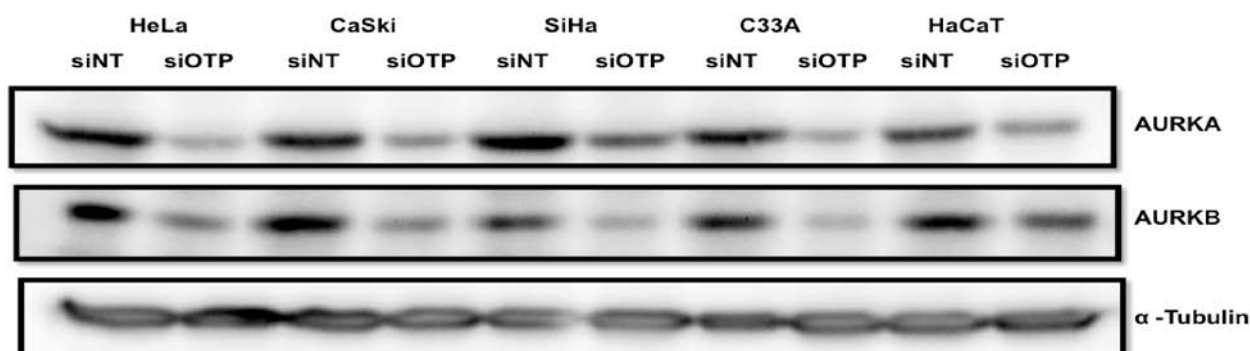


Figure 3.12. AURKA and AURKB ON-TARGETplus SMARTpool siRNA successfully decreased protein level. Cells were seeded and reverse transfected with either Aurora A kinase (AURKA) or Aurora B kinase (AURKB) ON-TARGETplus SMARTpool (siOTP) at a final concentration of 20nM and pellet was collected 24 h after transfection was performed. Non-targeting siRNA (siNT) was used as a control. Western blot imaging was acquired using Fusion ChemiDoc gel documentation system.

3.3 Discussion

The objective of this project was to use a synthetic lethality approach using a high-throughput siRNA screen to identify novel genes which when depleted are lethal only in HPV-transformed cervical cancer cells, with no (or minor) effect on other cells. This concept has been successfully applied in various other cancers. Luo *et al.* found a pathway involving PLK1 that is synthetically

lethal to Ras mutant cells (Luo et al., 2009). The inhibition of this pathway results in accumulation of cells in prometaphase resulting in the death of Ras mutant cells. In another study, a synthetic lethal siRNA screen identified target genes that potentiate the growth inhibitory outcome of gemcitabine in pancreatic cancers when silenced (Azorsa et al., 2009). The study found that the depletion of checkpoint kinase 1 (Chk1) is a putative therapeutic target for sensitizing pancreatic carcinoma cells to gemcitabine.

Although synthetic lethal screens have shown promising results, effective implementation of high-throughput siRNA screens necessitates optimized conditions that permit maximum transfection efficiency and low cytotoxicity. Therefore, for any high throughput siRNA screen, assay development must precede the actual screenings. Accordingly, all the cell lines used throughout the primary and validation siRNA screens were tested against several transfection conditions including seeding densities, transfection agents, and lipid concentrations.

A key measurement that precedes any high-throughput siRNA screen is the selection of a proper transfection agent with a suitable concentration that is neither highly diluted nor cytotoxic. Transfection reagents that induce a cytotoxic effect can adversely affect reproducibility and may vary gene expression after transfection (LaPan et al., 2008). Additionally, proper negative controls, particularly the Dharmacon non-targeting siRNA, were optimized. According to earlier reports, the Dharmacon non-targeting siRNA is more toxic to cells compared to another set of non-targeting siRNA such as Ambion (Thaker et al., 2010). This is a classic example that shows the importance of testing several positive and negative siRNA controls in addition to other optimization conditions.

The availability of commercial siRNA libraries, such as the kinome and druggable genome, has made focused library siRNA screens possible. In the present study, I performed a primary high throughput siRNA screen using the kinome library consisting of 779 genes from Dharmacon. This siGENOME library has a pool of four siRNAs each targeting the same gene within the well at different sites on the mRNA. I included three cell lines CaSki (cervical cancer HPV16 cell line), C33A (cervical cancer non-HPV cell line), and HaCaT (non-cervical cancer, non-HPV, spontaneously immortalized keratinocyte cell line). The screening revealed that two kinases, PLK1 and Wee1, severely affected all cell lines regardless of their HPV transformation status. The knockdown of both PLK1 and Wee1 resulted in very few cells going through S-phase as shown by

the nucleotide incorporation assay data. PLK1 is an essential cell cycle gene that has a low expression profile during G₁ and S phases (Strebhardt and Ullrich, 2006). It begins to rise during G₂ and peaks at the M phase of the cell cycle. It plays a significant role in ensuring the fidelity of the checkpoint controls. PLK1 is becoming a gene of interest in many cancer investigations as its depletion results in apoptosis. Wee1 is a protein kinase that regulates G₂ checkpoint in response to DNA damage. Wee1 phosphorylates and inactivates cyclin-dependent kinase 2-bound cyclin E, and consequently, controls the regulation of DNA replication through S-phase. Silencing Wee1 sensitizes many cancer cells, such as ovarian, colon, osteosarcoma, and lung, to DNA damage by irradiation (Wang et al., 2001, Wang et al., 2004b, PosthumaDeBoer et al., 2011). Therefore, it is not surprising that depleting PLK1 or Wee1 using siRNA would eventually result in low viability and lower cell number as well as blocking cells' entry into S-phase.

Although the viability assay and cell number revealed overlapping results of PLK1 and Wee1, the cytotoxicity assay was inconsistent with these data. For example, Wee1, but not PLK1, was within the top 50 hits based on the cytotoxicity assay. Such variations in this biological assay may occur as each assay has different principles, and targets different cellular events. The cytotoxicity assay is based on detecting the cytoplasmic adenylate kinase activity, which is a marker for loss of cell integrity (or cell death), whereas the resazurin cell viability assay is based on determining cellular metabolic capability (Cho et al., 2008, O'Brien et al., 2000). The siRNA that targeted PLK1 may have depleted the gene resulting in complete cell death within the first 24 h of transfection that was reflected by low cell count. The adenylate kinase, therefore, does exist in the culture media but may not be suitable to emit strong luminescence signal upon the completion of the experimental timeframe as it probably loses its enzymatic activity. This may explain the consistency of viability, cell number and the nucleotide incorporation assays of cells transfected with PLK1 siRNA in compare to the cytotoxicity assay result.

This project focuses on the identification of novel target genes that are lethal only to HPV-transformed cervical cancer cells. Among all the biological assays used throughout the primary screen, 54 genes were selected for further validation (Table 3.2). Among these 54 genes, there were some targets that severely affected CaSki, but not C33A including AURKA, AURKB, AURKC, GSG2, CNKSR1 and PRKCN. However, some of these genes were not validated by a secondary

screen to exclude siRNA off-target effects. The siGENOME SMARTpool siRNA, which was used in the primary screen, differs from the ON-TARGETplus SMARTpool smart pool siRNA (Dharmacon) that was used in the secondary screen, as the latter is a chemically modified siRNA (Jackson et al., 2006, Dua et al., 2011). Although another form of siRNA was used in the validation screen, the Aurora kinases A and B in addition to GSG2 (Haspin) were in the top hits that affected majority of HPV-transformed cervical cancer cells but not the non-HPV cells.

Haspin was a target hit that came through primary and validation screens. The depletion of Haspin affected at least two cervical cancer HPV-transformed cells (CaSki and HeLa), but the impact was less on the C33A. Haspin is a kinase that is involved in mitosis where it phosphorylates histone H3 at threonine-3 (hH3-Thr-3) and plays a crucial role in chromosome behaviour throughout cell division (Dai and Higgins, 2005, Dai et al., 2005, Tanaka et al., 1999). However, hH3-Thr-3 plays an imperative role in activating Aurora B. Both hH3-Thr-3 and Aurora B localize on the inner centromere. Wang *et al.* found that the hH3-Thr-3 places the chromosomal passenger complex (CPC) that encompasses Aurora B at the centromere to regulate selected targets of AURKB during mitosis (Wang et al., 2010). In another report, Wang and colleagues provided evidence of AURKB activity that triggers a positive feedback loop consisting of CPC-Haspin-hH3-Thr-3 to promote the generation of hH3-Thr-3 on chromatin (Wang et al., 2011a). These reports of AURKB-Haspin cross-talking and the implication of AURKB in different neoplastic disorders may pave the way for researchers to further investigate the role of Haspin in cancer models (Hegyí and Mehes, 2012, Gully et al., 2010, Yeung et al., 2008, Takeshita et al., 2013).

Aurora A and B are additional target hits that were validated throughout the secondary validation screen. Aurora kinases represent a family of three members (AURKA, AURKB, and AURKC) that belong to serine/threonine kinases, and these are highly required for cell cycle control (Katayama and Sen, 2010). Although they share large homology similarities, each member of the family has a distinct function. Aurora A primarily participates in centrosome function, cell mitotic entry, and spindle assembly. Aurora B, on the other hand, is involved in chromatin modifications, microtubule kinetochore attachment, spindle checkpoint, and cytokinesis (Bernard et al., 1998, Tang et al., 2006, Gautschi et al., 2008, Gautschi et al., 2006, Smith et al., 2005). I observed that in the primary screen, the depletion of AURKA strikingly resulted in low viability of CaSki cells, high adenylate

kinase activity, and few cells undergoing DNA replication. This effect was not seen in C33A cells when AURKA was depleted. These results were also reproducible when the validation screen was performed on a larger cervical cancer cell line panel. The depletion of the AURKA affected the growth of CaSki and HeLa with minor impact on SiHa cells. The major differences between the two types of cervical cancer cell lines tested in this project are: (i) the presence of the E6/E7 HPV oncogenes in the HPV-transformed cell lines and; (ii) the status of p53 as the HPV-induced cervical cancer cell lines have wild-type p53 whereas the non-HPV have mutant p53. In 2010, Shin *et al.* showed that the transfection of a wild type C33A cell line with HPV-E6 significantly increased the radiosensitivity of the cells when compared to vector-only transfected C33A (Shin et al., 2010). These findings support the idea that AURKA depletion may have triggered apoptotic pathway in the CaSki and HeLa HPV-transformed cells, but not the cervical cancer non-HPV C33A cells. Additionally, the HPV-transformed cervical cancer cell lines have a major difference among them as each cell type has different HPV DNA copy numbers, which may have contributed to the degree of sensitivity towards the depletion of AURKA.

I have also validated Aurora B, another aurora kinase family member, in the screen. Knocking down AURKB in the primary screen resulted in low viability and high adenylate kinase activity of the CaSki cells, suggesting cells death. This effect was further validated in HeLa cell line with less effect on SiHa cells. However, the C33A and HaCaT cells were not as remarkably affected by the depletion of AURKB as the HeLa or CaSki HPV-transformed cervical cancer cell lines. It has been reported that AURKB has an interactive and/or regulatory relationship with p53 (Ikezoe et al., 2010, Wu et al., 2011a). This cross talking between AURKB and p53 occurs at the centromere. Because the HPV-transformed cervical cancer cell lines differ from the non-HPV as the latter has a mutated p53 (Crook et al., 1991), this might be a reason that the depletion of AURKB has affected CaSki and HeLa more than C33A and HaCaT. Furthermore, as indicated in the previous section, the viral DNA copy number may have been a reason to why SiHa as an HPV-transformed cervical cancer cell line did not show similar patterns compared to HeLa and CaSki.

The results of this chapter have clearly demonstrated that siRNA high throughput synthetic lethal screen is a powerful tool to identify novel target genes in cancer models. Also, it shows the importance of optimizing proper screening conditions in a miniaturize screen prior to the actual

screening. Three mitotic regulators, AURKA, AURKB, and Haspin, have demonstrated strong lethality effect on HPV-transformed cervical cancer cell lines but not the non-HPVs. Due to the availability of commercialized small molecule inhibitors for Aurora A and B kinases and their known implications in different cancer types, Aurora B and Aurora A are the investigative subjects of Chapter 4 and Chapter 5 of this thesis, respectively.

4 Aurora B small molecule inhibitor, ZM447439, is not selective for HPV-transformed cell lines

4.1 Introduction

The primary and the secondary screens that were performed in this project validated top hits including GSG2 (Haspin), AURKB and AURKA. These hits were highly lethal in HPV-transformed cervical cancer cells but not the non-HPV panel. Obviously, all three target hits are mitotic regulators. Haspin, for example, phosphorylates histone H3 at threonine 3 (hH3Thr3). Haspin plays crucial role in chromosome alignment during mitosis. It was reported that the knockdown of Haspin by RNAi resulted in failure of metaphase chromosome alignment and activation of the spindle assembly checkpoint (Higgins, 2010). As Haspin phosphorylates histone H3 at threonine-3, it also provides a docking site for the Aurora B kinase (AURKB) complex at the centromere. Although Haspin has not previously been reported to be associated with cancer, Haspin-AURKB cross talk may help understand the role of Haspin in cancer and as a potential anti-cancer target.

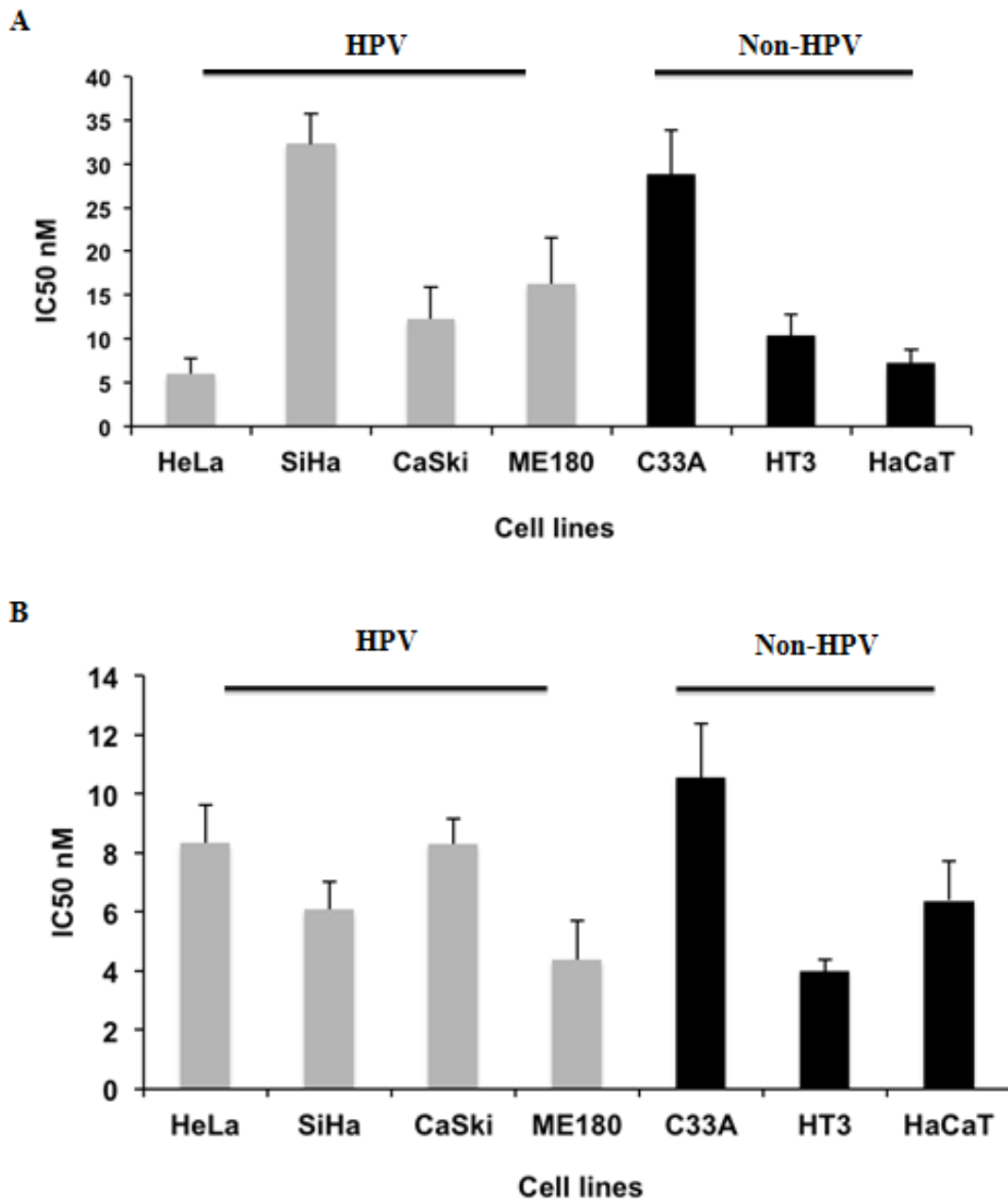
The Aurora kinase family comprises closely related threonine/serine kinases that play fundamental roles in the cell cycle (Carmena et al., 2009). As indicated in the previous chapter, these proteins are involved in the different stages of cell division, including centrosome duplication, spindle formation, chromosome alignment, mitotic checkpoint activation, and cytokinesis. AURKB is a member of the Aurora kinase family (Hegyi and Mehes, 2012, Katayama and Sen, 2010). *Aurora B* is located on chromosome 17p13.1, a region that is not normally amplified in human malignancies (Hegyi et al., 2012). Despite this, the mRNA and protein levels of Aurora B are increased in some neoplastic disorders such as colorectal cancer (Alferez et al., 2012). Aurora B is a key cell cycle component where its expression peaks at the G₂-M transition and is maximal during mitosis. Aurora B first localizes to the chromosome during prophase and then to the centromere during prophase and metaphase. It is activated by the inner centromeric protein (INCENP) and shows maximum activity during metaphase and telophase. The important substrates of Aurora B include the mitotic checkpoint proteins BubR1 and Mad2, INCENP, survivin, borealin, and histone H3 (Gabielli et al., 2011, Uehara et al., 2013). Aurora B phosphorylates histone H3 at Ser10 and is implicated in chromosome condensation and mitotic entry.

During the primary and secondary siRNA screening in this project, Aurora B was found to be a potential target that was more effective in HPV-transformed cervical cancer cells than in non-HPV cervical cancer cells. Based on this finding, this potential target gene was further investigated using the commercially available Aurora B inhibitor (ZM 447439), which is the focus of this chapter. The chapter also discusses whether these mitotic targets found throughout the screening processes were HPV-related hits.

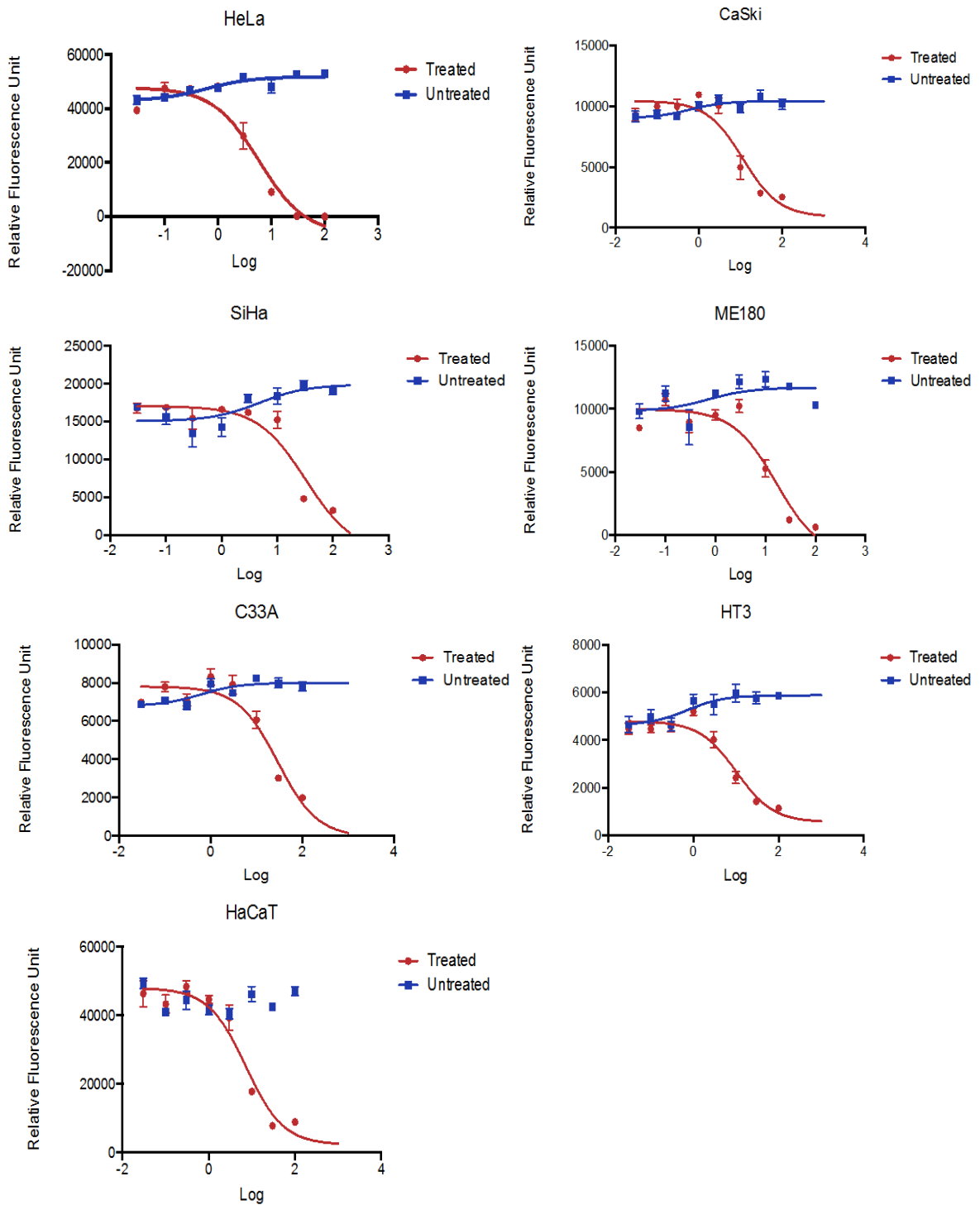
4.2 Results

4.2.1 Inhibiting AURKA, AURKB, and Haspin is specific to HPV-induced cell lines

Throughout the primary and secondary siRNA screening, the mitotic regulators Aurora A, Aurora B, and GSG2 (Haspin) were found to be potential targets that were more lethal to HPV-transformed cells. All these three genes are essential in mitosis. This observation raised the question whether interrupting mitosis may produce a similar phenotype. To test whether there was an HPV-selectivity of targeting these genes or it is only a consequence of targeting mitosis, two small-molecule inhibitors were introduced, the Polo-like kinase 1 (PLK1) mitotic small-molecule inhibitor (BI-2536) (Haupenthal et al., 2012), and paclitaxel (taxol). Both drugs were examined in a panel of HPV-transformed and non-HPV cancer cell lines using dose-response experiments. All cell lines were subject to the viability assay using resazurin dye. The results showed that, regardless of the HPV status of the cells, all cervical cancer cell lines in addition to HaCaT, non-cervical cancer, non-HPV cell line, were highly sensitive to both drugs (Figure 4.1 A and B), with IC_{50} in nanomolar range for each drug. This experiment demonstrates that HPV selective loss of viability with depletion of the newly discovered mitotic targets AURKA, AURKB, and GSG2 (Haspin) using siRNA, in cervical cancer (as indicated in Chapter 1) is not a generic targeting of mitosis effect but likely to reflect specific dependence of HPV-transformed cells on these targets. In other words, interrupting mitosis with the BI-2536 and taxol did not generate the same effect seen when AURKA, AURKB, or Haspin were depleted with siRNA.



C



D

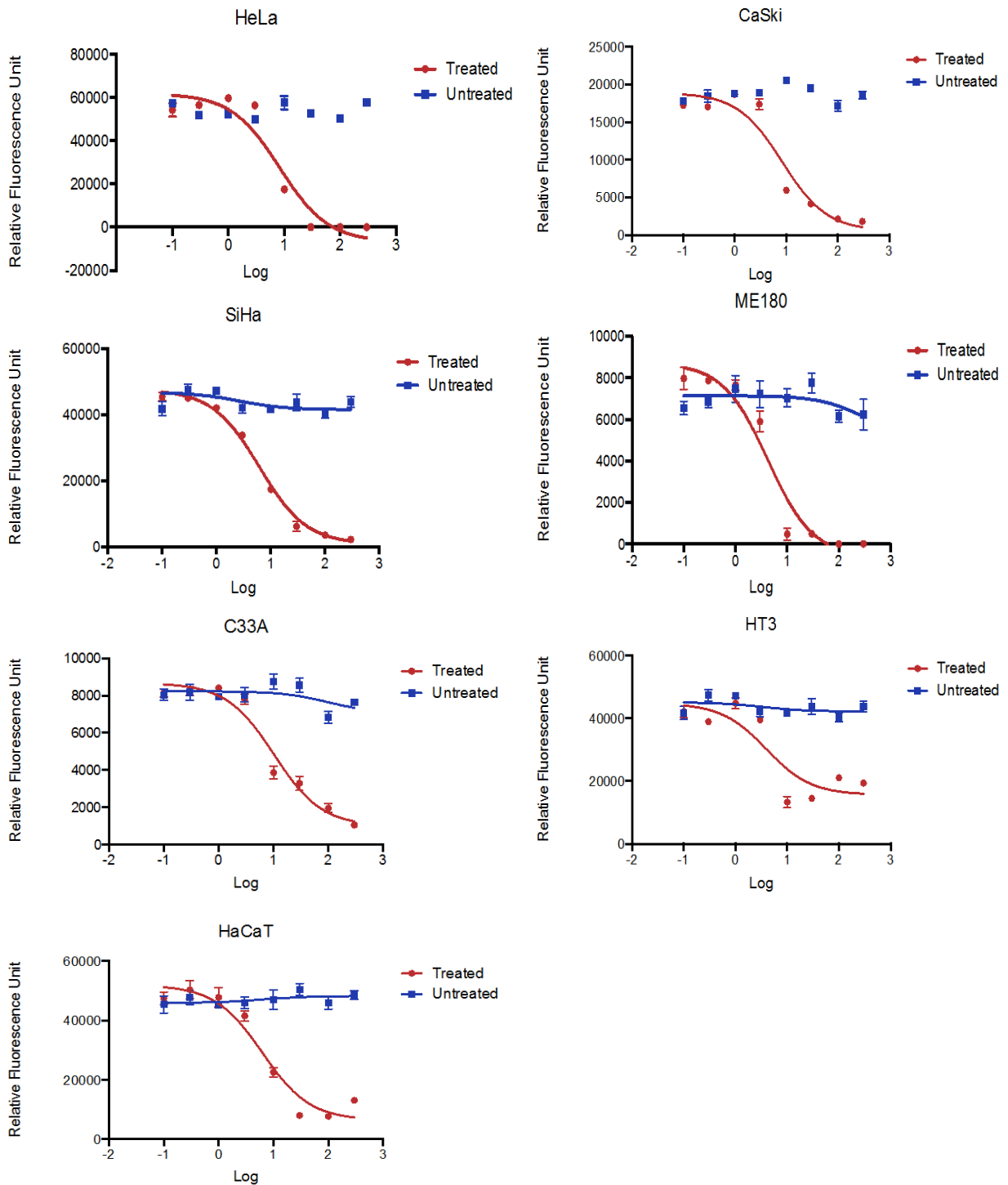
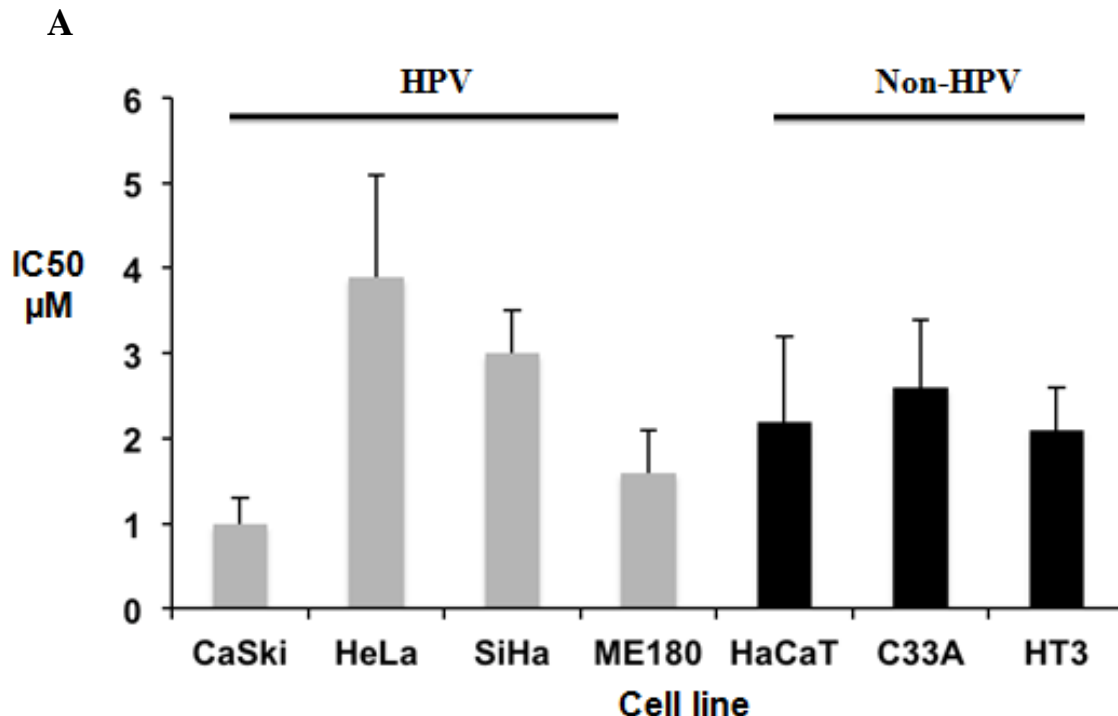


Figure 4.1. PLK1 small molecule inhibitor (BI-2536) and paclitaxel did not show selectivity towards either HPV or non-HPV cervical cancer cell lines. A Summary of the IC₅₀ values generated from a dose-response

experiment showing the effect of the paclitaxel (taxol) on a panel of HPV and non-HPV cervical cancer cell lines. **B** IC_{50} values for the same cell panel treated with the PLK1 inhibitor (BI-2536). In both experiments, cells were subject to a viability assay using the resazurin dye 44 μ M after 72 h of drug treatment (dose range 100-30-10-3-1 nM, 300 and 100 pM). Each point is the mean and standard error mean (SEM) of quadruplicate determinations. IC_{50} was calculated using GraphPad Prism V.6.0. In both **A** and **B** the small molecules affected all cell lines in nanomolar range regardless of their HPV transformation status. Dose-response curves of both experiments in all cell lines are shown in C (taxol) and D (BI-2536).

4.2.2 Aurora B small-molecule inhibitor (ZM 447439) selectivity

As indicated in the previous chapter, AURKB was a potential target that worth further investigations. In that regard, I took advantage of the commercially available small molecule inhibitor for AURKB (ZM447439) and investigated its effect on all HPV-transformed and non-HPV cervical cancer cell lines, and HaCaT cells. The calculated IC_{50} values demonstrated slight difference between HPV-transformed and non-HPV cervical cancer cell lines, including HaCaT. These data suggest that the Aurora B small molecule inhibitor ZM 447439 had no significant differential response that would make it a potential target in cervical cancer HPV-transformed or cervical cancer non-HPV cell lines using ZM447439.



B

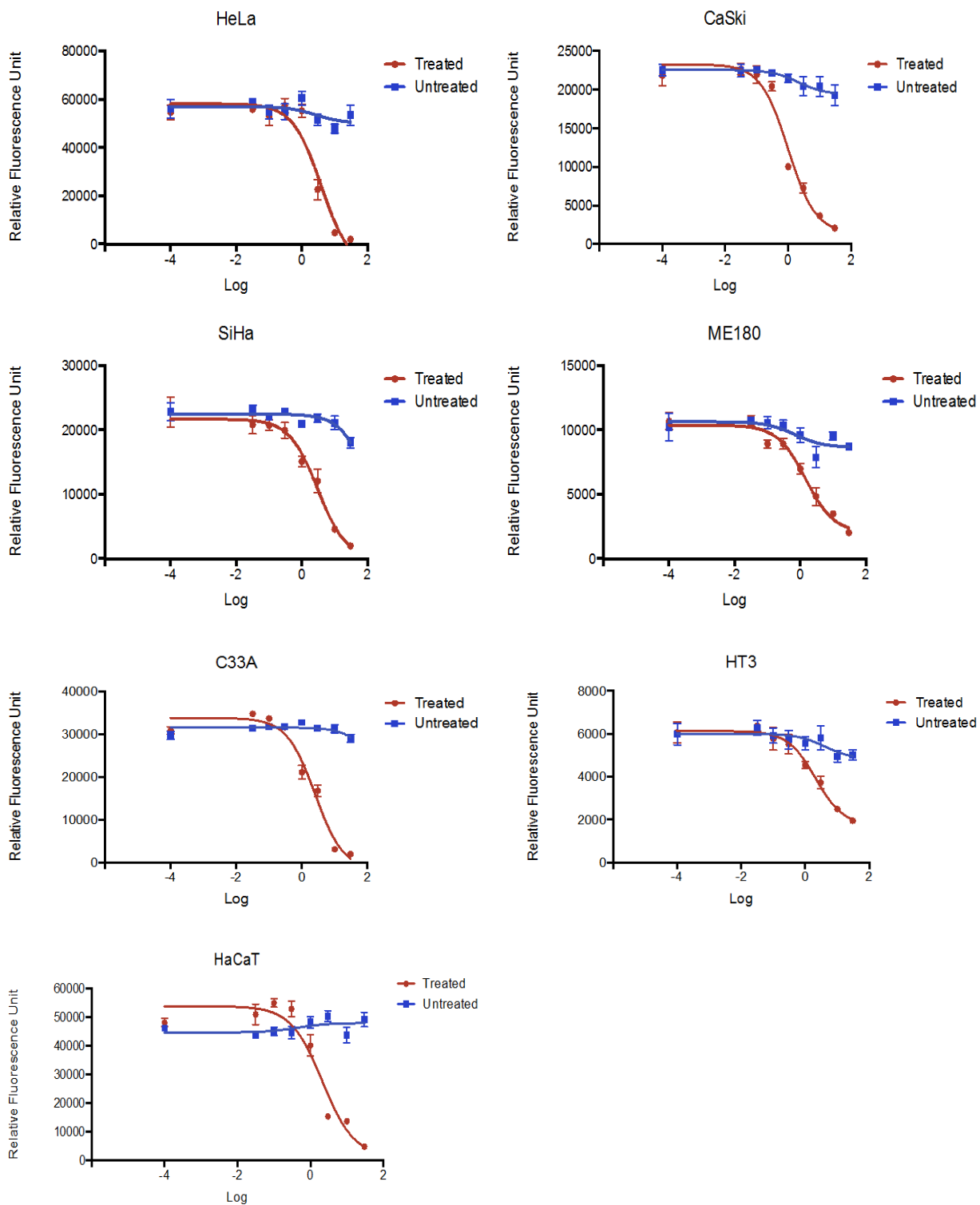
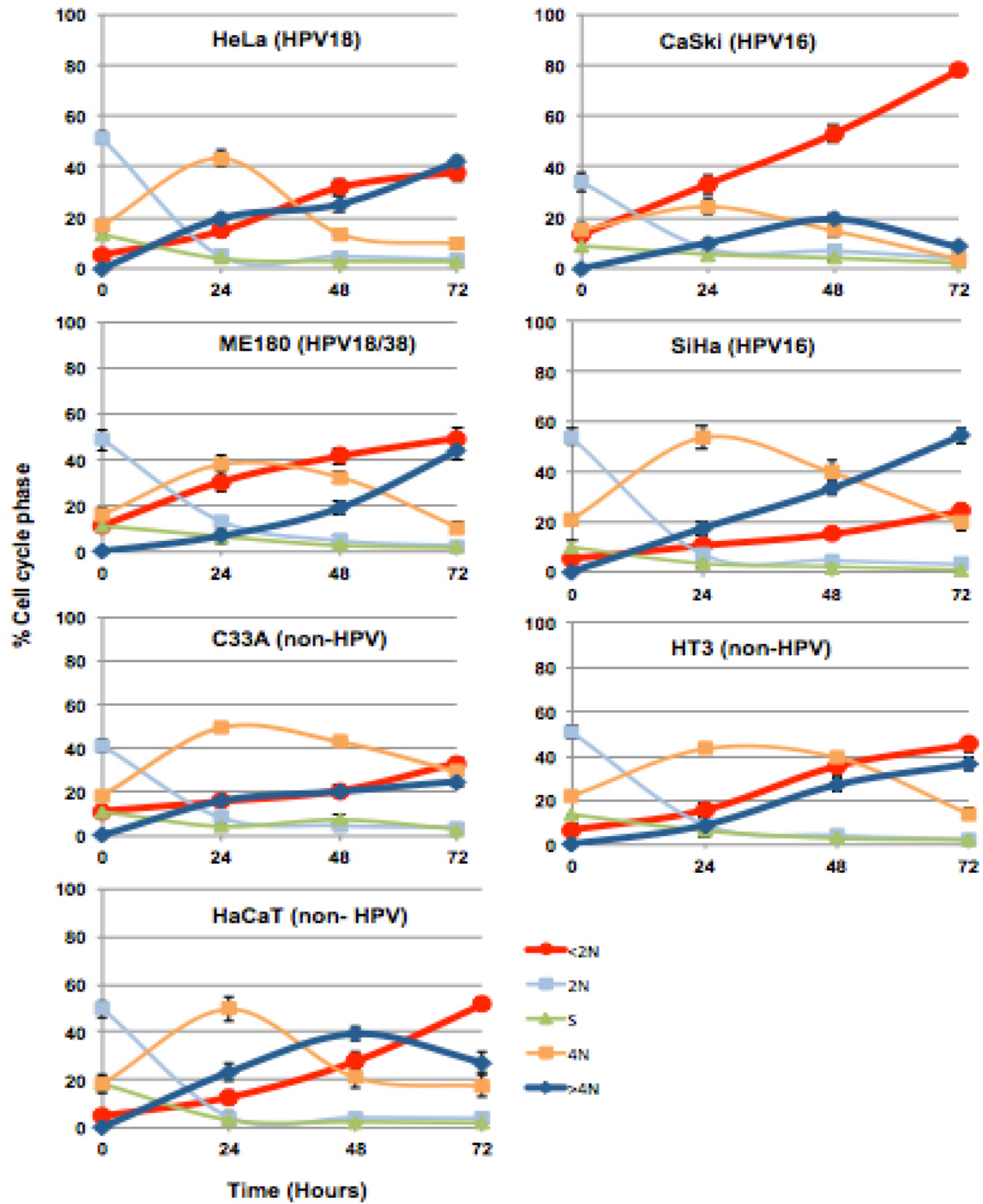


Figure 4.2. Aurora B small-molecule inhibitor ZM 447439 showed no selectivity towards HPV-transformed cervical cancer cells. **A)** Summary of the IC_{50} values for ZM 447439 in a panel of HPV-transformed and non-HPV cervical cancer cell lines, in addition to HaCaT, in a dose-response experiment. Cells were subject to viability assays using resazurin dye at final concentration of $44\mu\text{M}$ after 72 h of treatment with the inhibitor (dose range 30-10-3-1 μM – 300, 100 and 30 nM). Each point is the mean and standard error mean (SEM) of quadruplicate determinations. IC_{50} was calculated using GraphPad Prism V.6.0. All cell lines showed differential response to the treatment but did not demonstrate any selectivity based on HPV-transformation status. **B)** Dose-response curves of all cell lines treated with the ZM447439.

4.2.3 Suppression of Aurora B activity by ZM 447439 induces accumulation of 4N and >4N DNA contents

As previously shown that ZM 447439 did not show HPV selectivity, here I investigated the effect of this inhibition on both HPV-transformed cell lines and non-HPVs. All cells were subject to DNA content analysis using flow cytometry. Cells were treated with 5 μM ZM 447439 for 24, 48, and 72 h in addition to DMSO (vehicle) only treated cells. With 24 h of treatment, it was found that ZM 447439 resulted in accumulation of cells in G_2/M , induction of greater than 4N populations, and an obvious reduction in 2N population size regardless of HPV status (Figure 4.3). This effect was noticed in all cell lines including cervical cancer and non-cervical cancer, HaCaT, cells. After 48 h of treatment, the CaSki, and HaCaT cells reached their maximal >4N population, which indicates failure of cytokinesis. However, the remaining cell lines, HeLa, ME180, SiHa, C33A, and HT3, reached their maximal >4N population at 72 h of treatment. Additionally, treatment of cells with ZM 447439 resulted in a high apoptotic population in a time-dependent manner in all the tested cell lines, indicated by the increased sub-diploid population (<2N). These data suggest that the selectivity of the Aurora B small-molecule inhibitor ZM 447439 is not based on the HPV status of the cell line.

A



B

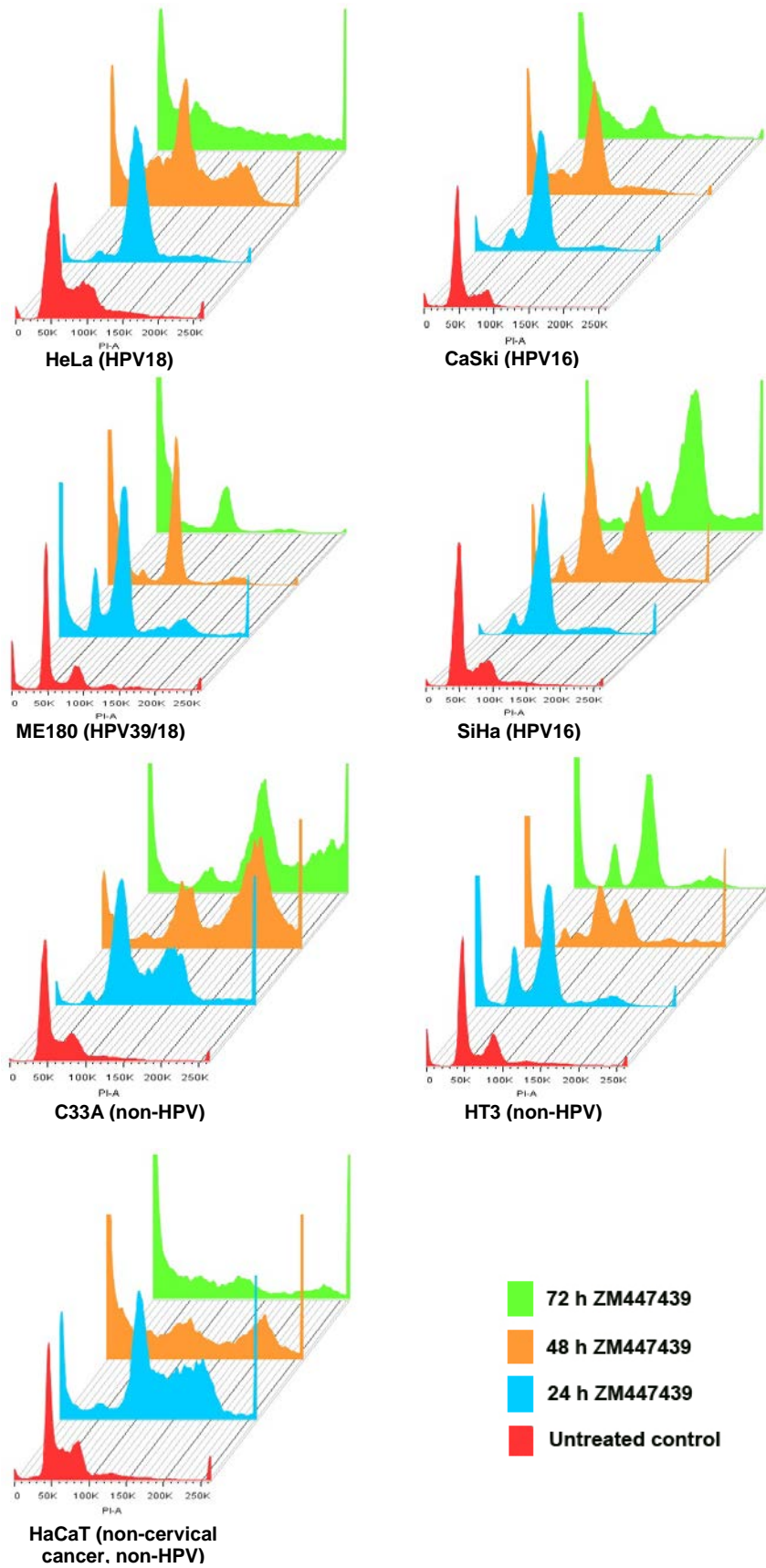


Figure 4.3. ZM447439 induced aneuploidy and high apoptotic profiles on time-dependent manner in all tested cell lines regardless of their HPV-transformation status. A) DNA content was analyzed using fluorescence-activated cell sorting (FACS). All cells were treated with 5 μ M ZM 447439 and collected at 24, 48, and 72 h. DMSO control only cells were collected after 24 hours and plotted as zero time on the graph. Each cell line had a negative control that was treated with the vehicle only (DMSO). The experiment was performed in three biological replicates and the error bars represent the SEM of three biological replicates. Data were processed using FlowJo V.2.0. B) Examples of the FACS histograms are shown from each tested cell line.

4.3 Discussion

Understanding the mechanism of cell division and faithful transmission of genetic materials from parental cells to daughter cells is a challenging area in cell biology. Cell division is a tightly regulated process where actively dividing cells pass through the cell cycle that comprises four defined stages including G₁, S, G₂, and M. At the end of the M (mitotic phase), cells undergo cytokinesis where they divide into two daughter cells. In the primary and secondary high-throughput screening carried out in this study, the siRNA depletion of three mitotic regulators, AURKA, AURKB, and Haspin, was found to be lethal for at least two HPV-transformed cell lines (HeLa and CaSki) with less effect on SiHa. The effect of depleting AURKB had severe impact on HaCaT viability but not as much on C33A (non-HPV cervical cancer cell line). The identification of the three mitotic regulators (AURKA, AURKB, and Haspin) may suggest that disrupting mitosis by targeting other mitotic regulators/events may result in the same HPV selectivity at least in CaSki and HeLa cell lines. The treatment of all HPV-transformed cervical cancer cell lines and the non-HPV cell lines with the Polo-like kinase 1 (PLK1) small molecule inhibitor (BI-2536) induced apoptosis in all the cells regardless of their HPV-transformation status. Harris and colleagues reported that the depletion of PLK1 by siRNA in medulloblastoma cell lines caused mitotic arrest (defect in mitosis followed by failure of cytokinesis), and induction of the apoptotic machinery (Harris et al., 2012). These findings were consistent with the report of Reagan-Shaw, where he showed that the depletion of PLK1 by siRNA caused the similar apoptotic outcome in prostate cancer cells (Reagan-Shaw and Ahmad, 2005). Earlier studies have shown that the knockdown of PLK1 by siRNA interrupts mitotic cell cycle progression through cell division cycle 25C (Cdc25C) and Cdc2/cyclin B1 positive feedback loop (Bu et al., 2008, Reagan-Shaw and Ahmad, 2005, Roshak et al., 2000). Additionally, several studies have demonstrated similar effect of PLK1 small molecule inhibitors such as MLN0905 and NMS-P937 (Valsasina et al., 2012, Shi et al., 2012). The use of these small molecule

inhibitors with different cancer cell lines resulted in significant increase in cells with 4N DNA content, which indicates considerable G₂/M block. This prolonged mitotic arrest was next followed by cell apoptosis. The data on the small molecule inhibitors and siRNA in the above studies was consistent with the findings of the present study where all cervical cancer cell lines, HPV-transformed and non-HPV, demonstrated high sensitivity to the PLK1 small molecule inhibitor indicating loss of viability at low (nanomolar) range.

As discussed earlier, the PLK1 small-molecule inhibitor was not found to be selective for HPV-transformed or non-HPV cervical cancer cell lines. To confirm this unselective response, another antimitotic agent, paclitaxel (taxol) was tested on the same panel. Taxol enhances tubulin polymerization and stabilizes microtubules and, subsequently, affect the normal breakdown of microtubules during cell division (Vyas and Kadow, 1995, Wan et al., 2004). This stabilization of the microtubule polymers enables chromosomes to achieve a metaphase spindle configuration, which consequently block the progression of mitosis and trigger apoptosis. In their study, Jordan *et. al.* showed that using taxol in low concentrations (10nM) in HeLa cells induces almost 90% mitosis block at the metaphase/anaphase transition eventually leading to apoptosis (Jordan et al., 1996). Our data on the use of taxol in the cervical cancer HPV-transformed and non-HPV cell lines was in agreement with the previous findings. Taken together, our data suggests that the use of two anti-mitotic small molecule inhibitors, PLK1- BI-2536 and taxol, showed no selectivity against cervical cancer HPV-transformed cell lines. Thus, confirming that the lethality in HeLa and CaSki cells as HPV-transformed cervical cancer cell lines that was produced when AURKA, AURKB, or Haspin were depleted using siRNA (as shown in Chapter 1) was in fact related to the HPV-transformation status of the cell, not a consequence of targeting mitosis or a mitotic event.

Aurora B kinase over-expression has been implicated in different malignancies; therefore, it is not surprising that several studies were carried out to unleash the importance of targeting AURKB as a potential therapy (Buczkwicz et al., 2013, Portella et al., 2011, Esposito et al., 2009). It has been described in the previous chapter that the depletion of AURKB by siRNA results in a lethal effect on the majority of HPV-transformed cervical cancer cell lines with minor effect on the C33A. Previous studies have shown that targeting AURKB prevents chromosomal alignment, and alteration of the spindle checkpoint function, followed by failure of cytokinesis and eventual loss of

cell viability (Ditchfield et al., 2003, Girdler F et al., 2006). The inhibition of AURKB activity was not only confirmed by RNAi study but also by using small-molecule inhibitors such as ZM447439 and AZD1152. Previous studies have demonstrated that the use of AZD1152 inhibitor induced polyploidy in acute myeloid leukaemia (AML) cell lines that indicate anti-proliferative activity of the drug, which in most cases led to apoptosis (Oke et al., 2009, Yang et al., 2007). Additionally, the drug was tested on Burkitt's, Hodgkin's lymphomas and multiple myeloma cell lines (Mori et al., 2011, Evans et al., 2008). It was noted that inhibition of AURKB activity resulted in accumulation of > 4N DNA content and induction of caspase-dependent apoptosis.

Another AURKB small-molecule inhibitor that has been widely used to inhibit AURKB activity is ZM447439. Previous reports have shown that ZM447439 inhibitor blocked cells in G₂/M transition, which leads to apoptosis by activating caspase 3 and 7 (Georgieva et al., 2010, Gadea and Ruderman, 2005). Zhang *et al.* (2011) further demonstrated that ZM447439 induced G₂/M cell cycle arrest and apoptosis in SiHa cervical cancer cell line (a HPV16-transformed cell line) (Zhang and Zhang, 2011). This report was focused on the synergistic effect between ZM447439 and cisplatin, a clinical approved chemotherapeutic agent. Therefore, the study included only SiHa as an HPV-transformed cervical cancer cell line and not non-HPV cell lines. These findings are consistent with the findings of the present study where the use of ZM447439 in cervical cancer cell lines induced significant G₂/M arrest within the first 24 hours of the treatment. This was followed by the induction of > 4N DNA content confirming the failure of cytokinesis and subsequent increase in the sub-diploid population. Interestingly, the small molecule inhibitor induced apoptosis in all the cervical cancer cell lines regardless of their HPV-transformation status and did not show any HPV selectivity. In contrast, the silencing of AURKB by siRNA (as indicated in Chapter 1) was lethally selective for at least CaSki and HeLa HPV-transformed cervical cancer cell lines.

The mode of action of siRNA and kinase small molecule inhibitors is completely different where the latter only inhibits the activity of the protein whilst the former degrades the messenger RNA (mRNA) and prevents protein translation. As siRNA prevents protein translation, it is then expected that protein-to-protein interactions will be completely lost. On the other hand, the majority of the small-molecule inhibitors target the kinase an ATP active site, and because there have been more than 500 kinases discovered in the human genome where each one has a ATP active site, there is

higher probability of cross-reactivity (Manning et al., 2002). For instance, using binding assays, VX-680 (Tozasertib), Aurora kinase inhibitor, was also found to bind to T3151 mutant of BCR-ALB1 (Carter et al., 2005, Harrington et al., 2004). Further characterization and co-crystallography of the T3151 mutant have supported this data (Young et al., 2006). Thus, despite the availability of large number of small molecule inhibitors, limited data are available on the selectivity of regularly used compounds.

In 2010, Harvard Medical School developed a new online library called Library of Integrated Network-based Cellular Signature (LINCS) that can be used to investigate the specificity of some small molecule inhibitors based on the binding assays for small-molecule kinase interactions (<https://lincs.hms.harvard.edu>) (Manning et al., 2002, Fabian et al., 2005). After using the online database to investigate the specificity of the ZM447439, it was found that the compound has several off-target effects. Additionally, AURKB make a part of the passenger chromosomal complex (CPC) together with surviving, borealin, and inner centromere protein (INCENP). The depletion of AURKB activity by siRNA tends to delocalise and destabilise other CPC members. This effect prevents the correct function of CPC at the centromere. In contrast, inhibiting AURKB activity by small molecules leaves the CPC intact and correctly localize. Taken together, these investigations might explain the non-selectivity of ZM447439 to the HPV-transformed cell lines when compared with the siRNA results.

The first result of this chapter confirms that the discovery of three mitotic regulators (AURKA, AURKB, and Haspin) as top siRNA screening hits, as shown in the previous chapter, was not a consequence of targeting mitosis. Indeed, the effect that was generated when these targets were depleted was actually selective to HPV-transformation status of the cells. This was demonstrated when mitosis was disrupted with two small molecule inhibitors, PLK1 and taxol, and showed no selectivity toward HPV-induced cervical cancer cell lines. Furthermore, the current chapter demonstrates that AURKB small molecule inhibitor, ZM447439, caused induction of > 4N DNA content indicating failure of cytokinesis followed by initiation of apoptosis. More importantly, the inhibitor did not show consistency with the siRNA results as the former did not show selectivity for the HPV-positive cell lines. In fact, all cell lines had the same effect regardless of their HPV-transformation status.

5 Aurora A small molecule inhibitor, MLN8237, is selective for HPV-transformed cervical cancer cells

5.1 Introduction

Aurora A kinase is a key mitotic regulator, which functions in centrosome assembly duplication and separation, microtubule to kinetochore attachment, spindle checkpoint and cytokinesis (Dar et al., 2010, Karthigeyan et al., 2010). It also plays a vital role in maintaining proper genomic integrity. Overexpression and gene amplification of Aurora A kinase has been reported in different cancer types and is associated with increased proliferation rates (Kops et al., 2005, Anand et al., 2003). The critical roles of Aurora A kinase in mitotic progression and its potential oncogenic activity has prompted the development of small molecule inhibitors as targeted anticancer therapeutic agents. Several Aurora kinases small molecule inhibitors have been developed. MLN8237 is an orally bioavailable compound that specifically targets Aurora A kinase. It exhibited high efficacy against many solid and hematological malignancies in preclinical models, and is currently in advanced clinical trials (Qi et al., 2013, Mosse et al., 2012, Matulonis et al., 2012, Dees et al., 2012, Gorgun et al., 2010).

The high-throughput synthetic lethal siRNA screens undertaken in this project identified Aurora A kinase as a validated hit that when depleted reduced the viability of HPV-transformed, but not the non-HPV cervical cancer cells. This observation was further validated to be specifically HPV-related in chapter 4 of this thesis where two mitotic small molecule inhibitors, taxol and BI-2536 PLK1 inhibitor, were tested and showed apoptotic phenotype regardless of cellular HPV-transformation. This evidence, in addition to the published reports that link Aurora A kinase to malignancies, suggested that Aurora A kinase was a likely target. In this chapter, the effect of inhibiting Aurora A kinase using the small molecule inhibitor MLN8237 in panels of HPV-transformed, non-HPV cervical cancer and non-cervical cancer cell lines was assessed. It shows that the sensitivity to MLN8237 is specifically HPV-related. Finally, the chapter demonstrates the efficacy of this compound *in vivo*, providing evidence of its therapeutic potential for the treatment of HPV-induced cervical cancer.

5.2 Results

5.2.1 MLN8237 showed selectivity for HPV-transformed cervical cancer cell lines

To determine the selectivity of MLN8237 for HPV-transformed cervical cancer cell lines, our panel of cervical cancer cells was subject to a resazurin-based viability dose-response experiment. The results showed that at least three HPV-transformed cells, HeLa, CaSki, and ME180, were highly sensitive to the inhibitor and indicated loss of viability with an IC_{50} of less than $1\mu M$, although SiHa did not demonstrate a similar trend (Figure 5.1A). The non-HPV cervical cancer cell lines revealed differential responses. The C33A had the highest IC_{50} ($14.3\mu M$) compared to the remaining panel either HPV or non-HPV. Furthermore, the HT3 showed a low IC_{50} ($2.1\mu M$) compared to the C33A but higher than HeLa, CaSki, and ME180 HPV-induced cell lines. Additionally, HaCaT as a non-HPV non-cervical cancer cell line showed a low IC_{50} value of $0.05\mu M$. The difference in sensitivity was not a consequence of differences in the proliferative rate of the cells, as the doubling-time of each cell line was similar (Figure 5.1B). Taken together, this data suggest HPV cell line selectivity that worth further investigation

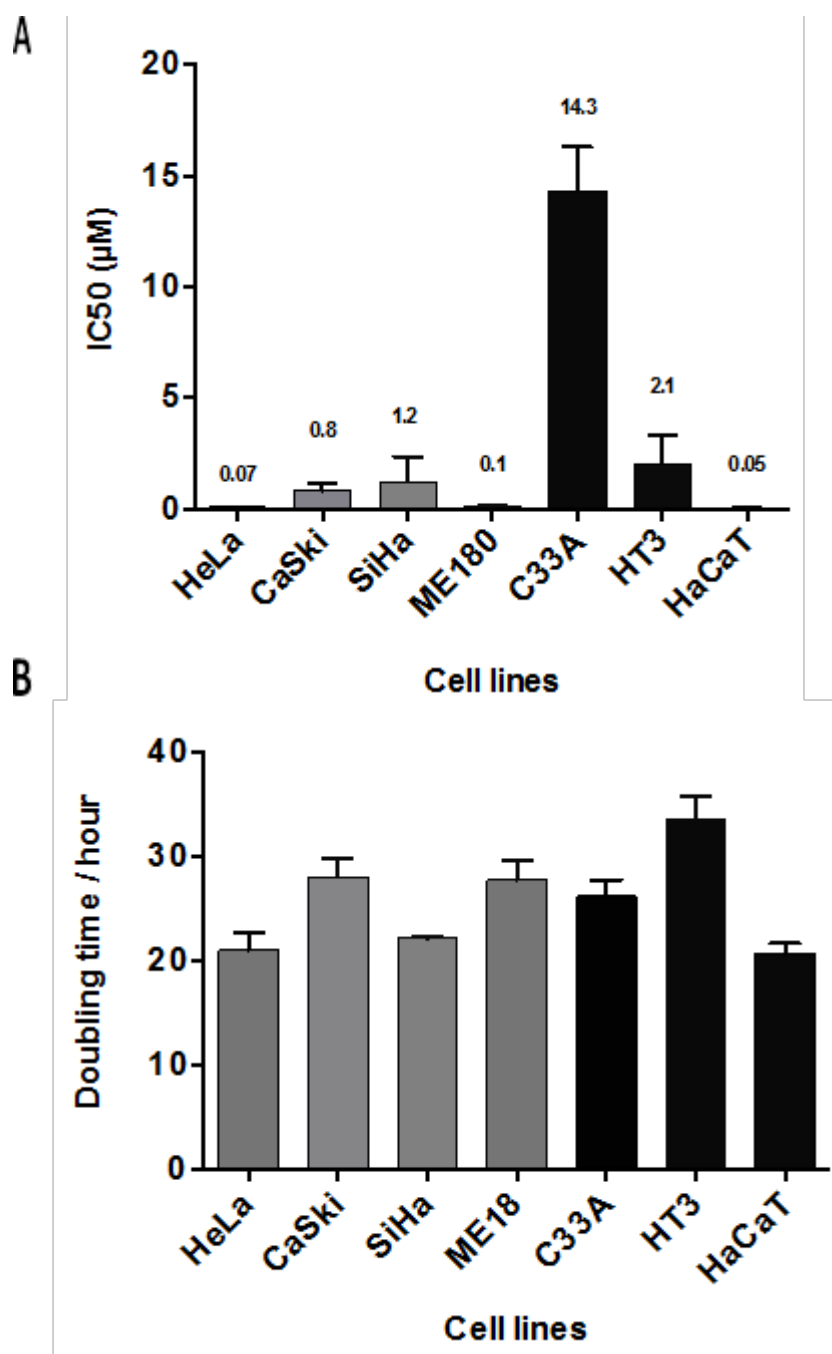


Figure 5.1. C33A non-HPV cervical cancer cell lines showed least sensitivity to MLN8237. A) Summary of the IC₅₀ values generated from a dose-response experiment showing the effect of the MLN8237 on a panel of HPV and non-HPV cervical cancer cell lines. Cells were subject to a viability assay using the resazurin dye at 44 µM after 72 h of drug treatment (dose range 30 µM to 30 nM). Each point is the mean and standard error mean (SEM) of quadruplicate determinations. IC₅₀ values were calculated using GraphPad Prism V.6.0. C33A non-HPV cervical cancer cell line had the highest IC₅₀ value compared to the remaining tested panel. All HPV-transformed cervical cancer cell lines together with HaCaT (non-HPV) had IC₅₀ values within nanomolars except for SiHa. The HT3 (non-HPV cervical cancer) had higher IC₅₀ compared

to the majority of the HPV-transformed cell lines. **B)** Doubling time experiment of the same tested panel. Cells were seeded for two days and then cell count was measured daily for 3 consecutive days. All cell lines had approximately similar patterns of duplication.

5.2.2 Non-HPV squamous cell carcinoma (SCC) showed resistance to MLN8237

The relative small number of non-HPV cervical cancers did not provide a good assessment of the selectivity of MLN8237 for HPV-induced cervical cancer. To extend the panel of non-HPV cancer cell lines, a panel of SCC cell lines was subjected to a MLN8237 dose-response experiment using the resazurin viability assay. SCC is a keratinocyte derived tumour type, the same target cell for HPV in cervical cancer, and thus provides a good comparison. The results demonstrated that Colo, FaDu and Detroit cell lines had IC_{50} in the range from 2 to 8 μ M (Figure 5.2), while it was not possible to determine an IC_{50} for KJD and SCC25 cell lines, which were above the highest dose used in the experiment (30 μ M). This data support the idea that non-HPV cell lines are less sensitive to the AURKA small molecule inhibitor, MLN8237, which may suggest HPV-transformation selectivity.

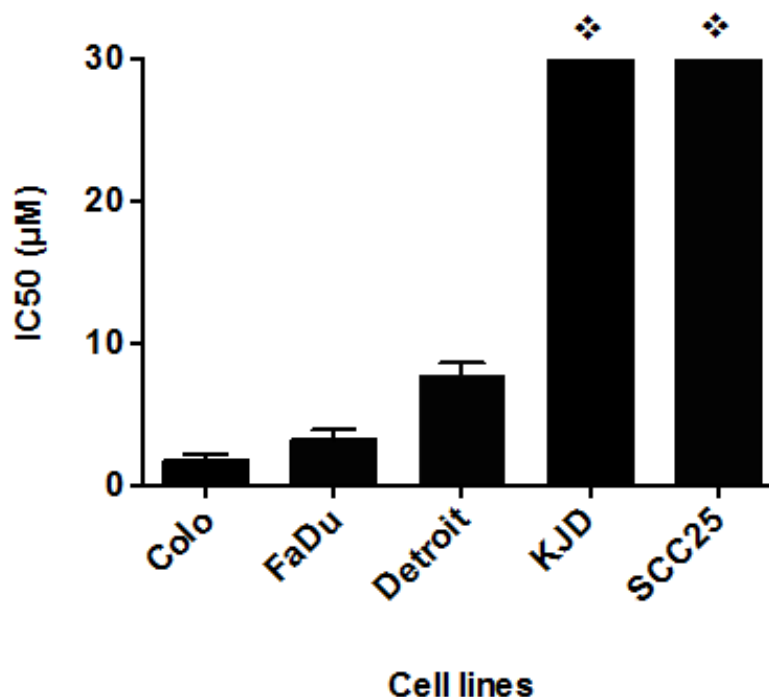
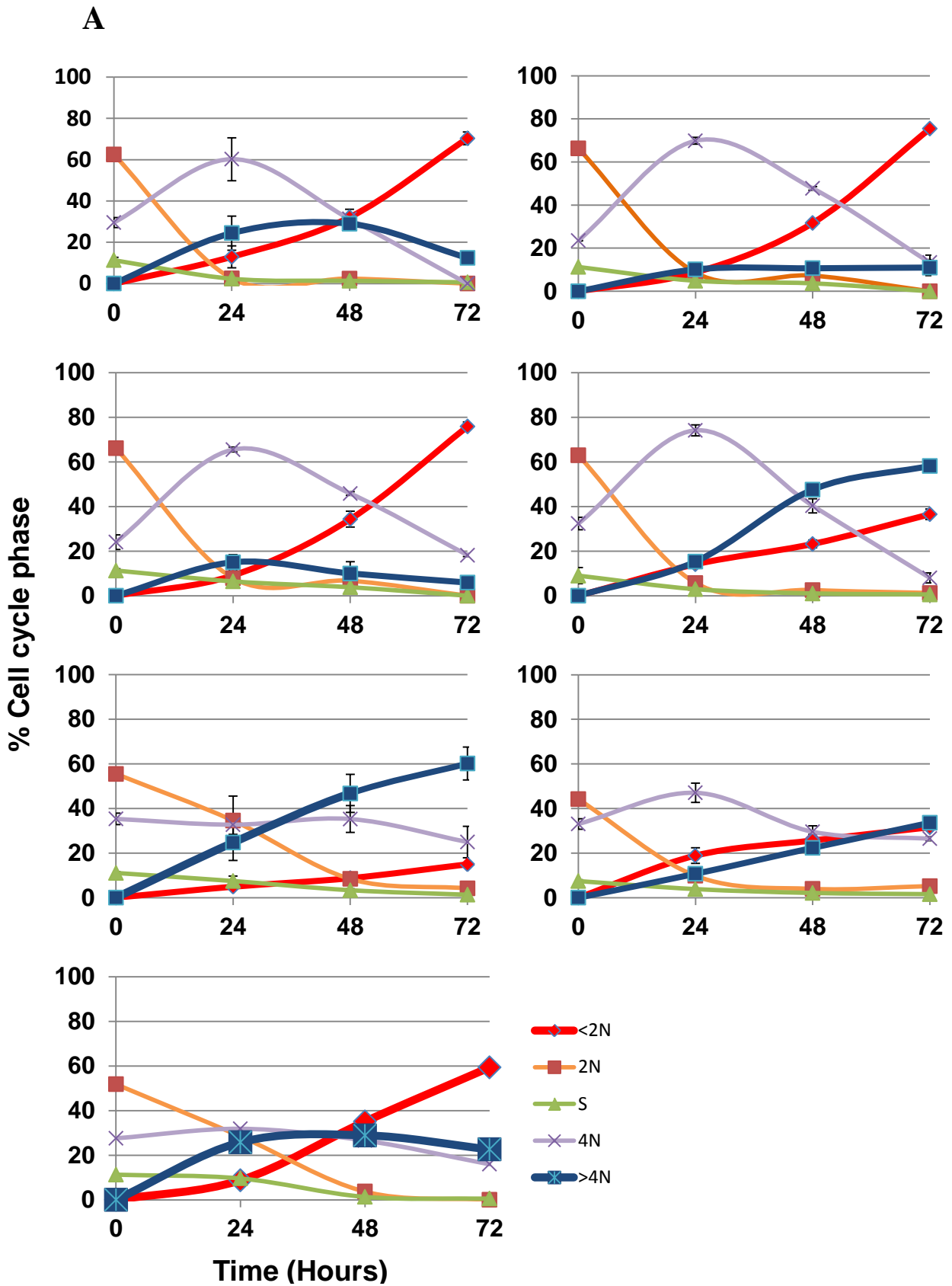


Figure 5.2. The non-HPV squamous cell carcinoma cell lines are less sensitive to MLN8237. Summary of the IC_{50} values generated from a dose-response experiment showing the effect of the MLN8237 on squamous cell

carcinoma (SSC) cell lines. Cells were subject to a viability assay using the resazurin dye at 44 μ M after 72 h of drug treatment (dose range 30 μ M to 30 nM). Each point is the mean and standard error mean (SEM) of quadruplicate determinations. IC₅₀ was calculated using GraphPad Prism V.6.0. (❖ KJD and SCC25 cell lines did not reach IC₅₀ within the tested dose range).

5.2.3 Treatment with MLN8237 induced apoptosis and polyploidy in cervical cancer cell lines

To investigate the effect of inhibiting AURKA with MLN8237 on cell cycle progression in the HPV-transformed and non-HPV cervical cancer cell lines, all cells were subjected to FACS analysis for DNA content. Cells were treated with 5 μ M MLN8237 for 24, 48, and 72 h in addition to DMSO only control (vehicle). Treatment of cell lines for 24 h with the inhibitor resulted in accumulation of cells in the 4N DNA population, induction of greater than 4N populations, a reduction in 2N population and decreased number of cells replicating DNA in all HPV-transformed cell lines and the HT3 non-HPV cell line (Figure 5.3). This effect was less obvious in the C33A and HaCaT cell lines. The latter two cell lines, however, induced higher >4N DNA content and S-phase population in comparison to the other cell lines. Treatment of cell lines with MLN8237 increased sub-diploid population (<2N) in a time-dependent manner in all cell lines. However, this trend was less in the C33A non-HPV cell line (Figure 5.3A and C). After 72 h of treatment, all HPV-transformed showed high sub-diploid population, HeLa 70%, Caski and ME180 75%, which indicates cell death (representative is shown in Figure 5.3B). The exception was SiHa where the sub-diploid population was 36%. By contrast, all the non-HPV cervical cancer cell lines, C33A and HT3, demonstrated low sub-diploid populations in comparison to the HPV-induced cell lines, 14%, and 31%, respectively. Indeed, high polyploidy population was noticed in the non-HPV cervical cancer cell lines after 72 h of treatment. Surprisingly, HaCaT as a non-HPV non-cervical cancer cell line demonstrated high apoptotic profile by 72 h indicated by a large population of <2N DNA. This is in fact is consistent with the IC₅₀ data where HaCaT showed high sensitivity to the compound. However, as the project aims to focus on non-HPV cervical cancer cell lines, these results provide evidence that treating HPV-transformed cervical cancer cells with MLN8237 induced cell death indicated by high sub-diploid population while non-HPV remains less sensitive to the compound.



B

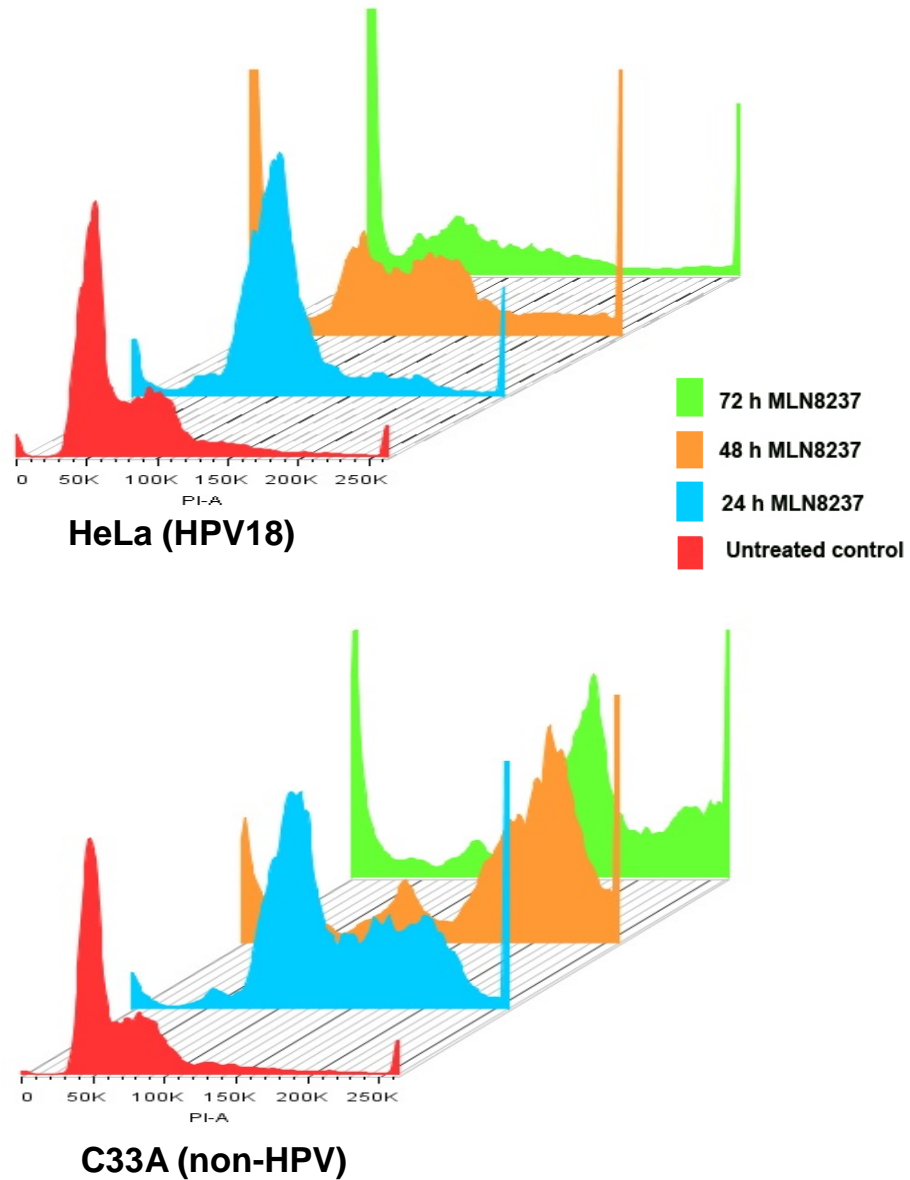


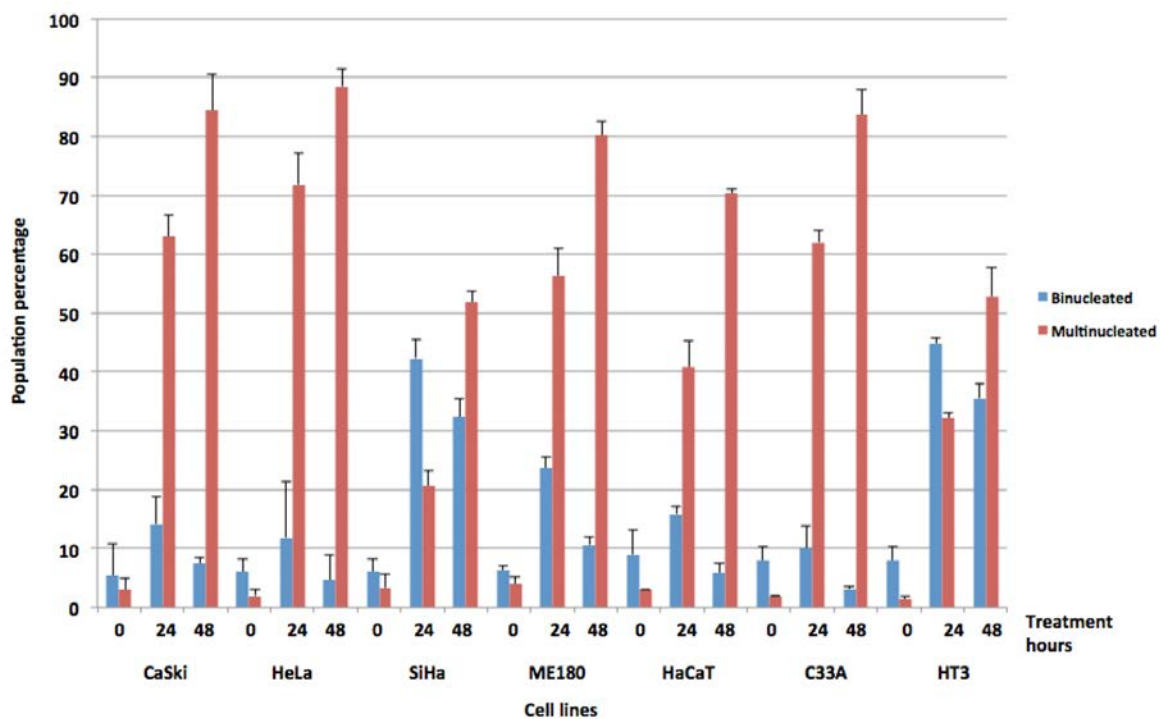
Figure 5.3. MLN8237 induced high apoptotic profile in HPV-transformed cervical cancer cell lines A) DNA content was analysed using fluorescence-activated cell sorting (FACS). All cells were treated with 5 μ M MLN8237 and collected at 24, 48, and 72 h. Each cell line had a negative control that was treated with the vehicle only (DMSO), which was collected in 24 h and plotted as zero on the graph. The error bars

represent a SEM of three biological replicates. **B)** Representative histograms of the HeLa and C33A to show induction of polyploidy in C33A and high apoptotic profile indicated by the increased subdiploid population in the HeLa cells. All data were processed using FlowJo V.2.0.

5.2.4 MLN8237 induced polyploidy of all tested cell lines tested using immunofluorescence staining

To confirm that the induction of 4N and >4N DNA contents was a consequence of failure of cytokinesis and that MLN8237 mediated DNA damage response, all cell lines were subject to immunofluorescence staining with the DAPI nuclear staining, α -tubulin staining of the cytoskeleton, and γ -H2AX as a DNA damage and/or replication stress marker. Percentage of binucleated or multinucleated cells after 24, and 48 h MLN8237 treatment is indicated (Figure 5.4A and B). The increased proportion of multinuclear cells varied between cell lines. However, the data showed no trend for either the HPV-transformed or the non-HPV cervical cancer cell lines. Indeed, all cells demonstrated marked failure of cytokinesis with increased multiple and fractured nuclei as shown by DAPI staining, a phenotype that is usually associated with aberrant mitosis. Also, all cells demonstrated DNA damage or recovery inhibition from replication stress as indicated by induction of γ -H2AX staining upon 48 h of treatment (representative cell lines are shown in Figure 5B). Collectively, this data strongly indicated that the accumulation of cells with 4N and >4N DNA contents was a consequence of failure of cytokinesis.

A



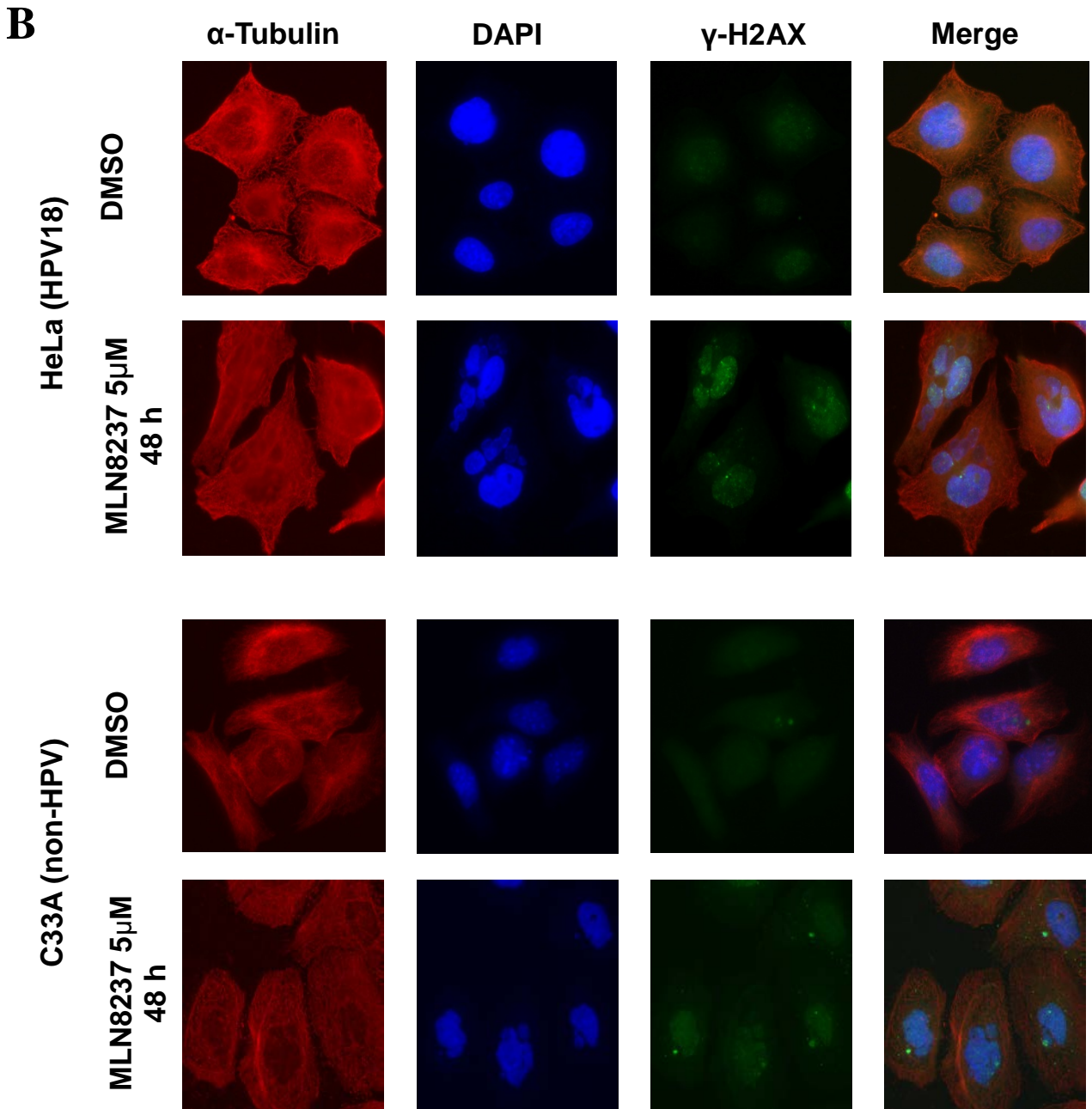
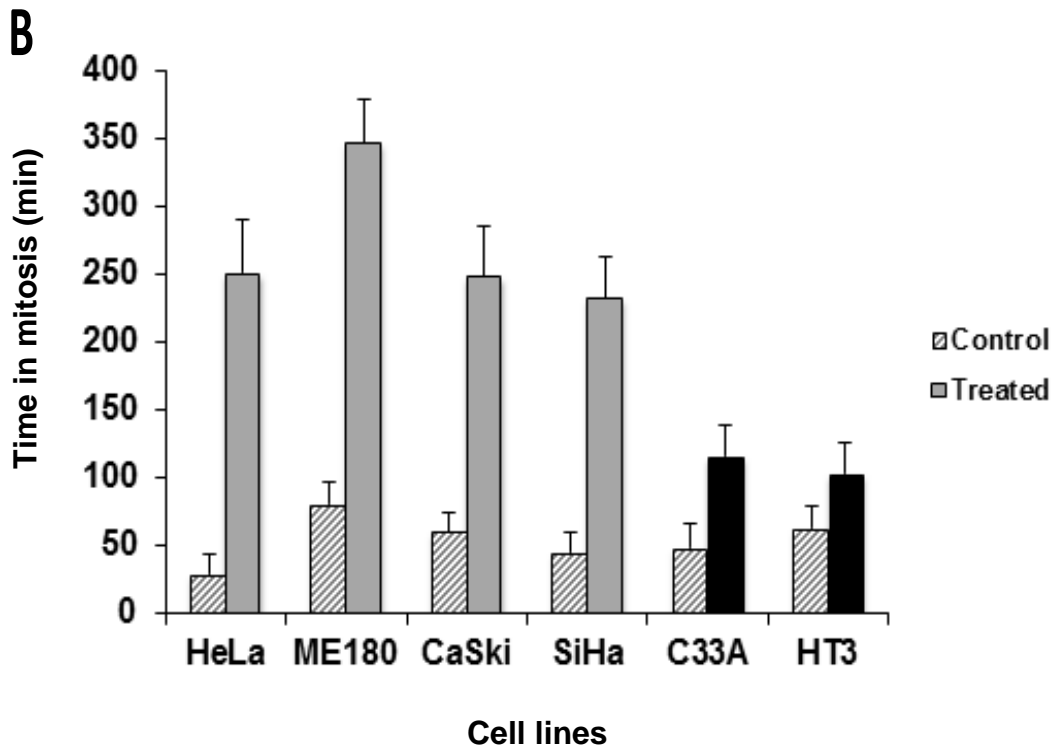
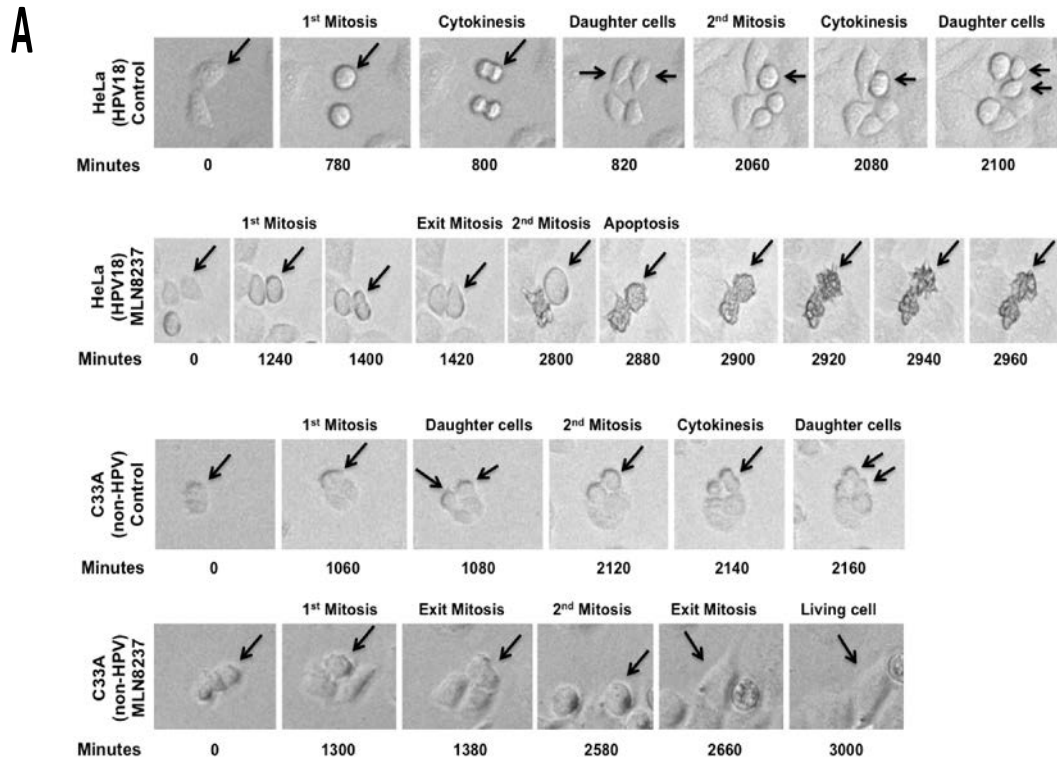
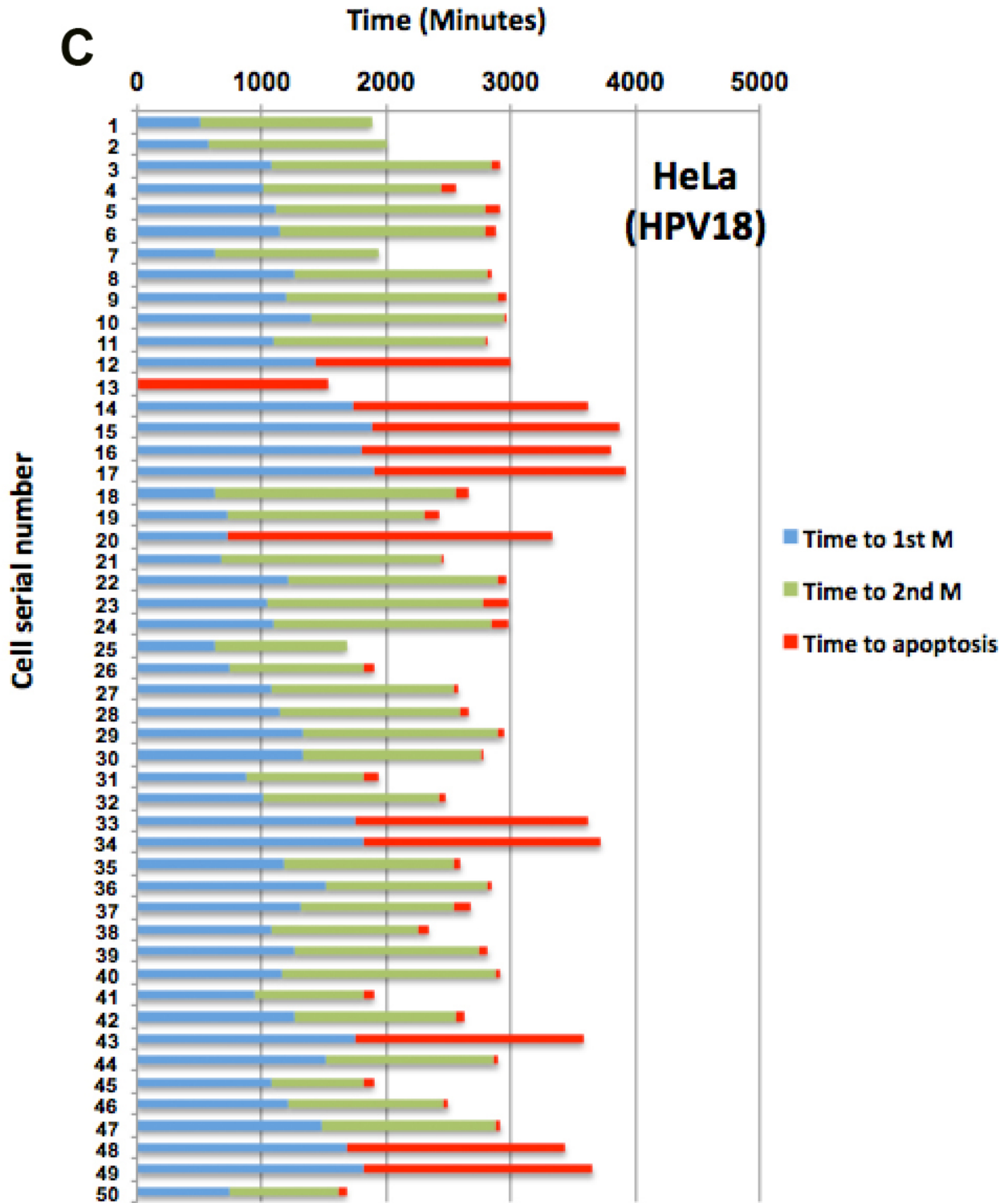


Figure 5.4. MLN8237 disrupt normal mitosis. A) Quantitation of bi-nucleated and multinucleated cells in DMSO control, 24, and 48 h of MLN8237 treatment. The error bars represent a mean of three biological replicates. B) Immunofluorescence staining of HeLa (cervical cancer HPV18 cell line) and (C33A cervical cancer non-HPV cell line) using an α -tubulin antibody (red), 4',6-diamidino-2-phenylindole (blue), and γ -H2AX antibody (green). Dimethyl sulfoxide (DMSO) was used as a control.

5.2.5 Time-lapse microscopy showed longer mitotic delay in HPV-transformed cell lines

Aurora A is a key mitotic regulator. To investigate whether HPV status affected the duration in mitosis upon inhibiting AURKA activity by MLN8237, all cell lines were subjected to a time-lapse microscopy for 72 h. Using transmitted light imaging it, the rounded mitosis morphology was readily discerned (Figure 5.5A). The results revealed that the normal mitosis duration of all cell lines tested was in the range of 30 to 80 minutes whereas HPV-transformed cell lines showed approximately 4 to 5 fold increase during first mitosis (Figure 5.4B). This prolonged mitosis was followed by failure of cytokinesis, clearly depicted by the daughter cells rejoining into a single cytoplasm (Figure 5.4A, frame 1420), and eventual loss of viability (frame 2880) featured by round shrinking cells and blebbing membrane as indicated in the time-lapse series. In contrast, non-HPV cervical cancer cell lines, C33A and HT3, showed remarkable lower mitotic delay when compared to the HPV-transformed cell lines with several cell cycles, indicating failure of cytokinesis. Also, the data revealed that remarkable proportion of the HPV-transformed cells underwent two mitoses before they die in the second mitosis (68% of HeLa and 52% of CaSki) (Figure 5.4C & D). This mitotic delay is likely to be due to the activation of the mitotic spindle assembly checkpoint, a reported consequence of inhibition of AURKA (Chan et al., 2012).





D

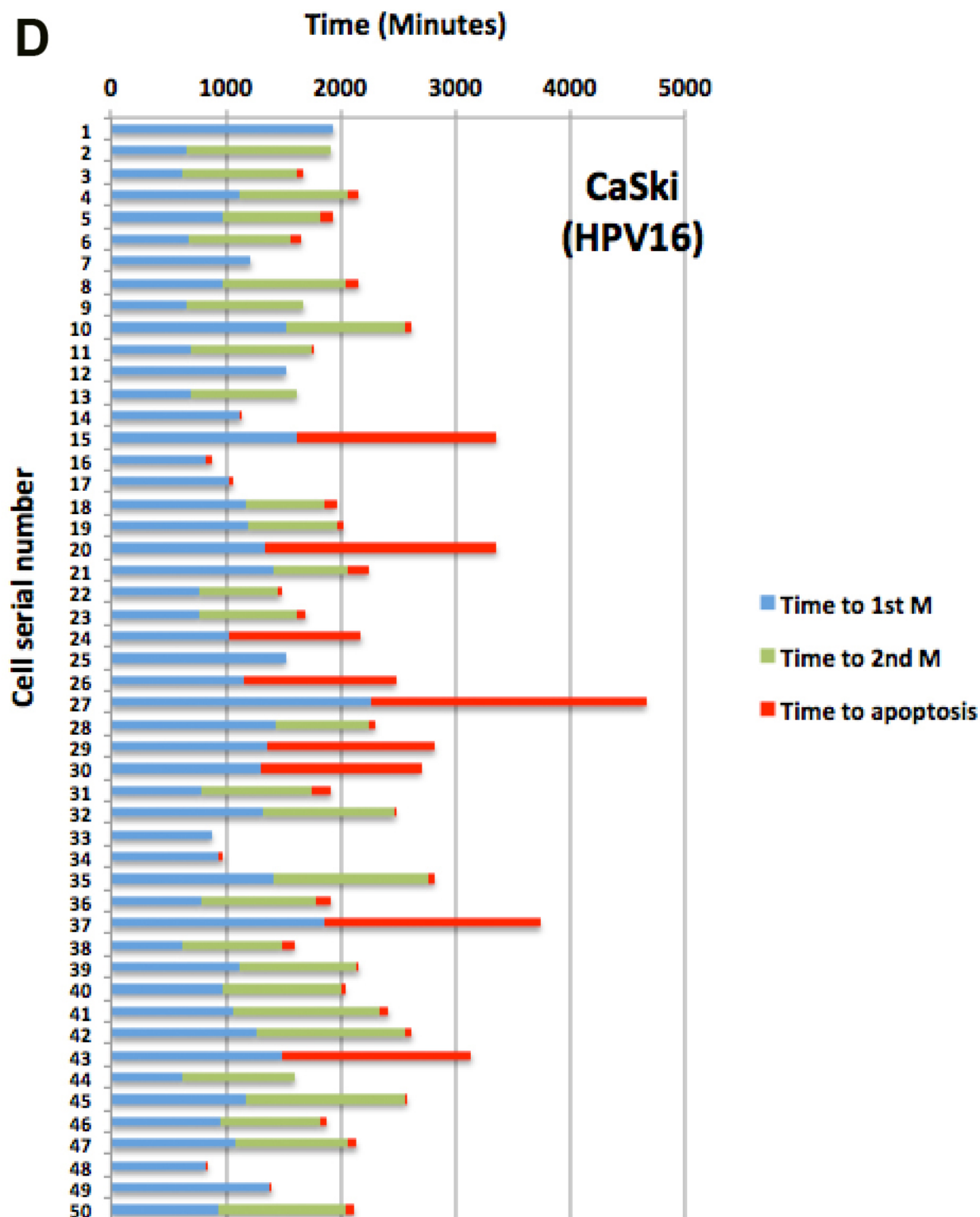


Figure 5.5. Time-lapse microscopy confirms high mitotic delay of HPV-transformed cells treated with MLN8237 followed by second mitosis and subsequent apoptosis. Cells were seeded in 6-well plates and then treated with 5 μ M MLN8237 or DMSO as a vehicle control for 72 h. **A** Representation of time in mitosis for HeLa and C33A in comparison to the control only cells. **B**) Representation of time in mitosis for each cell type, images were captured every 20 minutes interval time and at least 150 cells were counted in each condition and standard deviation was then calculated. **C** and **D** HeLa and CaSki, respectively, showing 50 cell-by-cell count that representing the time each cell needed to complete first mitosis and then enter the cell cycle and undergo second mitosis that was followed by apoptosis. Time-lapse series indicating that majority of HPV-induced cell line (HeLa-HPV18) goes at least through two cell cycles before they produce apoptotic phenotype whilst non-HPV (C33A) remains viable. The results were visualized and analyzed by ImageJ V1.46r.

5.2.6 Sensitivity to MLN8237 is a direct consequence of expression of HPV E7

To test whether one of the HPV encoded oncogenes was driving the sensitivity of the HPV-transformed cervical cancer cell lines to MLN8237, the C33A non-HPV cervical cancer and SCC25 non-HPV squamous cell carcinoma cell lines were transfected with HPV16 E7 oncogene. These were then assessed for their sensitivity to MLN8237. The data showed >50% reduction of IC₅₀ in C33A-HPV16-E7 and >30 fold reduction of the IC₅₀ in SCC25-HPV16-E7 cell line to 500 nM (Figure 5.6). This experiment may suggest that the expression of HPV E7 might be responsible for the increased sensitivity of the HPV-transformed cell lines.

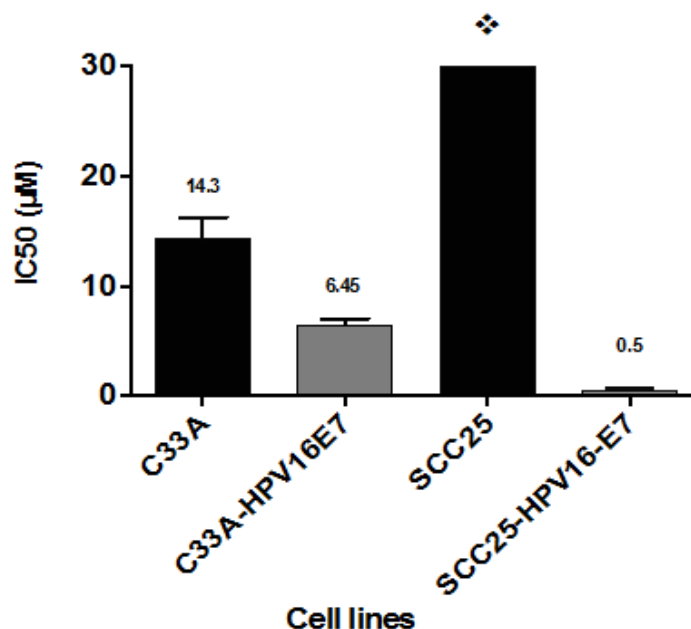


Figure 5.6. Transfection of non-HPV cell lines with HPV16 E7 increased sensitivity to MLN8237. Cells were transfected with the HPV16 E7 oncogene. The IC₅₀ was then calculated based on a dose-response

experiment (dose range 30 μ M to 30 μ M) using the resazurin viability assay at 44 μ M. Each point is the mean and standard error mean (SEM) of quadruplicate determinations. IC₅₀ was calculated using GraphPad Prism V.6.0. (SCC25 did not reach IC₅₀ within the tested dose range)

5.2.7 Over-expression of Mcl-1 reduced sensitivity to MLN8237

The time-lapse imaging revealed that the HPV-transformed cervical cancer cells were dying with a morphology that was typical of apoptotic cell death. To investigate contribution of apoptosis, particularly the intrinsic apoptotic mechanism to MLN8237 induced cell death, HeLa cell over-expressing either Bcl-2 or Mcl-1 anti-apoptotic proteins were examined for their sensitivity to MLN8237. The sensitivity of these cell lines to taxol or etoposide was used as a control. The results demonstrated significant higher IC₅₀ of the Mcl-1-HeLa, 4.7 μ M, in comparison to the parental HeLa ($P = 0.03$) and Bcl-2 overexpressing HeLa, which has relatively similar IC₅₀ value of 0.1 and 0.3 μ M, respectively (Figure 5.7A and C). The over expression of Mcl-1 also effectively protected HeLa cells from taxol (Figure 5.7B). However, Bcl-2 over-expression effectively protected HeLa cells from etoposide-induced apoptosis, demonstrated that the lack of effect on MLN8237-induced death was not due to failure of Bcl-2 function (Figure 5.7D).

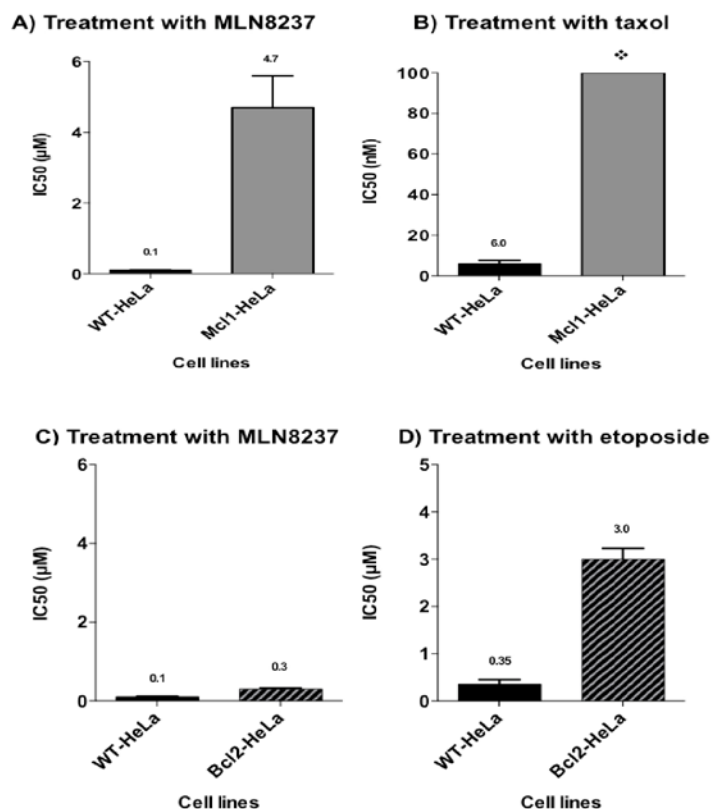


Figure 5.7. Mcl-1 over expression reduced the sensitivity to MLN8237. **A)** Summary of IC₅₀ of wild-type (WT) HeLa and HeLa over-expressing Mcl-1 generated by a dose-response experiment using MLN8237 at 30 μM to 30 nM dose range. **B)** Taxol was also included as a control at dose range of 100 nM to 100 pM on WT-HeLa and HeLa overexpressing Mcl-1. **C)** Summary of IC₅₀ of WT-HeLa and HeLa overexpressing Bcl-2 generated by a dose response experiment using MLN8237 at similar doses used in (A). **D)** Etoposide was included as a control at dose range of 50 μM to 50 nM on WT-HeLa and HeLa overexpressing Bcl-2. Each point is the mean and standard error mean (SEM) of quadruplicate determinations. IC₅₀ and *P* value were calculated using GraphPad Prism V.6.0. (❖Mcl-1-HeLa treated with taxol did not reach IC₅₀ within the tested dose range).

5.2.8 Assessing the mechanism of MLN8237-induced apoptosis in HPV and non-HPV cervical cancer cell lines

The ability of Mcl-1 over-expression to block MLN8237-dependent loss of viability indicated that the drug treatment was inducing an apoptotic death. As to determine the precise pathway, a panel of apoptotic components was examined by immunoblotting of the HPV-transformed or non-HPV cervical cancer cell lines after 24, 48, and 72 h MLN8237 treatment. The poly ADP ribose polymerase (PARP) showed cleaved PARP in all cell lines tested and was increasing a time-dependent manner (Figure 5.8). The levels of the anti-apoptotic Mcl-1, Bcl-2, and Bcl-x1 proteins

varied in each cell line, but MLN8237 treatment had little effect on the levels of any of these in any cell line. For the pro-apoptotic Bim, protein levels varied for each cell line but there was little effect of MLN8237 treatment. Only low levels of Bad and Noxa were detected, and although there was some increase in Bad levels observed with MLN8237 treatment this was cell line dependent and not selective for HPV expression. As expected, p53 was only readily detectible in the non-HPV cell lines and was not restored in the HPV-induced cervical cancer cell lines upon MLN8237 treatment. These data, as indicated by the PARP cleavage may demonstrates that apoptosis has been occurring in HPV-transformed cell lines independent of p53. However, the mechanism of apoptosis is unclear, but is sensitive to Mcl-1.

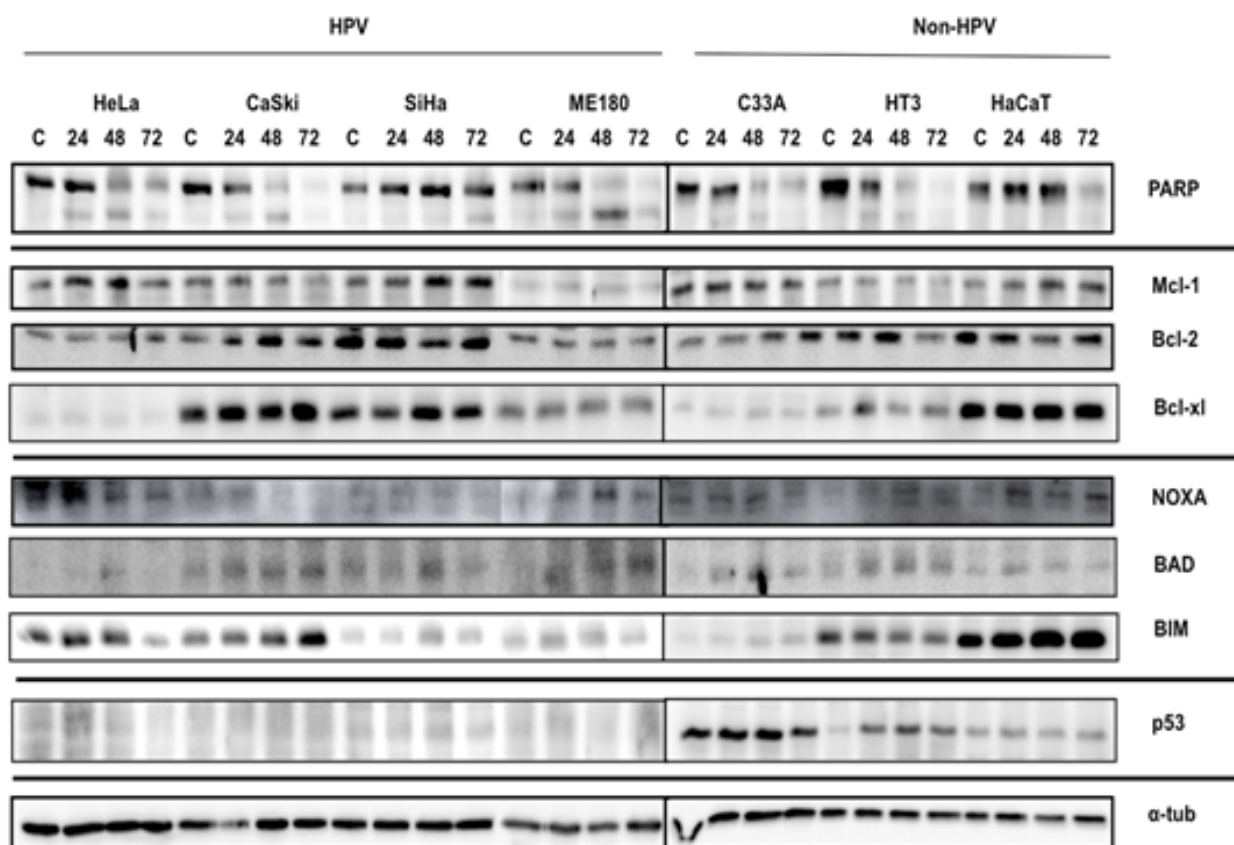


Figure 5.8. Analysis of cell lysate from cervical cancer HPV and non-HPV cell lines. Cells were seeded and pellet was collected after treatment of MLN8237 upon 24, 48, 72 h. Western blotting was then performed using PARP, the pro-apoptotic Bim, Bad and Noxa , and the anti-apoptotic Mcl-1, Bcl-2, and Bcl-xl. The p53 was only detectible in the non-HPV group confirming the apoptosis was occurring independent of p53. α-tubulin was used as a loading control. Experiment was performed in three biological replicates and Western blot imaging was acquired using Fusion ChemiDoc gel documentation system.

5.2.9 MLN8237 inhibits tumour growth in mouse xenograft model

To assess the ability of MLN8237 to inhibit tumour growth *in vivo*, nude mice were injected subcutaneously with either HeLa (HPV16), CaSki (HPV18), or C33A (non-HPV) cervical cancer cell lines in the flank tissue to induce growth of tumour. When the tumour size reached approximately 20-25 mm³, MLN8237 regimen at 30 mg/kg was initiated for 10 consecutive days. The results demonstrated no notable differences between the control and the treated groups within the first five days of the initiation of treatment (Figure 5.9). However, after five days, the tumour growth started increasing in the control group but declining in the treated groups regardless of the HPV-transformation status. At the end of the 10 days treatment period, both C33A and CaSki cell lines completely inhibited the tumour growth. This effect was noticed two days post-treatment in the HeLa group. Approximately four to five days post-treatment, tumour become palpable in the C33A (non-HPV) treated group, and all C33A treated group nude mice showed approximately 500 mm³ tumours by about 30 days post-treatment. Interestingly, both HPV-transformed cell lines, HeLa and CaSki, completed 50 days post-treatment with no detectible tumour growth in any of the MLN8237-treated animals. Excision of the original site of inoculation after the animals were sacrificed failed to reveal any residual tumour.

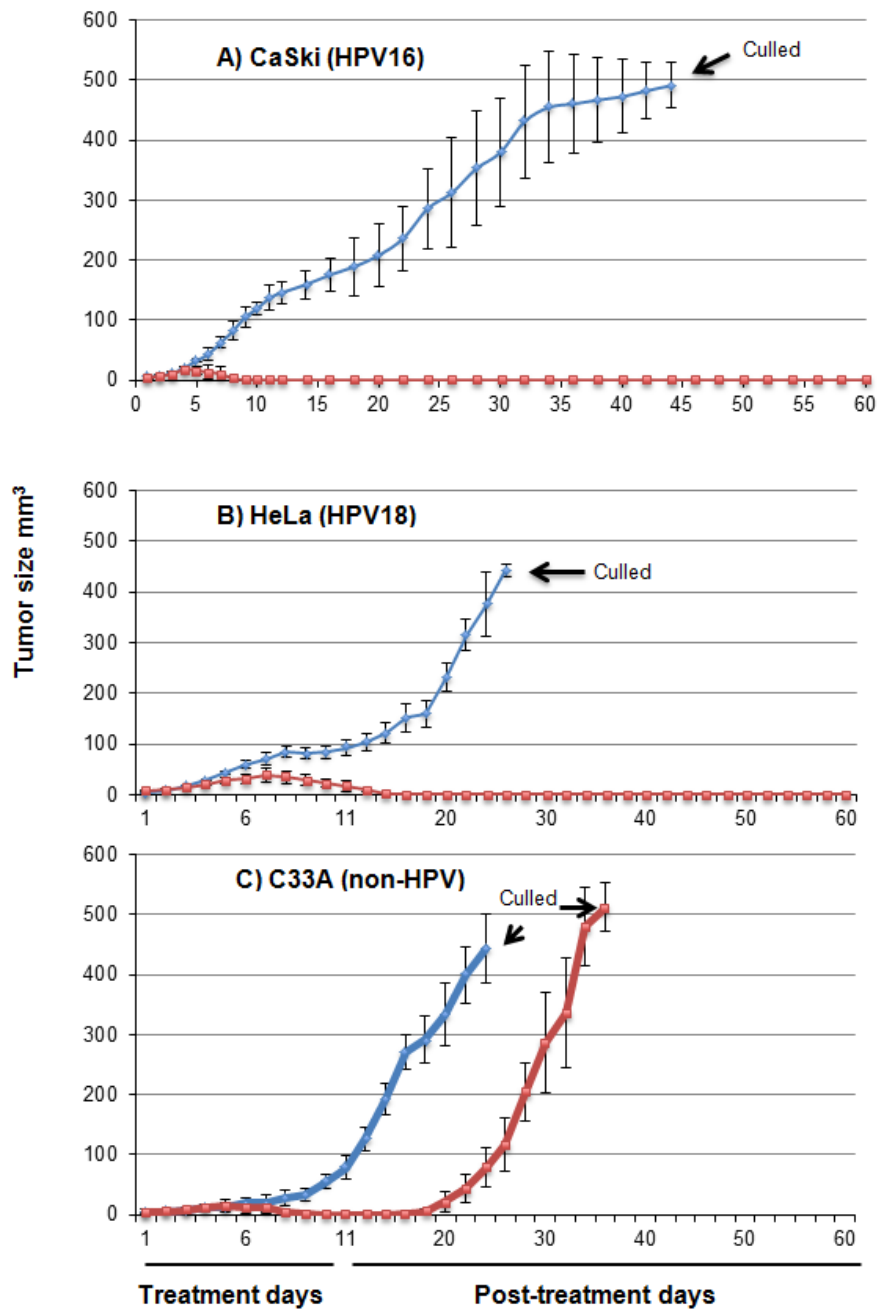


Figure 5.9. MLN8237 arrest tumour growth in vivo in a mouse xenograft model. 36 Mice were injected with 2.5 million of either CaSki (HPV16), HeLa (HPV18), or C33A (non-HPV) cervical cancer cells in the flank tissue. In each group, 6 mice were treated with the 30 mg/kg MLN8237 for 10 consecutive days and then followed up daily until culled; and 6 mice as control were only treated with tetracycline B in parallel with the treated group and were culled when the tumour size reach 500-600 mm³. **A** CaSki; **B** HeLa; **C** C33A. In both A and B, tumour growth was completely inhibited and no tumour growth was observed until 60 days. In the C33A tumour out growth was observed after treatment was stopped and mice were culled as indicated (■ red is treated; ◆ blue is control)

5.3 Discussion

The siRNA synthetic lethal screen performed as part of the thesis research identified and validated several potential target genes, including Aurora A kinase (AURKA), that selectively reduced the viability of majority of the HPV-transformed cells. Depletion of AURKA by siRNA showed strong lethality to at least two HPV-transformed cervical cancer cells (HeLa and CaSki). This effect was less observed in the C33A non-HPV cervical cancer and the HaCaT non-cervical cancer cells. These results confirmed AURKA as a valid target worthy of further investigation.

As a key mitotic regulator, AURKA localizes mainly to the centrosome and regulates centrosome maturation, entry into mitosis, development and function of the bipolar spindle, and cytokinesis. In G2 phase, AURKA associates with a crucial mitotic regulator, Polo-like kinase 1 (PLK1), which promotes its recruitment to the centrosome. This recruitment activates the Cyclin-dependent kinase (CDK)-activating phosphatase CDC25B and consequently the cell enters mitosis (Seki et al., 2008, Dutertre et al., 2004). Over-expression of AURKA is associated with the induction of aneuploidy and genomic instability that can contribute to tumorigenicity (Marumoto et al., 2005).

With the goal of further investigating the effect of specifically targeting AURKA in HPV-transformed cervical cancer cells, I evaluated the impact of the AURKA small molecule inhibitor, MLN8237, *in vitro* and *in vivo*. MLN8237 (alisertib) is an orally administered compound with preclinical activity against different neoplastic disorders and is currently undergoing Phase II clinical trials (Matulonis et al., 2012, Manfredi et al., 2011, Dees et al., 2012). Within 24 h of MLN8237 treatment, it increased the proportion of cells with >4N DNA content in all cell lines tested regardless of their HPV transformation status. The immunofluorescence staining and time lapse imaging revealed that the HPV-transformed cervical cancer cell lines had failed cytokinesis and underwent apoptosis beginning from 48 after they enter a second mitosis cycle upon drug addition. This was also supported by the FACS data that indicated large sub-diploid population of at least three cervical cancer HPV-transformed cell lines (HeLa, CaSki, and ME180). The exception was the SiHa (HPV16) line that has the lowest viral copy number amongst all the HPV-induced cervical cancer cell lines, which may contribute to their reduced sensitivity to the inhibitor (Poddighe et al., 1996). By contrast, the non-HPV cervical cancer cell lines, C33A and HT3, indicated increased proportion for cells with multinuclear phenotypes and the increased population

with >4N DNA content, representing polyploidy after 72 h of treatment. Surprisingly, HaCaT as a non-HPV non-cervical cancer cell line demonstrated high sensitivity to the compound. This sensitivity was confirmed with high apoptotic profile in the FACS data. The immunoblotting data of HaCaT indicated that BIM was increasing on a time-dependent manner. Although the reason of the sensitivity of HaCaT was not addressed, BIM may have contributed to induction of apoptosis.

Inhibition of AURKA leads to abnormal spindle formation (Dar et al., 2010). Cells undergo abnormal cell division upon the delay in mitotic entry and anaphase onset and, hence, cells develop polyploidy. Inhibition of AURKA may lead to chromosome mis-segregation and subsequently to apoptosis depending on how long cells spend in mitosis repairing damage (Hae-ock Lee et al., 2010). This is in agreement with the time-lapse microscopy results shown in this chapter. Specifically, all HPV-transformed cervical cancer cells were delayed in mitosis at least twice as long as the non-HPV cells. This mitotic delay was followed by delayed induction of apoptosis in the HPV-transformed cells upon the second mitotic cycle. Disruption of mitosis with antimitotic agents could be either death in mitosis, or adaptation followed by mitotic exit (mitotic slippage). Cell that survives the 4N DNA content may potentially continue DNA replication, arrest in G₁, or die via apoptosis (Rieder and Maiato, 2004). It has been reported that HeLa cells that has a deficient spindle assembly checkpoint escape mitotic arrest and enter another cell cycle with another DNA synthesis round when treated with taxol (Chin and Herbst, 2006). Also, BubR1-depleted HeLa cells underwent apoptosis within 48 h when treated with taxol whilst Mad2-depleted HeLa cells remained viable during that time and represented increased level of 4N DNA content. Also, control HeLa cells treated with monastrol, a mitotic kinesin Eg5 inhibitor, arrested cells in mitosis for about 229 ±19 minutes whilst Mad-2 depleted HeLa cells remained arrested for only 22 ±7 minutes. In another report, Tao *et al.*, indicated that the apoptotic event which was followed by treating cells with the mitotic kinesin Eg5 inhibitor needs mitotic slippage into G₁ phase during activated spindle checkpoint (Tao et al., 2005). The latter study demonstrated that activation of BubR1 and inactivation of survivin were required to initiate apoptosis after mitotic slippage. As indicated in the results section of this chapter, the time-lapse data showed a significantly longer mitotic arrest in the HPV-transformed cells compared with the non-HPV cells. Because the mechanism underlying this time difference was not addressed in this thesis, it can be speculated that several factors would have affected the duration of mitotic arrest. First, AURKA plays a crucial role in spindle assembly;

therefore, AURKA disruption could lead to defects in centrosome maturation and separation, deficient mitotic spindle formation, and failing chromosomal alignment (Nigg, 2001, Carmena and Earnshaw, 2003). Although it has been reported that these spindle assembly defects are associated with induction of spindle assembly checkpoint mitotic delay, some cells lacking functional AURKA are able to divide in the presence of these assembly defects (Hoar et al., 2007, Marumoto et al., 2003). This proposes that the function of the spindle assembly checkpoint is conceded upon AURKA inhibition. Secondly, the spindle checkpoint status of the tested cell lines was not investigated before and after drug treatment, which is an essential part that possibly could reveal the reason beyond this mitotic arrest delay, although mitotic arrest may evolves competent spindle checkpoint. Lastly, because function of the spindle checkpoint associates with several functioning proteins such as BubR1, Bub1, Bub3, Mad1, and Mad2 (Sudakin et al., 2001, Wu et al., 2000, Fang, 2002), neither of these proteins was checked in the present study, which may play a pivotal role in the mitotic arrest, mitotic slippage, and initiation of apoptosis upon mitotic slippage.

A major difference in the outcome that was noticed after treating the HPV-transformed and the non-HPV cell lines with MLN8237 was apoptosis. Although this apoptotic effect was confirmed by PARP immunoblotting, its mechanism remains unclear. In addition, the overexpression of the anti-apoptotic myeloid cell leukemia 1 (Mcl-1) in HeLa cells decreased the sensitivity of the cell to the MLN8237. This is in agreement of what has been previously reported that overexpression of Mcl-1 protects cells from apoptosis (Ploner et al., 2008, Zhang et al., 2011). The high sensitivity of the parental HeLa and the Bcl-2 overexpressing HeLa to the inhibitor may suggest the involvement of Noxa, Puma, or p73 in the induction of apoptosis of the HPV-transformed cervical cancer cell lines (Willis and Adams, 2005, Liu et al., 2010, Ploner et al., 2008). Moreover, transfection of the non-HPV cell lines, C33A and SCC25, with an HPV16-E7 oncogene increased their sensitivity to MLN8237 by >two fold. This may suggests that E7 is most likely increasing the sensitivity to apoptosis. E7 inhibits the function of the retinoblastoma protein (pRb), an essential negative regulator of cell cycle progression. The activity of pRb is largely associated with the members of the E2F family of transcription factors, which regulate both cell proliferation and apoptosis (Phillips and Vousden, 2001). E2F/Rbp complex has been reported to control transcription of several genes such as p14^{ARF}, p73, Apaf1, Caspases, Chk2, and BH3-only pro-apoptotic proteins (Hallstrom et al., 2008). E2F1 expression is associated with apoptosis, and loss of E2F1 or E2F3 suppresses

apoptosis in Rb-deficient mice embryos (Ziebold et al., 2001). E2F1 binds to the promoters of the Bcl-2 homology 3 (BH-3) only protein family members, PUMA, Noxa, Bim, and Hrk/DP5 (Hershko and Ginsberg, 2004), and inhibition of PUMA or Noxa expression dramatically reduces E2F1-induced apoptosis. Noxa and Puma are both pro-apoptotic proteins. Although there are several E2F target genes, the Mcl-1 data in the present work provide possible evidence of involvement of Mcl-1/Noxa or Puma in the apoptotic phenotype. There is therefore a link between HPV-E7 oncogene, pRb, E2F1, Noxa/Puma, and Mcl-1. Also, the knockdown of Noxa by a specific siRNA results in remarkable reduction in apoptosis in HeLa cells when compared to the control cell line (Mei et al., 2007). E7 may sensitize cells to apoptosis induction through Noxa or Puma by sequestering Mcl-1 function in the HPV-transformed cell lines. This is in agreement with my results showing that HeLa (HPV18) cell line overexpressing Mcl-1 became less sensitive to MLN8237. Taken together, these findings and published reports support the notion that E7 may have been a major cause of sensitizing cells to induction of apoptosis in the HPV-transformed cells and altered sensitivity in the E7 transfected non-HPV cell lines probably via Noxa or Puma/Mcl-1 mechanism. However, because E7 works in parallel with E6; therefore, a definite conclusion cannot be obtained without testing E6 in C33A and SCC25 cell lines.

Although there is a possible link between HPV-E7 and induction of apoptosis through Noxa or Puma, the connection between inhibiting AURKA and this HPV-transformed apoptotic selectivity remains obscure. A possible connection is that the loss of pRb function by HPV-E7 is associated with over-expression of p73 in cervical cancer and pre-malignant lesions (Brooks et al., 2002). E7-dependent activation of the p73 promoter disappeared in E7 mutants, which leads to functional pRb. This E7-dependent transactivation of p73 occurs via E2F1. P73 arises from an alternative splicing of the TAp73 primary transcript, a pro-apoptotic protein (Ozaki and Nakagawara, 2005). Over-expression of p73 is associated with the induction of apoptosis in some cancer cell lines (Jost et al., 1997). The use of MLN8054 results in p73-dependent apoptosis in H1299 and TE7 cancer cell lines (Dar et al., 2008). It is also known that E2 ubiquitin ligase (UBE2N), which binds Aurora A, is engaged in the activation of the nuclear-factor- κ B (NF- κ B) pathway (Ewart-Toland et al., 2003, (Deng et al., 2000). The binding of AURKA to UBE2N mediates the phosphorylation of I κ B α and consequently activates the NF- κ B pathway (Briassouli et al., 2007). The induction of Noxa or Puma, and the activation of p73 require the activation of the NF- κ B pathway (Martin et al., 2009).

All these previously described reports may suggest a model of how the inhibition of AURKA is selectively contributing to the HPV-transformed cellular apoptosis possibly by activating the NF- κ B pathway and induction of p73, Noxa, or Puma.

AURKA small molecule inhibitor MLN8237 has been widely used in different pre-clinical xenograft models. Görgün *et al.* indicated that treating myeloma xenograft model with 7.5mg/kg, 15mg/kg, and 30mg/kg for 21 consecutive days resulted in significant reduction of tumour size in comparison to the control group (Gorgun et al., 2010). However, this tumour growth inhibition was followed by tumour regrowth when treatment was ceased. Also, the study reported significant increase in the survival rate, particularly in the group treated with the 30mg/kg. It is important to mention that in the same report there was only one animal did not show tumour recurrence until after 58 days of treatment. The latter animal was within the group treated with 30mg/kg, which is a similar dose to what has been used in this thesis. Zhou and colleagues observed significant reduction in tumour size using a bladder cancer xenograft model when treated with 30mg/kg MLN8237 for 5 times/week for four weeks (Zhou et al., 2013). However, the report did not indicate whether tumour recurrence was observed. The aforementioned studies demonstrated significant capacity of MLN8237 when used as a single agent. Nevertheless, Mahadevan *et al.* demonstrated that MLN8237 was only able to induce modest antitumour activity when used at 10mg/kg and 30mg/kg in a mantle cell lymphoma xenograft model in comparison to the control group (Mahadevan et al., 2012). This is in agreement of what Qi and colleagues reported when used similar xenograft model (Qi et al., 2011). The present study also provides evidence that the AURKA small molecule inhibitor, MLN8237, was able to inhibit tumour growth *in vivo*. Although all C33A engrafted mice had tumour outgrowth once the treatment ceased, CaSki (HPV16) and HeLa (HPV18) xenograft models did not show tumour recurrence.

In conclusion, this chapter illustrates novel results using MLN8237 in a cervical cancer model. The inhibition of AURKA using MLN8237 induces polyploidy in the non-HPV cervical cancer cell lines, whereas the same degree of polyploidy was associated with apoptosis in the HPV-transformed cell lines. This finding was further confirmed in non-HPV SCC cell lines. Also, the transfection of the non-HPV C33A cervical cancer and the SCC25 squamous cell carcinoma cell lines with the oncogenic HPV-E7 dramatically increased the sensitivity of these cells to MLN8237, indicating a

role of E7 in this sensitivity. Furthermore, over-expression of Mcl-1, but not Bcl-2, in HeLa cells resulted in decreased sensitivity to MLN8237, suggesting that elevated Mcl-1 is likely to be a marker of reduced sensitivity to MLN8237 in HPV cervical cancers, and that the apoptosis induced by MLN8237 treatment is via a BH3-only protein that is inhibited by Mcl-1 but not Bcl-2. The only BH-3 only protein fitting this profile is Noxa. However, I have found little evidence for increased Noxa expression with MLN8237 treatment or reduction in Mcl-1 levels, suggesting the mechanism is possibly more complex. Finally, the inhibitor was tested in xenograft models using CaSki, HeLa, and C33A cells. Both CaSki and HeLa HPV-transformed xenograft models responded well to the treatment. Tumour growth was inhibited, and no tumour recurred even at 50 days post-treatment. However, in the non-HPV cervical cancer xenograft model using C33A cells, tumour inhibition was observed only during treatment, and tumour outgrowth occurred after the treatment ceased. These novel results suggest that MLN8237 is a promising therapeutic agent for cervical cancer caused by HPV types 16 and 18. Additionally, they pave the path for the investigation of the mechanistic cascades behind this apoptosis and polyploidy.

6 General discussion, conclusion, and future directions

6.1 General Discussion

Although many chemotherapeutic agents have shown promising effects in clinical settings, their adverse effects continue to be substantial and in many cases dose limiting, which can compromise the efficacy of the treatment. The development of safe and effective treatments in cancer remains a challenge, and the ability to identify selective targets that only kill cancer cells is a goal that has been only partially achieved in a few cancers. Most of the anti-cancer agents that are currently in use have been developed on the basis of their ability to kill rapidly dividing cells *in vitro*. Hence, these agents are also capable of killing rapidly dividing normal cells, such as the bone marrow and haemopoietic precursors. Although much is known about the molecular alterations that occur in cancers, it is difficult to directly translate these into a therapeutic context. In addition, the restoration of loss-of-function changes in tumour genes that occurs in patients is difficult to achieve. Because of these and many others reasons, the identification and development of selective anticancer agents, which do not directly target the genetic driver mutations may offer new opportunities for therapeutic intervention in cancers.

High-throughput synthetic lethal screening has been portrayed as a powerful tool to identify novel target genes. This concept has been utilized in the current thesis to identify novel target genes in cervical neoplasia, which when silenced kill only HPV-transformed cells and not others. The thesis describes the development of high-throughout siRNA screening from method optimization through assay development to the actual screenings and, finally, the validation of target hits. Additionally, it explains the selectivity of the Aurora B small molecule inhibitor (ZM447439) against HPV-induced and non-HPV cervical cancer cell lines. Finally, it demonstrates the significance of Aurora A kinase as a potential therapeutic target gene in HPV-transformed cervical neoplastic disorders, tested both *in vitro* and *in vivo*.

Although two different pools of siRNA were used throughout the primary and secondary screens of this project, six hits were confirmed to be synthetically lethal when depleted with the majority of HPV-transformed cells but not the non-HPV cervical cancer cell lines, although HaCaT as a non-HPV non-cervical cancer cell did not demonstrate similar results. Of these, three candidates,

namely, AURKB, AURKA, and GSG2 (Haspin), were highly interesting since they are all mitotic regulators. Mitosis has been of interest to many researchers and pharmaceutical companies aiming to develop anticancer agents due to its exceptionally successful effect in clinic settings (Pasquier et al., 2006, Zhou et al., 2003, Mollinedo and Gajate, 2003). These three mitotic regulators were identified in a specific response to the HPV-transformation status of the cell. This was confirmed when two mitotic inhibitors, BI-2536 and paclitaxel, were used but neither one demonstrates selectivity to either HPV or non-HPV cell lines. BI-2536 is a selective PLK1 inhibitor, whereas paclitaxel is a microtubule inhibitor that causes mitotic arrest (Wissing et al., 2013, Frost et al., 2012, Gu et al., 2013).

Among the three hits, AURKA and AURKB belong to the Aurora family, which have pivotal, yet distinct, roles in mitosis (Warner et al., 2003, Carmena and Earnshaw, 2003). Due to their important roles in mitosis, their implication in cancers, and the availability of commercial small-molecule inhibitors for both AURKA and AURKB, both genes have been the investigative subjects in this thesis.

In the present work, AURKB small-molecule inhibitor ZM447439 was used to investigate the selectivity of the compound to HPV-transformed and non-HPV cervical cancer cell lines (Chapter 4). However, the data revealed no selectivity for the HPV-transformed over the non-HPV cervical cancer cell lines with the inhibitor in terms of viability. This was also confirmed by investigating the DNA content and nuclear structure by FACS, where all cells induced G₂/M arrest by 24 h of treatment and increasing polyploidy population in association with apoptosis in all cell lines tested after 48 and 72 h of treatment, regardless of the HPV transformation status of the cell lines. This finding is in agreement with previous reports where ZM447439-treated cells induced G₂/M arrest followed by 4N and 8N DNA content (Ditchfield et al., 2003). This impairment of AURKB activity possibly leads to cellular apoptosis through the activation of Caspase 3 and PARP cleavage. Because the knockdown of the AURKB using specific siRNA could exert a lethal effect only on the majority of HPV-transformed cervical cancer tested cells but not others, it is believed that the non-specificity of ZM447439 may have played a role in this phenotypic outcome (Portella et al., 2011, Hauf et al., 2003). Indeed, there is a major difference between depleting AURKB by a specific siRNA and using small molecule inhibitor as the former degrade the mRNA whereas the latter only

inhibit its protein activity. This major difference would lead to several phenotypic outcomes. Firstly, degrading AURKB mRNA results in a high percentage, approximately 80-85%, removal of the protein, which consequently leads to very low possibility of interaction with other proteins. AURKB is a major part of the chromosomal passenger complex (CPC) that plays a fundamental role during mitosis (Vader and Lens, 2008, Ruchaud et al., 2007). The knockdown of AURKB has been reported to affect the dynamics of Survivin, another CPC subunit and an essential mediator of centromere and midbody docking of AURKB during mitosis (Delacour-Larose et al., 2004). The loss of AURKB/Survivin interactions results in dysfunctional CPC that, consequently, leads to improper mitotic events. Moreover, AURKB is engaged in the function of the spindle checkpoint (Vader et al., 2007). Thus, preventing protein translation by specific AURKB siRNA may also result in spindle checkpoint disruption. Spindle checkpoint has several enzymatic and non-enzymatic proteins where they assembled at kinetochore in an orchestrated order upon entry into mitosis (Morrow et al., 2005). The depletion of AURKB by specific siRNA was shown to reduce Mps1, a spindle checkpoint kinase, binding to kinetochore (Saurin et al., 2011). Subsequent to this binding reduction, the level of Mad2, a non-enzymatic protein of the spindle checkpoint, was significantly declined. As described, all these essential protein-to-protein interactions may have decreased or even lost as upon degrading AURKB mRNA and, consequently, preventing protein translation.

Despite the effect of depleting AURKB using a specific siRNA, the use of small molecule inhibitor ZM447439 was not able to induce similar selectivity as described in Chapter 4 of this thesis. AURKB forms a part of the chromosomal passenger complex, CPC. It was noted that AURKB-mediated RNAi silencing resulted in relocalization and destabilization of other members of the CPC, such as borealin and survivin (Weiss et al., 2007). However, ZM447439 inhibited AURKB activity but left CPC members intact and consequently resulted in different phenotype. CPC is a key player in orchestrating chromosome segregation and control of cytokinesis. Also, as mentioned before, AURKB plays important roles in mitosis. Therefore, it is expected that when a crucial member of CPC such as AURKB is depleted, subsequent unregulated cell cycle events occur. These may include, chromosomal defects, kinetochore-microtubule attachment abnormalities, lagging chromosomes in anaphase, and failure of cytokinesis (Vagnarelli and Earnshaw, 2004, Tanaka, 2005). Additionally, some small molecule inhibitors exhibit unspecific inhibition and affect other

proteins (Arkin and Wells, 2004). ZM447439 was reported to have inhibitory effect on AURKA (Gadea and Ruderman, 2005). AURKA is another key player in mitosis and disrupting its activity may result in several mitotic events. Therefore, the effect that can be generated by using the ZM447439 might not be specific to AURKB functionality in comparison to siRNA. Instead, it could be a dual effect of inhibiting both AURKA and AURKB. Furthermore, when AURKB was tested using the online database of Library of Integrated Network-based Cellular Signature (LINCS), it was found that ZM447439 inhibits some other proteins (<https://lincs.hms.harvard.edu>). Because the main aim of this thesis was to identify a target gene that when silenced/inhibited affect only HPV-transformed cervical cancer cells but not others, and ZM447439 failed to achieve this aim. Therefore, further investigations of the target were not performed. Instead, investigations on the other Aurora family member, AURKA, were carried out.

In the present project, AURKA siRNA and the small molecule inhibitor MLN8237 showed selectivity to HPV-induced cervical cancer cell lines whilst non-HPV cell lines showed less sensitivity (discussed in Chapters 3 and 5). Further investigations using MLN8237 show apoptotic phenotype in the HPV-transformed cell lines, which was confirmed by DNA contents and time-lapse data. Additionally, the treatment of non-HPV cell lines transfected with HPV E7 oncogene sensitized the cells to the inhibitor, and, consequently, resulted in lower IC₅₀. The previous data was further supported by *in vivo* demonstration where the treatment of HPV-transformed and non-HPV cervical cancer xenograft models for 10 consecutive days with 30mg/kg of MLN8237 resulted in tumour inhibition. Interestingly, no tumour recurrence was observed for 50 days post-treatment in the HPV-induced groups whereas the non-HPV group showed tumour recurrence 4-5 days post-treatment. AURKA is a key mitotic player where it orchestrates different mitotic events, including centrosome maturation, entrance to mitosis, bipolar spindle assembly, chromosomal alignment, and cytokinesis (Marumoto et al., 2005). Therefore, disrupting an essential element as AURKA would result in many cellular events, possibly including apoptosis. Although there was no clear connection between AURKA and HPV, the ability of Mcl-1 over expression to protect against the MLN8237-driven cell death points to a possible link. Mcl-1 is a pro-survival gene that belongs to the Bcl-2 family (Kozopas et al., 1993). Mei and colleagues found that Mcl-1 colocalizes with Puma, a pro-apoptotic Bcl-2 protein, in the mitochondria and blocks the release of Puma-mediated cytochrome *c* release and subsequent activation of caspase 9 (Mei et al., 2005). The report also noted that Mcl-1

stability increases upon binding with Puma. It is known that HPV E7 oncogene degrades the pRb, which leads to the release of E2F1. Also, the loss of pRb function by oncogenic E7 increases E2F activity and the expression of p73, which has been reported to result in apoptosis in some cancer cell lines (Jost et al., 1997). In their report, Melino and co-workers found that p73-induced apoptosis is triggered by Puma (Melino et al., 2004). Also, Puma was required to translocate Bax, a pro-apoptotic Bcl-2 protein, to the mitochondria during p73-induced apoptosis. Based on these reports, it can be hypothesized that p73 may play a role in the selective apoptotic phenotype to the HPV-transformed cervical cancer cell lines. This p73-induced apoptosis may occur through Puma possibly by releasing E2F1 when pRb is degraded by the oncogenic E7. Although the previous possible model of induction of apoptosis does not provide a direct link between HPV and AURKA, it was reported that p73-induced apoptosis requires the activation of the NF- κ B pathway (Martin et al., 2009). This activation can only occur via mediation by UBE2N, which in fact binds to AURKA (Ewart-Toland et al., 2003). This could be a possible mechanism that links AURKA with the selective phenotypic outcome of HPV-transformed cervical cancer cell lines.

Although AURKA and AURKB were investigated in this thesis, GSG2/Haspin was also a mitotic regulator that showed selective lethality to HPV-transformed cervical cancer cell line, CaSki, when depleted by siRNA (discussed in Chapter 3). Haspin is a relatively novel gene that contributes to proper chromosome alignment and satisfaction of spindle assembly checkpoint (Dai et al., 2006). It has been also reported that silencing of Haspin using RNAi increased mitotic index, delayed exit from mitosis, and weakened the spindle checkpoint response to taxol (Higgins, 2010, Wang et al., 2010, Niedzialkowska et al., 2012). Haspin phosphorylates histone H3 at threonine-3 (H3T3ph), which provides a docking site for AURKB at the centromere (Wang et al., 2012). Inhibition of Haspin caused decreased H3T3ph phosphorylation and subsequent loss of centromeric AURKB. This obviously shows the strong relationship between AURKB and Haspin as key players during mitosis, which should be investigated in the future.

6.2 Conclusions and future directions

The work presented in this thesis has illustrated a robust siRNA high-throughput screening protocol that enabled the identification of novel target genes that when silenced kill only HPV-transformed cervical cancer cells but not others. Six novel genes were identified and confirmed by the screen,

and only two of them, Aurora A and Aurora B, were selected for further investigations. The study also shows that the ZM447439 AURKB inhibitor was not selective towards HPV-induced cell lines. Instead, all tested cell lines were affected with the inhibitor, irrespective of their HPV-transformation status. MLN8237, a selective AURKA inhibitor that is currently under phases I and II clinical trial, demonstrated significant lethal selectivity in HPV-transformed cervical cancer cell lines *in vitro*; this finding was also confirmed *in vivo* by using three different cervical cancer cell lines, namely, HeLa (HPV18), CaSki (HPV16), and C33A (non-HPV).

Several issues can be addressed on the basis of the findings of this study. In particular, the mechanistic pathway beyond the link between Aurora A kinase and HPV-induced cell lines selectivity is an interesting aspect of this study that needs further investigation. Indeed, further investigation is necessary to determine if the NF- κ B/AURKA signalling pathway activation is required to maintain induction of apoptosis in the HPV-transformed cervical cancer cell lines. An NF- κ B deficient model can be used to determine whether this AURKA/NF- κ B signalling cascade is required to maintain sufficient AURKA inhibitor-induced apoptosis. Also, as it was proposed in this thesis the pro-apoptotic Puma may play a role in inducing apoptosis in the HPV-transformed cervical cancer cell lines, the knockdown of Puma by specific siRNA followed by treatment of these cells with the MLN8237 inhibitor will reveal the role of Puma in this mechanism. Another interesting area of investigation is the determination of the spindle checkpoint status in all cell lines tested either before or after treatment. This will provide evidence in how the mitotic slippage occur and, also, pave the pathway to understand the reason beyond the prolonged mitotic arrest that occurs in the HPV-induced cell lines which was not noticed in the non-HPV panel. Additionally, depletion of different spindle checkpoint proteins such as Mad2 or BubR1 by specific siRNA followed by treatment with the MLN8237 would also help understanding the mechanism beyond the mitotic arrest that was determined using the time-lapse data in Chapter 5. As discussed in the previous chapter, these spindle checkpoint elements are essential in functional spindle checkpoint and their status in the tested cell lines should be investigated. Meanwhile, based on the findings of this project, initiation of clinical trial to treat cases with cervical cancer can be possibly performed.

On the other hand, another line of future work is the investigation of a selective Aurora B small-molecule inhibitor that is currently under clinical trial, such as AZD1152 (Portella et al., 2011) with

HPV-transformed and non-HPV cervical cancer cell lines to check for AURKB small-molecule inhibitor selectivity towards HPV-positive cell lines, which can be conducted by a dose-response experiment. This is would possibly be interesting as the siRNA screening data showed lethal selectivity towards the majority of HPV-induced cell lines. In addition, little is known about Haspin and, in fact, the relation between Haspin and cervical cancer was never built. However, a small molecule inhibitor developed by Chroma Therapeutics called (CHR-6494) was used in a panel of cell lines including HeLa and showed promising results by decreasing the viability of HeLa and some other cancer cell lines (Huertas et al., 2012). Therefore, Haspin is an interesting area that worth investigation using small molecule inhibitors and siRNA.

Bibliography

- ADHIM, Z., OTSUKI, N., KITAMOTO, J., MORISHITA, N., KAWABATA, M., SHIRAKAWA, T. & NIBU, K. 2013. Gene silencing with siRNA targeting E6/E7 as a therapeutic intervention against head and neck cancer-containing HPV16 cell lines. *Acta Otolaryngol*, 133, 761-71.
- AINSWORTH, J., THOMAS, M., BANKS, L., COUTLEE, F. & MATLASHEWSKI, G. 2008. Comparison of p53 and the PDZ domain containing protein MAGI-3 regulation by the E6 protein from high-risk human papillomaviruses. *Virology*, 5, 67.
- ALFEREZ, D. G., GOODLAD, R. A., ODEDRA, R., SINI, P., CRAFTER, C., RYAN, A. J., WEDGE, S. R., WRIGHT, N. A., ANDERSON, E. & WILKINSON, R. W. 2012. Inhibition of Aurora-B kinase activity confers antitumour efficacy in preclinical mouse models of early and advanced gastrointestinal neoplasia. *Int J Oncol*, 41, 1475-85.
- ALLAM, M., PATERSON, A., THOMSON, A., RAY, B., RAJAGOPALAN, C. & SARKAR, G. 2005. Large loop excision and cold coagulation for management of cervical intraepithelial neoplasia. *Int J Gynaecol Obstet*, 88, 38-43.
- ANAND, S., PENRHYN-LOWE, S. & VENKITARAMAN, A. R. 2003. AURORA-A amplification overrides the mitotic spindle assembly checkpoint, inducing resistance to Taxol. *Cancer Cell*, 3, 51-62.
- ANN L. COKER, C. D., KATHERINE S. EGGLESTON, CLAUDIA HOPENHAYN, JACLYN NEE, AND THOMAS TUCKER 2008. Smoking and survival among Kentucky women diagnosed with invasive cervical cancer: 1995-2005. *Gynecol Oncol.* , 112, 365-369.
- APT, D., WATTS, R. M., SUSKE, G. & BERNARD, H. U. 1996. High Sp1/Sp3 ratios in epithelial cells during epithelial differentiation and cellular transformation correlate with the activation of the HPV-16 promoter. *Virology*, 224, 281-91.
- ARAKI, K. & KONIECZNY, B. T. 2012. Utilizing a retroviral RNAi system to investigate in vivo mTOR functions in T cells. *Methods Mol Biol*, 821, 305-16.
- ARKIN, M. R. & WELLS, J. A. 2004. Small-molecule inhibitors of protein-protein interactions: progressing towards the dream. *Nat Rev Drug Discov*, 3, 301-17.

- ARROYO, M. & RAYCHAUDHURI, P. 1992. Retinoblastoma-repression of E2F-dependent transcription depends on the ability of the retinoblastoma protein to interact with E2F and is abrogated by the adenovirus E1A oncoprotein. *Nucleic Acids Res*, 20, 5947-54.
- ARTANDI, S. E. & DEPINHO, R. A. 2000. A critical role for telomeres in suppressing and facilitating carcinogenesis. *Curr Opin Genet Dev*, 10, 39-46.
- ASHKENAZI, A. 2002. Targeting death and decoy receptors of the tumour-necrosis factor superfamily. *Nat Rev Cancer*, 2, 420-30.
- ASHWORTH, A. 2008. A synthetic lethal therapeutic approach: poly(ADP) ribose polymerase inhibitors for the treatment of cancers deficient in DNA double-strand break repair. *J Clin Oncol*, 26, 3785-90.
- AZORSA, D. O., GONZALES, I. M., BASU, G. D., CHOUDHARY, A., ARORA, S., BISANZ, K. M., KIEFER, J. A., HENDERSON, M. C., TRENT, J. M., VON HOFF, D. D. & MOUSSES, S. 2009. Synthetic lethal RNAi screening identifies sensitizing targets for gemcitabine therapy in pancreatic cancer. *J Transl Med*, 7, 43.
- BADARACCO, G., SAVARESE, A., MICHELI, A., RIZZO, C., PAOLINI, F., CAROSI, M., CUTILLO, G., VIZZA, E., ARCANGELI, G. & VENUTI, A. 2010. Persistence of HPV after radio-chemotherapy in locally advanced cervical cancer. *Oncol Rep*, 23, 1093-9.
- BAI, L., WEI, L., WANG, J., LI, X. & HE, P. 2006. Extended effects of human papillomavirus 16 E6-specific short hairpin RNA on cervical carcinoma cells. *Int J Gynecol Cancer*, 16, 718-29.
- BAIN, J., PLATER, L., ELLIOTT, M., SHPIRO, N., HASTIE, C. J., MCLAUCHLAN, H., KLEVERNIC, I., ARTHUR, J. S., ALESSI, D. R. & COHEN, P. 2007. The selectivity of protein kinase inhibitors: a further update. *Biochem J*, 408, 297-315.
- BARBIE, TAMAYO P, BOEHM JS & KIM SY, M. S., DUNN IF, SCHINZEL AC, SANDY P, MEYLAN E, SCHOLL C, FRÖHLING S, CHAN EM, SOS ML, MICHEL K, MERMEL C, SILVER SJ, WEIR BA, REILING JH, SHENG Q, GUPTA PB, WADLOW RC, LE H, HOERSCH S, WITTNER BS, RAMASWAMY S, LIVINGSTON DM, SABATINI DM, MEYERSON M, THOMAS RK, LANDER ES, MESIROV JP, ROOT DE, GILLILAND DG, JACKS T, HAHN WC. 2009. Systematic RNA interference reveals that oncogenic KRAS-driven cancers require TBK1. *Nature*, 562, 108-12.

- BARROW-LAING, L., CHEN, W. & ROMAN, A. Low- and high-risk human papillomavirus E7 proteins regulate p130 differently. *Virology*, 400, 233-9.
- BARROW-LAING, L., CHEN, W. & ROMAN, A. 2010. Low- and high-risk human papillomavirus E7 proteins regulate p130 differently. *Virology*, 400, 233-9.
- BARTEK, J., BARTKOVA, J. & LUKAS, J. 1997. The retinoblastoma protein pathway in cell cycle control and cancer. *Exp Cell Res*, 237, 1-6.
- BEAMISH, H., WARRENER, R. & GABRIELLI, B. G. 2004. Analysis of checkpoint responses to histone deacetylase inhibitors. *Methods Mol Biol*, 281, 245-59.
- BEAUDENON, S. & HUIBREGTSE, J. M. 2008. HPV E6, E6AP and cervical cancer. *BMC Biochem*, 9 Suppl 1, S4.
- BEDELL, M. A., HUDSON, J. B., GOLUB, T. R., TURYK, M. E., HOSKEN, M., WILBANKS, G. D. & LAIMINS, L. A. 1991. Amplification of human papillomavirus genomes in vitro is dependent on epithelial differentiation. *J Virol*, 65, 2254-60.
- BENEDET, J. L., ODICINO, F., MAISONNEUVE, P., BELLER, U., CREASMAN, W. T., HEINTZ, A. P., NGAN, H. Y. & PECORELLI, S. 2003. Carcinoma of the cervix uteri. *Int J Gynaecol Obstet*, 83 Suppl 1, 41-78.
- BERGERS, G. & BENJAMIN, L. E. 2003. Tumourigenesis and the angiogenic switch. *Nat Rev Cancer*, 3, 401-10.
- BERNARD, H. U. 2005. The clinical importance of the nomenclature, evolution and taxonomy of human papillomaviruses. *J Clin Virol*, 32 Suppl 1, S1-6.
- BERNARD, H. U., BURK, R. D., CHEN, Z., VAN DOORSLAER, K., ZUR HAUSEN, H. & DE VILLIERS, E. M. 2010. Classification of papillomaviruses (PVs) based on 189 PV types and proposal of taxonomic amendments. *Virology*, 401, 70-9.
- BERNARD, M., SANSEAU, P., HENRY, C., COUTURIER, A. & PRIGENT, C. 1998. Cloning of STK13, a third human protein kinase related to Drosophila aurora and budding yeast Ipl1 that maps on chromosome 19q13.3-ter. *Genomics*, 53, 406-9.
- BERTOLINI, F., SHAKED, Y., MANCUSO, P. & KERBEL, R. S. 2006. The multifaceted circulating endothelial cell in cancer: towards marker and target identification. *Nat Rev Cancer*, 6, 835-45.
- BHATIA, S., TYKODI, S. S. & THOMPSON, J. A. 2009. Treatment of metastatic melanoma: an overview. *Oncology (Williston Park)*, 23, 488-96.

- BIRMINGHAM, A., SELFORS, L. M., FORSTER, T., WROBEL, D., KENNEDY, C. J., SHANKS, E., SANTOYO-LOPEZ, J., DUNICAN, D. J., LONG, A., KELLEHER, D., SMITH, Q., BEIJERSBERGEN, R. L., GHAZAL, P. & SHAMU, C. E. 2009. Statistical methods for analysis of high-throughput RNA interference screens. *Nat Methods*, 6, 569-75.
- BISCHOF, O., NACERDDINE, K. & DEJEAN, A. 2005. Human papillomavirus oncoprotein E7 targets the promyelocytic leukemia protein and circumvents cellular senescence via the Rb and p53 tumour suppressor pathways. *Mol Cell Biol*, 25, 1013-24.
- BJORNSTI, M. A. & HOUGHTON, P. J. 2004. The TOR pathway: a target for cancer therapy. *Nat Rev Cancer*, 4, 335-48.
- BLAKAJ, D. M., FERNANDEZ-FUENTES, N., CHEN, Z., HEGDE, R., FISER, A., BURK, R. D. & BRENOWITZ, M. 2009. Evolutionary and biophysical relationships among the papillomavirus E2 proteins. *Front Biosci (Landmark Ed)*, 14, 900-17.
- BLASCO, M. A., LEE, H. W., HANDE, M. P., SAMPER, E., LANSDORP, P. M., DEPINHO, R. A. & GREIDER, C. W. 1997. Telomere shortening and tumour formation by mouse cells lacking telomerase RNA. *Cell*, 91, 25-34.
- BLUME-JENSEN, P. & HUNTER, T. 2001. Oncogenic kinase signalling. *Nature*, 411, 355-65.
- BODILY, J. & LAIMINS, L. A. 2011. Persistence of human papillomavirus infection: keys to malignant progression. *Trends Microbiol*, 19, 33-9.
- BODNAR, A. G., OUELLETTE, M., FROLKIS, M., HOLT, S. E., CHIU, C. P., MORIN, G. B., HARLEY, C. B., SHAY, J. W., LICHTSTEINER, S. & WRIGHT, W. E. 1998. Extension of life-span by introduction of telomerase into normal human cells. *Science*, 279, 349-52.
- BONATI, M. & GARATTINI, S. 2009. Controlling cervical cancer. *Pharmacoeconomics*, 27, 91-3.
- BORGNE, A. & MEIJER, L. 1996. Sequential dephosphorylation of p34(cdc2) on Thr-14 and Tyr-15 at the prophase/metaphase transition. *J Biol Chem*, 271, 27847-54.
- BOTTALICO, D., CHEN, Z., DUNNE, A., OSTOLOZA, J., MCKINNEY, S., SUN, C., SCHLECHT, N. F., FATAHZADEH, M., HERRERO, R., SCHIFFMAN, M. & BURK, R. D. 2011. The oral cavity contains abundant known and novel human papillomaviruses from the Betapapillomavirus and Gammapapillomavirus genera. *J Infect Dis*, 204, 787-92.
- BOXMAN, I. L., MULDER, L. H., NOYA, F., DE WAARD, V., GIBBS, S., BROKER, T. R., TEN KATE, F., CHOW, L. T. & TER SCHEGGET, J. 2001. Transduction of the E6 and E7 genes of epidermodysplasia- verruciformis-associated human papillomaviruses alters human

- keratinocyte growth and differentiation in organotypic cultures. *J Invest Dermatol*, 117, 1397-404.
- BOYD, A. S., STASKO, T. S. & TANG, Y. W. 2011. Basaloid squamous cell carcinoma of the skin. *J Am Acad Dermatol*, 64, 144-51.
- BRIASSOULI, P., CHAN, F., SAVAGE, K., REIS-FILHO, J. S. & LINARDOPOULOS, S. 2007. Aurora-A regulation of nuclear factor-kappaB signaling by phosphorylation of I κ B α . *Cancer Res*, 67, 1689-95.
- BROOKS, L. A., SULLIVAN, A., O'NIONS, J., BELL, A., DUNNE, B., TIDY, J. A., EVANS, D. J., OSIN, P., VOUSDEN, K. H., GUSTERSON, B., FARRELL, P. J., STOREY, A., GASCO, M., SAKAI, T. & CROOK, T. 2002. E7 proteins from oncogenic human papillomavirus types transactivate p73: role in cervical intraepithelial neoplasia. *Br J Cancer*, 86, 263-8.
- BROUGH, R., FRANKUM, J. R., COSTA-CABRAL, S., LORD, C. J. & ASHWORTH, A. 2011. Searching for synthetic lethality in cancer. *Curr Opin Genet Dev*, 21, 34-41.
- BROWN, L. F., GUIDI, A. J., SCHNITT, S. J., VAN DE WATER, L., IRUELA-ARISPE, M. L., YEO, T. K., TOGNAZZI, K. & DVORAK, H. F. 1999. Vascular stroma formation in carcinoma in situ, invasive carcinoma, and metastatic carcinoma of the breast. *Clin Cancer Res*, 5, 1041-56.
- BRZEZNIAK, C., CARTER, C. A. & GIACCONE, G. 2013. Dacomitinib, a new therapy for the treatment of non-small cell lung cancer. *Expert Opin Pharmacother*, 14, 247-53.
- BU, Y., YANG, Z., LI, Q. & SONG, F. 2008. Silencing of polo-like kinase (Plk) 1 via siRNA causes inhibition of growth and induction of apoptosis in human esophageal cancer cells. *Oncology*, 74, 198-206.
- BUCZKOWICZ, P., ZARGHOONI, M., BARTELS, U., MORRISON, A., MISURACA, K. L., CHAN, T., BOUFFET, E., HUANG, A., BECHER, O. & HAWKINS, C. 2013. Aurora kinase B is a potential therapeutic target in pediatric diffuse intrinsic pontine glioma. *Brain Pathol*, 23, 244-53.
- BULLARD DUNN, K. 2010. Retrorectal tumours. *Surg Clin North Am*, 90, 163-71, Table of Contents.
- BURD, E. M. 2003. Human papillomavirus and cervical cancer. *Clin Microbiol Rev*, 16, 1-17.

- CAMPISI, J. & D'ADDA DI FAGAGNA, F. 2007. Cellular senescence: when bad things happen to good cells. *Nat Rev Mol Cell Biol*, 8, 729-40.
- CANAANI, D. 2009. Methodological approaches in application of synthetic lethality screening towards anticancer therapy. *Br J Cancer*, 100, 1213-8.
- CAPRI, S., GASPARINI, R., PANATTO, D. & DEMARTEAU, N. 2011. Cost-consequences evaluation between bivalent and quadrivalent HPV vaccines in Italy: the potential impact of different cross-protection profiles. *Gynecol Oncol*, 121, 514-21.
- CARMELIET, P., FERREIRA, V., BREIER, G., POLLEFEYT, S., KIECKENS, L., GERTSENSTEIN, M., FAHRIG, M., VANDENHOECK, A., HARPAL, K., EBERHARDT, C., DECLERCQ, C., PAWLING, J., MOONS, L., COLLEN, D., RISAU, W. & NAGY, A. 1996. Abnormal blood vessel development and lethality in embryos lacking a single VEGF allele. *Nature*, 380, 435-9.
- CARMENA, M. & EARNSHAW, W. C. 2003. The cellular geography of aurora kinases. *Nat Rev Mol Cell Biol*, 4, 842-54.
- CARMENA, M., RUCHAUD, S. & EARNSHAW, W. C. 2009. Making the Auroras glow: regulation of Aurora A and B kinase function by interacting proteins. *Curr Opin Cell Biol*, 21, 796-805.
- CARTER, T. A., WODICKA, L. M., SHAH, N. P., VELASCO, A. M., FABIAN, M. A., TREIBER, D. K., MILANOV, Z. V., ATTERIDGE, C. E., BIGGS, W. H., 3RD, EDEEN, P. T., FLOYD, M., FORD, J. M., GROTZFELD, R. M., HERRGARD, S., INSKO, D. E., MEHTA, S. A., PATEL, H. K., PAO, W., SAWYERS, C. L., VARMUS, H., ZARRINKAR, P. P. & LOCKHART, D. J. 2005. Inhibition of drug-resistant mutants of ABL, KIT, and EGF receptor kinases. *Proc Natl Acad Sci U S A*, 102, 11011-6.
- CASTLE, P. E., RODRIGUEZ, A. C., PORRAS, C., HERRERO, R., SCHIFFMAN, M., GONZALEZ, P., HILDESHEIM, A. & BURK, R. D. 2007. A comparison of cervical and vaginal human papillomavirus. *Sex Transm Dis*, 34, 849-55.
- CHAN, D. A. & GIACCIA, A. J. 2011. Harnessing synthetic lethal interactions in anticancer drug discovery. *Nat Rev Drug Discov*, 10, 351-64.
- CHAN, E., KACHNIC, L. A. & THOMAS, C. R., JR. 2009. Anal cancer: progress on combined-modality and organ preservation. *Curr Probl Cancer*, 33, 302-26.

- CHAN, K. S., KOH, C. G. & LI, H. Y. 2012. Mitosis-targeted anti-cancer therapies: where they stand. *Cell Death Dis*, 3, e411.
- CHASE, D. M., KALOUYAN, M. & DISAIA, P. J. 2009. Colposcopy to evaluate abnormal cervical cytology in 2008. *Am J Obstet Gynecol*, 200, 472-80.
- CHEN, Q., ZHANG, X., JIANG, Q., CLARKE, P. R. & ZHANG, C. 2008. Cyclin B1 is localized to unattached kinetochores and contributes to efficient microtubule attachment and proper chromosome alignment during mitosis. *Cell Res*, 18, 268-80.
- CHEN, X. S., GARCEA, R. L., GOLDBERG, I., CASINI, G. & HARRISON, S. C. 2000. Structure of small virus-like particles assembled from the L1 protein of human papillomavirus 16. *Mol Cell*, 5, 557-67.
- CHIN, G. M. & HERBST, R. 2006. Induction of apoptosis by monastrol, an inhibitor of the mitotic kinesin Eg5, is independent of the spindle checkpoint. *Mol Cancer Ther*, 5, 2580-91.
- CHO, M. H., NILES, A., HUANG, R., INGLESE, J., AUSTIN, C. P., RISS, T. & XIA, M. 2008. A bioluminescent cytotoxicity assay for assessment of membrane integrity using a proteolytic biomarker. *Toxicol In Vitro*, 22, 1099-106.
- CHRISTOFORI, G. 2003. Changing neighbours, changing behaviour: cell adhesion molecule-mediated signalling during tumour progression. *EMBO J*, 22, 2318-23.
- CO., M. 2008. Human Papillomavirus, Monographs in Medicine. *Whitehouse Station*.
- COBRINIK, D. 2005. Pocket proteins and cell cycle control. *Oncogene*, 24, 2796-809.
- CONEJO-GARCIA, J. R., BUCKANOVICH, R. J., BENENCIA, F., COURREGES, M. C., RUBIN, S. C., CARROLL, R. G. & COUKOS, G. 2005. Vascular leukocytes contribute to tumour vascularization. *Blood*, 105, 679-81.
- CROOK, T., WREDE, D. & VOUSDEN, K. H. 1991. p53 point mutation in HPV negative human cervical carcinoma cell lines. *Oncogene*, 6, 873-5.
- CRUSIUS, K., RODRIGUEZ, I. & ALONSO, A. 2000. The human papillomavirus type 16 E5 protein modulates ERK1/2 and p38 MAP kinase activation by an EGFR-independent process in stressed human keratinocytes. *Virus Genes*, 20, 65-9.
- DAI, B., YOO, S. Y., BARTHOLOMEUSZ, G., GRAHAM, R. A., MAJIDI, M., YAN, S., MENG, J., JI, L., COOMBES, K., MINNA, J. D., FANG, B. & ROTH, J. A. 2013. KEAP1-dependent synthetic lethality induced by AKT and TXNRD1 inhibitors in lung cancer. *Cancer Res*.

- DAI, J. & HIGGINS, J. M. 2005. Haspin: a mitotic histone kinase required for metaphase chromosome alignment. *Cell Cycle*, 4, 665-8.
- DAI, J., SULLIVAN, B. A. & HIGGINS, J. M. 2006. Regulation of mitotic chromosome cohesion by Haspin and Aurora B. *Dev Cell*, 11, 741-50.
- DAI, J., SULTAN, S., TAYLOR, S. S. & HIGGINS, J. M. 2005. The kinase haspin is required for mitotic histone H3 Thr 3 phosphorylation and normal metaphase chromosome alignment. *Genes Dev*, 19, 472-88.
- DAO, L. D., DUFFY, A., VAN TINE, B. A., WU, S. Y., CHIANG, C. M., BROKER, T. R. & CHOW, L. T. 2006. Dynamic localization of the human papillomavirus type 11 origin binding protein E2 through mitosis while in association with the spindle apparatus. *J Virol*, 80, 4792-800.
- DAR, A. A., BELKHIRI, A., ECSEDY, J., ZAIKA, A. & EL-RIFAI, W. 2008. Aurora kinase A inhibition leads to p73-dependent apoptosis in p53-deficient cancer cells. *Cancer Res*, 68, 8998-9004.
- DAR, A. A., GOFF, L. W., MAJID, S., BERLIN, J. & EL-RIFAI, W. 2010. Aurora kinase inhibitors--rising stars in cancer therapeutics? *Mol Cancer Ther*, 9, 268-78.
- DAVIES, S. P., REDDY, H., CAIVANO, M. & COHEN, P. 2000. Specificity and mechanism of action of some commonly used protein kinase inhibitors. *Biochem J*, 351, 95-105.
- DAVIS, R. J. 2000. Signal transduction by the JNK group of MAP kinases. *Cell*, 103, 239-52.
- DE BOER, L., OAKES, V., BEAMISH, H., GILES, N., STEVENS, F., SOMODEVILLA-TORRES, M., DESOUZA, C. & GABRIELLI, B. 2008. Cyclin A/cdk2 coordinates centrosomal and nuclear mitotic events. *Oncogene*, 27, 4261-8.
- DE OLIVEIRA, J. C., BRASSESCO, M. S., PEZUK, J. A., MORALES, A. G., VALERA, E. T., MONTALDI, A. P., SAKAMOTO-HOJO, E. T., SCRIDELI, C. A. & TONE, L. G. 2012. In vitro PLK1 inhibition by BI 2536 decreases proliferation and induces cell-cycle arrest in melanoma cells. *J Drugs Dermatol*, 11, 587-92.
- DE VILLIERS, E. M., FAUQUET, C., BROKER, T. R., BERNARD, H. U. & ZUR HAUSEN, H. 2004a. Classification of papillomaviruses. *Virology*, 324, 17-27.
- DE VILLIERS, E. M., GUNST, K., STEIN, H. & SCHERUBL, H. 2004b. Esophageal squamous cell cancer in patients with head and neck cancer: Prevalence of human papillomavirus DNA sequences. *Int J Cancer*, 109, 253-8.

- DE VINCENZO, R., AMADIO, G., RICCI, C., LICAMELI, A., FERRANDINA, G., CAPELLI, G. & SCAMBIA, G. 2009. Treatment of cervical cancer in Italy: strategies and their impact on the women. *Vaccine*, 27 Suppl 1, A39-45.
- DEES, E. C., COHEN, R. B., VON MEHREN, M., STINCHCOMBE, T. E., LIU, H., VENKATAKRISHNAN, K., MANFREDI, M., FINGERT, H., BURRIS, H. A., 3RD & INFANTE, J. R. 2012. Phase I study of aurora A kinase inhibitor MLN8237 in advanced solid tumours: safety, pharmacokinetics, pharmacodynamics, and bioavailability of two oral formulations. *Clin Cancer Res*, 18, 4775-84.
- DELACOUR-LAROSE, M., MOLLA, A., SKOUFIAS, D. A., MARGOLIS, R. L. & DIMITROV, S. 2004. Distinct dynamics of Aurora B and Survivin during mitosis. *Cell Cycle*, 3, 1418-26.
- DELURY, C. P., MARSH, E. K., JAMES, C. D., BOON, S. S., BANKS, L., KNIGHT, G. L. & ROBERTS, S. 2013. The role of protein kinase A regulation of the E6 PDZ-binding domain during the differentiation-dependent life cycle of human papillomavirus type 18. *J Virol*, 87, 9463-72.
- DEMASI, J., HUH, K. W., NAKATANI, Y., MUNGER, K. & HOWLEY, P. M. 2005. Bovine papillomavirus E7 transformation function correlates with cellular p600 protein binding. *Proc Natl Acad Sci U S A*, 102, 11486-91.
- DENG, L., WANG, C., SPENCER, E., YANG, L., BRAUN, A., YOU, J., SLAUGHTER, C., PICKART, C. & CHEN, Z. J. 2000. Activation of the I κ B kinase complex by TRAF6 requires a dimeric ubiquitin-conjugating enzyme complex and a unique polyubiquitin chain. *Cell*, 103, 351-61.
- DEPHOURE, N., ZHOU, C., VILLEN, J., BEAUSOLEIL, S. A., BAKALARSKI, C. E., ELLEDGE, S. J. & GYGI, S. P. 2008. A quantitative atlas of mitotic phosphorylation. *Proc Natl Acad Sci U S A*, 105, 10762-7.
- DEVAULT, A., GUEYDON, E. & SCHWOB, E. 2008. Interplay between S-cyclin-dependent kinase and Dbf4-dependent kinase in controlling DNA replication through phosphorylation of yeast Mcm4 N-terminal domain. *Mol Biol Cell*, 19, 2267-77.
- DI LEONARDO, A., KHAN, S. H., LINKE, S. P., GRECO, V., SEIDITA, G. & WAHL, G. M. 1997. DNA rereplication in the presence of mitotic spindle inhibitors in human and mouse fibroblasts lacking either p53 or pRb function. *Cancer Res*, 57, 1013-9.

- DIMRI, G. P., LEE, X., BASILE, G., ACOSTA, M., SCOTT, G., ROSKELLEY, C., MEDRANO, E. E., LINSKENS, M., RUBELJ, I., PEREIRA-SMITH, O. & ET AL. 1995. A biomarker that identifies senescent human cells in culture and in aging skin in vivo. *Proc Natl Acad Sci U S A*, 92, 9363-7.
- DING, Z., WU, C. J., JASKELIOFF, M., IVANOVA, E., KOST-ALIMOVA, M., PROTOPOPOV, A., CHU, G. C., WANG, G., LU, X., LABROT, E. S., HU, J., WANG, W., XIAO, Y., ZHANG, H., ZHANG, J., ZHANG, J., GAN, B., PERRY, S. R., JIANG, S., LI, L., HORNER, J. W., WANG, Y. A., CHIN, L. & DEPINHO, R. A. 2012. Telomerase reactivation following telomere dysfunction yields murine prostate tumours with bone metastases. *Cell*, 148, 896-907.
- DITCHFIELD, C., JOHNSON, V. L., TIGHE, A., ELLSTON, R., HAWORTH, C., JOHNSON, T., MORTLOCK, A., KEEN, N. & TAYLOR, S. S. 2003. Aurora B couples chromosome alignment with anaphase by targeting BubR1, Mad2, and Cenp-E to kinetochores. *J Cell Biol*, 161, 267-80.
- DOI, N., ZENNO, S., UEDA, R., OHKI-HAMAZAKI, H., UI-TEI, K. & SAIGO, K. 2003. Short-interfering-RNA-mediated gene silencing in mammalian cells requires Dicer and eIF2C translation initiation factors. *Curr Biol*, 13, 41-6.
- DONG, Y., LI, A., WANG, J., WEBER, J. D. & MICHEL, L. S. 2010. Synthetic lethality through combined Notch-epidermal growth factor receptor pathway inhibition in basal-like breast cancer. *Cancer Res*, 70, 5465-74.
- DOORBAR, J., QUINT, W., BANKS, L., BRAVO, I. G., STOLER, M., BROKER, T. R. & STANLEY, M. A. 2012. The biology and life-cycle of human papillomaviruses. *Vaccine*, 30 Suppl 5, F55-70.
- DRAPER, E., BISSETT, S. L., HOWELL-JONES, R., WAIGHT, P., SOLDAN, K., JIT, M., ANDREWS, N., MILLER, E. & BEDDOWS, S. 2013. A randomized, observer-blinded immunogenicity trial of Cervarix((R)) and Gardasil((R)) Human Papillomavirus vaccines in 12-15 year old girls. *PLoS One*, 8, e61825.
- DUA, P., YOO, J. W., KIM, S. & LEE, D. K. 2011. Modified siRNA structure with a single nucleotide bulge overcomes conventional siRNA-mediated off-target silencing. *Mol Ther*, 19, 1676-87.

- DUENAS-GONZALEZ, A., CETINA, L., CORONEL, J. & MARTINEZ-BANOS, D. 2010. Pharmacotherapy options for locally advanced and advanced cervical cancer. *Drugs*, 70, 403-32.
- DUTERTRE, S., CAZALES, M., QUARANTA, M., FROMENT, C., TRABUT, V., DOZIER, C., MIREY, G., BOUCHE, J. P., THEIS-FEBVRE, N., SCHMITT, E., MONSARRAT, B., PRIGENT, C. & DUCOMMUN, B. 2004. Phosphorylation of CDC25B by Aurora-A at the centrosome contributes to the G2-M transition. *J Cell Sci*, 117, 2523-31.
- DUTTA, T., BURGESS, M., MCMILLAN, N. A. & PAREKH, H. S. 2010. Dendrosome-based delivery of siRNA against E6 and E7 oncogenes in cervical cancer. *Nanomedicine*, 6, 463-70.
- DYSON, N. 1998. The regulation of E2F by pRB-family proteins. *Genes Dev*, 12, 2245-62.
- DYSON, N., BERNARDS, R., FRIEND, S. H., GOODING, L. R., HASSELL, J. A., MAJOR, E. O., PIPAS, J. M., VANDYKE, T. & HARLOW, E. 1990. Large T antigens of many polyomaviruses are able to form complexes with the retinoblastoma protein. *J Virol*, 64, 1353-6.
- EICHTEN, A., WESTFALL, M., PIETENPOL, J. A. & MUNGER, K. 2002. Stabilization and functional impairment of the tumour suppressor p53 by the human papillomavirus type 16 E7 oncoprotein. *Virology*, 295, 74-85.
- EKSTROM, J., BZHALAVA, D., SVENBACK, D., FORSLUND, O. & DILLNER, J. 2011. High throughput sequencing reveals diversity of Human Papillomaviruses in cutaneous lesions. *Int J Cancer*, 129, 2643-50.
- EL-ARMOUCHE, A., SINGH, J., NAITO, H., WITTKOPPER, K., DIDIE, M., LAATSCH, A., ZIMMERMANN, W. H. & ESCHENHAGEN, T. 2007. Adenovirus-delivered short hairpin RNA targeting PKCalpha improves contractile function in reconstituted heart tissue. *J Mol Cell Cardiol*, 43, 371-6.
- ELHAJOUJI, A., CUNHA, M. & KIRSCH-VOLDERS, M. 1998. Spindle poisons can induce polyploidy by mitotic slippage and micronucleate mononucleates in the cytokinesis-block assay. *Mutagenesis*, 13, 193-8.
- ELMORE, S. 2007. Apoptosis: a review of programmed cell death. *Toxicol Pathol*, 35, 495-516.

- ESPOSITO, F., LIBERTINI, S., FRANCO, R., ABAGNALE, A., MARRA, L., PORTELLA, G. & CHIEFFI, P. 2009. Aurora B expression in post-puberal testicular germ cell tumours. *J Cell Physiol*, 221, 435-9.
- EVANS, R. P., NABER, C., STEFFLER, T., CHECKLAND, T., MAXWELL, C. A., KEATS, J. J., BELCH, A. R., PILARSKI, L. M., LAI, R. & REIMAN, T. 2008. The selective Aurora B kinase inhibitor AZD1152 is a potential new treatment for multiple myeloma. *Br J Haematol*, 140, 295-302.
- EWART-TOLAND, A., BRIASSOULI, P., DE KONING, J. P., MAO, J. H., YUAN, J., CHAN, F., MACCARTHY-MORROGH, L., PONDER, B. A., NAGASE, H., BURN, J., BALL, S., ALMEIDA, M., LINARDOPOULOS, S. & BALMAIN, A. 2003. Identification of Stk6/STK15 as a candidate low-penetrance tumour-susceptibility gene in mouse and human. *Nat Genet*, 34, 403-12.
- FABIAN, M. A., BIGGS, W. H., 3RD, TREIBER, D. K., ATTERIDGE, C. E., AZIMIOARA, M. D., BENEDETTI, M. G., CARTER, T. A., CICERI, P., EDEEN, P. T., FLOYD, M., FORD, J. M., GALVIN, M., GERLACH, J. L., GROTZFELD, R. M., HERRGARD, S., INSKO, D. E., INSKO, M. A., LAI, A. G., LELIAS, J. M., MEHTA, S. A., MILANOV, Z. V., VELASCO, A. M., WODICKA, L. M., PATEL, H. K., ZARRINKAR, P. P. & LOCKHART, D. J. 2005. A small molecule-kinase interaction map for clinical kinase inhibitors. *Nat Biotechnol*, 23, 329-36.
- FANG, G. 2002. Checkpoint protein BubR1 acts synergistically with Mad2 to inhibit anaphase-promoting complex. *Mol Biol Cell*, 13, 755-66.
- FANG, G., YU, H. & KIRSCHNER, M. W. 1998. The checkpoint protein MAD2 and the mitotic regulator CDC20 form a ternary complex with the anaphase-promoting complex to control anaphase initiation. *Genes Dev*, 12, 1871-83.
- FELDSER, D. M. & GREIDER, C. W. 2007. Short telomeres limit tumour progression in vivo by inducing senescence. *Cancer Cell*, 11, 461-9.
- FILIPPOVA, M., SONG, H., CONNOLLY, J. L., DERMODY, T. S. & DUERKSEN-HUGHES, P. J. 2002. The human papillomavirus 16 E6 protein binds to tumour necrosis factor (TNF) R1 and protects cells from TNF-induced apoptosis. *J Biol Chem*, 277, 21730-9.
- FLAHERTY, K. 2010. Advances in drug development. BRAF validation in melanoma. *Clin Adv Hematol Oncol*, 8, 31-4.

- FLAHERTY, K. T., HODI, F. S. & BASTIAN, B. C. 2010. Mutation-driven drug development in melanoma. *Curr Opin Oncol*, 22, 178-83.
- FLORES, E. R., ALLEN-HOFFMANN, B. L., LEE, D., SATTLER, C. A. & LAMBERT, P. F. 1999. Establishment of the human papillomavirus type 16 (HPV-16) life cycle in an immortalized human foreskin keratinocyte cell line. *Virology*, 262, 344-54.
- FORD, H. L. & PARDEE, A. B. 1999. Cancer and the cell cycle. *J Cell Biochem*, Suppl 32-33, 166-72.
- FRAZER, I. H. 2004. Prevention of cervical cancer through papillomavirus vaccination. *Nat Rev Immunol*, 4, 46-54.
- FROST, A., MROSS, K., STEINBILD, S., HEDBOM, S., UNGER, C., KAISER, R., TROMMESHAEUSER, D. & MUNZERT, G. 2012. Phase i study of the Plk1 inhibitor BI 2536 administered intravenously on three consecutive days in advanced solid tumours. *Curr Oncol*, 19, e28-35.
- FULDA, S. 2010. Evasion of apoptosis as a cellular stress response in cancer. *Int J Cell Biol*, 2010, 370835.
- GABRIELLI, B., CHIA, K. & WARRENER, R. 2011. Finally, how histone deacetylase inhibitors disrupt mitosis! *Cell Cycle*, 10, 2658-61.
- GABRIELLI, B. G., SARCEVIC, B., SINNAMON, J., WALKER, G., CASTELLANO, M., WANG, X. Q. & ELLEM, K. A. 1999. A cyclin D-Cdk4 activity required for G2 phase cell cycle progression is inhibited in ultraviolet radiation-induced G2 phase delay. *J Biol Chem*, 274, 13961-9.
- GADEA, B. B. & RUDERMAN, J. V. 2005. Aurora kinase inhibitor ZM447439 blocks chromosome-induced spindle assembly, the completion of chromosome condensation, and the establishment of the spindle integrity checkpoint in *Xenopus* egg extracts. *Mol Biol Cell*, 16, 1305-18.
- GALLUZZI, L. & KROEMER, G. 2008. Necroptosis: a specialized pathway of programmed necrosis. *Cell*, 135, 1161-3.
- GAO, D., NOLAN, D. J., MELLICK, A. S., BAMBINO, K., MCDONNELL, K. & MITTAL, V. 2008. Endothelial progenitor cells control the angiogenic switch in mouse lung metastasis. *Science*, 319, 195-8.

- GAO, Q., KUMAR, A., SINGH, L., HUIBREGTSE, J. M., BEAUDENON, S., SRINIVASAN, S., WAZER, D. E., BAND, H. & BAND, V. 2002. Human papillomavirus E6-induced degradation of E6TP1 is mediated by E6AP ubiquitin ligase. *Cancer Res*, 62, 3315-21.
- GAO, Q., SRINIVASAN, S., BOYER, S. N., WAZER, D. E. & BAND, V. 1999. The E6 oncoproteins of high-risk papillomaviruses bind to a novel putative GAP protein, E6TP1, and target it for degradation. *Mol Cell Biol*, 19, 733-44.
- GARCIA-CLOSAS, R., CASTELLSAGUE, X., BOSCH, X. & GONZALEZ, C. A. 2005. The role of diet and nutrition in cervical carcinogenesis: a review of recent evidence. *Int J Cancer*, 117, 629-37.
- GARLAND, S. M., HERNANDEZ-AVILA, M., WHEELER, C. M., PEREZ, G., HARPER, D. M., LEODOLTER, S., TANG, G. W., FERRIS, D. G., STEBEN, M., BRYAN, J., TADDEO, F. J., RAILKAR, R., ESSER, M. T., SINGS, H. L., NELSON, M., BOSLEGO, J., SATTLER, C., BARR, E. & KOUTSKY, L. A. 2007. Quadrivalent vaccine against human papillomavirus to prevent anogenital diseases. *N Engl J Med*, 356, 1928-43.
- GAUTSCHI, O., HEIGHWAY, J., MACK, P. C., PURNELL, P. R., LARA, P. N., JR. & GANDARA, D. R. 2008. Aurora kinases as anticancer drug targets. *Clin Cancer Res*, 14, 1639-48.
- GAUTSCHI, O., MACK, P. C., DAVIES, A. M., LARA, P. N., JR. & GANDARA, D. R. 2006. Aurora kinase inhibitors: a new class of targeted drugs in cancer. *Clin Lung Cancer*, 8, 93-8.
- GAVET, O. & PINES, J. 2010. Progressive activation of CyclinB1-Cdk1 coordinates entry to mitosis. *Dev Cell*, 18, 533-43.
- GAVRILOV, K. & SALTZMAN, W. M. 2012. Therapeutic siRNA: principles, challenges, and strategies. *Yale J Biol Med*, 85, 187-200.
- GENTHER, S. M., STERLING, S., DUENSING, S., MUNGER, K., SATTLER, C. & LAMBERT, P. F. 2003. Quantitative role of the human papillomavirus type 16 E5 gene during the productive stage of the viral life cycle. *J Virol*, 77, 2832-42.
- GEORGIEVA, I., KOYCHEV, D., WANG, Y., HOLSTEIN, J., HOPFENMULLER, W., ZEITZ, M. & GRABOWSKI, P. 2010. ZM447439, a novel promising aurora kinase inhibitor, provokes antiproliferative and proapoptotic effects alone and in combination with bio- and chemotherapeutic agents in gastroenteropancreatic neuroendocrine tumour cell lines. *Neuroendocrinology*, 91, 121-30.

- GEWIRTZ, D. A. 2014. The four faces of autophagy: implications for cancer therapy. *Cancer Res*, 74, 647-51.
- GIRDLER F, GASCOIGNE KE, EYERS PA, HARTMUTH S, CRAFTER C, FOOTE KM, KEEN NJ & SS., T. 2006. Validating Aurora B as an anti-cancer drug target. *J Cell Sci.*, 119, 3664-75.
- GIROGLOU, T., FLORIN, L., SCHAFER, F., STREECK, R. E. & SAPP, M. 2001. Human papillomavirus infection requires cell surface heparan sulfate. *J Virol*, 75, 1565-70.
- GIULIANO, A. R., TORTOLERO-LUNA, G., FERRER, E., BURCHELL, A. N., DE SANJOSE, S., KJAER, S. K., MUNOZ, N., SCHIFFMAN, M. & BOSCH, F. X. 2008. Epidemiology of human papillomavirus infection in men, cancers other than cervical and benign conditions. *Vaccine*, 26 Suppl 10, K17-28.
- GLICK, S. B., CLARKE, A. R., BLANCHARD, A. & WHITAKER, A. K. 2012. Cervical cancer screening, diagnosis and treatment interventions for racial and ethnic minorities: a systematic review. *J Gen Intern Med*, 27, 1016-32.
- GOMIS, R. R., ALARCON, C., HE, W., WANG, Q., SEOANE, J., LASH, A. & MASSAGUE, J. 2006. A FoxO-Smad synexpression group in human keratinocytes. *Proc Natl Acad Sci U S A*, 103, 12747-52.
- GONCALVES, C. V., QUINTANA, S. M., MARCOLIN, A. C., DUARTE, G., COSTA, J. S., KARAM, F. & BIANCHI, M. S. 2009. Microinvasive carcinoma of the uterine cervix in a 14-year-old adolescent: case report and literature review. *Sao Paulo Med J*, 127, 105-7.
- GONZALEZ, R. J. & TARLOFF, J. B. 2001. Evaluation of hepatic subcellular fractions for Alamar blue and MTT reductase activity. *Toxicol In Vitro*, 15, 257-9.
- GORDON, M. D. & NUSSE, R. 2006. Wnt signaling: multiple pathways, multiple receptors, and multiple transcription factors. *J Biol Chem*, 281, 22429-33.
- GORGUN, G., CALABRESE, E., HIDESHIMA, T., ECSEDY, J., PERRONE, G., MANI, M., IKEDA, H., BIANCHI, G., HU, Y., CIRSTEANU, D., SANTO, L., TAI, Y. T., NAHAR, S., ZHENG, M., BANDI, M., CARRASCO, R. D., RAJE, N., MUNSHI, N., RICHARDSON, P. & ANDERSON, K. C. 2010. A novel Aurora-A kinase inhibitor MLN8237 induces cytotoxicity and cell-cycle arrest in multiple myeloma. *Blood*, 115, 5202-13.

- GOTTSCHLING, M., GOKER, M., KOHLER, A., LEHMANN, M. D., STOCKFLETH, E. & NINDL, I. 2009. Cutaneotropic human beta-/gamma-papillomaviruses are rarely shared between family members. *J Invest Dermatol*, 129, 2427-34.
- GREEN, D. R. & KROEMER, G. 2004. The pathophysiology of mitochondrial cell death. *Science*, 305, 626-9.
- GREENBERG, R. A. 2005. Telomeres, crisis and cancer. *Curr Mol Med*, 5, 213-8.
- GREIDER, C. W. 2012. Molecular biology. Wnt regulates TERT--putting the horse before the cart. *Science*, 336, 1519-20.
- GRIVENNIKOV, S. I., GRETEN, F. R. & KARIN, M. 2010. Immunity, inflammation, and cancer. *Cell*, 140, 883-99.
- GU, Q., XING, J. Z., HUANG, M., ZHANG, X. & CHEN, J. 2013. Nanoformulation of paclitaxel to enhance cancer therapy. *J Biomater Appl*, 28, 298-307.
- GU, W., PAYNE, E., SUN, S., BURGESS, M. & MCMILLAN, N. A. 2011. Inhibition of cervical cancer cell growth in vitro and in vivo with dual shRNAs. *Cancer Gene Ther*, 18, 219-27.
- GUADAMILLAS, M. C., CERESO, A. & DEL POZO, M. A. 2011. Overcoming anoikis--pathways to anchorage-independent growth in cancer. *J Cell Sci*, 124, 3189-97.
- GULLY, C. P., ZHANG, F., CHEN, J., YEUNG, J. A., VELAZQUEZ-TORRES, G., WANG, E., YEUNG, S. C. & LEE, M. H. 2010. Antineoplastic effects of an Aurora B kinase inhibitor in breast cancer. *Mol Cancer*, 9, 42.
- GUO, C. P., LIU, K. W., LUO, H. B., CHEN, H. B., ZHENG, Y., SUN, S. N., ZHANG, Q. & HUANG, L. 2011. Potent anti-tumour effect generated by a novel human papillomavirus (HPV) antagonist peptide reactivating the pRb/E2F pathway. *PLoS One*, 6, e17734.
- HACKETT, J. A. & GREIDER, C. W. 2002. Balancing instability: dual roles for telomerase and telomere dysfunction in tumorigenesis. *Oncogene*, 21, 619-26.
- HAE-OCK LEE, OO-KYUNG LEE & LEE, H. 2010. Targeting mitotic kinases for anti-cancer treatment. *Emerging Signaling Pathways in Tumour Biology*, 157-184.
- HAGTING, A., JACKMAN, M., SIMPSON, K. & PINES, J. 1999. Translocation of cyclin B1 to the nucleus at prophase requires a phosphorylation-dependent nuclear import signal. *Curr Biol*, 9, 680-9.

- HAHN, W. C., COUNTER, C. M., LUNDBERG, A. S., BEIJERSBERGEN, R. L., BROOKS, M. W. & WEINBERG, R. A. 1999a. Creation of human tumour cells with defined genetic elements. *Nature*, 400, 464-8.
- HAHN, W. C., STEWART, S. A., BROOKS, M. W., YORK, S. G., EATON, E., KURACHI, A., BEIJERSBERGEN, R. L., KNOLL, J. H., MEYERSON, M. & WEINBERG, R. A. 1999b. Inhibition of telomerase limits the growth of human cancer cells. *Nat Med*, 5, 1164-70.
- HALLSTROM, T. C., MORI, S. & NEVINS, J. R. 2008. An E2F1-dependent gene expression program that determines the balance between proliferation and cell death. *Cancer Cell*, 13, 11-22.
- HANAHAN, D. & WEINBERG, R. A. 2011. Hallmarks of cancer: the next generation. *Cell*, 144, 646-74.
- HARA, E., TSURUI, H., SHINOZAKI, A., NAKADA, S. & ODA, K. 1991. Cooperative effect of antisense-Rb and antisense-p53 oligomers on the extension of life span in human diploid fibroblasts, TIG-1. *Biochem Biophys Res Commun*, 179, 528-34.
- HARDWICK, K. G., JOHNSTON, R. C., SMITH, D. L. & MURRAY, A. W. 2000. MAD3 encodes a novel component of the spindle checkpoint which interacts with Bub3p, Cdc20p, and Mad2p. *J Cell Biol*, 148, 871-82.
- HARMEY, J. H. & BOUCHIER-HAYES, D. 2002. Vascular endothelial growth factor (VEGF), a survival factor for tumour cells: implications for anti-angiogenic therapy. *Bioessays*, 24, 280-3.
- HARRINGTON, E. A., BEBBINGTON, D., MOORE, J., RASMUSSEN, R. K., AJOSE-ADEOGUN, A. O., NAKAYAMA, T., GRAHAM, J. A., DEMUR, C., HERCEND, T., DIU-HERCEND, A., SU, M., GOLEC, J. M. & MILLER, K. M. 2004. VX-680, a potent and selective small-molecule inhibitor of the Aurora kinases, suppresses tumour growth in vivo. *Nat Med*, 10, 262-7.
- HARRIS, P. S., VENKATARAMAN, S., ALIMOVA, I., BIRKS, D. K., DONSON, A. M., KNIPSTEIN, J., DUBUC, A., TAYLOR, M. D., HANDLER, M. H., FOREMAN, N. K. & VIBHAKAR, R. 2012. Polo-like kinase 1 (PLK1) inhibition suppresses cell growth and enhances radiation sensitivity in medulloblastoma cells. *BMC Cancer*, 12, 80.
- HARTWELL, L. H. & WEINERT, T. A. 1989. Checkpoints: controls that ensure the order of cell cycle events. *Science*, 246, 629-34.

- HARWOOD, C. A., SURENTERAN, T., SASIENI, P., PROBY, C. M., BORDEA, C., LEIGH, I. M., WOJNAROWSKA, F., BREUER, J. & MCGREGOR, J. M. 2004. Increased risk of skin cancer associated with the presence of epidermodysplasia verruciformis human papillomavirus types in normal skin. *Br J Dermatol*, 150, 949-57.
- HAUF, S., COLE, R. W., LATERRA, S., ZIMMER, C., SCHNAPP, G., WALTER, R., HECKEL, A., VAN MEEL, J., RIEDER, C. L. & PETERS, J. M. 2003. The small molecule Hesperadin reveals a role for Aurora B in correcting kinetochore-microtubule attachment and in maintaining the spindle assembly checkpoint. *J Cell Biol*, 161, 281-94.
- HAUPENTHAL, J., BIHRER, V., KORKUSUZ, H., KOLLMAR, O., SCHMITHALS, C., KRIENER, S., ENGELS, K., PLELI, T., BENZ, A., CANAMERO, M., LONGERICH, T., KRONENBERGER, B., RICHTER, S., WAIDMANN, O., VOGL, T. J., ZEUZEM, S. & PIIPER, A. 2012. Reduced efficacy of the Plk1 inhibitor BI 2536 on the progression of hepatocellular carcinoma due to low intratumoural drug levels. *Neoplasia*, 14, 410-9.
- HAUPT, R. M. & SINGS, H. L. 2011. The efficacy and safety of the quadrivalent human papillomavirus 6/11/16/18 vaccine gardasil. *J Adolesc Health*, 49, 467-75.
- HAYFLICK, L. 2000. The illusion of cell immortality. *Br J Cancer*, 83, 841-6.
- HE, S., ZHANG, D., CHENG, F., GONG, F. & GUO, Y. 2009. Applications of RNA interference in cancer therapeutics as a powerful tool for suppressing gene expression. *Mol Biol Rep*, 36, 2153-63.
- HEGEMANN, B., HUTCHINS, J. R., HUDECZ, O., NOVATCHKOVA, M., RAMESEDER, J., SYKORA, M. M., LIU, S., MAZANEK, M., LENART, P., HERICHE, J. K., POSER, I., KRAUT, N., HYMAN, A. A., YAFFE, M. B., MECHTLER, K. & PETERS, J. M. 2011. Systematic phosphorylation analysis of human mitotic protein complexes. *Sci Signal*, 4, rs12.
- HEGYI, K., EGERVARI, K., SANDOR, Z. & MEHES, G. 2012. Aurora kinase B expression in breast carcinoma: cell kinetic and genetic aspects. *Pathobiology*, 79, 314-22.
- HEGYI, K. & MEHES, G. 2012. Mitotic failures in cancer: Aurora B kinase and its potential role in the development of aneuploidy. *Pathol Oncol Res*, 18, 761-9.
- HEILMANN, A. M. & DYSON, N. J. 2012. Phosphorylation puts the pRb tumour suppressor into shape. *Genes Dev*, 26, 1128-30.

- HEMANN, M. T., STRONG, M. A., HAO, L. Y. & GREIDER, C. W. 2001. The shortest telomere, not average telomere length, is critical for cell viability and chromosome stability. *Cell*, 107, 67-77.
- HENDERSON, M. C. & AZORSA, D. O. 2013. High-throughput RNAi screening for the identification of novel targets. *Methods Mol Biol*, 986, 89-95.
- HENGARTNER, M. O. 2000. The biochemistry of apoptosis. *Nature*, 407, 770-6.
- HERSHKO, T. & GINSBERG, D. 2004. Up-regulation of Bcl-2 homology 3 (BH3)-only proteins by E2F1 mediates apoptosis. *J Biol Chem*, 279, 8627-34.
- HERZIG, M., SAVARESE, F., NOVATCHKOVA, M., SEMB, H. & CHRISTOFORI, G. 2007. Tumour progression induced by the loss of E-cadherin independent of beta-catenin/Tcf-mediated Wnt signaling. *Oncogene*, 26, 2290-8.
- HIGGINS, J. M. 2010. Haspin: a newly discovered regulator of mitotic chromosome behavior. *Chromosoma*, 119, 137-47.
- HOAR, K., CHAKRAVARTY, A., RABINO, C., WYSONG, D., BOWMAN, D., ROY, N. & ECSEDY, J. A. 2007. MLN8054, a small-molecule inhibitor of Aurora A, causes spindle pole and chromosome congression defects leading to aneuploidy. *Mol Cell Biol*, 27, 4513-25.
- HOLMGREN, S. C., PATTERSON, N. A., OZBUN, M. A. & LAMBERT, P. F. 2005. The minor capsid protein L2 contributes to two steps in the human papillomavirus type 31 life cycle. *J Virol*, 79, 3938-48.
- HOZAK, P., HASSAN, A. B., JACKSON, D. A. & COOK, P. R. 1993. Visualization of replication factories attached to nucleoskeleton. *Cell*, 73, 361-73.
- HUANG, C., JIANG, T., ZHU, L., LIU, J., CAO, J., HUANG, K. J. & QIU, Z. J. 2011. STAT3-targeting RNA interference inhibits pancreatic cancer angiogenesis in vitro and in vivo. *Int J Oncol*, 38, 1637-44.
- HUANG, F. W., HODIS, E., XU, M. J., KRYUKOV, G. V., CHIN, L. & GARRAWAY, L. A. 2013. Highly recurrent TERT promoter mutations in human melanoma. *Science*, 339, 957-9.
- HUERTAS, D., SOLER, M., MORETO, J., VILLANUEVA, A., MARTINEZ, A., VIDAL, A., CHARLTON, M., MOFFAT, D., PATEL, S., MCDERMOTT, J., OWEN, J., BROTHERTON, D., KRIGE, D., CUTHILL, S. & ESTELLER, M. 2012. Antitumour activity of a small-molecule inhibitor of the histone kinase Haspin. *Oncogene*, 31, 1408-18.

- HUH, K. W., DEMASI, J., OGAWA, H., NAKATANI, Y., HOWLEY, P. M. & MUNGER, K. 2005. Association of the human papillomavirus type 16 E7 oncoprotein with the 600-kDa retinoblastoma protein-associated factor, p600. *Proc Natl Acad Sci U S A*, 102, 11492-7.
- HUNG, S. C., WU, I. H., HSUE, S. S., LIAO, C. H., WANG, H. C., CHUANG, P. H., SUNG, S. Y. & HSIEH, C. L. 2010. Targeting 11 cell adhesion molecule using lentivirus-mediated short hairpin RNA interference reverses aggressiveness of oral squamous cell carcinoma. *Mol Pharm*, 7, 2312-23.
- IKEZOE, T., YANG, J., NISHIOKA, C. & YOKOYAMA, A. 2010. p53 is critical for the Aurora B kinase inhibitor-mediated apoptosis in acute myelogenous leukemia cells. *Int J Hematol*, 91, 69-77.
- INSINGA, R. P., GLASS, A. G. & RUSH, B. B. 2004. Diagnoses and outcomes in cervical cancer screening: a population-based study. *Am J Obstet Gynecol*, 191, 105-13.
- IZQUIERDO, M. 2005. Short interfering RNAs as a tool for cancer gene therapy. *Cancer Gene Ther.*, 12, 217-27.
- JACKMAN, M., LINDON, C., NIGG, E. A. & PINES, J. 2003. Active cyclin B1-Cdk1 first appears on centrosomes in prophase. *Nat Cell Biol*, 5, 143-8.
- JACKSON, A. L., BURCHARD, J., LEAKE, D., REYNOLDS, A., SCHELTER, J., GUO, J., JOHNSON, J. M., LIM, L., KARPILOW, J., NICHOLS, K., MARSHALL, W., KHVOROVA, A. & LINSLEY, P. S. 2006. Position-specific chemical modification of siRNAs reduces "off-target" transcript silencing. *RNA*, 12, 1197-205.
- JACKSON, D. A. & POMBO, A. 1998. Replicon clusters are stable units of chromosome structure: evidence that nuclear organization contributes to the efficient activation and propagation of S phase in human cells. *J Cell Biol*, 140, 1285-95.
- JAIN, R. K. & DUDA, D. G. 2003. Role of bone marrow-derived cells in tumour angiogenesis and treatment. *Cancer Cell*, 3, 515-6.
- JANG, C. W., CHEN, C. H., CHEN, C. C., CHEN, J. Y., SU, Y. H. & CHEN, R. H. 2002. TGF-beta induces apoptosis through Smad-mediated expression of DAP-kinase. *Nat Cell Biol*, 4, 51-8.
- JANG, M. K., KWON, D. & MCBRIDE, A. A. 2009. Papillomavirus E2 proteins and the host BRD4 protein associate with transcriptionally active cellular chromatin. *J Virol*, 83, 2592-600.

- JEN, J., HARPER, J. W., BIGNER, S. H., BIGNER, D. D., PAPADOPOULOS, N., MARKOWITZ, S., WILLSON, J. K., KINZLER, K. W. & VOGELSTEIN, B. 1994. Deletion of p16 and p15 genes in brain tumours. *Cancer Res*, 54, 6353-8.
- JEONG, K. W., KIM, H. Z., KIM, S., KIM, Y. S. & CHO, J. 2007. Human papillomavirus type 16 E6 protein interacts with cystic fibrosis transmembrane regulator-associated ligand and promotes E6-associated protein-mediated ubiquitination and proteasomal degradation. *Oncogene*, 26, 487-99.
- JOHANSSON, C., SOMBERG, M., LI, X., BACKSTROM WINQUIST, E., FAY, J., RYAN, F., PIM, D., BANKS, L. & SCHWARTZ, S. 2012. HPV-16 E2 contributes to induction of HPV-16 late gene expression by inhibiting early polyadenylation. *EMBO J*, 31, 3212-27.
- JONSON, ROGERS LM, RAMAKRISHNAN S & JR., D. L. 2008. Gene silencing with siRNA targeting E6/E7 as a therapeutic intervention in a mouse model of cervical cancer. *Gynecol Oncol*, 111, 356-64.
- JORDAN, M. A., WENDELL, K., GARDINER, S., DERRY, W. B., COPP, H. & WILSON, L. 1996. Mitotic block induced in HeLa cells by low concentrations of paclitaxel (Taxol) results in abnormal mitotic exit and apoptotic cell death. *Cancer Res*, 56, 816-25.
- JOST, C. A., MARIN, M. C. & KAEHLIN, W. G., JR. 1997. p73 is a simian [correction of human] p53-related protein that can induce apoptosis. *Nature*, 389, 191-4.
- KAERN, J., TROPE, C., SUNDFOER, K. & KRISTENSEN, G. B. 1996. Cisplatin/5-fluorouracil treatment of recurrent cervical carcinoma: a phase II study with long-term follow-up. *Gynecol Oncol*, 60, 387-92.
- KAHLE, K. T., KOZONO, D., NG, K., HSIEH, G., ZINN, P. O., NITTA, M. & CHEN, C. C. 2010. Functional genomics to explore cancer cell vulnerabilities. *Neurosurg Focus*, 28, E5.
- KAI, K., TAKAI, N., NASU, K., KIRA, N., ISHII, T., KASHIMA, K. & NARAHARA, H. 2009. Metastatic uterine cervical cancer originating in the lung: a case report. *Gynecol Obstet Invest*, 68, 269-71.
- KAPLAN, R. N., RIBA, R. D., ZACHAROULIS, S., BRAMLEY, A. H., VINCENT, L., COSTA, C., MACDONALD, D. D., JIN, D. K., SHIDO, K., KERNS, S. A., ZHU, Z., HICKLIN, D., WU, Y., PORT, J. L., ALTORKI, N., PORT, E. R., RUGGERO, D., SHMELKOV, S. V., JENSEN, K. K., RAFII, S. & LYDEN, D. 2005. VEGFR1-positive haematopoietic bone marrow progenitors initiate the pre-metastatic niche. *Nature*, 438, 820-7.

- KARIN, M., CAO, Y., GRETEN, F. R. & LI, Z. W. 2002. NF-kappaB in cancer: from innocent bystander to major culprit. *Nat Rev Cancer*, 2, 301-10.
- KARTHIGEYAN, D., PRASAD, S. B., SHANDILYA, J., AGRAWAL, S. & KUNDU, T. K. 2010. Biology of Aurora A kinase: Implications in cancer manifestation and therapy. *Med Res Rev*.
- KATAYAMA, H. & SEN, S. 2010. Aurora kinase inhibitors as anticancer molecules. *Biochim Biophys Acta*, 1799, 829-39.
- KATO, J., MATSUSHIME, H., HIEBERT, S. W., EWEN, M. E. & SHERR, C. J. 1993. Direct binding of cyclin D to the retinoblastoma gene product (pRb) and pRb phosphorylation by the cyclin D-dependent kinase CDK4. *Genes Dev*, 7, 331-42.
- KERBEL, R. S. 2008. Tumour angiogenesis. *N Engl J Med*, 358, 2039-49.
- KHAN, S. H. & WAHL, G. M. 1998. p53 and pRb prevent rereplication in response to microtubule inhibitors by mediating a reversible G1 arrest. *Cancer Res*, 58, 396-401.
- KIETPEERAKOOL, C. & SRISOMBOON, J. 2009. Medical treatment of cervical intraepithelial neoplasia II, III: an update review. *Int J Clin Oncol*, 14, 37-42.
- KIM, K. & LAMBERT, P. F. 2002. E1 protein of bovine papillomavirus 1 is not required for the maintenance of viral plasmid DNA replication. *Virology*, 293, 10-4.
- KOLLAREDDY, M., ZHELEVA, D., DZUBAK, P., BRAHMKSHATRIYA, P. S., LEPSIK, M. & HAJDUCH, M. 2012. Aurora kinase inhibitors: progress towards the clinic. *Invest New Drugs*, 30, 2411-32.
- KOPS, G. J., WEAVER, B. A. & CLEVELAND, D. W. 2005. On the road to cancer: aneuploidy and the mitotic checkpoint. *Nat Rev Cancer*, 5, 773-85.
- KOZOPAS, K. M., YANG, T., BUCHAN, H. L., ZHOU, P. & CRAIG, R. W. 1993. MCL1, a gene expressed in programmed myeloid cell differentiation, has sequence similarity to BCL2. *Proc Natl Acad Sci U S A*, 90, 3516-20.
- KYO, S. & INOUE, M. 2002. Complex regulatory mechanisms of telomerase activity in normal and cancer cells: how can we apply them for cancer therapy? *Oncogene*, 21, 688-97.
- LA TORRE, G., DE WAURE, C., CHIARADIA, G., MANNOCCI, A. & RICCIARDI, W. 2007. HPV vaccine efficacy in preventing persistent cervical HPV infection: a systematic review and meta-analysis. *Vaccine*, 25, 8352-8.

- LAPAN, P., ZHANG, J., PAN, J. & HANEY, S. 2008. Quantitative optimization of reverse transfection conditions for 384-well siRNA library screening. *Assay Drug Dev Technol*, 6, 683-91.
- LARA-GONZALEZ, P., SCOTT, M. I., DIEZ, M., SEN, O. & TAYLOR, S. S. 2011. BubR1 blocks substrate recruitment to the APC/C in a KEN-box-dependent manner. *J Cell Sci*, 124, 4332-45.
- LARA-GONZALEZ, P., WESTHORPE, F. G. & TAYLOR, S. S. 2012. The spindle assembly checkpoint. *Curr Biol*, 22, R966-80.
- LAURA G CURRIN, R. H. J., KAREN M LINKLATER, VIVIAN MAK, HENRIK MØLLER, AND ELIZABETH A DAVIES 2009. Inequalities in the incidence of cervical cancer in South East England 2001–2005: an investigation of population risk factors. *BMC Public Health*, 10.1186/1471-2458-9-62.
- LEONHARDT, H., RAHN, H. P., WEINZIERL, P., SPORBERT, A., CREMER, T., ZINK, D. & CARDOSO, M. C. 2000. Dynamics of DNA replication factories in living cells. *J Cell Biol*, 149, 271-80.
- LEUNG, R. K. & WHITTAKER, P. A. 2005. RNA interference: from gene silencing to gene-specific therapeutics. *Pharmacol Ther*, 107, 222-39.
- LEVINE, B. & KROEMER, G. 2008. Autophagy in the pathogenesis of disease. *Cell*, 132, 27-42.
- LEVITZKI, A. & GAZIT, A. 1995. Tyrosine kinase inhibition: an approach to drug development. *Science*, 267, 1782-8.
- LI, J., MEYER, A. N. & DONOGHUE, D. J. 1997a. Nuclear localization of cyclin B1 mediates its biological activity and is regulated by phosphorylation. *Proc Natl Acad Sci U S A*, 94, 502-7.
- LI, Y., GORBEA, C., MAHAFFEY, D., RECHSTEINER, M. & BENEZRA, R. 1997b. MAD2 associates with the cyclosome/anaphase-promoting complex and inhibits its activity. *Proc Natl Acad Sci U S A*, 94, 12431-6.
- LIN, E. Y., NGUYEN, A. V., RUSSELL, R. G. & POLLARD, J. W. 2001. Colony-stimulating factor 1 promotes progression of mammary tumours to malignancy. *J Exp Med*, 193, 727-40.

- LIU, Q., MOLDOVEANU, T., SPRULES, T., MATTA-CAMACHO, E., MANSUR-AZZAM, N. & GEHRING, K. 2010. Apoptotic regulation by MCL-1 through heterodimerization. *J Biol Chem*, 285, 19615-24.
- LIU, Q. & WANG, H. G. 2012. Anti-cancer drug discovery and development: Bcl-2 family small molecule inhibitors. *Commun Integr Biol*, 5, 557-65.
- LIU, X., CLEMENTS, A., ZHAO, K. & MARMORSTEIN, R. 2006. Structure of the human Papillomavirus E7 oncoprotein and its mechanism for inactivation of the retinoblastoma tumour suppressor. *J Biol Chem*, 281, 578-86.
- LIU, Y., XING, H., HAN, X., SHI, X., LIANG, F., CHENG, G., LU, Y. & MA, D. 2008. Apoptosis of HeLa cells induced by cisplatin and its mechanism. *J Huazhong Univ Sci Technolog Med Sci*, 28, 197-9.
- LOMONOSOVA, E. & CHINNADURAI, G. 2008. BH3-only proteins in apoptosis and beyond: an overview. *Oncogene*, 27 Suppl 1, S2-19.
- LONGWORTH, M. S. & LAIMINS, L. A. 2004. The binding of histone deacetylases and the integrity of zinc finger-like motifs of the E7 protein are essential for the life cycle of human papillomavirus type 31. *J Virol*, 78, 3533-41.
- LOWE, S. W., CEPERO, E. & EVAN, G. 2004. Intrinsic tumour suppression. *Nature*, 432, 307-15.
- LUO, J., EMANUELE, M. J., LI, D., CREIGHTON, C. J., SCHLABACH, M. R., WESTBROOK, T. F., WONG, K. K. & ELLEDGE, S. J. 2009. A genome-wide RNAi screen identifies multiple synthetic lethal interactions with the Ras oncogene. *Cell*, 137, 835-48.
- LYNG, H., SUNDFOR, K. & ROFSTAD, E. K. 2000. Changes in tumour oxygen tension during radiotherapy of uterine cervical cancer: relationships to changes in vascular density, cell density, and frequency of mitosis and apoptosis. *Int J Radiat Oncol Biol Phys*, 46, 935-46.
- MA, H., SAMARABANDU, J., DEVDHAR, R. S., ACHARYA, R., CHENG, P. C., MENG, C. & BEREZNEY, R. 1998. Spatial and temporal dynamics of DNA replication sites in mammalian cells. *J Cell Biol*, 143, 1415-25.
- MAGNUSSEN, G. I., HOLM, R., EMILSEN, E., ROSNES, A. K., SLIPICEVIC, A. & FLORENES, V. A. 2012. High expression of Wee1 is associated with poor disease-free survival in malignant melanoma: potential for targeted therapy. *PLoS One*, 7, e38254.
- MAHADEVAN, D., STEJSKAL, A., COOKE, L. S., MANZIELLO, A., MORALES, C., PERSKY, D. O., FISHER, R. I., MILLER, T. P. & QI, W. 2012. Aurora A inhibitor

- (MLN8237) plus vincristine plus rituximab is synthetic lethal and a potential curative therapy in aggressive B-cell non-Hodgkin lymphoma. *Clin Cancer Res*, 18, 2210-9.
- MALUMBRES, M. & BARBACID, M. 2006. Is Cyclin D1-CDK4 kinase a bona fide cancer target? *Cancer Cell*, 9, 2-4.
- MALUREANU, L. A., JEGANATHAN, K. B., HAMADA, M., WASILEWSKI, L., DAVENPORT, J. & VAN DEURSEN, J. M. 2009. BubR1 N terminus acts as a soluble inhibitor of cyclin B degradation by APC/C(Cdc20) in interphase. *Dev Cell*, 16, 118-31.
- MANFREDI, M. G., ECSEDY, J. A., CHAKRAVARTY, A., SILVERMAN, L., ZHANG, M., HOAR, K. M., STROUD, S. G., CHEN, W., SHINDE, V., HUCK, J. J., WYSONG, D. R., JANOWICK, D. A., HYER, M. L., LEROY, P. J., GERSHMAN, R. E., SILVA, M. D., GERMANOS, M. S., BOLEN, J. B., CLAIBORNE, C. F. & SELLS, T. B. 2011. Characterization of Alisertib (MLN8237), an investigational small-molecule inhibitor of aurora A kinase using novel in vivo pharmacodynamic assays. *Clin Cancer Res*, 17, 7614-24.
- MANNING, G., WHYTE, D. B., MARTINEZ, R., HUNTER, T. & SUDARSANAM, S. 2002. The protein kinase complement of the human genome. *Science*, 298, 1912-34.
- MARGOLIS, R. L., LOHEZ, O. D. & ANDREASSEN, P. R. 2003. G1 tetraploidy checkpoint and the suppression of tumorigenesis. *J Cell Biochem*, 88, 673-83.
- MARTIN, A. G., TRAMA, J., CRIGHTON, D., RYAN, K. M. & FEARNHEAD, H. O. 2009. Activation of p73 and induction of Noxa by DNA damage requires NF-kappa B. *Aging (Albany NY)*, 1, 335-49.
- MARTINEZ, P. & BLASCO, M. A. 2010. Role of shelterin in cancer and aging. *Aging Cell*, 9, 653-66.
- MARUMOTO, T., HONDA, S., HARA, T., NITTA, M., HIROTA, T., KOHMURA, E. & SAYA, H. 2003. Aurora-A kinase maintains the fidelity of early and late mitotic events in HeLa cells. *J Biol Chem*, 278, 51786-95.
- MARUMOTO, T., ZHANG, D. & SAYA, H. 2005. Aurora-A - a guardian of poles. *Nat Rev Cancer*, 5, 42-50.
- MARXER, M., MA, H. T., MAN, W. Y. & POON, R. Y. 2013. p53 deficiency enhances mitotic arrest and slippage induced by pharmacological inhibition of Aurora kinases. *Oncogene*.
- MASSAGUE, J. 2008. TGFbeta in Cancer. *Cell*, 134, 215-30.

- MASSIMI, P., SHAI, A., LAMBERT, P. & BANKS, L. 2008. HPV E6 degradation of p53 and PDZ containing substrates in an E6AP null background. *Oncogene*, 27, 1800-4.
- MATHEW, R. & WHITE, E. 2011. Autophagy, stress, and cancer metabolism: what doesn't kill you makes you stronger. *Cold Spring Harb Symp Quant Biol*, 76, 389-96.
- MATSUMOTO, Y., MABUCHI, S., MURAJI, M., MORII, E. & KIMURA, T. 2010. Squamous cell carcinoma of the uterine cervix producing granulocyte colony-stimulating factor: a report of 4 cases and a review of the literature. *Int J Gynecol Cancer*, 20, 417-21.
- MATULONIS, U. A., SHARMA, S., GHAMANDE, S., GORDON, M. S., DEL PRETE, S. A., RAY-COQUARD, I., KUTARSKA, E., LIU, H., FINGERT, H., ZHOU, X., DANAEI, H. & SCHILDER, R. J. 2012. Phase II study of MLN8237 (alisertib), an investigational Aurora A kinase inhibitor, in patients with platinum-resistant or -refractory epithelial ovarian, fallopian tube, or primary peritoneal carcinoma. *Gynecol Oncol*, 127, 63-9.
- MCCRIDE, A. A., OLIVEIRA, J. G. & MCPHILLIPS, M. G. 2006. Partitioning viral genomes in mitosis: same idea, different targets. *Cell Cycle*, 5, 1499-502.
- MCINTOSH, P. B., MARTIN, S. R., JACKSON, D. J., KHAN, J., ISAACSON, E. R., CALDER, L., RAJ, K., GRIFFIN, H. M., WANG, Q., LASKEY, P., ECCLESTON, J. F. & DOORBAR, J. 2008. Structural analysis reveals an amyloid form of the human papillomavirus type 16 E1-E4 protein and provides a molecular basis for its accumulation. *J Virol*, 82, 8196-203.
- MCLAUGHLIN-DRUBIN, M. E., HUH, K. W. & MUNGER, K. 2008. Human papillomavirus type 16 E7 oncoprotein associates with E2F6. *J Virol*, 82, 8695-705.
- MCLAUGHLIN-DRUBIN, M. E. & MUNGER, K. 2009. Oncogenic activities of human papillomaviruses. *Virus Res*, 143, 195-208.
- MCPHILLIPS, M. G., OLIVEIRA, J. G., SPINDLER, J. E., MITRA, R. & MCCRIDE, A. A. 2006. Brd4 is required for e2-mediated transcriptional activation but not genome partitioning of all papillomaviruses. *J Virol*, 80, 9530-43.
- MEEK, D. W. 2000. The role of p53 in the response to mitotic spindle damage. *Pathol Biol (Paris)*, 48, 246-54.
- MEHLEN, P. & PUISIEUX, A. 2006. Metastasis: a question of life or death. *Nat Rev Cancer*, 6, 449-58.

- MEI, Y., DU, W., YANG, Y. & WU, M. 2005. Puma(*)Mcl-1 interaction is not sufficient to prevent rapid degradation of Mcl-1. *Oncogene*, 24, 7224-37.
- MEI, Y., XIE, C., XIE, W., TIAN, X., LI, M. & WU, M. 2007. Noxa/Mcl-1 balance regulates susceptibility of cells to camptothecin-induced apoptosis. *Neoplasia*, 9, 871-81.
- MELINO, G., BERNASSOLA, F., RANALLI, M., YEE, K., ZONG, W. X., CORAZZARI, M., KNIGHT, R. A., GREEN, D. R., THOMPSON, C. & VOUSDEN, K. H. 2004. p73 Induces apoptosis via PUMA transactivation and Bax mitochondrial translocation. *J Biol Chem*, 279, 8076-83.
- MERALDI, P., DRAVIAM, V. M. & SORGER, P. K. 2004. Timing and checkpoints in the regulation of mitotic progression. *Dev Cell*, 7, 45-60.
- MICHEL, L. S., LIBERAL, V., CHATTERJEE, A., KIRCHWEGGER, R., PASCHE, B., GERALD, W., DOBLES, M., SORGER, P. K., MURTY, V. V. & BENEZRA, R. 2001. MAD2 haplo-insufficiency causes premature anaphase and chromosome instability in mammalian cells. *Nature*, 409, 355-9.
- MIDDLETON, K., PEH, W., SOUTHERN, S., GRIFFIN, H., SOTLAR, K., NAKAHARA, T., EL-SHERIF, A., MORRIS, L., SETH, R., HIBMA, M., JENKINS, D., LAMBERT, P., COLEMAN, N. & DOORBAR, J. 2003. Organization of human papillomavirus productive cycle during neoplastic progression provides a basis for selection of diagnostic markers. *J Virol*, 77, 10186-201.
- MILLIGAN, S. G., VEERAPRADITSIN, T., AHAMET, B., MOLE, S. & GRAHAM, S. V. 2007. Analysis of novel human papillomavirus type 16 late mRNAs in differentiated W12 cervical epithelial cells. *Virology*, 360, 172-81.
- MILLS, G. B., LU, Y. & KOHN, E. C. 2001. Linking molecular therapeutics to molecular diagnostics: inhibition of the FRAP/RAFT/TOR component of the PI3K pathway preferentially blocks PTEN mutant cells in vitro and in vivo. *Proc Natl Acad Sci U S A*, 98, 10031-3.
- MINAKUCHI, Y., TAKESHITA, F., KOSAKA, N., SASAKI, H., YAMAMOTO, Y., KOUNO, M., HONMA, K., NAGAHARA, S., HANAI, K., SANO, A., KATO, T., TERADA, M. & OCHIYA, T. 2004. Atelocollagen-mediated synthetic small interfering RNA delivery for effective gene silencing in vitro and in vivo. *Nucleic Acids Res*, 32, e109.

- MISHRA, L., DERYNCK, R. & MISHRA, B. 2005. Transforming growth factor-beta signaling in stem cells and cancer. *Science*, 310, 68-71.
- MISRA, J. S., SRIVASTAVA, S., SINGH, U. & SRIVASTAVA, A. N. 2009. Risk-factors and strategies for control of carcinoma cervix in India: hospital based cytological screening experience of 35 years. *Indian J Cancer*, 46, 155-9.
- MITCHELL, M. F., HITTELMAN, W. N., HONG, W. K., LOTAN, R. & SCHOTTENFELD, D. 1994. The natural history of cervical intraepithelial neoplasia: an argument for intermediate endpoint biomarkers. *Cancer Epidemiol Biomarkers Prev*, 3, 619-26.
- MIZUSHIMA, N. 2007. Autophagy: process and function. *Genes Dev*, 21, 2861-73.
- MOLLINEDO, F. & GAJATE, C. 2003. Microtubules, microtubule-interfering agents and apoptosis. *Apoptosis*, 8, 413-50.
- MONK, HUANG HQ, CELLA D, 3RD, L. H. & STUDY., G. O. G. 2005. Quality of life outcomes from a randomized phase III trial of cisplatin with or without topotecan in advanced carcinoma of the cervix: a Gynecologic Oncology Group Study. *J Clin Oncol.*, 23, 4617-25.
- MONTEIRO, D. L., TRAJANO, A. J., DA SILVA, K. S. & RUSSOMANO, F. B. 2006. Pre-invasive cervical disease and uterine cervical cancer in Brazilian adolescents: prevalence and related factors. *Cad Saude Publica*, 22, 2539-48.
- MOODY, C. A., FRADET-TURCOTTE, A., ARCHAMBAULT, J. & LAIMINS, L. A. 2007. Human papillomaviruses activate caspases upon epithelial differentiation to induce viral genome amplification. *Proc Natl Acad Sci U S A*, 104, 19541-6.
- MORALES, C. P., HOLT, S. E., OUELLETTE, M., KAUR, K. J., YAN, Y., WILSON, K. S., WHITE, M. A., WRIGHT, W. E. & SHAY, J. W. 1999. Absence of cancer-associated changes in human fibroblasts immortalized with telomerase. *Nat Genet*, 21, 115-8.
- MORI, N., ISHIKAWA, C., SENBA, M., KIMURA, M. & OKANO, Y. 2011. Effects of AZD1152, a selective Aurora B kinase inhibitor, on Burkitt's and Hodgkin's lymphomas. *Biochem Pharmacol*, 81, 1106-15.
- MORRIS, E. J. & DYSON, N. J. 2001. Retinoblastoma protein partners. *Adv Cancer Res*, 82, 1-54.
- MORROW, C. J., TIGHE, A., JOHNSON, V. L., SCOTT, M. I., DITCHFIELD, C. & TAYLOR, S. S. 2005. Bub1 and aurora B cooperate to maintain BubR1-mediated inhibition of APC/CCdc20. *J Cell Sci*, 118, 3639-52.

- MOSSE, Y. P., LIPSITZ, E., FOX, E., TEACHEY, D. T., MARIS, J. M., WEIGEL, B., ADAMSON, P. C., INGLE, M. A., AHERN, C. H. & BLANEY, S. M. 2012. Pediatric phase I trial and pharmacokinetic study of MLN8237, an investigational oral selective small-molecule inhibitor of Aurora kinase A: a Children's Oncology Group Phase I Consortium study. *Clin Cancer Res*, 18, 6058-64.
- MUELLER, P. R., COLEMAN, T. R., KUMAGAI, A. & DUNPHY, W. G. 1995. Myt1: a membrane-associated inhibitory kinase that phosphorylates Cdc2 on both threonine-14 and tyrosine-15. *Science*, 270, 86-90.
- MULLER, P. A. & VOUSDEN, K. H. 2014. Mutant p53 in cancer: new functions and therapeutic opportunities. *Cancer Cell*, 25, 304-17.
- MUNGER, K., WERNES, B. A., DYSON, N., PHELPS, W. C., HARLOW, E. & HOWLEY, P. M. 1989. Complex formation of human papillomavirus E7 proteins with the retinoblastoma tumour suppressor gene product. *EMBO J*, 8, 4099-105.
- MUSACCHIO, A. & SALMON, E. D. 2007. The spindle-assembly checkpoint in space and time. *Nat Rev Mol Cell Biol*, 8, 379-93.
- NAKAYAMA, K. & NAKAYAMA, K. 1998. Cip/Kip cyclin-dependent kinase inhibitors: brakes of the cell cycle engine during development. *Bioessays*, 20, 1020-9.
- NAKAYAMA, K. I., HATAKEYAMA, S. & NAKAYAMA, K. 2001. Regulation of the cell cycle at the G1-S transition by proteolysis of cyclin E and p27Kip1. *Biochem Biophys Res Commun*, 282, 853-60.
- NAM, J. H., KIM, S. H., KIM, J. H., KIM, Y. M., KIM, Y. T. & MOK, J. E. 2002. Nonradical treatment is as effective as radical surgery in the management of cervical cancer stage IA1. *Int J Gynecol Cancer*, 12, 480-4.
- NARECHANIA, A., CHEN, Z., DESALLE, R. & BURK, R. D. 2005. Phylogenetic incongruence among oncogenic genital alpha human papillomaviruses. *J Virol*, 79, 15503-10.
- NAUD, P., DE CARVALHO, N., TEIXEIRA, J. & BORBA, P. Sep. 17-22-2011. HPV-16/18 Vaccine: Sustained Immunogenicity And Efficacy Up To 9.4 Years. *IPV Conference*, Berlin
- NEBANE, N. M., CORIC, T., WHIG, K., MCKELLIP, S., WOODS, L., SOSA, M., SHEPPARD, R., RASMUSSEN, L., BJORNSTI, M. A. & WHITE, E. L. 2013. High-Throughput RNA Interference Screening: Tricks of the Trade. *J Lab Autom*.
- NEVINS, J. R. 2001. The Rb/E2F pathway and cancer. *Hum Mol Genet*, 10, 699-703.

- NIEDZIALKOWSKA, E., WANG, F., POREBSKI, P. J., MINOR, W., HIGGINS, J. M. & STUKENBERG, P. T. 2012. Molecular basis for phosphospecific recognition of histone H3 tails by Survivin paralogues at inner centromeres. *Mol Biol Cell*, 23, 1457-66.
- NIEHRS, C. & ACEBRON, S. P. 2012. Mitotic and mitogenic Wnt signalling. *EMBO J*, 31, 2705-13.
- NIGG, E. A. 2001. Mitotic kinases as regulators of cell division and its checkpoints. *Nat Rev Mol Cell Biol*, 2, 21-32.
- NIJMAN, S. M. 2011. Synthetic lethality: general principles, utility and detection using genetic screens in human cells. *FEBS Lett*, 585, 1-6.
- NIJMAN, S. M. & FRIEND, S. H. 2013. Cancer. Potential of the synthetic lethality principle. *Science*, 342, 809-11.
- NILSSON, J., YEKEZARE, M., MINSHULL, J. & PINES, J. 2008. The APC/C maintains the spindle assembly checkpoint by targeting Cdc20 for destruction. *Nat Cell Biol*, 10, 1411-20.
- NISHIKAWA, R., JI, X. D., HARMON, R. C., LAZAR, C. S., GILL, G. N., CAVENEE, W. K. & HUANG, H. J. 1994. A mutant epidermal growth factor receptor common in human glioma confers enhanced tumorigenicity. *Proc Natl Acad Sci U S A*, 91, 7727-31.
- NISHITANI, H. & LYGEROU, Z. 2004. DNA replication licensing. *Front Biosci*, 9, 2115-32.
- NISHITANI, H., TARAVIRAS, S., LYGEROU, Z. & NISHIMOTO, T. 2001. The human licensing factor for DNA replication Cdt1 accumulates in G1 and is destabilized after initiation of S-phase. *J Biol Chem*, 276, 44905-11.
- NOVAK, B. & TYSON, J. J. 1993. Numerical analysis of a comprehensive model of M-phase control in *Xenopus* oocyte extracts and intact embryos. *J Cell Sci*, 106 (Pt 4), 1153-68.
- NOYA, F., CHIEN, W. M., BROKER, T. R. & CHOW, L. T. 2001. p21cip1 Degradation in differentiated keratinocytes is abrogated by costabilization with cyclin E induced by human papillomavirus E7. *J Virol*, 75, 6121-34.
- NOZAWA, H., CHIU, C. & HANAHAN, D. 2006. Infiltrating neutrophils mediate the initial angiogenic switch in a mouse model of multistage carcinogenesis. *Proc Natl Acad Sci U S A*, 103, 12493-8.
- NYITRAY, SMITH D, VILLA L, LAZCANO-PONCE E, ABRAHAMSEN M, PAPENFUSSM & AR, G. 2010. Prevalence of and Risk Factors for Anal Human Papillomavirus Infection in Men Who Have Sex with Women: A Cross-National Study. *J Infect Dis.*, 5.

- O'BRIEN, J., WILSON, I., ORTON, T. & POGNAN, F. 2000. Investigation of the Alamar Blue (resazurin) fluorescent dye for the assessment of mammalian cell cytotoxicity. *Eur J Biochem*, 267, 5421-6.
- O'KEEFE, R. T., HENDERSON, S. C. & SPECTOR, D. L. 1992. Dynamic organization of DNA replication in mammalian cell nuclei: spatially and temporally defined replication of chromosome-specific alpha-satellite DNA sequences. *J Cell Biol*, 116, 1095-110.
- OKE, A., PEARCE, D., WILKINSON, R. W., CRAFTER, C., ODEDRA, R., CAVENAGH, J., FITZGIBBON, J., LISTER, A. T., JOEL, S. & BONNET, D. 2009. AZD1152 rapidly and negatively affects the growth and survival of human acute myeloid leukemia cells in vitro and in vivo. *Cancer Res*, 69, 4150-8.
- OLDHAM, S. & HAFEN, E. 2003. Insulin/IGF and target of rapamycin signaling: a TOR de force in growth control. *Trends Cell Biol*, 13, 79-85.
- OZAKI, T. & NAKAGAWARA, A. 2005. p73, a sophisticated p53 family member in the cancer world. *Cancer Sci*, 96, 729-37.
- OZPOLAT, B., SOOD, A. K. & LOPEZ-BERESTEIN, G. 2014. Liposomal siRNA nanocarriers for cancer therapy. *Adv Drug Deliv Rev*, 66, 110-6.
- P, O. C., RHYS-EVANS, P. H., MODJTAHEDI, H. & ECCLES, S. A. 2002. The role of c-erbB receptors and ligands in head and neck squamous cell carcinoma. *Oral Oncol*, 38, 627-40.
- PAAVONEN, J., NAUD, P., SALMERON, J., WHEELER, C. M., CHOW, S. N., APTER, D., KITCHENER, H., CASTELLSAGUE, X., TEIXEIRA, J. C., SKINNER, S. R., HEDRICK, J., JAISAMRARN, U., LIMSON, G., GARLAND, S., SZAREWSKI, A., ROMANOWSKI, B., AOKI, F. Y., SCHWARZ, T. F., POPPE, W. A., BOSCH, F. X., JENKINS, D., HARDT, K., ZAHAF, T., DESCAMPS, D., STRUYF, F., LEHTINEN, M. & DUBIN, G. 2009. Efficacy of human papillomavirus (HPV)-16/18 AS04-adjuvanted vaccine against cervical infection and precancer caused by oncogenic HPV types (PATRICIA): final analysis of a double-blind, randomised study in young women. *Lancet*, 374, 301-14.
- PACEK, M. & WALTER, J. C. 2004. A requirement for MCM7 and Cdc45 in chromosome unwinding during eukaryotic DNA replication. *EMBO J*, 23, 3667-76.
- PARDALI, K., KURISAKI, A., MOREN, A., TEN DIJKE, P., KARDASSIS, D. & MOUSTAKAS, A. 2000. Role of Smad proteins and transcription factor Sp1 in

- p21(Waf1/Cip1) regulation by transforming growth factor-beta. *J Biol Chem*, 275, 29244-56.
- PARKER, L. L. & PIWNICA-WORMS, H. 1992. Inactivation of the p34cdc2-cyclin B complex by the human WEE1 tyrosine kinase. *Science*, 257, 1955-7.
- PASQUIER, E., HONORE, S. & BRAGUER, D. 2006. Microtubule-targeting agents in angiogenesis: where do we stand? *Drug Resist Updat*, 9, 74-86.
- PECORELLI, S. & ODICINO, F. 2003. Cervical cancer staging. *Cancer J*, 9, 390-4.
- PECORELLI, S., ZIGLIANI, L. & ODICINO, F. 2009. Revised FIGO staging for carcinoma of the cervix. *Int J Gynaecol Obstet*, 105, 107-8.
- PENNA, C., FAMBRINI, M., FALLANI, M. G., PIERALLI, A., SCARSELLI, G. & MARCHIONNI, M. 2005. Laser CO2 conization in postmenopausal age: risk of cervical stenosis and unsatisfactory follow-up. *Gynecol Oncol*, 96, 771-5.
- PEPPER, M. S., FERRARA, N., ORCI, L. & MONTESANO, R. 1992. Potent synergism between vascular endothelial growth factor and basic fibroblast growth factor in the induction of angiogenesis in vitro. *Biochem Biophys Res Commun*, 189, 824-31.
- PERALTA-ZARAGOZA, O., BERMUDEZ-MORALES, V. H., PEREZ-PLASENCIA, C., SALAZAR-LEON, J., GOMEZ-CERON, C. & MADRID-MARINA, V. 2012. Targeted treatments for cervical cancer: a review. *Onco Targets Ther*, 5, 315-28.
- PETAJA, T., PEDERSEN, C., PODER, A., STRAUSS, G., CATTEAU, G., THOMAS, F., LEHTINEN, M. & DESCAMPS, D. 2011. Long-term persistence of systemic and mucosal immune response to HPV-16/18 AS04-adjuvanted vaccine in preteen/adolescent girls and young women. *Int J Cancer*, 129, 2147-57.
- PETTERSSON, B. F., ANDERSSON, S., HELLMAN, K. & HELLSTROM, A. C. 2010. Invasive carcinoma of the uterine cervix associated with pregnancy: 90 years of experience. *Cancer*.
- PFISTER, H. 2003. Chapter 8: Human papillomavirus and skin cancer. *J Natl Cancer Inst Monogr*, 52-6.
- PHILLIPS, A. C. & VOUSDEN, K. H. 2001. E2F-1 induced apoptosis. *Apoptosis*, 6, 173-82.
- PIETSCH, E. C. & MURPHY, M. E. 2008. Low risk HPV-E6 traps p53 in the cytoplasm and induces p53-dependent apoptosis. *Cancer Biol Ther*, 7, 1916-8.

- PIM, D., BERGANT, M., BOON, S. S., GANTI, K., KRANJEC, C., MASSIMI, P., SUBBAIAH, V. K., THOMAS, M., TOMAIC, V. & BANKS, L. 2012. Human papillomaviruses and the specificity of PDZ domain targeting. *FEBS J*, 279, 3530-7.
- PIM, D., COLLINS, M. & BANKS, L. 1992. Human papillomavirus type 16 E5 gene stimulates the transforming activity of the epidermal growth factor receptor. *Oncogene*, 7, 27-32.
- PLANAS-SILVA, M. D. & WEINBERG, R. A. 1997. The restriction point and control of cell proliferation. *Curr Opin Cell Biol*, 9, 768-72.
- PLONER, C., KOFLER, R. & VILLUNGER, A. 2008. Noxa: at the tip of the balance between life and death. *Oncogene*, 27 Suppl 1, S84-92.
- PODDIGHE, P. J., BULTEN, J., KERSTENS, H. M., ROBBEN, J. C., MELCHERS, W. J. & HANSELAAR, A. G. 1996. Human papilloma virus detection by in situ hybridisation signal amplification based on biotinylated tyramine deposition. *Clin Mol Pathol*, 49, M340-4.
- PORCELLI, L., QUATRALE, A. E., MANTUANO, P., SILVESTRIS, N., BRUNETTI, A. E., CALVERT, H., PARADISO, A. & AZZARITI, A. 2012. Synthetic lethality to overcome cancer drug resistance. *Curr Med Chem*, 19, 3858-73.
- PORTELLA, G., PASSARO, C. & CHIEFFI, P. 2011. Aurora B: a new prognostic marker and therapeutic target in cancer. *Curr Med Chem*, 18, 482-96.
- PORTER, L. A. & DONOGHUE, D. J. 2003. Cyclin B1 and CDK1: nuclear localization and upstream regulators. *Prog Cell Cycle Res*, 5, 335-47.
- POSTHUMADEBOER, J., WURDINGER, T., GRAAT, H. C., VAN BEUSECHEM, V. W., HELDER, M. N., VAN ROYEN, B. J. & KASPERS, G. J. 2011. WEE1 inhibition sensitizes osteosarcoma to radiotherapy. *BMC Cancer*, 11, 156.
- PRASANTH, S. G., MENDEZ, J., PRASANTH, K. V. & STILLMAN, B. 2004. Dynamics of pre-replication complex proteins during the cell division cycle. *Philos Trans R Soc Lond B Biol Sci*, 359, 7-16.
- PROSKURYAKOV, S. Y. & GABAI, V. L. 2010. Mechanisms of tumour cell necrosis. *Curr Pharm Des*, 16, 56-68.
- PUTRAL, L. N., BYWATER, M. J., GU, W., SAUNDERS, N. A., GABRIELLI, B. G., LEGGATT, G. R. & MCMILLAN, N. A. 2005. RNA interference against human papillomavirus oncogenes in cervical cancer cells results in increased sensitivity to cisplatin. *Mol Pharmacol*, 68, 1311-9.

- QI, W., COOKE, L. S., LIU, X., RIMSZA, L., ROE, D. J., MANZIOLLI, A., PERSKY, D. O., MILLER, T. P. & MAHADEVAN, D. 2011. Aurora inhibitor MLN8237 in combination with docetaxel enhances apoptosis and anti-tumour activity in mantle cell lymphoma. *Biochem Pharmacol*, 81, 881-90.
- QI, W., SPIER, C., LIU, X., AGARWAL, A., COOKE, L. S., PERSKY, D. O., CHEN, D., MILLER, T. P. & MAHADEVAN, D. 2013. Alisertib (MLN8237) an investigational agent suppresses Aurora A and B activity, inhibits proliferation, promotes endo-reduplication and induces apoptosis in T-NHL cell lines supporting its importance in PTCL treatment. *Leuk Res*, 37, 434-9.
- QIAN, B. Z. & POLLARD, J. W. 2010. Macrophage diversity enhances tumour progression and metastasis. *Cell*, 141, 39-51.
- RAK, J., YU, J. L., KLEMENT, G. & KERBEL, R. S. 2000. Oncogenes and angiogenesis: signaling three-dimensional tumour growth. *J Invest Dermatol Symp Proc*, 5, 24-33.
- RAMOZ, N., RUEDA, L. A., BOUADJAR, B., MONTOYA, L. S., ORTH, G. & FAVRE, M. 2002. Mutations in two adjacent novel genes are associated with epidermodysplasia verruciformis. *Nat Genet*, 32, 579-81.
- REAGAN-SHAW, S. & AHMAD, N. 2005. Silencing of polo-like kinase (Plk) 1 via siRNA causes induction of apoptosis and impairment of mitosis machinery in human prostate cancer cells: implications for the treatment of prostate cancer. *FASEB J*, 19, 611-3.
- RIBATTI, D., NICO, B., CRIVELLATO, E. & VACCA, A. 2007. Macrophages and tumour angiogenesis. *Leukemia*, 21, 2085-9.
- RICH, T., ALLEN, R. L. & WYLLIE, A. H. 2000. Defying death after DNA damage. *Nature*, 407, 777-83.
- RICHARDS, K. F., BIENKOWSKA-HABA, M., DASGUPTA, J., CHEN, X. S. & SAPP, M. 2013. Multiple heparan sulfate binding site engagements are required for the infectious entry of human papillomavirus type 16. *J Virol*, 87, 11426-37.
- RIEDER, C. L. & MAIATO, H. 2004. Stuck in division or passing through: what happens when cells cannot satisfy the spindle assembly checkpoint. *Dev Cell*, 7, 637-51.
- ROBATI, M., HOLTZ, D. & DUNTON, C. J. 2008. A review of topotecan in combination chemotherapy for advanced cervical cancer. *Ther Clin Risk Manag*, 4, 213-8.

- ROJAS-ESPAILLAT, L. A. & ROSE, P. G. 2005. Management of locally advanced cervical cancer. *Curr Opin Oncol*, 17, 485-92.
- ROMANOWSKI, B., DE BORBA, P. C., NAUD, P. S., ROTELI-MARTINS, C. M., DE CARVALHO, N. S., TEIXEIRA, J. C., AOKI, F., RAMJATTAN, B., SHIER, R. M., SOMANI, R., BARBIER, S., BLATTER, M. M., CHAMBERS, C., FERRIS, D., GALL, S. A., GUERRA, F. A., HARPER, D. M., HEDRICK, J. A., HENRY, D. C., KORN, A. P., KROLL, R., MOSCICKI, A. B., ROSENFELD, W. D., SULLIVAN, B. J., THOMING, C. S., TYRING, S. K., WHEELER, C. M., DUBIN, G., SCHUIND, A., ZAHAF, T., GREENACRE, M. & SGRIOBHADAIR, A. 2009. Sustained efficacy and immunogenicity of the human papillomavirus (HPV)-16/18 AS04-adjuvanted vaccine: analysis of a randomised placebo-controlled trial up to 6.4 years. *Lancet*, 374, 1975-85.
- ROSHAK, A. K., CAPPER, E. A., IMBURGIA, C., FORNWALD, J., SCOTT, G. & MARSHALL, L. A. 2000. The human polo-like kinase, PLK, regulates cdc2/cyclin B through phosphorylation and activation of the cdc25C phosphatase. *Cell Signal*, 12, 405-11.
- RUCHAUD, S., CARMENA, M. & EARNSHAW, W. C. 2007. Chromosomal passengers: conducting cell division. *Nat Rev Mol Cell Biol*, 8, 798-812.
- RUTZ, S. & SCHEFFOLD, A. 2004. Towards in vivo application of RNA interference - new toys, old problems. *Arthritis Res Ther*, 6, 78-85.
- SAELENS, X., FESTJENS, N., VANDE WALLE, L., VAN GURP, M., VAN LOO, G. & VANDENABEELE, P. 2004. Toxic proteins released from mitochondria in cell death. *Oncogene*, 23, 2861-74.
- SAHA, B., ADHIKARY, A., RAY, P., SAHA, S., CHAKRABORTY, S., MOHANTY, S., DAS, K., MUKHERJEE, S., MAZUMDAR, M., LAHIRI, L., HOSSAIN, D. M., SA, G. & DAS, T. 2012. Restoration of tumour suppressor p53 by differentially regulating pro- and anti-p53 networks in HPV-18-infected cervical cancer cells. *Oncogene*, 31, 173-86.
- SAIT, K. H. 2011. Knowledge, attitudes, and practices regarding cervical cancer screening among physicians in the Western Region of Saudi Arabia. *Saudi Med J*, 32, 1155-60.
- SALCEDO, M., TAJA, L., UTRERA, D., CHAVEZ, P., HIDALGO, A., PEREZ, C., BENITEZ, L., CASTANEDA, C., DELGADO, R. & GARIGLIO, P. 2002. Changes in retinoblastoma gene expression during cervical cancer progression. *Int J Exp Pathol*, 83, 275-86.

- SAURIN, A. T., VAN DER WAAL, M. S., MEDEMA, R. H., LENS, S. M. & KOPS, G. J. 2011. Aurora B potentiates Mps1 activation to ensure rapid checkpoint establishment at the onset of mitosis. *Nat Commun*, 2, 316.
- SAWAYA, MCCONNELL KJ, KULASINGAM SL, LAWSON HW, KERLIKOWSKE K, MELNIKOW J, LEE NC, GILDENGORIN G, MYERS ER & AE., W. 2003. Risk of cervical cancer associated with extending the interval between cervical-cancer screenings. *N Engl J Med.*, 349, 1501-9.
- SAWAYA, G. F., SUNG, H. Y., KEARNEY, K. A., MILLER, M., KINNEY, W., HIATT, R. A. & MANDELBLATT, J. 2001. Advancing age and cervical cancer screening and prognosis. *J Am Geriatr Soc*, 49, 1499-504.
- SCHIFFMAN, M., HERRERO, R., DESALLE, R., HILDESHEIM, A., WACHOLDER, S., RODRIGUEZ, A. C., BRATTI, M. C., SHERMAN, M. E., MORALES, J., GUILLEN, D., ALFARO, M., HUTCHINSON, M., WRIGHT, T. C., SOLOMON, D., CHEN, Z., SCHUSSLER, J., CASTLE, P. E. & BURK, R. D. 2005. The carcinogenicity of human papillomavirus types reflects viral evolution. *Virology*, 337, 76-84.
- SCHOLL, FRÖHLING S, DUNN IF, SCHINZEL AC & BARBIE DA, K. S., SILVER SJ, TAMAYO P, WADLOW RC, RAMASWAMY S, DÖHNER K, BULLINGER L, SANDY P, BOEHM JS, ROOT DE, JACKS T, HAHN WC, GILLILAND DG. 2009a. Synthetic lethal interaction between oncogenic KRAS dependency and STK33 suppression in human cancer cells. *Cell*, 137, 821-34.
- SCHOLL, FRÖHLING S, DUNN IF & SCHINZEL AC, B. D., KIM SY, SILVER SJ, TAMAYO P, WADLOW RC, RAMASWAMY S, DÖHNER K, BULLINGER L, SANDY P, BOEHM JS, ROOT DE, JACKS T, HAHN WC, GILLILAND DG. 2009b. Synthetic lethal interaction between oncogenic KRAS dependency and STK33 suppression in human cancer cells. *Cell*, 137, 821-34.
- SCHWARZ, T. F., HUANG, L. M., MEDINA, D. M., VALENCIA, A., LIN, T. Y., BEHRE, U., CATTEAU, G., THOMAS, F. & DESCAMPS, D. 2012. Four-year follow-up of the immunogenicity and safety of the HPV-16/18 AS04-adjuvanted vaccine when administered to adolescent girls aged 10-14 years. *J Adolesc Health*, 50, 187-94.
- SCHWARZ, T. F., KOCKEN, M., PETAJA, T., EINSTEIN, M. H., SPACZYNSKI, M., LOUWERS, J. A., PEDERSEN, C., LEVIN, M., ZAHAF, T., PONCELET, S., HARDT, K.,

- DESCAMPS, D. & DUBIN, G. 2010. Correlation between levels of human papillomavirus (HPV)-16 and 18 antibodies in serum and cervicovaginal secretions in girls and women vaccinated with the HPV-16/18 AS04-adjuvanted vaccine. *Hum Vaccin*, 6, 1054-61.
- SEKI, A., COPPINGER, J. A., JANG, C. Y., YATES, J. R. & FANG, G. 2008. Bora and the kinase Aurora a cooperatively activate the kinase Plk1 and control mitotic entry. *Science*, 320, 1655-8.
- SEOANE, J., LE, H. V., SHEN, L., ANDERSON, S. A. & MASSAGUE, J. 2004. Integration of Smad and forkhead pathways in the control of neuroepithelial and glioblastoma cell proliferation. *Cell*, 117, 211-23.
- SHAIKH, F., SANEHI, P. & RAWAL, R. 2012. Molecular screening of compounds to the predicted Protein-Protein Interaction site of Rb1-E7 with p53- E6 in HPV. *Bioinformation*, 8, 607-12.
- SHANNON, J., THOMAS, D. B., RAY, R. M., KESTIN, M., KOETSAWANG, A., KOETSAWANG, S., CHITNARONG, K., KIVIAT, N. & KUYPERS, J. 2002. Dietary risk factors for invasive and in-situ cervical carcinomas in Bangkok, Thailand. *Cancer Causes Control*, 13, 691-9.
- SHEHNAZ K. HUSSAIN, M. M. M., LISA G. JOHNSON, QIN DU, MARI MALKKI, HUI-WEN WILKERSON, FEDERICO M. FARIN, JOSEPH J. CARTER, DENISE A. GALLOWAY, JANET R. DALING, EFFIE W. PETERSDORF, AND STEPHEN M. SCHWARTZ 2009. Cervical and Vulvar Cancer Risk in Relation to Joint Effects of Cigarette Smoking and Genetic Variation in Interleukin 2. *Cancer Epidemiol Biomarkers Prev.* , 17, 1790-99.
- SHERR, C. J. 2000. Cell cycle control and cancer. *Harvey Lect*, 96, 73-92.
- SHERR, C. J. & ROBERTS, J. M. 1999. CDK inhibitors: positive and negative regulators of G1-phase progression. *Genes Dev*, 13, 1501-12.
- SHI, J. Q., LASKY, K., SHINDE, V., STRINGER, B., QIAN, M. G., LIAO, D., LIU, R., DRISCOLL, D., NESTOR, M. T., AMIDON, B. S., RAO, Y., DUFFEY, M. O., MANFREDI, M. G., VOS, T. J., N, D. A. & HYER, M. L. 2012. MLN0905, a small-molecule plk1 inhibitor, induces antitumour responses in human models of diffuse large B-cell lymphoma. *Mol Cancer Ther*, 11, 2045-53.
- SHIMADA, M. & KOMATSU, K. 2009. Emerging connection between centrosome and DNA repair machinery. *J Radiat Res*, 50, 295-301.

- SHIN, H. J., KIM, J. Y., HAMPSON, L., PYO, H., BAEK, H. J., ROBERTS, S. A., HENDRY, J. H. & HAMPSON, I. N. 2010. Human papillomavirus 16 E6 increases the radiosensitivity of p53-mutated cervical cancer cells, associated with up-regulation of aurora A. *Int J Radiat Biol*, 86, 769-79.
- SHIN, M. K., BALSITIS, S., BRAKE, T. & LAMBERT, P. F. 2009. Human papillomavirus E7 oncoprotein overrides the tumour suppressor activity of p21Cip1 in cervical carcinogenesis. *Cancer Res*, 69, 5656-63.
- SHWEIKI, D., ITIN, A., SOFFER, D. & KESHET, E. 1992. Vascular endothelial growth factor induced by hypoxia may mediate hypoxia-initiated angiogenesis. *Nature*, 359, 843-5.
- SIMA, N., WANG, W., KONG, D., DENG, D., XU, Q., ZHOU, J., XU, G., MENG, L., LU, Y., WANG, S. & MA, D. 2008. RNA interference against HPV16 E7 oncogene leads to viral E6 and E7 suppression in cervical cancer cells and apoptosis via upregulation of Rb and p53. *Apoptosis*, 13, 273-81.
- SINGH, S., NARANG, A. S. & MAHATO, R. I. 2011. Subcellular fate and off-target effects of siRNA, shRNA, and miRNA. *Pharm Res*, 28, 2996-3015.
- SIOUD, M. 2010. Advances in RNA sensing by the immune system: separation of siRNA unwanted effects from RNA interference. *Methods Mol Biol*, 629, 33-52.
- SMITH, J. S., LINDSAY, L., HOOTS, B., KEYS, J., FRANCESCHI, S., WINER, R. & CLIFFORD, G. M. 2007. Human papillomavirus type distribution in invasive cervical cancer and high-grade cervical lesions: a meta-analysis update. *Int J Cancer*, 121, 621-32.
- SMITH, S. L., BOWERS, N. L., BETTICHER, D. C., GAUTSCHI, O., RATSCHILLER, D., HOBAN, P. R., BOOTON, R., SANTIBANEZ-KOREF, M. F. & HEIGHWAY, J. 2005. Overexpression of aurora B kinase (AURKB) in primary non-small cell lung carcinoma is frequent, generally driven from one allele, and correlates with the level of genetic instability. *Br J Cancer*, 93, 719-29.
- SOO, K., O'ROURKE, M. P., KHOO, P. L., STEINER, K. A., WONG, N., BEHRINGER, R. R. & TAM, P. P. 2002. Twist function is required for the morphogenesis of the cephalic neural tube and the differentiation of the cranial neural crest cells in the mouse embryo. *Dev Biol*, 247, 251-70.
- SPAHN, M., BADER, P., WESTERMANN, D., ECHTLE, D. & FROHNEBERG, D. 2005. Bladder carcinoma during pregnancy. *Urol Int*, 74, 153-9.

- STRAUSS, H. G., HAENSGEN, G., DUNST, J., HAYWARD, C. R., BURGER, H. U., SCHERHAG, A. & KOELBL, H. 2008. Effects of anemia correction with epoetin beta in patients receiving radiochemotherapy for advanced cervical cancer. *Int J Gynecol Cancer*, 18, 515-24.
- STREBHARDT, K. & ULLRICH, A. 2006. Targeting polo-like kinase 1 for cancer therapy. *Nat Rev Cancer*, 6, 321-30.
- STUBENRAUCH, F. & LAIMINS, L. A. 1999. Human papillomavirus life cycle: active and latent phases. *Semin Cancer Biol*, 9, 379-86.
- SUDAKIN, V., CHAN, G. K. & YEN, T. J. 2001. Checkpoint inhibition of the APC/C in HeLa cells is mediated by a complex of BUBR1, BUB3, CDC20, and MAD2. *J Cell Biol*, 154, 925-36.
- TAKAHASHI, T., BOKU, N., MURAKAMI, H., NAITO, T., TSUYA, A., NAKAMURA, Y., ONO, A., MACHIDA, N., YAMAZAKI, K., WATANABE, J., RUIZ-GARCIA, A., IMAI, K., OHKI, E. & YAMAMOTO, N. 2012. Phase I and pharmacokinetic study of dacomitinib (PF-00299804), an oral irreversible, small molecule inhibitor of human epidermal growth factor receptor-1, -2, and -4 tyrosine kinases, in Japanese patients with advanced solid tumours. *Invest New Drugs*, 30, 2352-63.
- TAKESHITA, M., KOGA, T., TAKAYAMA, K., IJICHI, K., YANO, T., MAEHARA, Y., NAKANISHI, Y. & SUEISHI, K. 2013. Aurora-B overexpression is correlated with aneuploidy and poor prognosis in non-small cell lung cancer. *Lung Cancer*, 80, 85-90.
- TANAKA, H., YOSHIMURA, Y., NOZAKI, M., YOMOGIDA, K., TSUCHIDA, J., TOSAKA, Y., HABU, T., NAKANISHI, T., OKADA, M., NOJIMA, H. & NISHIMUNE, Y. 1999. Identification and characterization of a haploid germ cell-specific nuclear protein kinase (Haspin) in spermatid nuclei and its effects on somatic cells. *J Biol Chem*, 274, 17049-57.
- TANAKA, T., MANGALA, L. S., VIVAS-MEJIA, P. E., NIEVES-ALICEA, R., MANN, A. P., MORA, E., HAN, H. D., SHAHZAD, M. M., LIU, X., BHAVANE, R., GU, J., FAKHOURY, J. R., CHIAPPINI, C., LU, C., MATSUO, K., GODIN, B., STONE, R. L., NICK, A. M., LOPEZ-BERESTEIN, G., SOOD, A. K. & FERRARI, M. 2010. Sustained small interfering RNA delivery by mesoporous silicon particles. *Cancer Res*, 70, 3687-96.
- TANAKA, T. U. 2005. Chromosome bi-orientation on the mitotic spindle. *Philos Trans R Soc Lond B Biol Sci*, 360, 581-9.
-

- TANG, C. J., LIN, C. Y. & TANG, T. K. 2006. Dynamic localization and functional implications of Aurora-C kinase during male mouse meiosis. *Dev Biol*, 290, 398-410.
- TANG, Z., BHARADWAJ, R., LI, B. & YU, H. 2001. Mad2-Independent inhibition of APCCdc20 by the mitotic checkpoint protein BubR1. *Dev Cell*, 1, 227-37.
- TAO, W., SOUTH, V. J., ZHANG, Y., DAVIDE, J. P., FARRELL, L., KOHL, N. E., SEPP-LORENZINO, L. & LOBELL, R. B. 2005. Induction of apoptosis by an inhibitor of the mitotic kinesin KSP requires both activation of the spindle assembly checkpoint and mitotic slippage. *Cancer Cell*, 8, 49-59.
- TARAILO, M., TARAILO, S. & ROSE, A. M. 2007. Synthetic lethal interactions identify phenotypic "interologs" of the spindle assembly checkpoint components. *Genetics*, 177, 2525-30.
- TAYLOR, S. S. & MCKEON, F. 1997. Kinetochore localization of murine Bub1 is required for normal mitotic timing and checkpoint response to spindle damage. *Cell*, 89, 727-35.
- THAKER, N. G., MCDONALD, P. R., ZHANG, F., KITCHENS, C. A., SHUN, T. Y., POLLACK, I. F. & LAZO, J. S. 2010. Designing, optimizing, and implementing high-throughput siRNA genomic screening with glioma cells for the discovery of survival genes and novel drug targets. *J Neurosci Methods*, 185, 204-12.
- THOMAS, M. & BANKS, L. 1999. Human papillomavirus (HPV) E6 interactions with Bak are conserved amongst E6 proteins from high and low risk HPV types. *J Gen Virol*, 80 (Pt 6), 1513-7.
- TIPTON, A. R., TIPTON, M., YEN, T. & LIU, S. T. 2011. Closed MAD2 (C-MAD2) is selectively incorporated into the mitotic checkpoint complex (MCC). *Cell Cycle*, 10, 3740-50.
- TOMITA, L. Y., LONGATTO FILHO, A., COSTA, M. C., ANDREOLI, M. A., VILLA, L. L., FRANCO, E. L. & CARDOSO, M. A. 2010. Diet and serum micronutrients in relation to cervical neoplasia and cancer among low-income Brazilian women. *Int J Cancer*, 126, 703-14.
- TRAN, J., RAK, J., SHEEHAN, C., SAIBIL, S. D., LACASSE, E., KORNELUK, R. G. & KERBEL, R. S. 1999. Marked induction of the IAP family antiapoptotic proteins survivin and XIAP by VEGF in vascular endothelial cells. *Biochem Biophys Res Commun*, 264, 781-8.

- UEHARA, R., TSUKADA, Y., KAMASAKI, T., POSER, I., YODA, K., GERLICH, D. W. & GOSHIMA, G. 2013. Aurora B and Kif2A control microtubule length for assembly of a functional central spindle during anaphase. *J Cell Biol*, 202, 623-36.
- UNEMORI, E. N., FERRARA, N., BAUER, E. A. & AMENTO, E. P. 1992. Vascular endothelial growth factor induces interstitial collagenase expression in human endothelial cells. *J Cell Physiol*, 153, 557-62.
- VADER, G., CRUIJSEN, C. W., VAN HARN, T., VROMANS, M. J., MEDEMA, R. H. & LENS, S. M. 2007. The chromosomal passenger complex controls spindle checkpoint function independent from its role in correcting microtubule kinetochore interactions. *Mol Biol Cell*, 18, 4553-64.
- VADER, G. & LENS, S. M. 2008. The Aurora kinase family in cell division and cancer. *Biochim Biophys Acta*, 1786, 60-72.
- VAGNARELLI, P. & EARNSHAW, W. C. 2004. Chromosomal passengers: the four-dimensional regulation of mitotic events. *Chromosoma*, 113, 211-22.
- VALSASINA, B., BERIA, I., ALLI, C., ALZANI, R., AVANZI, N., BALLINARI, D., CAPPELLA, P., CARUSO, M., CASOLARO, A., CIAVOLELLA, A., CUCCHI, U., DE PONTI, A., FELDER, E., FIORENTINI, F., GALVANI, A., GIANELLINI, L. M., GIORGINI, M. L., ISACCHI, A., LANSEN, J., PESENTI, E., RIZZI, S., ROCCHETTI, M., SOLA, F. & MOLL, J. 2012. NMS-P937, an orally available, specific small-molecule polo-like kinase 1 inhibitor with antitumour activity in solid and hematologic malignancies. *Mol Cancer Ther*, 11, 1006-16.
- VAN DELFT, M. F. & HUANG, D. C. 2006. How the Bcl-2 family of proteins interact to regulate apoptosis. *Cell Res*, 16, 203-13.
- VERSTOVSEK, S. 2013. Ruxolitinib: an oral Janus kinase 1 and Janus kinase 2 inhibitor in the management of myelofibrosis. *Postgrad Med*, 125, 128-35.
- VIVANCO, I. & SAWYERS, C. L. 2002. The phosphatidylinositol 3-Kinase AKT pathway in human cancer. *Nat Rev Cancer*, 2, 489-501.
- VOULGARI, A. & PINTZAS, A. 2009. Epithelial-mesenchymal transition in cancer metastasis: mechanisms, markers and strategies to overcome drug resistance in the clinic. *Biochim Biophys Acta*, 1796, 75-90.

- VYAS, D. M. & KADOW, J. F. 1995. Paclitaxel: a unique tubulin interacting anticancer agent. *Prog Med Chem*, 32, 289-337.
- WALCZAK, H. & KRAMMER, P. H. 2000. The CD95 (APO-1/Fas) and the TRAIL (APO-2L) apoptosis systems. *Exp Cell Res*, 256, 58-66.
- WALTER, J. & NEWPORT, J. 2000. Initiation of eukaryotic DNA replication: origin unwinding and sequential chromatin association of Cdc45, RPA, and DNA polymerase alpha. *Mol Cell*, 5, 617-27.
- WAN, Y. F., GUO, X. Q., WANG, Z. H., YING, K. & YAO, M. H. 2004. Effects of paclitaxel on proliferation and apoptosis in human acute myeloid leukemia HL-60 cells. *Acta Pharmacol Sin*, 25, 378-84.
- WANG, F., DAI, J., DAUM, J. R., NIEDZIALKOWSKA, E., BANERJEE, B., STUKENBERG, P. T., GORBSKY, G. J. & HIGGINS, J. M. 2010. Histone H3 Thr-3 phosphorylation by Haspin positions Aurora B at centromeres in mitosis. *Science*, 330, 231-5.
- WANG, F., ULYANOVA, N. P., DAUM, J. R., PATNAIK, D., KATENEVA, A. V., GORBSKY, G. J. & HIGGINS, J. M. 2012. Haspin inhibitors reveal centromeric functions of Aurora B in chromosome segregation. *J Cell Biol*, 199, 251-68.
- WANG, F., ULYANOVA, N. P., VAN DER WAAL, M. S., PATNAIK, D., LENS, S. M. & HIGGINS, J. M. 2011a. A positive feedback loop involving Haspin and Aurora B promotes CPC accumulation at centromeres in mitosis. *Curr Biol*, 21, 1061-9.
- WANG, J. W. & RODEN, R. B. 2013. Virus-like particles for the prevention of human papillomavirus-associated malignancies. *Expert Rev Vaccines*, 12, 129-41.
- WANG, J. Y., KNUDSEN, E. S. & WELCH, P. J. 1994. The retinoblastoma tumour suppressor protein. *Adv Cancer Res*, 64, 25-85.
- WANG, Q., GRIFFIN, H., SOUTHERN, S., JACKSON, D., MARTIN, A., MCINTOSH, P., DAVY, C., MASTERSON, P. J., WALKER, P. A., LASKEY, P., OMARY, M. B. & DOORBAR, J. 2004a. Functional analysis of the human papillomavirus type 16 E1=E4 protein provides a mechanism for in vivo and in vitro keratin filament reorganization. *J Virol*, 78, 821-33.
- WANG, Q., KENNEDY, A., DAS, P., MCINTOSH, P. B., HOWELL, S. A., ISAACSON, E. R., HINZ, S. A., DAVY, C. & DOORBAR, J. 2009a. Phosphorylation of the human

- papillomavirus type 16 E1--E4 protein at T57 by ERK triggers a structural change that enhances keratin binding and protein stability. *J Virol*, 83, 3668-83.
- WANG, S., PANG, T., GAO, M., KANG, H., DING, W., SUN, X., ZHAO, Y., ZHU, W., TANG, X., YAO, Y. & HU, X. 2013. HPV E6 induces eIF4E transcription to promote the proliferation and migration of cervical cancer. *FEBS Lett*, 587, 690-7.
- WANG, S. L., YAO, H. H. & QIN, Z. H. 2009b. Strategies for short hairpin RNA delivery in cancer gene therapy. *Expert Opin Biol Ther*, 9, 1357-68.
- WANG, Y., DECKER, S. J. & SEBOLT-LEOPOLD, J. 2004b. Knockdown of Chk1, Wee1 and Myt1 by RNA interference abrogates G2 checkpoint and induces apoptosis. *Cancer Biol Ther*, 3, 305-13.
- WANG, Y., LI, J., BOOHER, R. N., KRAKER, A., LAWRENCE, T., LEOPOLD, W. R. & SUN, Y. 2001. Radiosensitization of p53 mutant cells by PD0166285, a novel G(2) checkpoint abrogator. *Cancer Res*, 61, 8211-7.
- WANG, Z., RAO, D. D., SENZER, N. & NEMUNAITIS, J. 2011b. RNA interference and cancer therapy. *Pharm Res*, 28, 2983-95.
- WARNER, S. L., BEARSS, D. J., HAN, H. & VON HOFF, D. D. 2003. Targeting Aurora-2 kinase in cancer. *Mol Cancer Ther*, 2, 589-95.
- WATERS, J. P., POBER, J. S. & BRADLEY, J. R. 2013. Tumour necrosis factor and cancer. *J Pathol*, 230, 241-8.
- WEINBERG, R. 2006. The Biology of Cancer. *Garland Science*.
- WEINSTEIN, I. B. 2002. Cancer. Addiction to oncogenes--the Achilles heal of cancer. *Science*, 297, 63-4.
- WEISS, W. A., TAYLOR, S. S. & SHOKAT, K. M. 2007. Recognizing and exploiting differences between RNAi and small-molecule inhibitors. *Nat Chem Biol*, 3, 739-44.
- WHYTE, P., BUCHKOVICH, K. J., HOROWITZ, J. M., FRIEND, S. H., RAYBUCK, M., WEINBERG, R. A. & HARLOW, E. 1988. Association between an oncogene and an anti-oncogene: the adenovirus E1A proteins bind to the retinoblastoma gene product. *Nature*, 334, 124-9.
- WILLIAMS, G. H. & STOEBER, K. 2012. The cell cycle and cancer. *J Pathol*, 226, 352-64.
- WILLIS, S. N. & ADAMS, J. M. 2005. Life in the balance: how BH3-only proteins induce apoptosis. *Curr Opin Cell Biol*, 17, 617-25.

- WILSON, R., FEHRMANN, F. & LAIMINS, L. A. 2005. Role of the E1--E4 protein in the differentiation-dependent life cycle of human papillomavirus type 31. *J Virol*, 79, 6732-40.
- WILSON, V. G., WEST, M., WOYTEK, K. & RANGASAMY, D. 2002. Papillomavirus E1 proteins: form, function, and features. *Virus Genes*, 24, 275-90.
- WISSING, M. D., MENDONCA, J., KORTENHORST, M. S., KAELEBER, N. S., GONZALEZ, M., KIM, E., HAMMERS, H., VAN DIEST, P. J., CARDUCCI, M. A. & KACHHAP, S. K. 2013. Targeting prostate cancer cell lines with polo-like kinase 1 inhibitors as a single agent and in combination with histone deacetylase inhibitors. *FASEB J*, 27, 4279-93.
- WOLF, P., SEIDL, H., BACK, B., BINDER, B., HOFLEER, G., QUEHENBERGER, F., HOFFMANN, C., KERL, H., STARK, S., PFISTER, H. J. & FUCHS, P. G. 2004. Increased prevalence of human papillomavirus in hairs plucked from patients with psoriasis treated with psoralen-UV-A. *Arch Dermatol*, 140, 317-24.
- WONG, P. G., WINTER, S. L., ZAIKA, E., CAO, T. V., OGUZ, U., KOOMEN, J. M., HAMLIN, J. L. & ALEXANDROW, M. G. 2011. Cdc45 limits replicon usage from a low density of preRCs in mammalian cells. *PLoS One*, 6, e17533.
- WU, H., LAN, Z., LI, W., WU, S., WEINSTEIN, J., SAKAMOTO, K. M. & DAI, W. 2000. p55CDC/hCDC20 is associated with BUBR1 and may be a downstream target of the spindle checkpoint kinase. *Oncogene*, 19, 4557-62.
- WU, K. J., GRANDORI, C., AMACKER, M., SIMON-VERMOT, N., POLACK, A., LINGNER, J. & DALLA-FAVERA, R. 1999. Direct activation of TERT transcription by c-MYC. *Nat Genet*, 21, 220-4.
- WU, L., MA, C. A., ZHAO, Y. & JAIN, A. 2011a. Aurora B interacts with NIR-p53, leading to p53 phosphorylation in its DNA-binding domain and subsequent functional suppression. *J Biol Chem*, 286, 2236-44.
- WU, S. Y., SINGHANIA, A., BURGESS, M., PUTRAL, L. N., KIRKPATRICK, C., DAVIES, N. M. & MCMILLAN, N. A. 2011b. Systemic delivery of E6/7 siRNA using novel lipidic particles and its application with cisplatin in cervical cancer mouse models. *Gene Ther*, 18, 14-22.
- WU, X. Z., CHEN, D. & XIE, G. R. 2007. Bone marrow-derived cells: roles in solid tumour. Minireview. *Neoplasma*, 54, 1-6.

- WYCKOFF, J., WANG, W., LIN, E. Y., WANG, Y., PIXLEY, F., STANLEY, E. R., GRAF, T., POLLARD, J. W., SEGALL, J. & CONDEELIS, J. 2004. A paracrine loop between tumour cells and macrophages is required for tumour cell migration in mammary tumours. *Cancer Res*, 64, 7022-9.
- YANG, J., CHANG, E., CHERRY, A. M., BANGS, C. D., OEI, Y., BODNAR, A., BRONSTEIN, A., CHIU, C. P. & HERRON, G. S. 1999. Human endothelial cell life extension by telomerase expression. *J Biol Chem*, 274, 26141-8.
- YANG, J., IKEZOE, T., NISHIOKA, C., TASAKA, T., TANIGUCHI, A., KUWAYAMA, Y., KOMATSU, N., BANDOBASHI, K., TOGITANI, K., KOEFFLER, H. P., TAGUCHI, H. & YOKOYAMA, A. 2007. AZD1152, a novel and selective aurora B kinase inhibitor, induces growth arrest, apoptosis, and sensitization for tubulin depolymerizing agent or topoisomerase II inhibitor in human acute leukemia cells in vitro and in vivo. *Blood*, 110, 2034-40.
- YANG, J., MANI, S. A., DONAHER, J. L., RAMASWAMY, S., ITZYKSON, R. A., COME, C., SAVAGNER, P., GITELMAN, I., RICHARDSON, A. & WEINBERG, R. A. 2004. Twist, a master regulator of morphogenesis, plays an essential role in tumour metastasis. *Cell*, 117, 927-39.
- YANG, J., MANI, S. A. & WEINBERG, R. A. 2006. Exploring a new twist on tumour metastasis. *Cancer Res*, 66, 4549-52.
- YEUNG, S. C., GULLY, C. & LEE, M. H. 2008. Aurora-B kinase inhibitors for cancer chemotherapy. *Mini Rev Med Chem*, 8, 1514-25.
- YOU, J., CROYLE, J. L., NISHIMURA, A., OZATO, K. & HOWLEY, P. M. 2004. Interaction of the bovine papillomavirus E2 protein with Brd4 tethers the viral DNA to host mitotic chromosomes. *Cell*, 117, 349-60.
- YOUNG, M. A., SHAH, N. P., CHAO, L. H., SEELIGER, M., MILANOV, Z. V., BIGGS, W. H., 3RD, TREIBER, D. K., PATEL, H. K., ZARRINKAR, P. P., LOCKHART, D. J., SAWYERS, C. L. & KURIYAN, J. 2006. Structure of the kinase domain of an imatinib-resistant Abl mutant in complex with the Aurora kinase inhibitor VX-680. *Cancer Res*, 66, 1007-14.

- YU, J. H., LIN, B. Y., DENG, W., BROKER, T. R. & CHOW, L. T. 2007. Mitogen-activated protein kinases activate the nuclear localization sequence of human papillomavirus type 11 E1 DNA helicase to promote efficient nuclear import. *J Virol*, 81, 5066-78.
- YUGAWA, T. & KIYONO, T. 2009. Molecular mechanisms of cervical carcinogenesis by high-risk human papillomaviruses: novel functions of E6 and E7 oncoproteins. *Rev Med Virol*, 19, 97-113.
- ZANIER, CHARBONNIER S, BALTZINGER M, NOMINÉ Y, ALTSCHUH D & G., T. 2005. Kinetic analysis of the interactions of human papillomavirus E6 oncoproteins with the ubiquitin ligase E6AP using surface plasmon resonance. *J Mol Biol.*, 349, 401-12.
- ZEHBE, I., RATSCH, A., ALUNNI-FABBRONI, M., BURZLAFF, A., BAKOS, E., DURST, M., WILANDER, E. & TOMMASINO, M. 1999. Overriding of cyclin-dependent kinase inhibitors by high and low risk human papillomavirus types: evidence for an in vivo role in cervical lesions. *Oncogene*, 18, 2201-11.
- ZENG, L., IMAMOTO, A. & ROSNER, M. R. 2008. Raf kinase inhibitory protein (RKIP): a physiological regulator and future therapeutic target. *Expert Opin Ther Targets*, 12, 1275-87.
- ZHANG, B., CHEN, W. & ROMAN, A. 2006. The E7 proteins of low- and high-risk human papillomaviruses share the ability to target the pRB family member p130 for degradation. *Proc Natl Acad Sci U S A*, 103, 437-42.
- ZHANG, H., GUTTIKONDA, S., ROBERTS, L., UZIEL, T., SEMIZAROV, D., ELMORE, S. W., LEVERSON, J. D. & LAM, L. T. 2011. Mcl-1 is critical for survival in a subgroup of non-small-cell lung cancer cell lines. *Oncogene*, 30, 1963-8.
- ZHANG, W., LI, J., KANGINAKUDRU, S., ZHAO, W., YU, X. & CHEN, J. J. 2010. The human papillomavirus type 58 E7 oncoprotein modulates cell cycle regulatory proteins and abrogates cell cycle checkpoints. *Virology*, 397, 139-44.
- ZHANG, X., MAR, V., ZHOU, W., HARRINGTON, L. & ROBINSON, M. O. 1999. Telomere shortening and apoptosis in telomerase-inhibited human tumour cells. *Genes Dev*, 13, 2388-99.
- ZHOU, J., GUPTA, K., AGGARWAL, S., ANEJA, R., CHANDRA, R., PANDA, D. & JOSHI, H. C. 2003. Brominated derivatives of noscapine are potent microtubule-interfering agents that perturb mitosis and inhibit cell proliferation. *Mol Pharmacol*, 63, 799-807.

- ZHOU, N., SINGH, K., MIR, M. C., PARKER, Y., LINDNER, D., DREICER, R., ECSIEDY, J. A., ZHANG, Z., TEH, B. T., ALMASAN, A. & HANSEL, D. E. 2013. The investigational Aurora kinase A inhibitor MLN8237 induces defects in cell viability and cell-cycle progression in malignant bladder cancer cells in vitro and in vivo. *Clin Cancer Res*, 19, 1717-28.
- ZIEBOLD, U., REZA, T., CARON, A. & LEES, J. A. 2001. E2F3 contributes both to the inappropriate proliferation and to the apoptosis arising in Rb mutant embryos. *Genes Dev*, 15, 386-91.
- ZOU, L. & STILLMAN, B. 2000. Assembly of a complex containing Cdc45p, replication protein A, and Mcm2p at replication origins controlled by S-phase cyclin-dependent kinases and Cdc7p-Dbf4p kinase. *Mol Cell Biol*, 20, 3086-96.

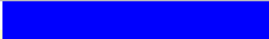






Appendix 1 Customized high-content imaging protocols for the tested cell lines.

Image Acquisition	
Objective	10x
Camera Name	ORCA-ER;0.63
Acquisition Camera Mode	Standard (1024x1024;2x2)
AutoFocus Camera Mode	AutoFocus (1024x1024;4x4)
AutoFocus Field Interval	1

AutoFocus Parameters	
Fine Focus Step Size	17.6
Fine Focus Plane Count	9
Coarse Focus Step Size	70.4
Coarse Focus Plane Count	9
Smart Focus Plane Count	21
Use Extended Range Focusing	False
Apply Backlash Correction	False
AutoFocus Method	STANDARD
Use Relaxed Pass/Fail Criteria	False
Focus Edge Threshold	0
Focus Adjustment	0
Focus Score Min Ratio	0.2
Focus Score Mid Ratio	0.4
Focus Score Max Ratio	0.5
Focus Exposure Time for AutoExpose (seconds)	0.1

Scan Limits	
Max Fields for Well	4
Min Objects for Well	No Limit
Max Sparse Fields for Well	No Limit
Min Objects for Field	N/A
Max Sparse Wells for Plate	N/A

Assay Parameters	
PixelSize	2.048
Type_1_EventDefinition	0
Type_2_EventDefinition	0
Type_3_EventDefinition	0
AvgIntenCh2LevelHigh	100
AvgIntenCh2LevelHigh_CC	3
AvgIntenCh2LevelLow	0
AvgIntenCh2LevelLow_CC	99
MinRef/AvgObjectCountPerField	2
ObjectAreaCh1LevelHigh	1000000000000
ObjectAreaCh1LevelHigh_CC	1
ObjectAreaCh1LevelLow	0
ObjectAreaCh1LevelLow_CC	1
ObjectAvgIntenCh1LevelHigh	4095
ObjectAvgIntenCh1LevelHigh_CC	1
ObjectAvgIntenCh1LevelLow	150
ObjectAvgIntenCh1LevelLow_CC	1
ObjectShapeLWRCh1LevelHigh	1.3
ObjectShapeLWRCh1LevelHigh_CC	1
ObjectShapeLWRCh1LevelLow	0.5
ObjectShapeLWRCh1LevelLow_CC	1
ObjectShapeP2ACh1LevelHigh	1000
ObjectShapeP2ACh1LevelHigh_CC	1
ObjectShapeP2ACh1LevelLow	0
ObjectShapeP2ACh1LevelLow_CC	1
ObjectTotalIntenCh1LevelHigh	10000000000
ObjectTotalIntenCh1LevelHigh_CC	0
ObjectTotalIntenCh1LevelLow	0
ObjectTotalIntenCh1LevelLow_CC	1
ObjectVarIntenCh1LevelHigh	1000000
ObjectVarIntenCh1LevelHigh_CC	1
ObjectVarIntenCh1LevelLow	1000000
ObjectVarIntenCh1LevelLow_CC	1
TotalIntenCh2LevelHigh	12000
TotalIntenCh2LevelHigh_CC	2
TotalIntenCh2LevelLow	0
TotalIntenCh2LevelLow_CC	99
UseMicrometers	0
VarIntenCh2LevelHigh	1000000
VarIntenCh2LevelHigh_CC	1
VarIntenCh2LevelLow	1000000
VarIntenCh2LevelLow_CC	1
BackgroundCorrectionCh1	-50
BackgroundCorrectionCh2	-50
MaskModifierCh2	0
ObjectSegmentationCh1	-2
ObjectSmoothFactorCh1	1
ObjectTypeCh1	0
RejectBorderObjectsCh1	1
UseReferenceWells	0

Channel 1: Channel1			
Dye	XF93 - Hoechst		
Apply Illumination Correction	False		
Apply Background Correction	True		
Gain	25		
Use Apotome	False		
Z Offset	0.00		
Exposure Parameters			
Method	Fixed		
Exposure Time (seconds)	0.015		
Object Identification			
Method	FixedThreshold		
Value	92		
Object Selection Parameter		Min	Max
ObjectAreaCh1		20	200
ObjectShapeP2ACh1		0	2
ObjectShapeLWRCh1		0	2
ObjectAvgIntenCh1		0	32767
ObjectTotalIntenCh1		0	9999999
Display Options			
Composite Color (Hex)	#0000FF		
SelectedObject	#0000FF		
RejectedObject	#FF7F00		
Channel 2: Channel2			
Dye	XF93 - Cy5		
Apply Illumination Correction	False		
Apply Background Correction	True		
Gain	25		
Use Apotome	False		
Z Offset	0.00		
Exposure Parameters			
Method	Fixed		
Exposure Time (seconds)	0.02		
Object Identification			
Method	None		
Value	0		
Object Selection Parameter		Min	Max
AvgIntenCh2		0	32767
TotalIntenCh2		0	1000000000
Display Options			
Composite Color (Hex)	#00FF00		
SelectedObject	#0000FF		
RejectedObject	#FF7F00		
MaskCh2	#00FF00		
Assay			
Assay Algorithm	TargetActivation.V3		
Assay Version	6.0 (Locally Installed Version: 6.0.0.3016)		
Focus Channel	1		
#Channels	2		

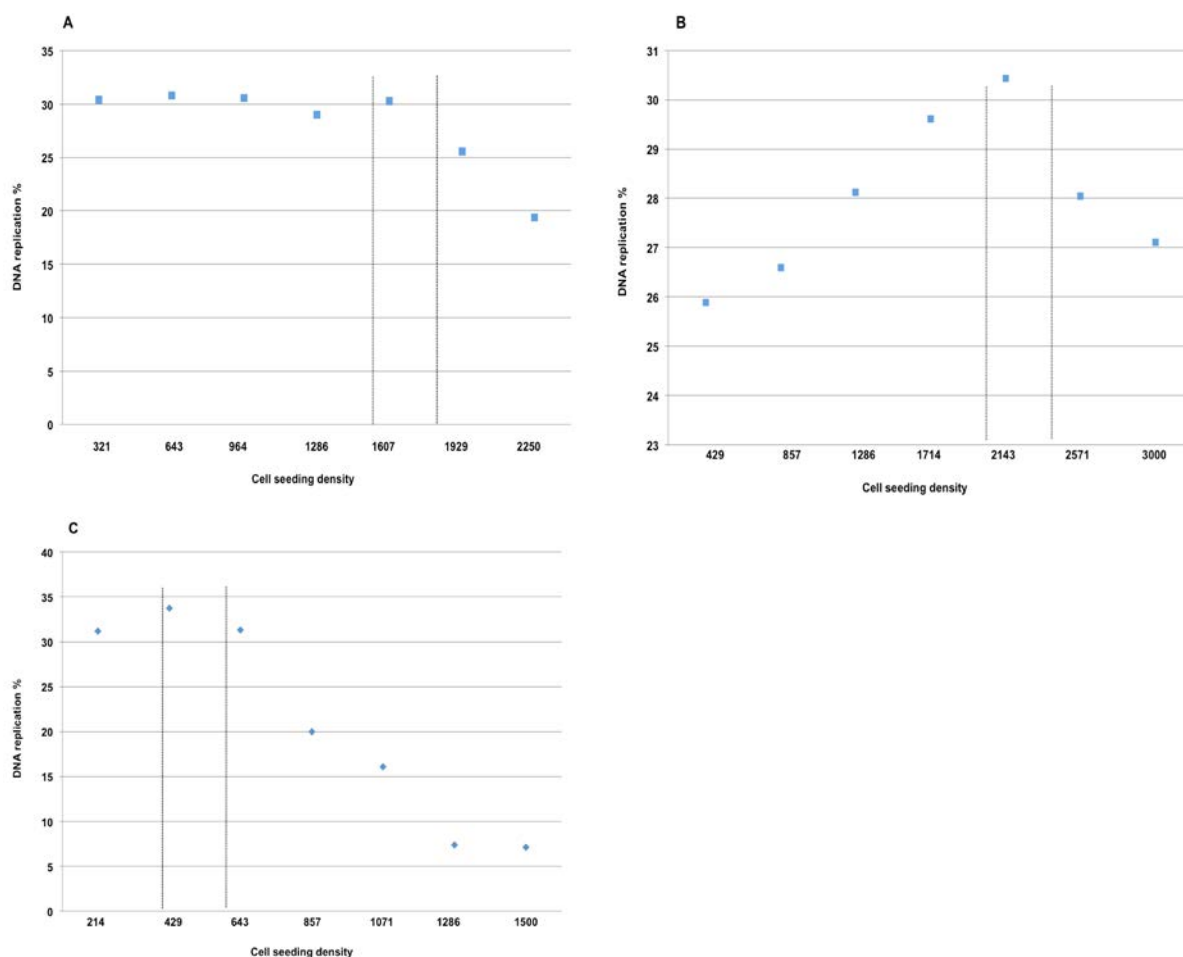
Well Feature Extents			
Feature Name	Lower Extent	Upper Extent	
%EventType1Objects	1	100	
%EventType2Objects	1	100	
%EventType3Objects	1	100	
%RESPONDER_AvgIntenCh2	1	100	
%RESPONDER_ObjectAreaCh1	0	100	
%RESPONDER_ObjectAvgIntenCh1	1	100	
%RESPONDER_ObjectShapeLWRCh1	0	100	
%RESPONDER_ObjectShapeP2ACH1	0	100	
%RESPONDER_ObjectTotalIntenCh1	1	100	
%RESPONDER_ObjectVarIntenCh1	0	100	
%RESPONDER_TotalIntenCh2	1	100	
%RESPONDER_VarIntenCh2	0	100	
%SelectedObjects	1	100	
CV_AvgIntenCh2	0	100	
CV_ObjectAreaCh1	0	100	
CV_ObjectAvgIntenCh1	0	100	
CV_ObjectShapeLWRCh1	0	100	
CV_ObjectShapeP2ACH1	0	100	
CV_ObjectTotalIntenCh1	0	100	
CV_ObjectVarIntenCh1	0	100	
CV_TotalIntenCh2	0	100	
CV_VarIntenCh2	0	100	
EventType1ObjectCount	1	100	
EventType2ObjectCount	1	100	
EventType3ObjectCount	1	100	
MEAN_AvgIntenCh2	1	100	
MEAN_ObjectAreaCh1	1	100	
MEAN_ObjectAvgIntenCh1	1	100	
MEAN_ObjectShapeLWRCh1	1	100	
MEAN_ObjectShapeP2ACH1	1	100	
MEAN_ObjectTotalIntenCh1	1	100	
MEAN_ObjectVarIntenCh1	1	100	
MEAN_TotalIntenCh2	1	100	
MEAN_VarIntenCh2	1	100	
SD_AvgIntenCh2	1	100	
SD_ObjectAreaCh1	1	100	
SD_ObjectAvgIntenCh1	1	100	
SD_ObjectShapeLWRCh1	1	100	
SD_ObjectShapeP2ACH1	1	100	
SD_ObjectTotalIntenCh1	1	100	
SD_ObjectVarIntenCh1	1	100	
SD_TotalIntenCh2	1	100	
SD_VarIntenCh2	1	100	
SE_AvgIntenCh2	0	100	
SE_ObjectAreaCh1	0	100	
SE_ObjectAvgIntenCh1	0	100	
SE_ObjectShapeLWRCh1	0	100	
SE_ObjectShapeP2ACH1	0	100	
SE_ObjectTotalIntenCh1	0	100	
SE_ObjectVarIntenCh1	0	100	
SE_TotalIntenCh2	0	100	
SE_VarIntenCh2	0	100	
SelectedObjectCount	1	100	
SelectedObjectCountPerValidField	1	100	
ValidFieldCount	1	100	
ValidObjectCount*	1	100	

* Indicates the default well feature for the Assay Protocol

** Indicates feature extents are dependent upon system reference well settings

Appendix 1. Detailed high-content imaging protocol for tested cell lines. Cells were labelled with 10nM EdU and were subject to the Click reaction. Following, all cells were fixed and stained with 400nM DAPI in 3% BSA. Positive nuclei for EdU together with cell numbers were detected by the ArrayScan VTI analyser using the above-mentioned detailed protocol.

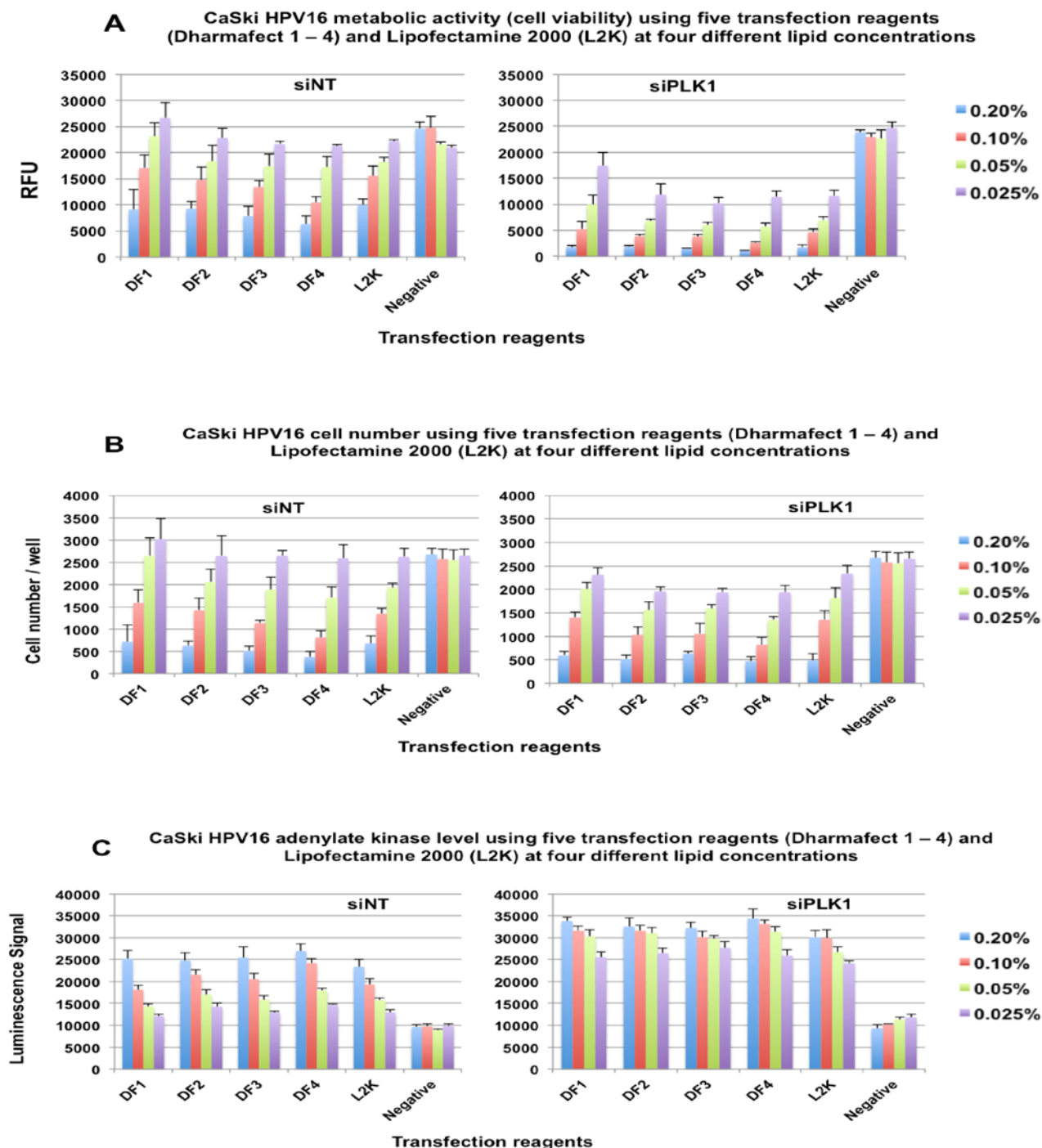
Appendix 2 Example of how cell seeding density was determined



Appendix 2. Examples of how cell seeding densities were determined in 384-well plates for different cells lines.

Optimal seeding density was determined when cells reached the highest DNA replication percentage within the indicated vertical lines. **A** CaSki cell line was seeded at a maximum cell seeding density and a dilution series was performed. Cells were then incubated at 37°C with 5% CO₂ for 72 h prior to harvesting. Cells were then labelled with 10nM EdU. Following, cells were subjected to click-reaction conditions and stained with 400nM DAPI in 3% BSA. Positive nuclei for EdU together with cell numbers were detected using the ArrayScan VTI analyser (Cellomics). Similar procedures were followed for **B** C33A, and **C** HaCaT.

Appendix 3 Example of other transfection reagents and concentrations



Appendix 3. Examples of how DharmaFECT 3 was determined as the best transfection reagents. Five transfection reagents (DharmaFECT 1 – 4) and Lipofectamine 2000 (L2K) were evaluated at four different lipid

concentrations (0.2%, 0.1%, 0.05%, and 0.025%). This is only a representative example from CaSki cell line. Cells were reversed transfected with siRNA against Polo-like kinase 1 (siPLK1) or non-targeting siRNA (siNT) at a final concentration of 50nM. Cells were then incubated at 37°C with 5% CO₂ for 72 h prior to harvesting. After incubation, cells were assayed for: **A** metabolic activity (cell viability) by adding the resazurin dye was into each well at a 44µM final concentration, and plates were incubated for 75 min at 37°C with 5% CO₂ before being read by the FLOUStar plate reader for fluorescence detection; **B** cells were fixed and stained with 400nM DAPI stain in 3% BSA and a cell count was performed by the ArrayScan VTI analyser (Cellomics); **C** 8µl was recovered from the original transfection 384-well plates to new white 384-well plates, similar volume of the adenylate kinase substrate was added into each well and plates were incubated for 20 min at room temperature. Plates were then read by the FLUOStar plate reader for luminescence signal detection. Each data point in A, B, and C represents a mean of four replicates.

Appendix 4 siRNA primary screen candidates detail

Acc. Number	Gene Symbol	Gene ID	Z-score cell no.			Z-score viability			Z-score AK		Z-score Edu%		
			CaSki	C33A	HaCaT	CaSki	C33A	HaCaT	CaSki	C33A	CaSki	C33A	HaCaT
NM_004217	AURKB	9212	-2.19	-2.32	-0.55	0.65	0.36	0.52	2.03	-0.64	-1.19	0.41	0.77
NM_003600	AURKA	6790	-3.94	-2.18	-2.71	0.75	0.76	0.22	7.28	1.31	2.10	-0.84	-3.08
NM_003629	PIK3R3	8503	-2.54	-2.10	-1.06	0.47	0.35	0.33	1.98	-0.81	0.22	1.50	1.16
NM_007207	DUSP10	11221	0.44	-0.44	-0.25	0.13	0.50	0.48	0.19	1.13	0.02	-0.76	1.47
NM_004327	BCR	613	-1.23	0.00	-1.54	0.25	0.25	0.17	1.90	0.87	0.69	-0.44	-0.93
NM_002376	MARK3	4140	-1.83	-0.06	-1.73	0.13	0.23	0.40	1.34	-1.07	1.00	-0.59	0.21
NM_031965	GSG2	83903	-2.86	0.13	0.08	0.16	0.05	0.47	4.76	-0.21	2.34	-0.28	1.09
NM_006314	CNKSR1	10256	-1.91	-0.38	-2.36	0.28	0.67	0.20	1.65	2.22	-2.05	-1.61	1.94
NM_003691	STK16	8576	-0.83	-0.20	0.34	0.12	0.59	0.17	2.00	0.88	0.38	-0.82	-0.26
NM_002736	PRKAR2B	5577	-2.09	-1.86	-0.99	0.42	0.39	0.42	3.50	2.60	-0.01	-1.33	-0.42
NM_004431	EPHA2	1969	0.40	0.85	1.37	0.13	0.85	0.66	-0.13	-0.69	0.88	0.91	-0.02
NM_002969	MAPK12	6300	-2.78	0.50	-0.38	0.95	0.53	0.66	5.22	0.31	1.23	0.79	0.71
NM_006823	PKIA	5569	0.02	-0.75	1.77	0.17	0.65	0.18	-0.37	0.09	0.55	1.26	-0.49
NM_006218	PIK3CA	5290	-0.97	-0.70	0.64	0.55	0.42	0.29	-0.16	-1.61	0.04	-0.09	0.17
NM_004612	TGFBR1	7046	-1.73	0.44	0.28	0.31	0.44	0.32	3.25	0.40	1.76	1.10	-0.09
NM_002767	PRPSAP2	5636	-1.02	-0.67	0.21	0.41	0.26	0.48	2.24	-0.30	-1.20	0.28	0.49

NM_0028 43	PTPRJ	5795	-0.57	0.29	-0.50	0.41	0.35	1.00	0.00	-0.52	-1.67	1.01	0.82
NM_0331 18	MYLK2	85366	-2.59	-0.17	-2.27	0.45	0.81	0.27	1.64	1.08	-1.76	-2.03	1.44
NM_0312 72	TEX14	56155	-2.33	-1.41	-0.37	0.49	0.70	0.81	4.00	1.86	2.08	0.63	-0.75
NM_1334 94	NEK7	14060 9	0.49	0.81	-0.11	0.03	0.90	1.49	-0.10	-0.49	-0.64	0.77	-0.14
NM_0209 65	MAGI-3	26042 5	-1.55	-0.20	-0.86	0.28	0.09	0.06	1.39	-1.67	0.08	-0.12	0.28
NM_0000 24	ADRB2	154	-2.09	-0.12	-1.91	0.40	0.80	0.09	3.13	-0.92	1.18	-1.88	0.55
NM_0142 26	RAGE	5891	-0.08	0.36	-2.33	0.10	0.69	0.31	0.10	0.24	-0.22	-0.47	2.87
NM_0179 88	FLJ10074	55681	0.65	1.85	2.09	0.42	0.36	0.56	-0.27	-0.25	1.01	0.16	-1.21
NM_0145 86	HUNK	30811	-2.36	-0.92	-0.83	0.21	0.24	0.36	4.43	-0.84	2.10	0.18	0.87
NM_0066 09	MAP3K2	10746	0.19	0.18	-0.15	0.33	0.34	1.39	0.27	1.14	-0.80	-1.60	0.67
NM_0012 04	BMPR2	659	-0.90	-0.71	1.25	0.09	0.32	0.15	0.89	-0.10	1.38	-0.83	-0.52
NM_0058 13	PRKCN	23683	-2.69	0.00	0.55	0.11	0.42	0.36	3.69	0.06	0.76	0.04	-0.62
NM_0063 43	MERTK	10461	-2.10	0.66	-1.83	0.68	0.19	0.29	3.60	1.19	0.80	1.36	1.36
NM_0528 41	STK22C	81629	-1.21	-0.62	-0.84	0.11	0.52	0.27	-0.08	-0.95	-2.85	-1.25	-0.61
NM_1528 35	PDIK1L	14942 0	0.62	1.19	1.93	0.27	0.08	0.51	-0.49	-1.00	-0.52	-0.96	-0.72
NM_0049 38	DAPK1	1612	0.27	-2.64	-0.15	0.46	0.39	0.27	0.38	3.22	0.12	-0.93	0.47
NM_0018 26	CKS1B	1163	0.16	0.72	1.56	0.54	0.34	0.17	-0.32	-0.77	0.18	0.73	0.00
NM_0007 88	DCK	1633	-2.71	0.10	-2.51	0.79	0.17	0.05	2.60	-0.20	1.90	-0.80	1.72
NM_1781 70	NEK8	28408 6	-1.13	-0.35	-0.83	0.21	0.56	0.25	-0.21	-0.53	-1.54	-0.42	0.30

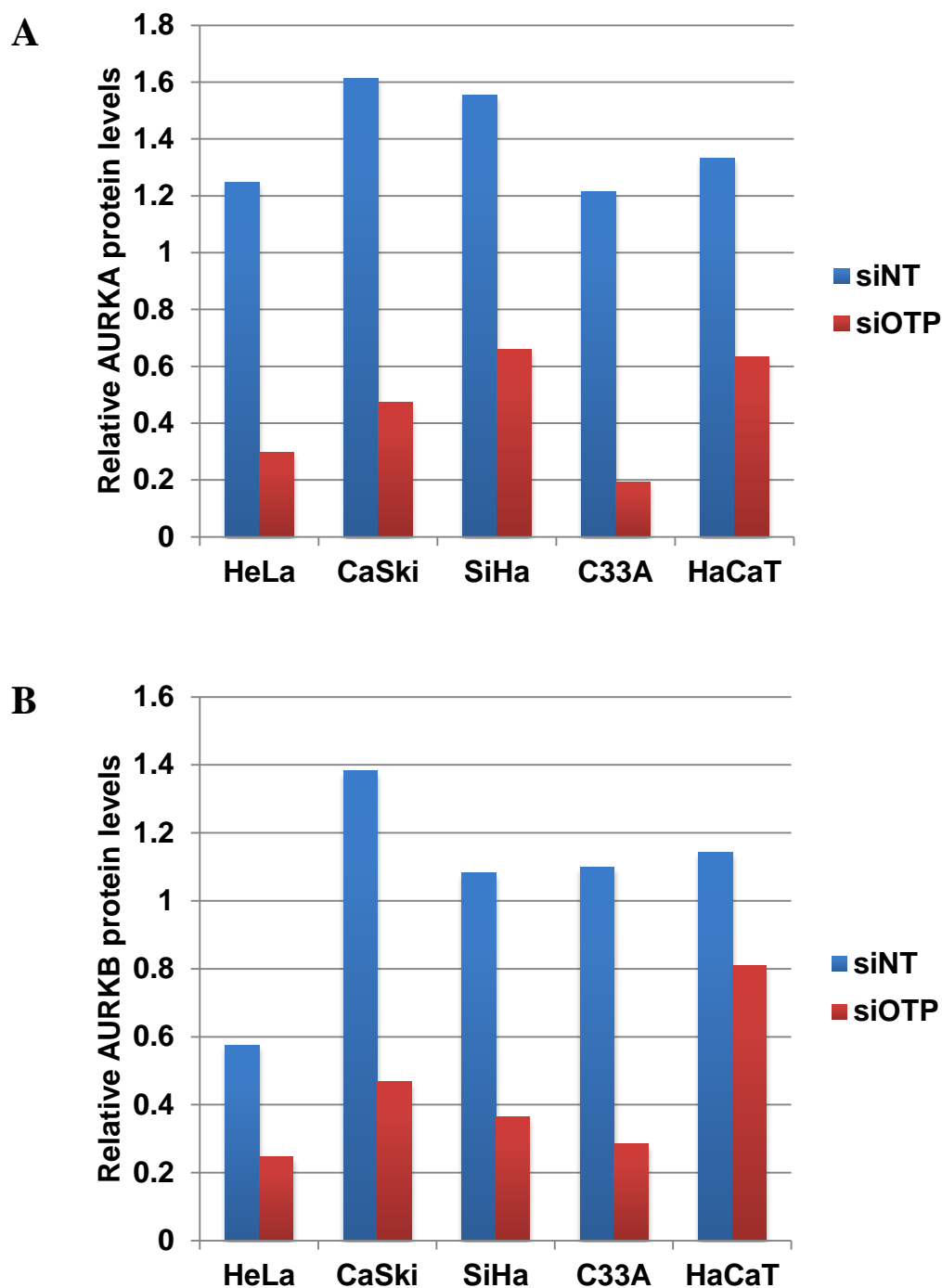
NM_0031 88	MAP3K7	6885	-1.37	-0.13	0.04	0.22	0.79	0.41	2.86	1.53	-0.34	-1.10	0.16
NM_0027 53	MAPK10	5602	0.61	0.09	1.66	0.28	0.63	0.30	-0.22	-0.83	-0.23	-0.20	-1.79
NM_0053 07	GRK4	2868	-1.90	-0.26	-0.70	0.47	0.55	0.42	1.90	-0.93	-0.90	0.10	0.60
NM_0045 86	RPS6KA3	6197	-1.44	-0.88	0.15	0.46	0.53	0.39	3.01	2.00	1.34	-0.28	0.07
NM_0000 20	ACVRL1	94	-0.70	0.93	-1.01	0.54	1.28	0.60	2.41	-0.18	2.29	1.50	-1.19
NM_1735 98	KSR2	28345 5	-2.65	0.06	-0.98	0.51	0.64	0.21	1.86	-0.53	2.24	-0.42	0.98
NM_0159 85	ANGPT4	51378	0.01	0.33	-0.43	0.23	0.15	0.32	-0.80	-0.62	-1.92	-1.70	0.81
NM_0320 37	SSTK	83983	-1.31	0.69	0.24	0.22	0.58	0.18	1.26	-0.73	-0.09	-0.20	-0.28
NM_0071 99	IRAK3	11213	-0.89	0.59	-0.73	0.12	0.52	0.69	3.46	1.28	0.86	-0.41	1.73
NM_0052 28	EGFR	1956	0.47	0.61	0.86	0.50	0.97	0.58	-0.58	-0.94	0.33	0.59	-0.80
NM_0036 47	DGKE	8526	-1.40	-0.06	-0.41	0.23	0.22	0.44	2.16	0.81	-1.14	-0.95	-0.10
NM_0031 77	SYK	6850	-0.53	-1.09	-0.50	0.36	0.08	0.72	1.01	0.24	-2.12	-1.38	0.14
NM_0157 16	MINK	50488	-1.77	0.55	-0.62	0.35	0.16	0.08	1.03	-1.40	1.93	-0.81	-0.65
NM_0027 58	MAP2K6	5608	-2.14	-1.33	0.16	0.31	0.84	0.79	1.87	-1.38	0.89	1.01	-0.29
NM_0036 88	CASK	8573	-1.65	-1.40	1.01	0.21	0.15	0.33	0.01	-1.19	-0.73	1.10	-1.00
NM_0203 97	CAMK1D	57118	0.62	0.30	1.88	0.25	1.00	0.49	-0.85	0.51	0.07	0.70	-1.84
NM_0031 60	AURKC	6795	-2.48	-0.41	-0.72	0.16	1.23	0.50	4.86	-0.24	0.89	0.54	-0.46

Gene symbol	Catalogue number
AURKB	M-003326-02
AURKA	M-003545-09
PIK3R3	M-019546-00
DUSP10	M-003965-01
BCR	M-003875-04
MARK3	M-003517-03
GSG2	M-005327-00
CNKSR1	M-012217-00
STK16	M-004054-00
PRKAR2B	M-007673-00
EPHA2	M-003116-01
MAPK12	M-003590-00
PKIA	M-012321-00
PIK3CA	M-003018-01
TGFBR1	M-003929-01
PRPSAP2	M-006795-01
PTPRJ	M-008476-01
MYLK2	M-005352-02
TEX14	M-005386-01
NEK7	M-003795-02
MAGI-3	M-009453-01
ADRB2	M-005426-01
RAGE	M-004838-01
FLJ10074	M-005318-00
CSNK1D	M-003478-00

HUNK	M-004214-01
MAP3K2	M-003582-01
BMP2	M-005309-02
PRKCN	M-005029-01
MERTK	M-003155-01
STK22C	M-004050-01
PD1K1L	M-005011-02
DAPK1	M-004417-02
CKS1B	M-004586-01
DCK	M-006710-00
NEK8	M-004866-00
MAP3K7	M-003790-05
MAPK10	M-004324-00
GRK4	M-004625-00
RPS6KA3	M-003026-01
ACVRL1	M-005302-02
KSR2	M-005322-01
ANGPT4	M-007803-00
SSTK	M-005034-00
IRAK3	M-004762-00
EGFR	M-003114-01
DGKE	M-011493-00
SYK	M-003176-03
MINK	M-004861-02
MAP2K6	M-003967-00
CASK	M-005311-01
CAMK1D	M-004946-00

AURKC	M-019573-01
-------	-------------

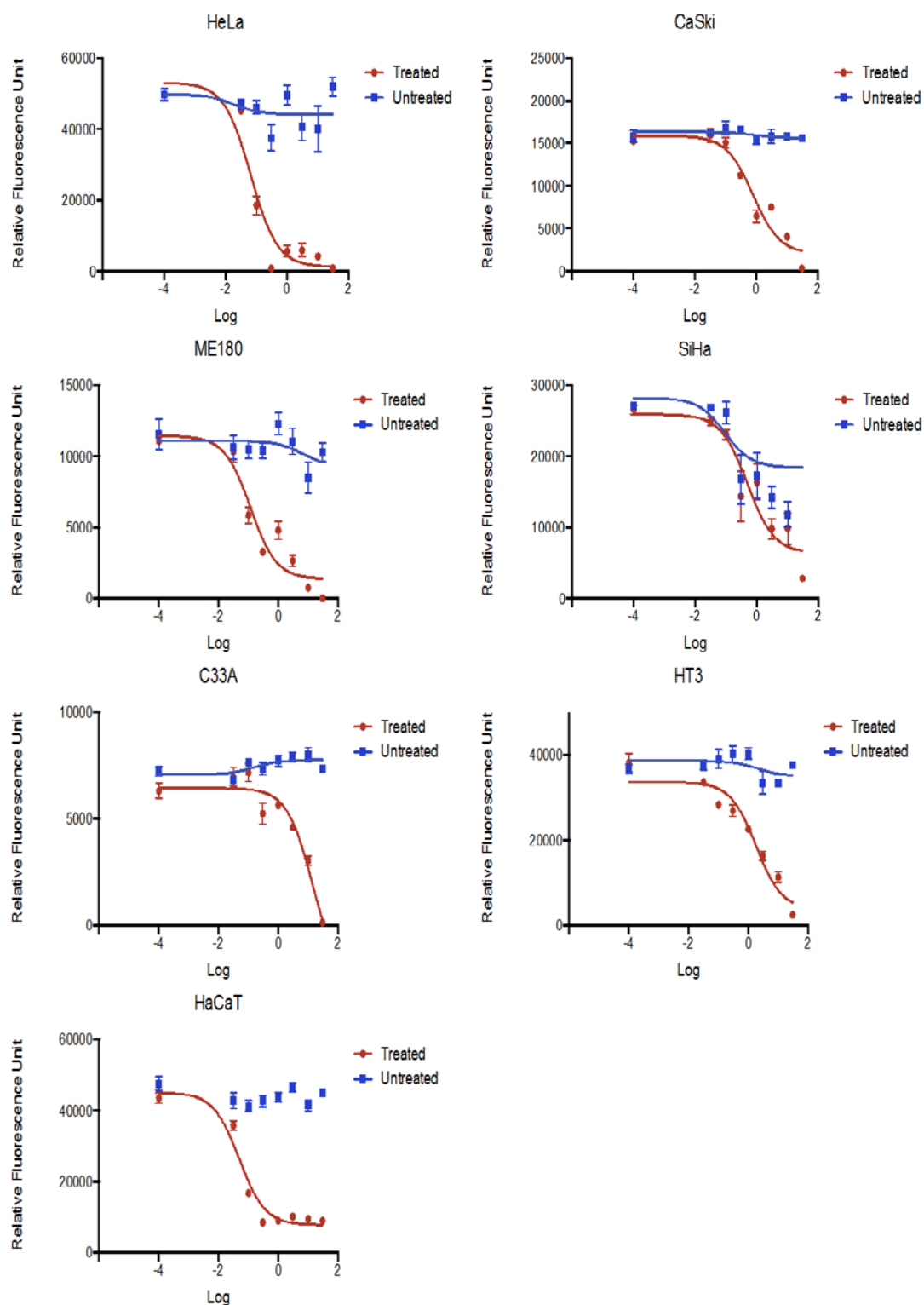
Appendix 4. Primary siRNA screen hit details. As presented in this thesis, the primary siRNA screen revealed 54 target genes that were further validated in a secondary screen. This appendix provide detailed information about their Z-scores, Gene ID, catalogue number from Dharmacon (Vendor ID), gene symbols, and accession numbers.

Appendix 5 Relative AURKA and AURKB protein levels

Appendix 5. Relative AURK and AURKB protein levels. Cells were seeded and transfected with either AURKA or AURKB ON-TARGETplus SMARTpool siRNA for 72 h. Non-targeting siRNA was used as a negative control. Pellet cells were subject to immunoblotting as shown in Figure 3.12 in Chapter 3. Both Figure A and

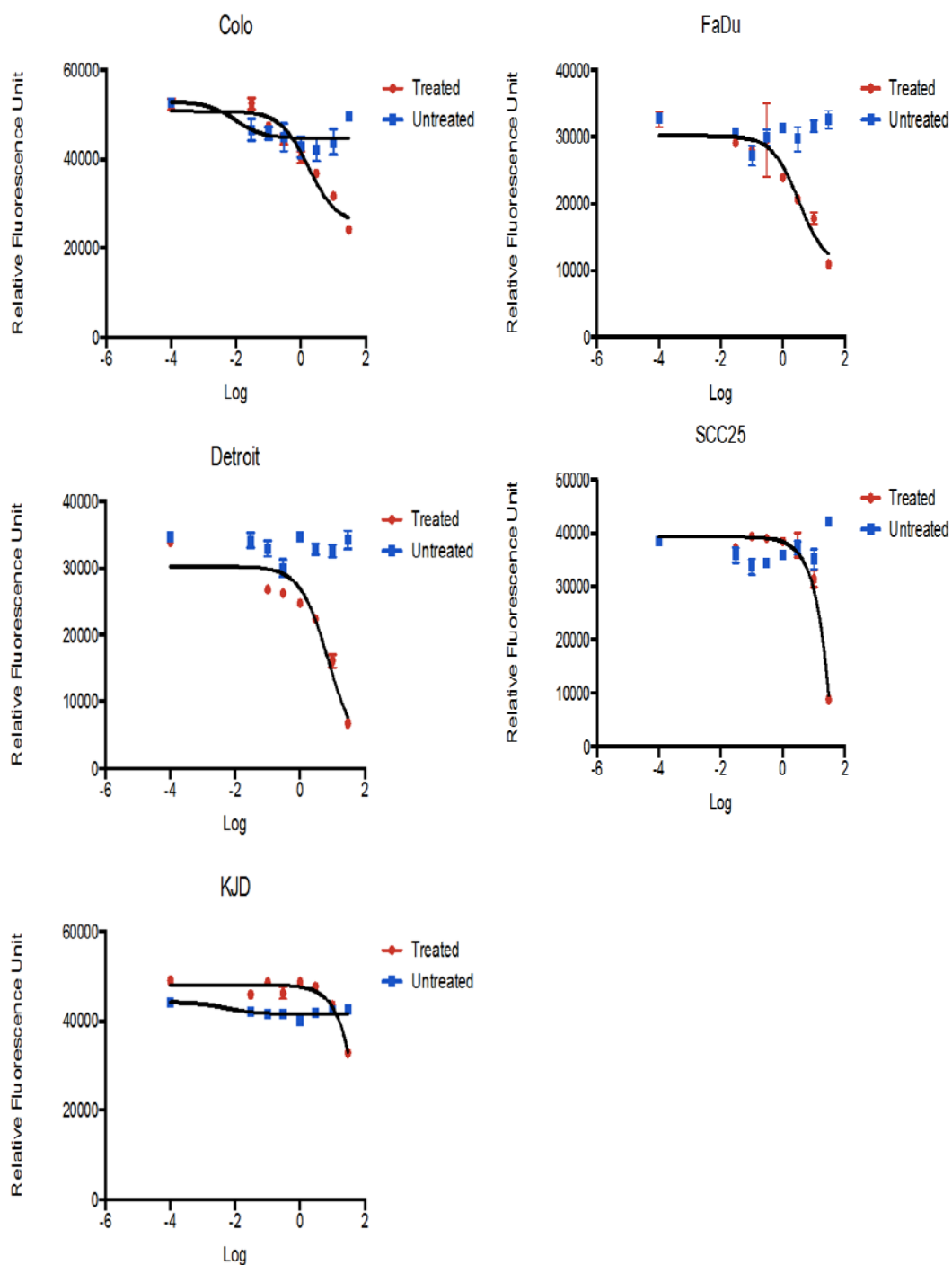
B show quantification of AURKA and AURKB protein levels, respectively; normalized to α -tubulin loading control.

Appendix 6 Dose-response for cervical cancer HPV and non-HPV cell lines treated with MLN8237.



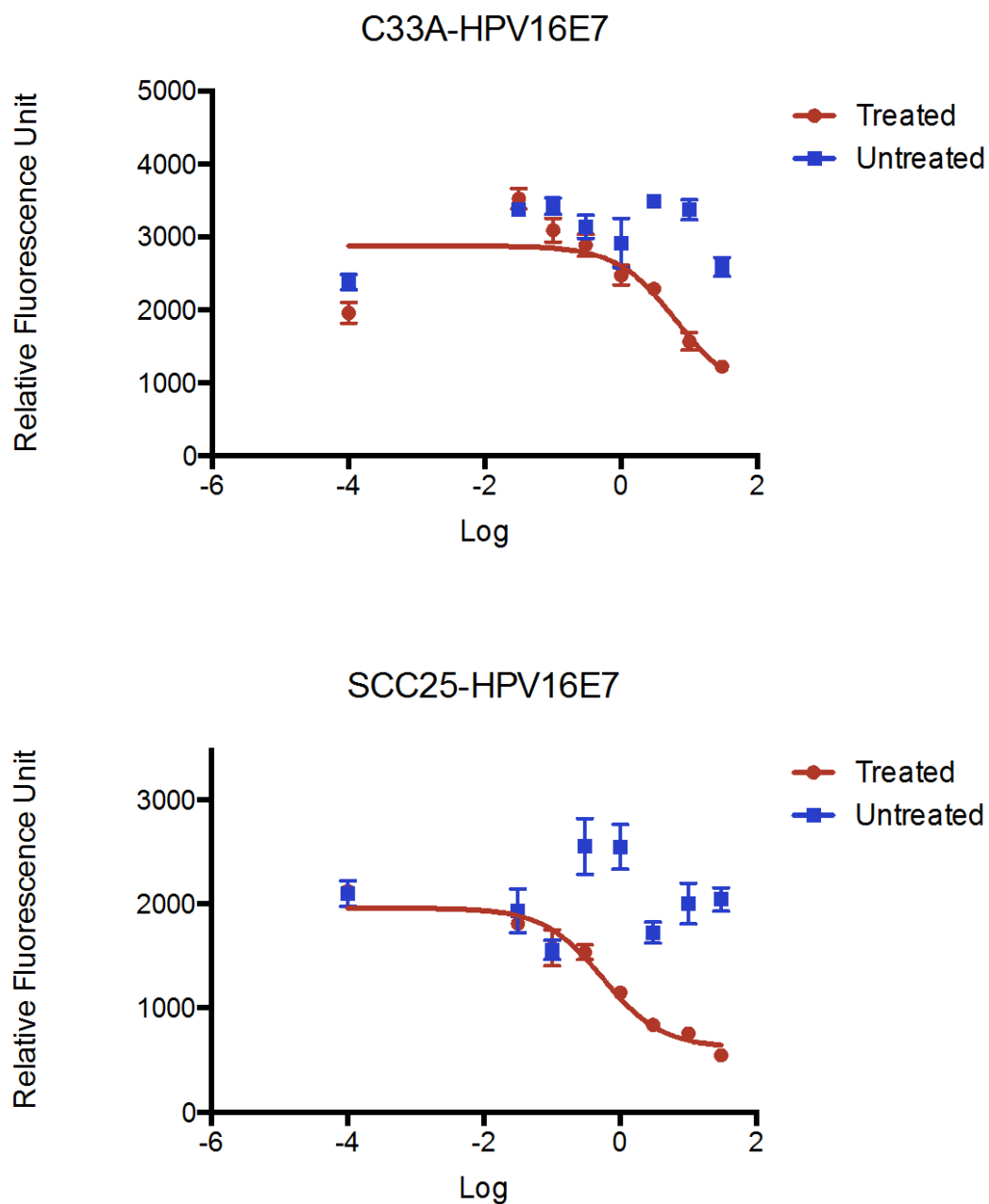
Appendix 6. Dose-response curves for HPV and non-HPV cervical cancer cells treated with MLN8237. Cells were seeded and incubated overnight at 37°C with 5% CO₂. Upon incubation, AURKA small molecule inhibitor (MLN8237) was introduced at a range of 30-10-3-1µM – 300, 100 and 30nM and incubated at the same incubation conditions for 72 h. Cells were subject to the viability assay based on resazurin dye that was used at a final concentration of 44µM. Fluorescence signal was detected using FLUOStart microplate reader. As indicated in these curves, HeLa, ME180, and HaCaT were affected with low concentration of the compound whereas SiHa and HT3 were less affected. C33A (cervical cancer non-HPV) showed less sensitivity to the MLN8237 compared to the remaining tested cell lines. All curves and IC₅₀ values were generated using GraphPad Prism V6.0.

Appendix 7 Dose-response for cervical cancer squamous cell carcinoma (SCC) cell lines treated with MLN8237.



Appendix 7. Dose-response curves for SCC cells treated with MLN8237. Same experimental protocol as indicated in Appendix 5 was followed for this experiment. The curves demonstrated that both SCC-25 and KJD cell lines had very low sensitivity to the small molecule compared to the Colo, FaDu, and Detroit. All curves and IC₅₀ values were generated using GraphPad Prism V6.0.

Appendix 8 Dose-response for C33A and SCC-25 HPV16E7-transfected cell lines treated with MLN8237.



Appendix 8. Dose-response curves for C33A and SCC25 HPV16E7-transfected cell lines treated with MLN8237. Cells were seeded and incubated overnight at 37°C with 5% CO₂. Upon incubation, AURKA small molecule inhibitor (MLN8237) was introduced at a range of 30µM to 30nM and incubated at the same incubation

conditions for 72 h. Cells were subject to the viability assay based on resazurin dye that was used at a final concentration of 44 μ M. Fluorescence signal was detected using FLUOStart microplate reader. Both cell lines showed higher sensitivity to the MLN8237 when compared with the curves in Appendix 5 and 6 of the parental cell lines. The SCC25 in particular showed dramatic reduction in the IC₅₀ value from very low sensitive (in the parental cell line) to high sensitivity (in the HPV16E7 transfected cells). The case was similar with the C33A where low IC₅₀ was observed in this curve compared to the one generated from the parental cell line. All curves and IC₅₀ values were generated using GraphPad Prism V6.0.